Linear Matrix Inequality Approach to H_∞ Loop Shaping Control Problem

Thesis submitted in partial fulfillment of the requirements for the degree of

DOCTOR OF PHILOSOPHY

by

SOURAV PATRA

Department of Electrical Engineering
Indian Institute of Technology, Kharagpur
West Bengal, INDIA 721302
[November 2007]

Dedicated to

My Family

Department of Electrical Engineering
Indian Institute of Technology, Kharagpur
Kharagpur, India 721302.

Certificate

This is to certify that the thesis entitled **Linear Matrix Inequality Approach to H_∞ Loop Shaping Control Problem**, submitted by **Sourav Patra**, a Research Scholar, in the *Department of Electrical Engineering*, *Indian Institute of Technology*, *Kharagpur*, *India*, for the award of the degree of **Doctor of Philosophy**, is a record of an original research work carried out by him under our supervision and guidance. The thesis fulfills all requirements as per the regulations of this Institute and in our opinion, it has reached the standard needed for submission. Neither this thesis nor any part of it has been submitted for any degree or academic award elsewhere.

Dr. Goshaidas Ray
Professor,
Department of Electrical Engineering,
Indian Institute of Technology, Kharagpur
India 721302.

Dr. Siddhartha Sen
Professor,
Department of Electrical Engineering,
Indian Institute of Technology, Kharagpur
India 721302.

Acknowledgment

I would like to take opportunity to acknowledge the help and support of a number of people who have contributed directly or otherwise to the work presented in this thesis.

First of all, I would like to express my gratitude to my supervisors, Professor Goshaidas Ray and Professor Siddhartha Sen who not only guided me throughout the research but also provided reassurance during difficult times.

I would like to express my sincere thanks to the Head of the Department of Electrical Engineering, IIT Kharagpur for providing me all facilities to carry out my research work. I also express my sincere gratitude to the members of doctoral scrutiny committee and all the faculty members of the department. They have made my stay so much fruitful and educative.

I also thank my fellow research scholars, we together discussed and shared our ideas, problems, our frustration, and our moments of triumph. I am grateful to all my hall-mates for the enjoyable time I had shared with them.

Finally, but perhaps most importantly, I would like to thank my family. I am grateful to my father for giving me the freedom to be what I wanted to be and for always being there when I needed him. I am also grateful to my *Jethu*, *Jethima*, *Dada* and *Indrani* for their constant support, love and encouragement. I would like to dedicate this thesis to them.

Sourav Patra
IIT, Khragpur

Abstract

The aim of this work is to recast the H_∞ loop shaping control problems with different design constraints in linear matrix inequality (LMI) framework. It facilitates to design robust controller in convex optimization approach which is computationally superior and easily solvable using available LMI solver. The H_∞ loop shaping method is a two-steps design procedure. In first step, the open-loop singular values are shaped in order to meet closed-loop design specifications; whereas second step is involved with controller synthesis that ensures robustness with respect to unstructured uncertainty of the system. In the present work, a new method has been proposed for pre-compensator selection to shape singular values of the open-loop plant. Subsequently, the condition number of the pre-compensator is also minimized to reduce loop deterioration and the corresponding problem has been formulated in LMI framework.

Exploiting the H_∞ loop shaping control problem in parametric form, a general design framework is obtained. However, it needs an iterative algorithm to calculate the robust stability margin. In the present work, the parametric problem has been formulated in LMI form that circumvents some computational difficulties of Riccati equation based state-space approach. On the other hand, from implementation point of view, the full-order H_∞ loop shaping controller is disadvantageous as its order is high. Here, an alternative method is proposed to design lower-order H_∞ loop shaping controller in four-block framework. To show the performance of lower order controller the method has been applied to a physical problem, load frequency control of inter-connected power system where robustness is achieved against load disturbances and parametric uncertainty of the system.

Further in this work, a local stabilization problem of uncertain LTI plant has been addressed with bounded control input constraint. It is a linear case of actuator saturation problem. Later, considering saturation nonlinearity, two different techniques have

been proposed to design robust controller in H_∞ loop shaping framework. One is in LPV approach and other has been addressed by representing the saturation problem in equivalent Lur'e type system. In the thesis, to elucidate the effectiveness of the proposed methods several numerical examples have been illustrated.

Key words: *H_∞ loop shaping control, linear matrix inequality (LMI), bilinear matrix inequality (BMI), normalized coprime factorization, static controller, Popov stability criteria, linear parameter varying (LPV) system, load frequency control (LFC).*

Contents

List of symbols and acronyms

Symbols

$\Re$	The set of real numbers
$\Re^n$	The set of real $(n \times 1)$ vectors
$\Re^{m \times n}$	The set of real $m \times n$ matrices
L_2	The Hilbert space of square integrable functions
j	Imaginary unit= $\sqrt{-1}$
$c(.)$	Condition number
$\sigma(.)$	Singular value
$\bar{\sigma}(.)$	Maximum singular value
$\underline{\sigma}(.)$	Minimum singular value
μ	Structured singular value
$\\|(.)\\|_2$	Eucladian norm
$\\|(.)\\|_H$	Hankel norm
$\\|(.)\\|_\infty$	Infinity norm
$\in$	Belongs to
$\subset$	Subset of
$<$	Less than
$\leq$	Less than or equal to
$\ll$	Much less than
$>$	Greater than
$\geq$	Greater than or equal to
$\gg$	Much greater than
$\neq$	Not equal to
$\Rightarrow$	Implies to
$\approx$	Approximately equal to

$\forall$	For all
$\exists$	There exists
$:$	Such that
$\rightarrow$	Tends to
$\mapsto$	Maps to
$\pm n$	Variation from $-n$ to $+n$
$y \in [a, b]$	$a \leq y \leq b$ where $y, a, b \in \Re$
$\sup_{x \in \chi} f(x)$	Supremum of $f(x)$ over $x \in \chi$
$\inf_{x \in \chi} f(x)$	Infimum of $f(x)$ over $x \in \chi$
0	Null matrix with appropriate dimension
I_n	Identity matrix with n number of rows and columns
X^T	Transpose of matrix X
X^*	Complex conjugate transpose of matrix X
X^{-1}	Inverse of X
X^{-T}	Transpose of X^{-1} or Inverse of X^T
X^{-*}	Complex conjugate transpose of X^{-1}
$X^\dagger$	Pseudo Inverse of X
$\rho(X)$	Spectral radius of X
$\lambda(X)$	Eigen values of X
$X > 0$	Positive definite matrix X
$X < 0$	Negative definite matrix X
$det(X)$	Determinant of X
$Tr(X)$	Trace of X
$rank(X)$	Rank of X
$diag(x_1, \ldots, x_n)$	A diagonal matrix whose diagonal elements are $x_1,, x_2, \ldots\ x_n$
$\left[\begin{array}{c\|c} A & B \\ \hline C & D \end{array}\right]$	Transfer function of a system $G(s) = C(sI - A)^{-1}B + D$
$\begin{bmatrix} A(\theta) & B(\theta) \\ C(\theta) & D(\theta) \end{bmatrix}$	The State-space matrices of a linear parameter varying system where θ is varying vector of parameters
G^T	Transpose of a real-rational system G
G^{-1}	Inverse of real-rational system G
$Co\{.\}$	Convex hull
$\varepsilon_1(P)$	An ellipsoid $\{x : x^T P x \leq 1\}$
$\varepsilon_\alpha(P)$	An ellipsoid $\{x : x^T P x \leq \alpha\}$
$\square$	End of proof

Acronyms

ARE	Algebraic Riccati Equation
ARI	Algebraic Riccati Inequality
BMI	Bilinear Matrix Inequality
EVP	Eigen Value Problem
GEVP	Generalized Eigen Value Problem
LFC	Load Frequency Control
LFT	Linear Fractional Transformation
LLFT	Lower Linear Fractional Transformation
LMI	Linear Matrix Inequality
LMIP	Linear Matrix Inequality Problem
LPV	Linear Parameter Varying
LTI	Linear Time Invariant
MIMO	Multiple Input Multiple Output
NLCF	Normalized Left Coprime Factorization
NRCF	Normalized Right Coprime Factorization
PID	Proportional Integral Derivative
RHS	Right Hand Side
SISO	Single Input Single Output
SVD	Singular Value Decomposition
TFM	Transfer Function Matrix

List of Figures

List of Tables

CHAPTER 1

Introduction

1.1 Background and motivation

A physical system can not be modeled exactly, neither can its behavior be predicted precisely taking into account all the exogenous signals of the plant. This limitation has compelled the control system community to broaden the arena of classical control to robust control theory for designing a closed-loop system that is insensitive to model uncertainty, disturbance and noise [25, 40, 66, 91, 106, 114]. Needless to say, there has been a quantum jump in number of research articles on robust control theory in recent times ([24, 27, 40, 66, 114] and references therein).

Although the analysis and synthesis tools for linear SISO plants have reached a matured stage [25], extension of these theories easily cannot be directed to multivariable systems [27, 73, 81]. Particularly, the cross-coupling and inadequate gain-phase information of MIMO plants create complexity in design [40, 91, 114]. To overcome these difficulties, a formidable interest has been generated in multivariable control and several successful design methods have been developed [27, 33, 40, 66, 73, 81, 91, 114]. Among them, the H_∞ synthesis is a popular and effective robust control design technique for multivariable systems [26, 33].

In early 80's, the concept of H_∞ control was first proposed to provide a better design trade-off between performance and stability of the closed-loop system [113]. This problem is cast as an optimization problem for minimizing the H_∞ norm of an objective function [26, 33]. The optimality as well as applicability of this method to multivariable systems enhance its popularity, however, its success is limited sometimes due to complexity of the design and high order of the controller [40, 114]. Note that, the synthesis of H_∞ controller is often carried out for an augmented plant which is formed by combining nominal plant with the appropriately chosen weights [26, 33, 40, 114]. These weights are selected on basis of the performance specifications. In selection stage, no information is available for the performance bound. If high performance bound is obtained, the weights are reselected and whole design process is repeated. Thus the selection of weights in H_∞ control is an iterative process and essentially depends on designer's experience and intuitions [40, 114]. In late 80's, Doyle-Glover-Khargonekar-Francis (DGKF) [26] and Doyle-Glover [38] methods were introduced to provide some systematic steps for H_∞ controller design where some assumptions were made to avoid singularity of the problem. In order to satisfy these assumptions, designer often requires to perform loop-shifting and transformation that again impart some extra burden to design. In the two design procedures mentioned above, coupled AREs are solved to synthesize a stabilizing controller and an iterative algorithm is used for calculating the performance bound [26, 40, 114].

On the other hand, the LMI approach to H_∞ control leads a remarkably simplified method for controller design [36, 49]. This technique provides a design platform where the number of assumptions is reduced, iterative algorithm for performance bound is bypassed and the solvability conditions are characterized by two symmetric positive-definite matrices. These two matrices are the stabilizing solutions of two ARIs. In [60], a correspondence has been drawn in between the DGKF method, Doyle-Glover method and LMI approach. Interestingly, the controller structure obtained in the first two methods can similarly be derived in LMI framework [35]. In view of the above discussions, the H_∞ synthesis problem comparatively becomes simpler into LMI approach and it is numerically attractive as the solutions are obtained in convex optimization framework [37].

Before the LMI approach was applied to H_∞ control, a breakthrough came in robust control theory. In early 90's, McFarlane and Glover introduced a method, termed as H_∞ loop shaping control by combining classical loop shaping concept with the H_∞ synthesis problem [64, 65]. This method shapes the open-loop singular values of the plant in order to satisfy the closed-loop design specifications and it accounts stability margin prior to controller synthesis. Like general H_∞ synthesis problem, here the weights are not selected in closed-loop structure (i.e., weights on error signal, control input etc. [114]) and to find the stability margin, whole design process is not required to perform. To obtain this value, an explicit formula has been derived in normalized coprime factorization framework [39, 64, 65]. It reduces design efforts and distinguishes the H_∞ loop shaping method from general H_∞ synthesis problem. This method ensures robustness of the closed-loop system against unstructured uncertainty which is described as perturbations to normalized coprime factors of the shaped plant [39, 64]. Interestingly, this robust stabilization problem can also be formulated in an equivalent four-block H_∞ framework which is similar to general H_∞ synthesis problem [65].

Hence, the design philosophy of H_∞ loop shaping control is different from general H_∞ synthesis problem. Its success depends on the achieved loop shape and corresponding robust stability margin, in other words, indirectly on proper weight selection [65]. Compared to multivariable plant, the weight selection is easier for SISO system and to this end, various weight selection procedures have been reported in the literature [1, 48, 55, 56, 61, 68, 70, 71, 109]. Specifically for weak cross-coupling, the shaping of singular values is done by diagonal weights, however, non-diagonal weights are needed for strongly coupled plants [70, 71, 91]. Moreover, this complexity also will increase as the dimension of the plant is increased and essentially, a systematic method is needed for weight selection. In H_∞ loop shaping method, another major concern is to achieve a good robust stability margin [64]. In this regard, no explicit relation exists between the weights and robust stability margin and to achieve this goal, designer often depends on classical concept and takes care of the factors which are causing for poor stability margin [64, 65, 114]. In addition to this, an important question is also raised in McFarlane-Glover H_∞ loop shaping method concerning uncertainty structure of the plant. As the stabilizing controller is designed in coprime factorization framework by describing the uncertainty as perturbations to normalized coprime factors of the shaped plant, logically a question comes: how does it ensure the robust stability against structured uncertainty or additive or multiplicative types of uncertainty of the nominal plant? In this regard the shaping weights play an important role and well-conditioned weights can ensure a good robust stability margin for the aforesaid uncertainties. On the other hand, even though controller appears in forward path of the closed-loop structure, the pre-specified open-loop shape is desired for successful design. To fulfill this goal, the well-conditioned weights and good robust stability margin are necessary, and thus weight selection process needs special attention of the design.

Parametric H_∞ loop shaping method provides a more generalized design methodology by introducing an additional free parameter. In [41], keeping the same design structure of McFarlane-Glover method, an additional known free parameter has been introduced in performance index to obtain a better trade-off between the sensitivity and complementary sensitivity functions of the closed-loop system. Unfortunately, when the free parameter is not equal to one, the parametric H_∞ loop shaping technique needs an iterative algorithm to calculate the performance bound [41], and hence, novelty of the H_∞ loop shaping method is lost. In state-space approach, the necessary and sufficient conditions for the existence of parametric H_∞ loop shaping controller have been derived in terms of stabilizing solutions of two AREs [41]. Immediately from this result, the McFarlane-Glover H_∞ loop shaping framework is obtained when the introduced parameter is set to one. Interestingly in [41], it has been shown that, the solvability condition is only dependent on the stabilizing solution of control ARE, whereas the other ARE gives stabilizing solution zero and jointly satisfies γ constraint for H_∞ synthesis (i.e., the spectral radius of the product of these two solutions is equal to zero which is always less than γ). Furthermore, exploiting the disturbance feed-forward structure of the generalized plant, an observer-based controller has also been realized and the problem is addressed as a state-feedback problem [41, 87, 114]. This approach imparts a more flexible design platform for H_∞ loop shaping control. Still a formulation is needed to avoid iterative algorithm of [41] for calculating the robust stability margin when the free parameter is not equal to one.

On the other hand, from implementation point of view the full-order H_∞ loop shaping controller is disadvantageous as the order of controller is high and depends on the order of the compensated plant [65, 114]. In control system literature, an increasing interest has been observed on design of a lower order controller, and most of the researchers have concentrated on static controller design ([16, 54, 101] and references therein) or model order reduction [40, 114]. In this context, a novel method has been reported in [74]-[76] for designing a static output feedback H_∞ loop shaping controller. Utilizing inherent structure of the H_∞ loop shaping control, sufficient conditions have been derived for the existence of a static controller. This method proposes effectively a reduced order controller design technique as the final loop shaping controller is obtained by cascading weights with the static controller [76]. Due to sufficient conditions, it is a conservative method, however, the non-convex rank minimization problem for controller order reduction is bypassed [36]. Moreover, it is easy to implement a tractable controller as the design constraints are posed in LMI form [14, 37]. The design has been performed in normalized coprime factorization framework, but, it is not always straightforward when the input saturation [78] and pole placement [19] constraints are taken into account. Specifically for these constraints, the equivalent four-block structure of H_∞ loop shaping control may be the most suitable platform for robust controller design and an effort is needed in this direction to design a static controller.

H_∞ loop shaping method presently has also been applied to different areas in control theory like, internal model control (IMC) [22], model predictive control (MPC) [82], controller parameters tuning [69, 95] etc. Subsequently, in control system literatures a large volume of works can be found where this method has been applied on various applications in different directions [3, 21, 30, 31, 50, 57, 63, 86, 92, 96, 97, 100, 115]. In spite of a huge success over a decade, less attention has been paid to H_∞ loop shaping control where input saturation has been taken into account. Particularly, the shaping of singular values of the open-loop plant becomes inaccurate when the LTI plant is subject to input saturation, and that in turn, leads to performance deterioration and inadequate stability margin information. In literature, few anti-windup schemes and ad-hoc methods have been adopted for H_∞ loop shaping control to suppress the undesirable effects of saturation [31, 78, 79, 96, 107] . Towards this objective, the observer-based structure of the controller has also been used in some practical applications for gain scheduling [70, 107]. However, one aspect is still not addressed so far for H_∞ loop shaping control: what will be performance and stability margin of the H_∞ loop shaping control when system goes into saturation? It is a non-trivial problem as saturation non-linearity is quite difficult to realize in coprime factorization framework as well as it becomes complex as the pre-compensator is a part of controller but not of the system. Moreover, as system operates in nonlinear region the explicit formula used for stability margin is no longer applicable and this method looses its novelty. To overcome these difficulties, the modification of compensators in an adaptive way may be a remedial step to tackle the effects of saturation in H_∞ loop shaping control, however, it imparts a difficult task to designer.

Related to saturation problem, an up-growing interest has been observed in recent times on analysis of stability and performance study of LTI plant in local or global sense [11, 18, 43, 47, 52, 59, 80, 83, 99]. When the saturation non-linearity is sector bounded, for local stabilization problem the applications of Circle and Popov absolute stability criteria are well-studied ([53, 72] and references therein). However, for global stability, a nonlinear feedback law is needed for open-loop stable plant [34] and to this end, the switching control becomes a popular design technique for closed-loop control [23, 84, 93]. The basic solution of these saturation problems lies on the theory of stability in the sense of Lyapunov. To prove stability, designer finds a candidate Lyapunov function which is positive definite in a region of state-space, known as region of attraction for the equilibrium point, and its derivative with respect to time becomes negative definite [47, 52, 53]. On the other hand, to design controller for LTI plant with input saturation constraint, the modeling of saturation non-linearity is essential. To this requirement, several modeling techniques have been reported in control system literatures where the sector bound condition has been taken into account. Among them, the polytopic modeling, Lur'e type system representation with dead zone nonlinearity etc. are the popular techniques in actuator saturation control [44, 47, 52, 102, 103, 104, 108]. In connection with polytopic modeling, some researchers have formulated the saturation control problem in linear parameter varying (LPV) framework [17, 67, 94] where the system state-space matrices are the affine function of some varying parameters [10, 111]. Meanwhile it has to be noted that, the H_∞ loop shaping method is not new to LPV framework, but it has already been applied to such systems [6, 30]. However, using LPV approach explicitly the saturation problem is not yet addressed in H_∞ loop shaping framework and to this direction, some design scopes can be extended [4, 5, 63, 88, 92, 98, 107]. On the other hand, the Lur'e type system representation is a well-known approach in actuator saturation problem. In this approach, the saturation nonlinearity is presented by a linear part in combination with the dead zone nonlinearity. In closed-loop structure, the nonlinear part is separated out and is connected in feedback with the remaining linear part. This feedback arrangement is commonly known as the Lur'e type system representation and for the stability of this type of system, the Popov absolute stability criteria is often adopted. Interestingly, the H_∞ loop shaping framework with input saturation nonlinearity can also be represented in Lur'e type system and a new design method can be proposed.

Since long back, the researchers have devoted more time in computational aspects of the design and their basic motive was to reduce the design complexity and time. To this end, the LMI approach in convex optimization framework is a significant contribution by the mathematicians and control system engineers. The designer quite often formulates various design problems with LMI constraints and using some algorithms, the problems are solved out. The interior point algorithm is one of the most popular and efficient algorithm for solving LMI problems [14]. Interestingly, these algorithms are readily available in some commercial software like, MATLAB and if one can formulate design problem in LMI framework, using available LMI solvers it can easily be solved out. Towards this objective, the concept of positive real lemma, bonded real lemma, passivity etc. are very essential and these can be found in some standard control system literatures [14, 105]. In the present work, using these concepts an effort has been made to formulate the H_∞ loop shaping control problems with different design constraints in LMI framework that yield some computational advantages in design. Before describing the specific problems studied by us, we shall like to make a brief of some of the relevant results which are already available in literatures.

1.2 Preliminaries

Relevant to this thesis, some basic materials have been presented in this section that has been used in subsequent chapters of this thesis. Most of the materials are standard, however, not self-contained and readers are suggested to see relevant references for details. In Chapters 4 and 6, some more preliminaries have also been included which will be needed for those particular chapters.

Singular Value Decomposition [46]

Singular value decomposition is an important mathematical tool for multivariable systems. It helps to find gains of the system in different input-output directions. Here, for a constant matrix, it is described as follows.

Let us consider $A \in \Re^{m\times n}$. Then, there exists unitary matrices

$$U = [u_1, u_2, \ldots, u_m] \in \Re^{m\times m} \text{ and } V = [v_1, v_2, \ldots, v_n] \in \Re^{n\times n}$$

such that

$$A = U\Sigma V^T \tag{1.1}$$

where, $UU^T = I_m$, $V^T V = I_n$, $\Sigma_{m\times n} = \left[\begin{array}{c|c} \Sigma_p & 0 \\ \hline 0 & 0 \end{array}\right]$, $p = \min(m, n)$ and $\Sigma_p = \mathrm{diag}(\sigma_1, \sigma_2, \ldots, \sigma_p)$. Also note that, $\sigma_1 \geq \sigma_2 \geq \cdots \geq \sigma_p > 0$ and σ_1, σ_p are respectively the maximum and minimum singular values of matrix A. The condition number of A is defined as $c(A) = \frac{\sigma_1}{\sigma_p}$ and it is always greater or equal to 1.

Some singular value inequalities [40, 46]

Here, some singular value inequalities are presented that have been used in Chapter 2. For proof, readers are suggested to see the above references. We consider, A and B are two matrices with compatible dimensions. Then,

$$\begin{array}{rcl} \bar{\sigma}(A+B) & \leq & \bar{\sigma}(A)+\bar{\sigma}(B) \\ \bar{\sigma}(AB) & \leq & \bar{\sigma}(A)\bar{\sigma}(B) \\ \underline{\sigma}(A)\bar{\sigma}(B) \leq & \bar{\sigma}(AB) & \leq \bar{\sigma}(A)\bar{\sigma}(B) \\ \underline{\sigma}(A)\underline{\sigma}(B) \leq & \underline{\sigma}(AB) & \leq \bar{\sigma}(A)\underline{\sigma}(B) \\ \bar{\sigma}(A^{-1}) & = & \dfrac{1}{\underline{\sigma}(A)}. \end{array}$$

L_2-norm [114]

The L_2-norm of a system $G(s) \in L_2$ is defined as follows:

$$\|G\|_2^2 = \frac{1}{2\pi}\int_{-\infty}^{\infty} Tr[G^T(-j\omega)G(j\omega)]d\omega = \frac{1}{2\pi j}\oint Tr[G^T(-s)G(s)]ds. \tag{1.2}$$

Note that, $\|G\|_2$ exists if and only if, $G(s)$ is strictly proper and has no poles on the imaginary axis.

H_∞-norm [114]

The H_∞ optimization theory deals with the H_∞-norm of a system $G(s)$. Note that, the H_∞ is the subspace of functions which are analytic and bounded in the open right-half of s-plane. The real rational subspace of H_∞ is denoted by $\Re H_\infty$ that consists of all proper, real rational stable transfer function matrices.

Consider a system $G \in \Re H_\infty$ and it is driven at frequency ω with a sinusoidal input of unit magnitude. At this frequency, $\bar{\sigma}(G(j\omega))$ is the largest possible size of the output for the corresponding sinusoidal input. Thus, the H_∞-norm provides the largest possible amplification over all frequencies of a unit sinusoidal input. In other words, the H_∞-norm of G is defined as

$$\|G\|_\infty = sup_{Re(s)>0}\bar{\sigma}(G(s)) = sup_{\omega\in\Re}\bar{\sigma}[G(j\omega)], \tag{1.3}$$

where "sup" means the supremum or the least upper bound of the function $\bar{\sigma}(G(j\omega))$. Interestingly, $\|G\|_\infty$ is also called the induced norm of mapping $u \mapsto Gu$ where u is the input of system and $u \in \Re H_2$, $\|u\|_2 = 1$. Hence, from the induced norm concept,

H_∞-norm of G can also be defined as

$$\|G\|_\infty := sup\{\|Gu\|_2 : u \in \Re H_2, \|u\|_2 = 1\}. \tag{1.4}$$

From this definition it is clear that, if output of the system is y and $G \in \Re H_\infty$, then for any input u with unit energy, the energy in y is bounded by $\|G\|_\infty$ when $t \geq 0$.

Hankel norm [40, 114]

To understand the Hankel norm of a stable system $G(s)$, one applies an input $u(t)$ up to $t = 0$ and measures the output $y(t)$ for $t > 0$. The Hankel norm is defined as the choice of $u(t)$ that maximizes the ratio of the 2-norm of these two signals. Mathematically it can be represented as

$$\|G(s)\|_H = max_{u(t)} \frac{\sqrt{\int_0^\infty \|y(\tau)\|_2^2 d\tau}}{\sqrt{\int_{-\infty}^0 \|u(\tau)\|_2^2 d\tau}}. \tag{1.5}$$

The Hankel norm is like an induced norm from past input to future output. It can also be shown that the Hankel norm is equal to

$$\|G(s)\|_H = \sqrt{\rho(PQ)} \tag{1.6}$$

where, P and Q are the controllability and observability gramian matrices. These matrices are obtained as the unique positive definite solutions of the following Lyapunov equations:

$$AP + PA^* + BB^* = 0$$

$$A^*Q + QA + C^*C = 0$$

where, the minimal realization of $G(s)$ is described by the state-space matrices (A, B, C, D). If the degree of G is n, the corresponding Hankel singular values are the positive square roots of the eigenvalues of PQ, *i.e.*, $\sigma_i = \sqrt{\lambda_i(PQ)}$, $i = 1, \ldots, n$ where $\sigma_1 \geq \sigma_2 \geq \cdots \geq \sigma_n \geq 0$. Then, the Hankel norm of G denoted as $\|G\|_H$ is σ_1. The Hankel and H_∞-norms are closely related as follows:

$$\|G(s)\|_H = \sigma_1 \leq \|G(s)\|_\infty \leq 2\sum_{i=1}^{n} \sigma_i. \tag{1.7}$$

Spectral factorization [33, 114]

Let us consider a square transfer function matrix $G(s)$ that satisfies the following conditions:

$$\left.\begin{array}{c} G(s), G(s)^{-1} \in \Re L_\infty \\ G(-s)^T = G(s) \\ G(\infty) > 0 \end{array}\right\} \tag{1.8}$$

where, the first condition indicates $G(s), G(s)^{-1}$ are proper and have no poles on the imaginary axis. The second condition yields, $G(s)$ has pole and zero symmetry about the imaginary axis. Using spectral factorization, $G(s)$ can be represented as follows:

$$G(s) = G_0(-s)^T G_0(s) \tag{1.9}$$

where, $G_0(s)$ is a spectral factor and $G_0(s), G_0(s)^{-1} \in \Re H_\infty$.

Similarly, the transfer function matrix $G(s)$ satisfying (1.8) can also be represented as follows using co-spectral factorization.

$$G(s) = G_0(s) G_0(-s)^T \tag{1.10}$$

where, $G_0(s), G_0(s)^{-1} \in \Re H_\infty$.

Linear Fractional Transformation [40, 114]

A wide variety of feedback arrangements can be presented in a standard form using linear fractional transformation and it is frequently used in H_∞ optimization control. In Figure 1.1, the lower LFT structure has been shown.

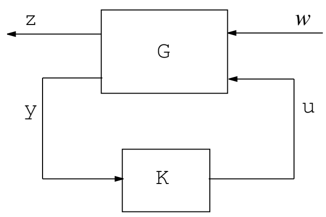

Figure 1.1: Lower Linear Fractional Transformation

The LLFT is denoted as $T_{zw} = F_l(G, K)$. If $\left[\begin{array}{c} z \\ \hline y \end{array}\right] = \left[\begin{array}{c|c} g_{11} & g_{12} \\ \hline g_{21} & g_{22} \end{array}\right] \left[\begin{array}{c} w \\ \hline u \end{array}\right]$,

$$T_{zw} = F_l(G, K) = g_{11} + g_{12}K\left(I - g_{22}K\right)^{-1} g_{21} \tag{1.11}$$

when $det(I - g_{22}K) \neq 0$. Similarly, the upper LFT can also be defined (see references). Note that, the plant $G(s)$ can also be represented in state-space form

$$\left.\begin{aligned} \dot{x} &= Ax + B_1 w + B_2 u \\ z &= C_1 x + D_{11} w + D_{12} u \\ y &= C_2 x + D_{21} w + D_{22} u \end{aligned}\right\} \tag{1.12}$$

Using the packet-matrix notation, from (1.12) we get

$$G(s) = \left[\begin{array}{c|cc} A & B_1 & B_2 \\ \hline C_1 & D_{11} & D_{12} \\ C_2 & D_{21} & D_{22} \end{array}\right].$$

Small gain theorem [114]

To ensure internal stability of the closed-loop system, quite often, the small gain theorem is used in robust control theory. It is conservative, however, simple and effective for determining the closed-loop stability.

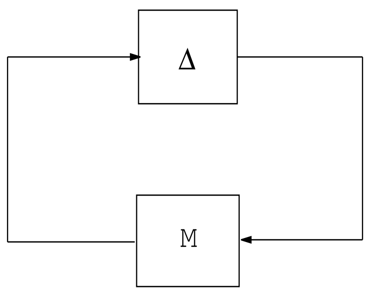

Figure 1.2: Closed-loop system

The small gain theorem states that, the closed-loop system shown in Figure 1.2 is internally stable, if

$$\bar{\sigma}(\Delta(j\omega))\bar{\sigma}(M(j\omega)) < 1 \ \ \forall\, \omega \in \Re$$

where $\Delta, M \in \Re H_\infty$.

Linear Matrix Inequality [14, 105]

An optimization problem with convex constraints can be posed in LMI framework. The LMI is a convex constraint with the following form.

$$F(x) = F_0 + \sum_{i=1}^{m} x_i F_i > 0 \tag{1.13}$$

where, $x = [x_1 \ x_2 \ \dots \ x_m]^T \in \Re^m$ and $F_i = F_i^T \in \Re^{n\times n}$. In (1.13), x is the variable and $F_i, \ i = 0, \dots, m$ are the fixed symmetric matrices. $F(x)$ is an affine function of x and (1.13) indicates the positive definiteness of the constraint. The above strict LMI is feasible if the set $\{x : F(x) > 0\}$ is nonempty and $F(x) \geq 0$ yields nonstrict LMI constraint. Interestingly, multiple LMIs can also be expressed in a single LMI constraint. For example, if $F_i(x) > 0$ for $i = 1, \dots, n$, then it equivalently can be expressed as the following single LMI:

$$diag(F_1(x), F_2(x), \dots, F_n(x)) > 0.$$

Therefore, it is usual to make no distinction between a set of LMIs and a single LMI.

Interestingly, the affine function is a sufficient property to prove a constraint to be an LMI. Note that, a function is an affine function of a variable x, if

$$f(x) = f_0 + f_1(x) \tag{1.14}$$

where, $f(x) : \Re^m \mapsto \Re^n, \ f_0 \in \Re^n$ and $f_1(\alpha_1 x_1 + \alpha_2 x_2) = \alpha_1 f_1(x_1) + \alpha_2 f_1(x_2)$ for all $\alpha_1, \ \alpha_2 \in \Re$ and $x_1, \ x_2 \in \Re^m$. Another important property of LMI is that it forms a convex constraint on the variable. In (1.13), the set $\{x : F(x) > 0\}$ is convex. Note that, a set S is convex if for all $x_1, \ x_2 \in S$ and $\delta \in [0, 1], \ \delta x_1 + (1 - \delta)x_2 \in S$.

We shall discuss some standard problems that are commonly encountered in the convex optimization framework. An LMIP is subject to find the feasible solution for a set of convex constraints. In EVP, the maximum eigenvalue of a matrix is minimized subject to an LMI constraint when that matrix affinely depends on a variable. The EVP is in the following form:

$$\begin{aligned} &\text{Minimize} && \lambda \\ &\text{subject to} && \lambda I - A(x) > 0, B(x) > 0 \end{aligned} \tag{1.15}$$

where, A and B are symmetric matrices and affinely depend on the variable x. Another commonly encountered problem is GEVP which is quasiconvex in nature. Here, the maximum generalized eigenvalue of a pair of matrices are minimized subject to an LMI constraint and the general form of the problem is as follows:

$$\begin{aligned} \text{Minimize} \quad & \lambda \\ \text{subject to} \quad & \lambda B(x) - A(x) > 0, B(x) > 0, C(x) > 0 \end{aligned} \tag{1.16}$$

where, A, B and C are the symmetric matrices that are affinely dependent on the variable x.

Schur complement lemma [14, 36]

This lemma converts the convex nonlinear inequality to LMI constraint. If x is the variable, $Q(x) = Q(x)^T, R(x) = R(x)^T$ and $S(x)$ depend affinely on x, then the convex nonlinear inequalities

$$R(x) > 0, Q(x) - S(x)R(x)^{-1}S(x)^T > 0 \tag{1.17}$$

can be expressed equivalently as

$$\begin{bmatrix} Q(x) & S(x) \\ S(x)^T & R(x) \end{bmatrix} > 0, \tag{1.18}$$

which is an LMI constraint. In other way, if (1.18) is satisfied it yields

$$\begin{aligned} R(x) &> 0 \\ Q(x) &- S(x)R(x)^{-1}S(x)^T > 0 \end{aligned} \tag{1.19}$$

or, equivalently

$$\begin{aligned} Q(x) &> 0 \\ R(x) &- S(x)^TQ(x)^{-1}S(x)^T > 0 \end{aligned} \tag{1.20}$$

where, $Q(x)-S(x)R(x)^{-1}S(x)^T > 0$ and $R(x)-S(x)^TQ(x)^{-1}S(x)^T > 0$ are respectively the Schur complement of $R(x)$ and $Q(x)$. In other words, the nonlinear inequalities (1.19) and (1.20) can be represented as the LMI (1.18).

The matrix norm constraint $\|Z(x)\|_2 < 1$ where $Z(x) \in \Re^{p\times q}$ and depends affinely on x, is represented as LMI

$$\begin{bmatrix} I & Z(x) \\ Z(x)^T & I \end{bmatrix} > 0$$

from the fact that $\lambda_{max}(Z(x)^T Z(x)) < 1$ implies that $y^T Z(x)^T Z(x) y - y^T y < 0$ for all $y \in \Re^{q\times 1}$, i.e., $Z(x)^T Z(x) < I$.

Bounded real lemma [14]

The performance and robustness issues in feedback system design can be posed as objectives for certain closed-loop transfer matrices of the form $\|T_{zw}\|_\infty < \gamma$ (see (1.11)). The bounded real lemma provides a means to establish certain conditions that are equivalent to $\|T_{zw}\|_\infty < \gamma$. This lemma can be explained as follows:

Consider a system

$$\left.\begin{aligned} \dot{x} &= Ax + Bu \\ y &= Cx + Du \end{aligned}\right\} \tag{1.21}$$

where $A \in \Re^{n\times n},\ B \in \Re^{n\times p},\ C \in \Re^{q\times n},\ D \in \Re^{q\times p}$ and $x(0) = 0$. The transfer function matrix between u to y is $G = C(sI - A)^{-1}B + D$ and its H_∞-norm is less than γ, if and only if, (i) $(\gamma^2 I - D^T D) > 0$ and (ii) there exists $P = P^T > 0$ such that for stable A

$$(A^T P + PA + C^T C) + (PB + C^T D)(\gamma^2 I - D^T D)^{-1}(B^T P + D^T C) < 0. \tag{1.22}$$

Using Schur complement lemma, (1.22) can be written as

$$\begin{bmatrix} A^T P + PA + C^T C & PB + C^T D \\ B^T P + D^T C & D^T D - \gamma^2 I \end{bmatrix} < 0. \tag{1.23}$$

Elimination lemma [14]

Consider the inequality

$$\Psi + U^T \Phi^T V + V^T \Phi U < 0 \tag{1.24}$$

where $\Psi \in \Re^{n\times n}$ is a given symmetric matrix; U, V are two matrices with column dimension n, and Φ is the unknown matrix with compatible dimension. There exists a solution Φ, if and only if

$$\begin{aligned} W_U^T \Psi W_U &< 0 \\ W_V^T \Psi W_V &< 0 \end{aligned} \tag{1.25}$$

are hold. W_U and W_V are respectively the two matrices whose columns are the bases of the null spaces of U and V.

Completion lemma [14]

Let $P \in \Re^{n\times n}$ and $Q \in \Re^{n\times n}$ be two symmetric positive definite matrices. There exists a matrix $\tilde{P} \in \Re^{2n\times 2n}$ whose left upper $n \times n$ block is P and Q is the left upper $n \times n$ block of $\tilde{P}^{-1}$, if and only if,

$$\begin{bmatrix} P & I \\ I & Q \end{bmatrix} \geq 0. \tag{1.26}$$

S-Procedure [14]

In optimization technique, quite often, a set of quadratic constraints are handled by multipliers using S-procedure. There are many situations in control engineering where several quadratic inequalities are combined into a single quadratic LMI form.

Let $f_0, \ldots, f_p$ be quadratic functions of the variable $x \in \Re^n$ and

$$f_i(x) = x^T T_i x + 2u_i^T x + v_i,\ i = 0, \ldots, p$$

where $T_i = T_i^T$. We consider the following conditions as:

$$f_0(x) \geq 0\ \forall\ x \text{ such that } f_i(x) \geq 0 \text{ for } i = 1, \ldots, p. \tag{1.27}$$

Now, if there exist $\tau_1 \geq 0, \ldots, \tau_p \geq 0$ such that $\forall x$,

$$f_0(x) - \sum_{i=1}^{p} \tau_i f_i(x) \geq 0, \tag{1.28}$$

then (1.27) holds. Again note that, (1.28) can be written as

$$\begin{bmatrix} T_0 & u_0 \\ u_0^T & v_0 \end{bmatrix} - \sum_{i=1}^{p} \tau_i \begin{bmatrix} T_i & u_i \\ u_i^T & v_i \end{bmatrix} \geq 0. \tag{1.29}$$

Now, the S procedure will be presented for the quadratic forms with strict inequalities. Let, $T_0, \ldots, T_p \in R^{n\times n}$ be symmetric matrices with following conditions:

$$x^T T_0 x > 0\ \forall\ x \neq 0 \text{ such that } x^T T_i x \geq 0,\ i = 1, \ldots, p. \tag{1.30}$$

If there exists $\tau_1, \ldots, \tau_p$ such that

$$T_0 - \sum_{i=1}^{p} \tau_i T_i > 0 \tag{1.31}$$

then, (1.30) holds.

Ellipsoidal inequality [14]

The ellipsoid constraints are important in LMI approach. An ellipsoid described by

$$x^T P^{-1} x < 1, \ P = P^T > 0 \tag{1.32}$$

can be expressed in an LMI form using Schur complement lemma as follows:

$$\begin{bmatrix} 1 & x^T \\ x & P \end{bmatrix} > 0. \tag{1.33}$$

Bilinear matrix inequality [105]

A BMI is of the following form:

$$F(x, y) = F_0 + \sum_{i=1}^{m} x_i F_i + \sum_{j=1}^{n} y_j G_j + \sum_{i=1}^{m} \sum_{j=1}^{n} x_i y_j H_{ij} > 0 \tag{1.34}$$

where G_j, H_{ij} and F_i are symmetric matrices with same dimension and $x \in \Re^m, \ y \in \Re^n$. When y is fixed, (1.34) is LMI in x and for fixed value of x, it is an LMI in y. The BMI problem is not a convex problem. The BMIs are more difficult to handle computationally than LMIs and normally, some iterative algorithms are used to find the solutions of BMI problems.

1.3 Organization of the thesis

The thesis consists of seven chapters and it is organized as follows:

Chapter 2: H_∞ loop shaping control

In this chapter, the McFarlane-Glover H_∞ loop shaping method has been reviewed in detail along with design steps and weight selection procedure. Related to this method, both the normalized coprime factorization and its equivalent four-block synthesis frameworks have been illustrated to depict different uncertainty structures of the plant. In addition, some useful derivations and remarks also have been presented. Later, two new algorithms have been proposed for pre-compensator selection to facilitate H_∞ loop shaping control, where second algorithm is posed in LMI framework leading to minimize the condition number of the designed weight. Finally, a numerical example has been illustrated to show the effectiveness of the proposed algorithms.

Chapter 3: Parametric H_∞ loop shaping control

This chapter provides a general framework for H_∞ loop shaping control from where the McFarlane-Glover method (discussed in Chapter 2) is obtained by setting the parameter is equal to one. Here, an effort has been made to provide the solutions of parametric H_∞ loop shaping control in LMI framework and a correspondence has also been drawn with the state-space method. Further, exploiting the disturbance feed-forward structure of the problem, the observer-based H_∞ loop shaping controller has been realized in LMI framework. Particularly, this chapter consists of two design frameworks for parametric H_∞ loop shaping control, one is formulated in LMI framework and other is in Riccati equation based state-space approach. The results of this chapter are illustrated through a numerical example.

Chapter 4: Static H_∞ loop shaping control

The methods discussed so far in Chapters 2 and 3 are for designing the full-order controller. This order is normally high and it is equal to the order of the compensated plant. Implementation of such controllers for higher order compensated plant lead to high cost, poor reliability and potential problems in maintenance. In this chapter, a new set of sufficient conditions has been derived for the existence of a static H_∞ loop shaping controller that results to elevate the problems associated with the high order controller. The existence of such loop-shaping controller is obtained in four-block H_∞ synthesis framework which is equivalent to the normalized coprime factor robust stabilization problem. The attractiveness of the proposed method is shown by formulating the problem in LMI form which can efficiently be solved by using standard LMI solvers. The effectiveness of the proposed method is elucidated through some numerical examples. At end of this chapter, a case study has been carried out for designing a robust controller for load frequency control problem of two-area inter-connected power system.

Using the proposed method, a static H_∞ loop shaping controller for the solution of load frequency control problem has been designed to ensure robustness against the parametric uncertainty and load disturbances of the system. The performance of the controller has been compared with the full-order controller. Finally, to ensure performance robustness against the parametric uncertainty of the system the real μ analysis has been carried out.

Chapter 5: Local stabilization with bounded control inputs via H_∞ loop shaping approach

In this chapter, the local stabilization problem of LTI plant has been addressed with bounded control inputs. For closed-loop stability, a parametric H_∞ loop shaping controller is designed leading to maximize the region of attraction when control inputs are bounded by pre-specified limits. The introduced parameter is computed in LMI framework from design constraints to achieve a better trade-off among design objectives. Further, this design problem has also been extended for uncertain LTI plant whose uncertainty is described as perturbations to normalized coprime factors of the shaped plant. By this approach, an output feedback H_∞ loop shaping controller is designed such that, with bounded control inputs the local stabilization is accomplished for certain level of uncertainty of the LTI plant and subsequently, the region of attraction is also maximized. The synthesis problems have been formulated in LMI framework. To show the effectiveness of the proposed technique, some numerical examples are demonstrated.

Chapter 6: Robust control with input saturation: H_∞ loop shaping approach

In this chapter, two different approaches are introduced to design robust H_∞ loop shaping controller for LTI plant with input saturation constraint. In the first method, the shaped plant with input saturation has been represented by an equivalent polytopic LPV system. Then, using vertex property of the polytopic LPV plant, H_∞ loop shaping controllers are designed at each vertex of the polytope, and subsequently these controllers are scheduled by adopting certain interpolation method. The scheduled controller locally ensures robust stability and L_2-performance of the closed-loop system due to vertex property of the polytopic LPV shaped plant. In second method, the H_∞ loop shaping framework with input saturation nonlinearity has been transformed into an equivalent Lur'e type system. Then, Popov stability criterion has been used to design a robust controller that ensures certain degree of stability margin against unstructured uncertainty of the plant. Finally, an example has been illustrated to show the effectiveness of the proposed methods.

Chapter 7: Conclusions

This is the concluding chapter in which we summarize the main results of our work and also make some suggestions regarding further studies along the lines of the present work.

CHAPTER 2

H_∞ loop shaping control

The H_∞ loop shaping design method is a combination of classical loop shaping concept and H_∞ optimization technique that optimally establishes a balance between robust performance and stability of the closed-loop system. The term "loop shaping" for multivariable system refers to singular value shaping of the open-loop plant which is needed in order to meet closed-loop design specifications. Quite often, this method is also called as McFarlane-Glover H_∞ loop shaping method. Here, the controller is designed to ensure robust stability against the normalized coprime factor uncertainty description of the shaped plant. In this chapter, the H_∞ loop shaping method has been revisited and related to this method, some useful remarks and derivations are presented. Mainly, the focus is paid on weighting functions selection and its role to H_∞ loop shaping control.

2.1 Introduction

The loop shaping technique is an old and well established method in linear control theory [25]. This method imparts robustness to closed-loop system by appropriately choosing the loop gain in different frequency regions, however, it needs uncertainty information and precise performance specifications of the system. The uncertainty description is often introduced in the plant model in terms of its upper bound, whereas disturbance attenuation, speed of response, percentage of overshoot, bandwidth etc. are normally dictated as performance specifications for the closed-loop system [25, 114]. Based on these requirements, a desired loop shape is chosen to which a stable, minimum phase proper rational transfer function is fitted and from there, a stabilizing controller is obtained.

In robust control theory, the closed-loop system is designed to ensure a pre-specified level of performance and stability of the system irrespective of uncertainty and exogenous signals (disturbance, noise) of the plant [114]. In this design framework, always a fundamental trade-off is demanded between robustness and performance of the system and to fulfill it, a performance index is optimized. This index is involved with some weight functions which are selected on the basis of uncertainty, sensitivity and complementary sensitivity functions of the desired closed-loop system. Sometimes, depending on design requirements weights are also selected for measured output signal, error signal, control input signal etc [25, 40, 114]. In terms of these weight functions, the loop gain bounds are calculated in different frequency region that satisfies some robustness conditions. This frequency region is divided into three parts (see Figure 2.1). In first region i.e., in lower range, the loop gain bound is high (for good tracking and disturbance rejection); whereas in high frequency range loop gain is low (for noise suppression) and in intermediate frequencies, loop-gain typically controls the gain and phase margins. However in intermediate region, the roll-off rate and bandwidth are kept within a specified limit to obtain desirable shapes for sensitivity and complementary sensitivity transfer functions of the closed-loop system. Based on these concepts, a desired loop shape is chosen such that it satisfies all conditions in the whole frequency range and finally, a stabilizing robust controller is obtained.

To illustrate the preceding method, a SISO nominal plant G is considered with multiplicative model uncertainty Δ such that the number of right hand side poles of both the nominal and perturbed plants is same [25]. This model uncertainty arises due to inevitable discrepancy between the true plant and its model. The main role of controller is to achieve an acceptable trade-off between performance (tracking or regulation) and robustness to plant uncertainty. Here, two weight functions W_Δ and W_p are selected satisfying

$$|\Delta(j\omega)| < |W_\Delta(j\omega)| \text{ and } \|W_p(j\omega)S(j\omega)\|_\infty < 1,$$

where S is the sensitivity function of the desired closed-loop system. The term weighted sensitivity function $W_p(j\omega)S(j\omega)$ can be made small at low frequencies with a high loop gain, yielding good tracking and disturbance rejection performance. On the other hand, the uncertain system is robustly stable if the complementary sensitivity function $T(j\omega)$ satisfies the following bound

$$\|W_\Delta(j\omega)T(j\omega)\|_\infty \leq 1,$$

where $W_\Delta(j\omega)$ is the weight function bounding the plant uncertainty. Meanwhile it is noted that, T is the complementary sensitivity function that satisfies

$$S + T = 1.$$

Hence for robust performance, the condition

$$\||W_\Delta T| + |W_p S|\|_\infty < 1 \tag{2.1}$$

must be satisfied and in low frequency range,

$$|W_p(j\omega)| \gg 1 \text{ and } |S(j\omega)| \ll 1.$$

Since, $|S(j\omega)| = |\frac{1}{1+L(j\omega)}|$ where $L(j\omega)$ is the loop transfer function, at low frequency range loop gain $|L(j\omega)| \gg 1$. Hence,

$$|S(j\omega)| \approx \frac{1}{|L(j\omega)|} \text{ and } |T(j\omega)| = \left|\frac{L(j\omega)}{1+L(j\omega)}\right| \approx 1.$$

Now, the condition (2.1) can be simplified as

$$|W_\Delta(j\omega)| + \frac{|W_p(j\omega)|}{|L(j\omega)|} < 1 \tag{2.2}$$

from where, the loop gain bound is obtained as follows:

$$|L(j\omega)| > \frac{|W_p(j\omega)|}{1 - |W_\Delta(j\omega)|}. \tag{2.3}$$

Similarly, at high frequency range the loop gain bound can be expressed as $|L(j\omega)| < \frac{1-|W_p(j\omega)|}{|W_\Delta(j\omega)|}$. Note that, these bounds are the function of weights from where, a desired loop shape can be selected as shown in Figure 2.1.

The loop shaping method discussed above is quite easier for SISO system. Whereas for MIMO case, it becomes complex as loop gain is specified by its singular values (in lower frequency range, minimum singular value of the loop transfer function matrix

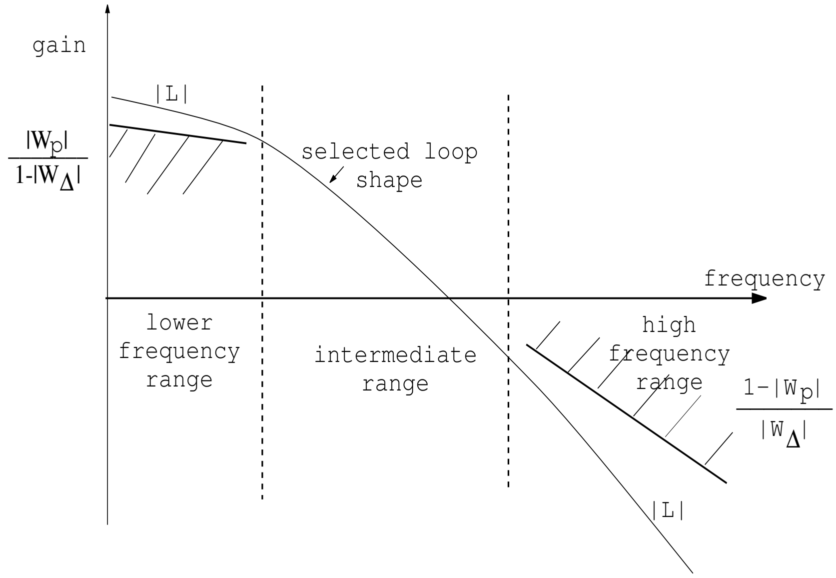

Figure 2.1: Loop gain bounds

must be grater than the specified bound and in higher frequency range, the maximum singular value will be less than the specified bound); precise information regarding gain and phase margin can not be obtained (like SISO plant) and the cross-coupling makes the weight selection difficult for design [91]. Moreover for MIMO system, some extra attentions also have to be taken to ensure the selected weight is stable and minimum phase. Keeping all these factors in mind, the graphical loop shaping method for SISO system has been extended to MIMO system, however, comparatively an easier loop shaping method can be obtained in H_∞ framework to provide an optimal trade-off between performance and robustness of the system [26, 114]. In H_∞ synthesis, a weighted mixed sensitivity minimization problem is solved to design a stabilizing controller. However in this structure, some difficulties still exist for weight selection and in performance bound (γ) calculation. In H_∞ synthesis, the selected weights are not appropriate until a good performance bound is obtained and to know it, whole design process has to be completed that in result, provides extra burden to designer and makes the weight selection procedure iterative in nature. It is well-known that the additive or multiplicative type of uncertainty described in the form of a stable rational transfer function indicates perturbation to the nominal plant model. However, it may not be always true for real system and in this context, coprime factor uncertainty description of the system is the most general presentation for unstructured uncertain system.

The H_∞ loop shaping method proposed by McFarlane-Glover is a sensible and promising method for designing robust controller [65]. This method combines classical loop shaping concept with robust stabilization problem and ensures closed-loop stability against the uncertainty of normalized coprime factors of the shaped plant. This method effectively is a two-stage controller design technique where in the first stage, open-loop singular values are shaped with frequency dependent weights according to closed-loop objectives are addressed. The function of second stage is the robust stabilization of the shaped-plant with regard to coprime factor uncertainty using H_∞ optimization method. Unfortunately in MIMO system, still designer gets stumbling situation for selecting the proper weights, however, the experience and intuition can reduce the difficulty. In H_∞ loop shaping method, weights that shape open-loop singular values of the nominal plant, effectively meets closed-loop design specifications such as stability, good performance and certain robustness and accounts stability margin prior to controller synthesis.

In [64, 65], McFarlane and Glover illustrated the design philosophy of H_∞ loop shaping control. They have pointed out some typical aspects of the design and, some useful and important derivations also have been developed leading to establish the relations between weights, stability margin, nominal plant and controller (no explicit relation between the weights and stability margin!). Moreover, some guidelines of classical loop shaping control, a prerequisite for weight selection also have been discussed. In time of weight selection, designer often takes care of the factors like, right hand side poles and zeros, roll-off rate at cross-over frequency and pole-zero cancelation etc. These factors restrict system performances and also affect robust stability margin. A detail discussion on these aspects can be found in [40, 91, 114]. Moreover, it also has to be noted that, in H_∞ loop shaping framework the controller synthesis is greatly affected by condition number of the selected weights. It is concerned with loop deterioration and for well-conditioned weights, the deterioration is less [65].

In this method, the success of design hence depends on achieved loop shape and corresponding robust stability margin, in other words, indirectly on proper weight selection. For the system with weak cross-coupling, the singular value shaping can be done with diagonal weights, however, non-diagonal weights are needed for strongly coupled plant. Moreover, the complexity increases as dimension of the system increases and essentially, a systematic method is needed for weight selection. It can be seen in literature that, SVD is a mathematical tool that frequently has been adopted for selecting the proper weights in H_∞ loop shaping control [55, 71]. Some additional constraints also have been imposed in weight selection algorithm in order to tackle the other design parameters, as a result, a simultaneous weight selection framework is obtained that maximizes the robust stability margin.

In control system literatures, a number of systematic procedures can be found for weight selection to facilitate the H_∞ loop shaping control. Hyde proposed a technique for shaping the singular values of the scaled plant by reordering the inputs and outputs [48]. By reordering, the scaled plant is made diagonal as close as possible and from input-output plots, weights are selected. It needs design experience and is good for weakly-coupled plant. In [109], authors have considered weights as design parameters and have used the method of inequalities to select the weight functions. In their work, a two degree-of-freedom H_∞ loop shaping controller has been designed using an additional pre-compensator that is connected to the reference input. The weights are with specific form and order, and designed technique leads an optimization framework to maximize the robust stability margin of the system.

Papegeorgiou and Glover proposed a systematic method for weight selection using SVD approach by which non-diagonal weights can be designed [71]. This technique needs a diagonal TFM that gives desired shape of singular values by cascading with the nominal plant. Within the selected frequency range, SVD is carried out and ordering of singular values is maintained. This method does not consider stability margin in weight selection process. On the other hand, to maximize the robust stability margin, in [55] a simultaneous weight selection procedure in linear matrix inequality framework has been proposed. In this algorithm, two additional constraints are imposed to restrict the condition number of the weights. In [68], Nobakhti and Munro have presented a method for shaping the singular values of the multivariable plant that can be applied to H_∞ loop shaping control. Using the concept of Gershgorin disc, the method first selects a compensator to diagonalize the nominal plant and then, an additional diagonal weighting matrix is selected to achieve the desired loop shape. Another weight selection method has been proposed in [61] using hierarchical micro-genetic algorithm that manipulates the loop-shaping weighting function matrices in pursuit of the satisfaction of problem requirements. This method also provides a simultaneous optimization framework to maximize the robust stability margin. In [78], a method has been proposed for selecting the weights in presence of input saturation constraint. When control input is high and crosses saturation limit, gain of the weight is adjusted in an ad-hoc manner.

In literatures, although a large number of procedures are available for selecting the proper compensators for H_∞ loop shaping method, nowhere the condition number minimization issue is addressed to reduce the loop deterioration in presence of controller.

In this chapter, exploiting the matrix perturbation technique, a new method has been proposed for pre-compensator selection to facilitate the H_∞ loop shaping control. The work presented in [1] is extended with a view to develop two different algorithms that are useful to design pre-compensator for solution of H_∞ loop shaping control problem. More precisely, the second algorithm is formulated in LMI framework to minimize the condition number of the pre-compensator that in turn, significantly improves the loop properties.

The rest of the chapter is organized as follows. In Section 2.2, the design steps for H_∞ loop shaping control has been demonstrated. Section 2.3 describes the role of weight functions to this design method and some useful remarks have been given in Section 2.4. In Section 2.5, a new method has been proposed for weight selection followed by a numerical example which is illustrated in Section 2.6. Finally, the concluding remarks are drawn in Section 2.7.

2.2 Design steps for H_∞ loop shaping control

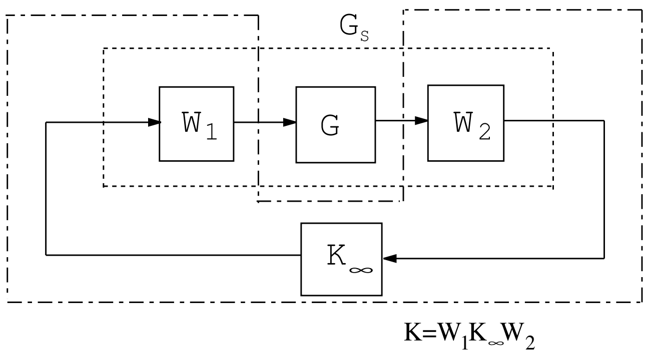

Figure 2.2: McFarlane-Glover H_∞ loop shaping method [65]

In this section, a brief outline has been presented for McFarlane-Glover H_∞ loop shaping method. The method essentially is a two-steps design procedure: first step is involved with loop shaping and second step includes the robust stabilization problem [65, 64].

In the H_∞ loop shaping design procedure, the attainment of performance specification depends on the selection of the weighting function matrices. In Figure 2.2, the shaped plant for H_∞ loop shaping control has been depicted where G, W_2 and W_1 are respectively the nominal plant, selected post and pre-compensator. Combining these compensators with nominal plant, the shaped plant is obtained, i.e., $G_S = W_2 G W_1$. The selection of both pre and post weighting function matrices are, therefore, the key element in attaining the performance requirements of the system and is the main point of this design technique. In normalized left coprime factorization framework, G_S is factorized as $M^{-1}N$ where $M, N \in \Re H_\infty$ and satisfies $MM^* + NN^* = I$. It helps to find the robust stability margin explicitly by using the non-iterative expression:

$$\epsilon_{max} = \left(1 - \left\| \begin{bmatrix} M & N \end{bmatrix} \right\|_H^2 \right)^{\frac{1}{2}} \tag{2.4}$$

where, ϵ_{max} is the maximum robust stability margin of the closed-loop system. If $\epsilon_{max} > 0.2$ (considered good, based on theory and practical experience), the design cycle proceeds, otherwise, weights are reselected [65].

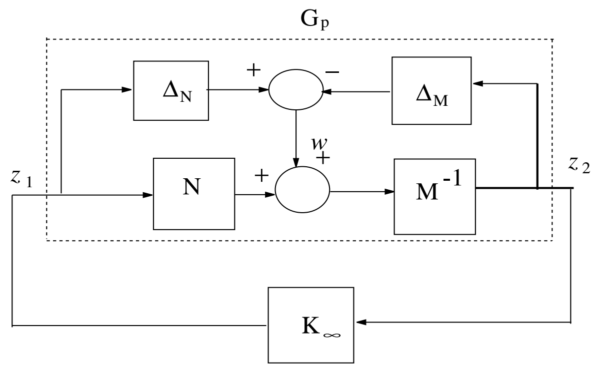

Figure 2.3: Robust stabilization problem in normalized left coprime factorization framework [65]

In second step, the stabilizing H_∞ controller K_∞ is synthesized for the shaped plant G_S describing the uncertainty as perturbations to normalized coprime factors of the shaped plant as shown in Figure 2.3 (here, it is shown for NLCF). $G_p = (M + \Delta_M)^{-1}$ $(N + \Delta_N)$ is the perturbed plant with unstructured uncertainties Δ_M and Δ_N. The motive behind the robust stabilization is to stabilize not only the nominal plant G, but also a family of perturbed plant G_p. The robust stabilizing controller K_∞ is designed such that

$$\inf_{K_\infty \text{stabilizing}} \left\| \begin{bmatrix} K_\infty \\ I \end{bmatrix} (I - G_S K_\infty)^{-1} M^{-1} \right\|_\infty \leq \frac{1}{\epsilon} = \gamma \tag{2.5}$$

is satisfied, in other way, $\left\| \begin{bmatrix} \Delta_N & \Delta_M \end{bmatrix} \right\|_\infty < \epsilon$ is ensured where $0 < \epsilon < \epsilon_{max}$. Finally, the loop shaping controller is obtained by combining the weighting fuctions W_1 and W_2

with K_∞ such that, it becomes $W_1K_\infty W_2$ as shown in Figure 2.2.

This design philosophy is different from general H_∞ synthesis problem. Here, the robust stability margin is the design indicator and it is calculated prior to controller synthesis using the relation (2.4). Although, (2.4) depicts an explicit relation between the robust stability margin and shaped plant, it can not give any quantitative measure for stability margin that explicitly depends on the selected weights [64, 65].

2.3 Role of weight functions

In this section, the emphasis is given on weight functions and its role to H_∞ loop shaping control. First, the compatibility of the selected loop shape is considered. The word 'compatible' yields a successful design correspond to the shaped plant that gives good robust stability margin with considerable loop deterioration. Interestingly, it has been observed that the degradation of desired loop shape occurs due to poor stability margin and large condition number of the weights. To illustrate the deterioration in loop shape at plant output and input for low and high frequencies (see Figure 2.2), the following expressions have been shown [64].

- For low frequency
  1. Loop gain at plant output:
     $\underline{\sigma}\left(GK\right) = \underline{\sigma}\left(GW_1K_\infty W_2\right) \geq \underline{\sigma}\left(W_2GW_1\right)\underline{\sigma}\left(K_\infty\right)/c\left(W_2\right)$
  2. Loop gain at plant input:
     $\underline{\sigma}\left(KG\right) = \underline{\sigma}\left(W_1K_\infty W_2G\right) \geq \underline{\sigma}\left(W_2GW_1\right)\underline{\sigma}\left(K_\infty\right)/c\left(W_1\right)$
- For high frequency
  1. Loop gain at plant output:
     $\bar{\sigma}\left(GK\right) = \bar{\sigma}\left(GW_1K_\infty W_2\right) \leq \bar{\sigma}\left(W_2GW_1\right)\bar{\sigma}\left(K_\infty\right)c\left(W_2\right)$
  2. Loop gain at plant input:
     $\bar{\sigma}\left(KG\right) = \bar{\sigma}\left(W_1K_\infty W_2G\right) \leq \bar{\sigma}\left(W_2GW_1\right)\bar{\sigma}\left(K_\infty\right)c\left(W_1\right)$

These inequalities are derived for closed-loop system where stabilizing controller makes the loop gain different from open-loop shape. In this context, it has been shown that at low and high frequency regions, the gain of K_∞ is restricted and it depends on robust stability margin and singular values of the shaped plant [64, 65]. For high value of robust stability margin, the loop deterioration is less if the selected weights are with well condition number. Hence, compatible loop shape not only demands a good robust stability margin but also needs proper weight selection.

On the other hand, in robust control theory to achieve the design objectives some transfer function matrices are often considered like, in between the reference input to measured output, disturbance signal to error signal, reference input to control input etc. and their gains are minimized subject to robust stability of the closed-loop system. In H_∞ loop shaping framework, simplifying the objective function (2.5), some bounds on these transfer functions are obtained (see [65] for detail) and interestingly, it has been observed that these bounds are function of robust stability margin, gain and condition number of the weights. In this regard to get an idea, at low frequency some relations have been shown below [65].

1. Gain from output disturbance to controller output:

$$\bar{\sigma}\left(K\left(I-GK\right)^{-1}\right) \leq \gamma c\left(W_1\right)/\underline{\sigma}\left(G\right)$$

2. Gain from output disturbance to controller input:

$$\bar{\sigma}\left(\left(I-GK\right)^{-1}\right) \leq \gamma \frac{1}{\underline{\sigma}\left(G\right)\underline{\sigma}\left(W_1\right)\underline{\sigma}(W_2)}$$

3. Gain from input disturbance to controller output:

$$\bar{\sigma}\left(K\left(I-GK\right)^{-1}G\right) \leq \gamma c\left(W_1\right)$$

4. Gain from input disturbance to plant output:

$$\bar{\sigma}\left(\left(I-GK\right)^{-1}G\right) \leq \frac{\gamma}{\underline{\sigma}\left(W_1\right)\underline{\sigma}(W_2)}$$

Here, the singular value bounds are dependent on maximum and minimum singular value of the nominal plant which are not in designer's hand to control. As for example, in the first inequality if the minimum singular value of nominal plant is high, an ill-conditioned pre-compensator may give a low upper bound for good robust stability margin. Similarly, the other inequalities can also be interpreted in terms of condition number and singular values of the weights. In brief, it can be concluded that in time of proper weight selection, not only the shaping of singular values of the nominal plant is important but also, its condition number and singular values have to be taken care of to get a good trade-off between performance and robustness of the closed-loop system. Hence, designer must be careful about the desired loop shape as well as selected weights to achieve a successful design.

In H_∞ loop shaping method, the controller ensures robust stability of the closed-loop system against the perturbations to normalized coprime factors of the shaped plant. The question is: how is it related with actual uncertainty which is present in the nominal plant? To get answer of this question, the normalized left coprime factor robust stabilization problem can be described in the following structure [7].

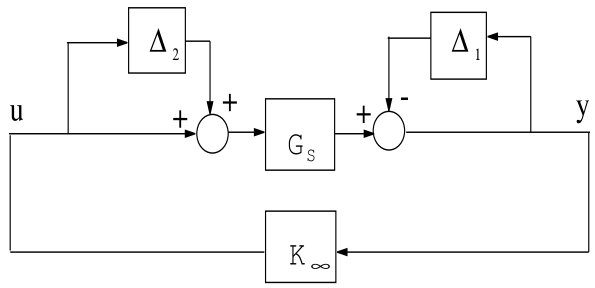

Figure 2.4: Input multiplicative and inverse output multiplicative uncertainty description

From Figure 2.4, we have

$$y = (M + M\Delta_1)^{-1} (N + N\Delta_2) u$$

where, $G_S = M^{-1}N$. With $\Delta_1 = M^{-1}\Delta_M$ and $\Delta_2 = N^{-1}\Delta_N$, Figure 2.4 depicts the same design structure as shown in Figure 2.3. Using this equivalent input-output uncertainty description, it can be related with actual uncertainty description of the nominal plant. Considering the actual uncertainty description of the nominal plant, the H_∞ loop shaping framework can be described as shown in Figure 2.5 [7].
Comparing Figure 2.4 and 2.5, we have

$$\begin{bmatrix} \Delta_{a1} & 0 \\ 0 & \Delta_{a2} \end{bmatrix} = \begin{bmatrix} W_2^{-1}\Delta_1 W_2 & 0 \\ 0 & W_1\Delta_2 W_1^{-1} \end{bmatrix}.$$

From this relation, it can be shown that the closed-loop system is robust stable if

$$\left\| \begin{bmatrix} \Delta_{a1} & 0 \\ 0 & \Delta_{a2} \end{bmatrix} \right\|_\infty < \frac{\epsilon}{\max\left(\sup_\omega c\left(W_2\right), \sup_\omega c\left(W_1\right)\right)}$$

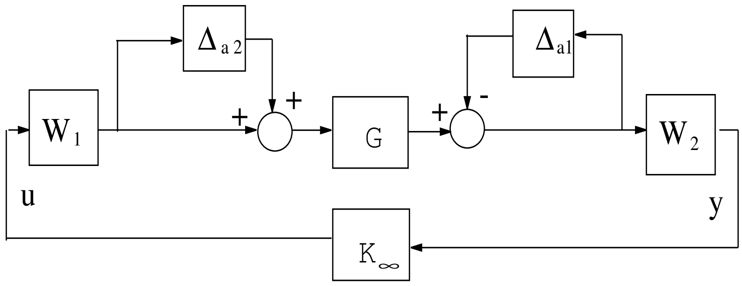

Figure 2.5: H_∞ loop shaping control with actual uncertainty description of the nominal plant

is satisfied, where ϵ is the robust stability margin obtained from coprime factor uncertainty description of the shaped plant. Note that in above inequality, the right hand side is always less than equal to ϵ and if, condition numbers of the weights are large, the robust stability margin will be different for actual uncertainty description of the nominal plant. Hence, for ill-conditioned weighting functions the stability issue is greatly affected.

Now, a different issue has to be discussed for actual control system with input saturation constraint that arises as a consequence of physical restriction of actuators. In H_∞ loop shaping framework when saturation element arises in between the pre-compensator and nominal plant, the robust controller synthesis becomes a nontrivial problem as the design is performed based on the shaped plant. To overcome this difficulty, it is required to adjust the gain of weights, that imparts again a complicated task to designer. In this respect, the structure of H_∞ loop shaping framework becomes advantageous for anti-windup control [48]. In anti-windup scheme, generally an additional loop is formed by monitoring the difference of the input and output signal to the saturation block and introducing integral action to this loop. In context of H_∞ loop shaping framework, the integrator of pre-compensator which is often used to get the high loop gain at low frequency region, is used to facilitate the anti-windup action.

In the next section, some useful derivations and remarks on H_∞ loop shaping control have been illustrated.

2.4 Some useful remarks

In preceding section, a discussion has been made on weight functions and its role to H_∞ loop shaping control. However a fact is not yet mentioned, that is, how the stability margin is explicitly related with the selected weights. It is an open and non-trivial problem of McFarlane-Glover H_∞ loop shaping method and in this section, some guidelines have been discussed for weight selection that yields good robust stability margin. In addition, the uncertainty structure related to this design framework has also been presented in detail.

First, we look into the equation (2.4) that gives an explicit relation between γ and G_S. From this equation, it is quite difficult perhaps impossible to find an explicit relation between the weight functions and γ. To establish this relation, one must separate out G and weight functions from the shaped plant G_S. But it is difficult, since the relation again is involved with the coprime factors of the shaped plant (see equation (2.4) where ϵ_{max} is the function of the Hankel norm of M and N). On the other hand, it is important to note that, the achievable γ_{opt} can be calculated before designing the stabilizing controller, where it depends only on the shaped plant. In [64], a detail discussion has been made on this topic and towards this direction, an explicit relation between stability margin and weights can not be obtained from (2.4). Hence, we concentrate on the performance index (2.5) that provides a relation between nominal plant G, weight functions W_1 and W_2 which are involved into the shaped plant G_S, controller K_∞ and the stability margin $\epsilon = \frac{1}{\gamma}$. In the following section, a derivation has been established that results some interesting expressions.

Let, $G_S \in C^{n\times n}$. Since the controller K_∞ is designed by satisfying (2.5), we have

$$\begin{aligned} (I + K_\infty^* K_\infty) &\leq \gamma^2 (I - K_\infty^* G_S^*)(M^*M)(I - G_S K_\infty) \\ \Rightarrow \begin{bmatrix} K_\infty^* & I \end{bmatrix} \begin{bmatrix} K_\infty \\ I \end{bmatrix} &\leq \gamma^2 (I - K_\infty^* W^* G^*)(M^*M)(I - GWK_\infty) \end{aligned} \tag{2.6}$$

(We consider only pre-compensator $W = W_1$ and post-compensator $W_2 = I$)

$$= \gamma^2 \begin{bmatrix} K_\infty \\ I \end{bmatrix}^* \begin{bmatrix} W & 0 \\ 0 & I \end{bmatrix}^* \begin{bmatrix} -G & I \end{bmatrix}^* (M^*M) \begin{bmatrix} -G & I \end{bmatrix} \begin{bmatrix} W & 0 \\ 0 & I \end{bmatrix} \begin{bmatrix} K_\infty \\ I \end{bmatrix}$$

$$\begin{aligned} &\Rightarrow \begin{bmatrix} K_\infty^* & I \end{bmatrix} \begin{bmatrix} K_\infty \\ I \end{bmatrix} \\ &\leq \begin{bmatrix} K_\infty \\ I \end{bmatrix}^* \left\{ \gamma^2 \begin{bmatrix} W & 0 \\ 0 & I \end{bmatrix}^* \begin{bmatrix} -G & I \end{bmatrix}^* (M^*M) \begin{bmatrix} -G & I \end{bmatrix} \begin{bmatrix} W & 0 \\ 0 & I \end{bmatrix} \right\} \begin{bmatrix} K_\infty \\ I \end{bmatrix} \end{aligned} \tag{2.7}$$

Let we define, $P = \gamma^2 \begin{bmatrix} W & 0 \\ 0 & I \end{bmatrix}^* \begin{bmatrix} -G & I \end{bmatrix}^* (M^*M) \begin{bmatrix} -G & I \end{bmatrix} \begin{bmatrix} W & 0 \\ 0 & I \end{bmatrix}$ and $Q = \begin{bmatrix} K_\infty \\ I \end{bmatrix} \in C^{2n\times n}$. Using SVD of Q, we have $Q = U\Sigma V^*$ where U and V are unitary matrices with $U \in C^{2n\times 2n}, \Sigma \in C^{2n\times n}, V \in C^{n\times n}$. Now from (2.7), we have

$$Q^*Q \leq Q^*PQ. \tag{2.8}$$

Replacing $Q = U\Sigma V^*$ in (2.8), we have

$$V\Sigma^*U^*U\Sigma V^* \leq V\Sigma^*U^*PU\Sigma V^*$$

$$\Rightarrow \Sigma^*\Sigma \leq \ \Sigma^*U^*PU\Sigma. \tag{2.9}$$

Since Q is with full rank, the structure of Σ can be defined as $\Sigma = \begin{bmatrix} \Sigma_1^{n\times n} \\ 0^{n\times n} \end{bmatrix}$ and replacing it in (2.9), we have

$$\begin{bmatrix} \Sigma_1^* & 0 \end{bmatrix} \begin{bmatrix} \Sigma_1 \\ 0 \end{bmatrix} \leq \begin{bmatrix} \Sigma_1^* & 0 \end{bmatrix} U^*PU \begin{bmatrix} \Sigma_1 \\ 0 \end{bmatrix}. \tag{2.10}$$

Since Σ_1 is non-singular, Σ_1^{-1} exists. Now, defining $U = \begin{bmatrix} U_1 & U_2 \end{bmatrix}$ and pre and post-multiplying (2.10) with Σ_1^{-1}, we have

$$I \leq U_1^*PU_1. \tag{2.11}$$

Remark 2.1: *From (2.10), it can be written as $U^*PU \geq I$. Since $UU^* = I$, we have $P \geq I$. This implies*

$$\underline{\sigma}(P) \geq 1$$

Using the expression for P, one can have the following relation.

$$\begin{aligned} & \underline{\sigma}\left(M \begin{bmatrix} -G & I \end{bmatrix} \begin{bmatrix} W & 0 \\ 0 & I \end{bmatrix} \right) \geq \gamma^{-1} \\ \Rightarrow \quad & \underline{\sigma}\left(\begin{bmatrix} -N & M \end{bmatrix} \right) \geq \gamma^{-1}. \end{aligned}$$

Since $NN^* + MM^* = I$, we have $\gamma \geq 1$ that does not conflict with the result of [65].

Hence, it is an alternative way by which one can prove that, the achieved γ is always grater or equal to one.

Remark 2.2: *In other way, from (2.11) we have*

$$\begin{aligned}\gamma^{-1} \leq \underline{\sigma}\left(M\begin{bmatrix} -G & I \end{bmatrix}\begin{bmatrix} W & 0 \\ 0 & I \end{bmatrix}U_1\right) &\leq \bar{\sigma}\left(M\begin{bmatrix} -G & I \end{bmatrix}\begin{bmatrix} W & 0 \\ 0 & I \end{bmatrix}\right)\underline{\sigma}(U_1) \\ &= \bar{\sigma}\left(\begin{bmatrix} -N & M \end{bmatrix}\right)\underline{\sigma}(U_1) = \underline{\sigma}(U_1).\end{aligned}$$

$$\Rightarrow \gamma^{-1} \leq \underline{\sigma}(U_1)$$

Since the columns of U_1 are the columns of unitary matrix U, $\underline{\sigma}(U_1) = 1$. Hence, $\gamma \geq 1$. Again simplifying this inequality, we have

$$\gamma^{-1} \leq \bar{\sigma}\left(M\begin{bmatrix} -G & I \end{bmatrix}\begin{bmatrix} W & 0 \\ 0 & I \end{bmatrix}\right) \leq \bar{\sigma}(M)\bar{\sigma}\left(\begin{bmatrix} -G & I \end{bmatrix}\right)\bar{\sigma}\left(\begin{bmatrix} W & 0 \\ 0 & I \end{bmatrix}\right)$$

Since, $\bar{\sigma}\left(\begin{bmatrix} -G & I \end{bmatrix}\right) = \sqrt{\lambda_{max}\left(I + GG^*\right)} = \sqrt{1 + \bar{\sigma}^2(G)}$ *and* $\bar{\sigma}(M) = \sqrt{\frac{1}{1+\underline{\sigma}^2(G_s)}}$ *(see [64] page 127), then*

$$\gamma^{-1} \leq \sqrt{\frac{1 + \bar{\sigma}^2(G)}{1 + \underline{\sigma}^2(G_S)}}\; max\left(\bar{\sigma}(W), 1\right)$$

$$\Rightarrow \gamma \geq \frac{1}{max\left(\bar{\sigma}(W), 1\right)}\sqrt{\frac{1 + \underline{\sigma}^2(G_S)}{1 + \bar{\sigma}^2(G)}}$$

It can be seen clearly from the above expression how shaped plant and maximum singular value of W influence the robust stability margin of the closed-loop system.

Now, the equivalent four-block structure of H_∞ loop shaping control will be presented. Only for this section, the NRCF of G_S is considered to compare and elaborate the results of [42]. Note that, without loss of generality, similar type of results can also be obtained in NLCF framework.

From Figure 2.6, we have

$$z = -M_r^{-1}(I - K_\infty G_s)^{-1}\begin{bmatrix} -K_\infty & I \end{bmatrix}\begin{bmatrix} w_1 \\ w_2 \end{bmatrix}$$

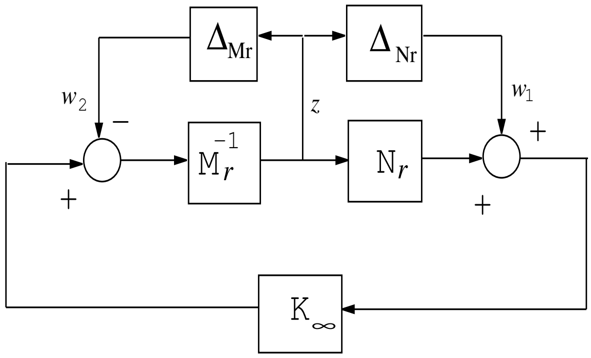

Figure 2.6: Robust stabilization problem in normalized right coprime factorization framework

where $G_S = N_r M_r^{-1}$. It also satisfies $\begin{bmatrix} -M_r^* & -N_r^* \end{bmatrix} \begin{bmatrix} -M_r \\ -N_r \end{bmatrix} = \begin{bmatrix} M_r^* & N_r^* \end{bmatrix} \begin{bmatrix} M_r \\ N_r \end{bmatrix} = I$. We assume that the number of outputs is greater than equal to the number of inputs of the shaped plant (this assumption is also considered in [42]). In robust stabilization framework, a stabilizing controller K_∞ is designed to minimize

$$\|T_{zw}\|_\infty = \left\| -M_r^{-1}(I - K_\infty G_s)^{-1} \begin{bmatrix} -K_\infty & I \end{bmatrix} \right\|_\infty . \tag{2.12}$$

Equivalently, without changing the ∞-norm of (2.12), we can rewrite

$$\begin{aligned} \|T_{zw}\|_\infty &= \left\| \begin{bmatrix} -M_r^* & -N_r^* \end{bmatrix} \begin{bmatrix} -M_r \\ -N_r \end{bmatrix} \left(-M_r^{-1}(I - K_\infty G_s)^{-1} \begin{bmatrix} -K_\infty & I \end{bmatrix} \right) \right\|_\infty \\ &= \left\| \begin{bmatrix} -M_r^* & -N_r^* \end{bmatrix} \right\|_\infty \left\| \begin{bmatrix} -M_r \\ -N_r \end{bmatrix} \left(-M_r^{-1}(I - K_\infty G_s)^{-1} \begin{bmatrix} -K_\infty & I \end{bmatrix} \right) \right\|_\infty \\ &= \left\| \begin{bmatrix} -M_r \\ -N_r \end{bmatrix} \left(-M_r^{-1}(I - K_\infty G_s)^{-1} \begin{bmatrix} -K_\infty & I \end{bmatrix} \right) \right\|_\infty \\ &= \left\| \begin{bmatrix} I \\ G_s \end{bmatrix} (I - K_\infty G_s)^{-1} \begin{bmatrix} -K_\infty & I \end{bmatrix} \right\|_\infty . \end{aligned} \tag{2.13}$$

Similarly, without loss of generality (2.12) can be rewritten as

$$\|T_{zw}\|_\infty = \left\| \begin{bmatrix} -N_r^* & -M_r^* \end{bmatrix} \begin{bmatrix} -N_r \\ -M_r \end{bmatrix} \left(-M_r^{-1}(I - K_\infty G_s)^{-1} \begin{bmatrix} -K_\infty & I \end{bmatrix} \right) \right\|_\infty$$

$$
\begin{aligned}
&= \left\| \begin{bmatrix} -N_r^* & -M_r^* \end{bmatrix} \right\|_\infty \left\| \begin{bmatrix} -N_r \\ -M_r \end{bmatrix} \left(-M_r^{-1}(I - K_\infty G_s)^{-1} \begin{bmatrix} -K_\infty & I \end{bmatrix} \right) \right\|_\infty \\
&= \left\| \begin{bmatrix} -N_r \\ -M_r \end{bmatrix} \left(-M_r^{-1}(I - K_\infty G_s)^{-1} \begin{bmatrix} -K_\infty & I \end{bmatrix} \right) \right\|_\infty \\
&= \left\| \begin{bmatrix} G_s \\ I \end{bmatrix} (I - K_\infty G_s)^{-1} \begin{bmatrix} -K_\infty & I \end{bmatrix} \right\|_\infty . \qquad (2.14)
\end{aligned}
$$

Remark 2.3: *The transfer function matrices shown in (2.13) and (2.14) are in four-block structure. If the objective signal vector is considered as* $\begin{bmatrix} z_2^T & z_1^T \end{bmatrix}^T$ *and exogenous signal vector as* $\begin{bmatrix} w_2^T & w_1^T \end{bmatrix}^T$*, two different design structures are then obtained that yield different types of uncertainty structure of the system.*

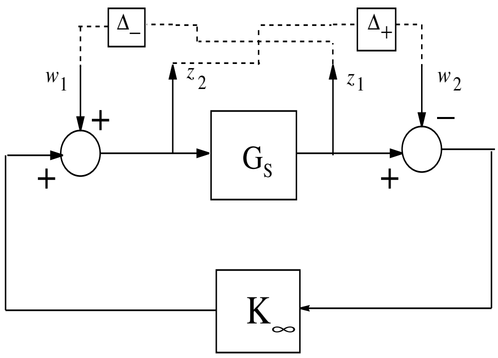

Figure 2.7: Additive and feedback type uncertainty structure

Figures 2.7 and 2.8 are related to (2.13) and (2.14) respectively. Both of these two structures, interestingly, belong to a general class of uncertainty structure which is mentioned in [42]. The general perturbation structure of the shaped plant is

$$G_{S\Delta} = ((I - \Delta_\times)G_S - \Delta_+)\,(I - \Delta_- G_S - \Delta_\div)^{-1} .$$

When $\Delta_\div$ and $\Delta_\times$ become zero, the uncertainty structure is like Figure 2.7 and similarly, the structure becomes as shown in Figure 2.8, when Δ_- and Δ_+ are zero.

Remark 2.4: *In [42], two equivalent sets of perturbed plants have been addressed corresponding to uncertainty structure shown in Figures 2.6 and 2.8. Similarly, a different*

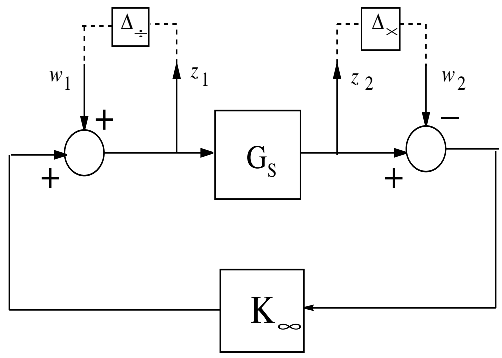

Figure 2.8: Output multiplicative and input inverse multiplicative uncertainty structure

set of perturbed plant has been developed as shown in Figure 2.7 which is equivalent to the above two sets (see Figures 2.6 and 2.8)

2.5 A method for weight selection

In this section, a method has been proposed to select a pre-compensator for solving H_∞ loop shaping control by considering the work of [1]. The post-compensator is assumed as an identity matrix with proper dimension. In Procedure 1, a simple and effective method is proposed in comparison with the simultaneous optimization technique discussed in [55]. In Procedure 2, an effort has been made to minimize the condition number of the pre-compensator that in turn, effectively reduces loop deterioration in presence of controller. Before describing the method, we need to represent a relation between a matrix A and its perturbed form $\bar{A}$ that will help to calculate the variation to be introduced in a nominal plant in order to shape the desired singular values of any closed-loop system. This idea has been utilized in the proposed algorithms.

Lemma 2.1 [1]: *Let $A, \bar{A} \in \boldsymbol{C}^{n\times n}$ and $\bar{A}$ is defined as*

$$\bar{A} = A\left(I + \Psi\right), \tag{2.15}$$

where $\Psi = V\Phi V^*$. $V = [v_1, v_2, \ldots, v_n]$ and $U = [u_1, u_2, \ldots, u_n]$ are two unitary matrices whose columns are respectively the eigenvectors of A^*A and $\bar{A}^*\bar{A}$. Then, $u_k = V\gamma_k$ provided γ_k is the k^{th} column eigenvector of Z^*Z, where Z is defined as $\left(D_\sigma\right)^{\frac{1}{2}}\left(I + \Phi\right)$, $\Phi \in \boldsymbol{C}^{n\times n}$ and $D_\sigma = diag\left(\sigma_n^2\left(A\right)\right) = V^*A^*AV$.

The proof of this lemma is given in [1]. Now, in order to select a pre-compensator that shapes the singular values of the open-loop plant based on design specifications, the frequency-by-frequency calculation has been performed and at each frequency, the TFM becomes a complex matrix. We consider, $G(j\omega)$ and $G_d(j\omega)$ are the two matrices at frequency ω which are respectively obtained from the nominal and desired shaped plant. These two plants are with same dimension. Here, G_d is a known TFM and it is chosen based on closed-loop design specification. In the following steps, dependence on $j\omega$ is omitted for simplicity of the notation.

Procedure 1

Using (2.15), the following relation can be formed at each frequency:

$$G_d = G\left(I + V\Phi V^*\right) = GV(I+\Phi)V^* = GW_1, \tag{2.16}$$

where Φ is unknown matrix and V is formed with the eigenvectors of G^*G such that $V^*G^*GV = D_\sigma = \text{diag}\left(\sigma_n^2(G)\right)$. It is assumed that G^*G has no eigenvalue at origin for all frequencies, hence, D_σ^{-1} exists. Now, simplifying (2.16), we have

$$\Phi = \left(D_\sigma^{-1}\right)(GV)^*\left(G_d - G\right)V, \tag{2.17}$$

where the pre-compensator matrix is $(I + V\Phi V^*)$. Since, G and G_d are known, V and Φ can be easily calculated at each frequency. Within the selected frequency range, each element of $(I + V\Phi V^*)$ is plotted and a stable, minimum-phase transfer function is fitted to each plot. The selection of W_1 is such that $G_S = GW_1$ contains no hidden modes.

Algorithm 1

Assumption: For all frequencies, $G^*(j\omega)\,G(j\omega)$ has no eigenvalue at origin.
Inputs: Nominal TFM $G(s)$ and the desired shaped plant $G_d(s)$.

Algorithmic steps:

1. Select the frequency range in which the shaping of singular values is mostly desired. Grid the frequency range.

2. At each frequency grid, compute $G(j\omega), V(j\omega), G_d(j\omega), D_\sigma(j\omega)$.

3. Compute Φ and $(I + V\Phi V^*)$, and store the data.

4. Plot each element of $(I + V\Phi V^*)$ with frequency. Fit each element of TFM with a stable, minimum-phase transfer function.

5. Perform co-spectral factorization to obtain stable, minimum phase pre-compensator.

Remark 2.5: *The perturbation Φ is not general, however, depends not only on G but also on G_d. The assumption for this algorithm is more conservative. However, the direct inversion of nominal plant G in (2.16) has been avoided by following the procedure as discussed above.*

Now, a different design technique is proposed to select a pre-compensator for solving H_∞ loop shaping control problem. In this procedure, the condition number minimization constraint is taken into account and finally, the proposed design method is formulated in LMI framework.

Procedure 2

Let $\alpha(s)$ and $\beta(s)$ are the two SISO transfer functions indicating the upper and lower bounds of the selected region for loop shape. At any frequency ω, $|\beta(j\omega)| \leq \sigma\left(G_S(j\omega)\right) \leq |\alpha(j\omega)|$, then, it can be written as

$$|\beta(j\omega)|^2 I \leq G_S^*(j\omega) G_S(j\omega) \leq |\alpha(j\omega)|^2 I \tag{2.18}$$

where, I is the identity matrix with proper dimension. For simplicity, $j\omega$ is henceforth omitted. Applying (2.16), the inequality (2.18) can be written as

$$|\beta|^2 I \leq V X^* V^* G^* G V X V^* \leq |\alpha|^2 I \tag{2.19}$$

where $X = I + \Phi$. Since, $\underline{\sigma}\left(G_S\right) > 0$, X is a non-singular matrix. Now, defining $F = V^* G^* G V$, (2.19) can be simplified as

$$\begin{aligned} |\beta|^2 \left(X X^*\right)^{-1} \leq F \leq |\alpha|^2 \left(X X^*\right)^{-1} \\ \Rightarrow |\beta|^2 I \leq F Q \leq |\alpha|^2 I \end{aligned} \tag{2.20}$$

where $Q = X X^*$.

Since, $F > 0$, (G^*G has no eigen value at origin) F^{-1} exists and it is obvious that

$$\underline{\sigma}\left(F^{-1}\right) I \leq F^{-1} \leq \bar{\sigma}\left(F^{-1}\right) I. \tag{2.21}$$

From (2.20) it can be written as

$$|\beta|^2 F^{-1} \leq Q \leq |\alpha|^2 F^{-1}.$$

Hence from (2.21),

$$|\beta|^2 \underline{\sigma}\left(F^{-1}\right) I \leq Q \leq |\alpha|^2 \bar{\sigma}\left(F^{-1}\right) I. \tag{2.22}$$

Let, $k = |\beta|^2 \underline{\sigma}\left(F^{-1}\right),\ k > 0$. Then (2.22) can be written as

$$|\beta|^2 \underline{\sigma}\left(F^{-1}\right) I \leq Q \leq \frac{|\alpha|^2 \bar{\sigma}\left(F^{-1}\right)}{|\beta|^2 \underline{\sigma}\left(F^{-1}\right)} |\beta|^2 \underline{\sigma}\left(F^{-1}\right) I. \tag{2.23}$$

Let, c is a number where $c \geq 1$ and also $c^2 \geq \frac{|\alpha|^2 \bar{\sigma}\left(F^{-1}\right)}{|\beta|^2 \underline{\sigma}\left(F^{-1}\right)}$, then (2.23) can be written as

$$kI \leq Q \leq c^2 kI. \tag{2.24}$$

Corollary 2.1: *At each frequency, a pre-compensator matrix W_1 has to be selected such that the singular values of GW_1 will lie in between $|\alpha|$ and $|\beta|$. If W_1 is formed as VXV^* from (2.16) where X is defined as $X = I + \Phi$, then $Q = XX^*$ can be obtained by solving the minimization problem:*
Minimize c^2
Subject to

$$\begin{aligned} |\beta|^2 I \leq FQ &\leq |\alpha|^2 I \\ Q &> 0 \\ kI \leq Q &\leq c^2 kI \end{aligned} \tag{2.25}$$

where, c^2 is the condition number of Q.

This optimization problem is in the form of a generalized eigenvalue problem (GEVP) in LMI framework.

Algorithm 2

Assumption: For all frequencies, $G^*(j\omega)G(j\omega)$ has no eigenvalue at origin.

Inputs: Nominal plant TFM $G(s)$ and two SISO transfer functions $\alpha(s)$ and $\beta(s)$.

Algorithmic steps:

1. Select the frequency range $[\omega_l, \quad \omega_h]$ in which the singular values of the nominal plant will be shaped. Grid the frequency range. The dense frequency grid will give the better result.

2. At each frequency grid compute $V(j\omega)$, $G(j\omega)$ and $F(j\omega) = (G(j\omega)V(j\omega))^* \times(G(j\omega)V(j\omega))$.

3. Solve the optimization problem (2.25) and get the solution Q. From Q, calculate X. The pre-compensator matrix $W_1 = VXV^*$ and store the data.

4. Plot each element of W_1 with frequency. Fit with a stable, minimum-phase transfer function to each element of W_1.

5. Perform co-spectral factorization to obtain stable, minimum phase pre-compensator.

Remark 2.6: *The Algorithm 2 can be easily implemented in MATLAB environment using LMI toolbox. Although (2.25) comprises two non-strict inequalities, for finding solutions using LMI toolbox these two are assumed as strict inequalities. In both the algorithms, the MATLAB command 'fitmag' has been used to fit the data points with a stable, minimum phase transfer function. Interestingly, even though each element of TFM becomes stable and minimum phase, it does not yield that overall TFM becomes minimum phase. Hence, co-spectral factorization is required to achieve this objective [33].*

2.6 Numerical example

To demonstrate the effectiveness of the proposed method, an example has been illustrated in this section. The simplified mathematical model of high-purity distillation column is considered [66]. It is an ill-conditioned plant with strong cross-coupling. In H_∞ loop shaping framework, to shape singular values of the open-loop plant two different non-diagonal weights have been obtained using two different algorithms proposed in the preceding section. The plant model is given below [66].

$$G(s) = \frac{e^{-\tau s}}{1+75s} \begin{bmatrix} 0.878 & 0.864 \\ 1.082 & 1.096 \end{bmatrix} \begin{bmatrix} k_1 & 0 \\ 0 & k_2 \end{bmatrix}$$

where,

$$0.8 \leq k_1 \leq 1.2$$
$$0.8 \leq k_2 \leq 1.2$$
$$0 \leq \tau \leq 1.$$

The nominal plant model is assumed using the mid values of k_1, k_2 and $\tau = 1$. The outputs of the plant are top composition and bottom composition and the inputs are reflux and boilup [66]. The time delay is simplified with a first order Padé approximation that introduces a zero to RHS of s-plane at 2 rad/min. This RHS zero restricts the closed loop bandwidth.

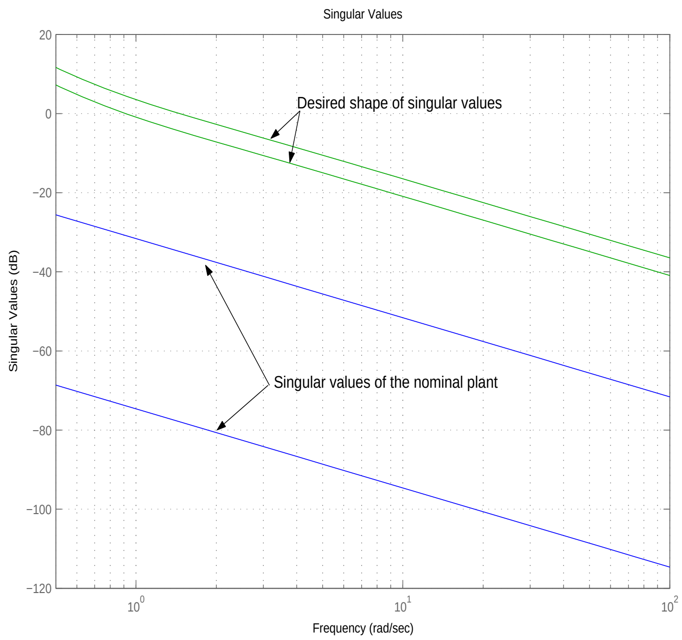

Figure 2.9: Singular values of the nominal plant and desired shape of singular values

In Figure 2.9, singular values of the nominal plant have been shown and its condition number is 142 at all frequencies. As mentioned in [48], the performance specifications are taken as follows: output should reach to 90% of its steady-state value within 30 minutes while the corresponding input channel of the system is excited with a step input, and the effect of cross-coupling on the other output channel should be less than 50% of steady state value of first output channel after the above specified time. To meet closed-loop design specifications, singular values are increased in both the high and low frequency regions, and a TFM is chosen as

$$G_d(s) = \begin{bmatrix} \frac{1.5(s+0.8)^2}{s^2(s+1.3)} & 0 \\ 0 & \frac{0.9(s+0.8)^2}{s^2(s+1.3)} \end{bmatrix}$$

for desired shape of singular values which are shown in Figure 2.9. The desired shape indicates boundaries of the loop shaping region, that is, all singular values of the shaped plant should lie in this region. Now, to shape singular values of the open-loop plant the proposed two algorithms have been adopted.

Since it is a two-input-two-output system, the TFM selected for desired shape has two SISO transfer functions at diagonal position whose gain plots indicate the desired shape of singular values. This selection is done on trial and error basis. For Algorithm 2, same transfer functions have been used to indicate the boundaries of the desired loop shape. Applying both the algorithms, frequency-by-frequency data points have been stored and the corresponding gain vs. frequency plots are shown in Figures 2.10-2.13. Then, each plot is fitted with a stable, minimum-phase transfer function and for fitting, the MATLAB command 'fitmag' has been used. Note that, the obtained TFM may or may not be minimum phase and to get a stable, minimum phase TFM, co-spectral factorization is performed. The corresponding designed pre-compensator TFM $W_1 = \begin{bmatrix} W_{11} & W_{12} \\ W_{21} & W_{22} \end{bmatrix}$ is as follows:

From Algorithm 1

$$W_{11}(s) = \frac{\begin{array}{c} 3546(s^9 + 3.9932s^8 + 6.2042s^7 + 5.0508s^6 + 2.5169s^5 + 0.8821s^4 + 0.2304s^3 \\ +0.0431s^2 + 0.0055s + 0.00047) \end{array}}{s^9 + 3.862s^8 + 5.429s^7 + 3.88s^6 + 1.761s^5 + 0.5826s^4 + 0.1496s^3 + 0.0246s^2 + 0.003s + 0.000194}$$

$$W_{12}(s) = \frac{\begin{array}{c} -3483(s^9 + 3.9831s^8 + 6.1843s^7 + 5.0148s^6 + 2.4924s^5 + 0.8653s^4 + 0.2150s^3 \\ +0.0413s^2 + 0.0053s + 0.000426) \end{array}}{s^9 + 3.862s^8 + 5.429s^7 + 3.88s^6 + 1.761s^5 + 0.5826s^4 + 0.1496s^3 + 0.0246s^2 + 0.003s + 0.000194}$$

$$W_{21}(s) = \frac{\begin{array}{c} -3483(s^{12} + 48.033s^{11} + 681.59s^{10} + 3465s^9 + 8530s^8 + 11438s^7 + 8753.9s^6 + 4005.2s^5 \\ +1203.6s^4 + 287.1088s^3 + 41.7456s^2 + 4.8952s + 0.1931) \end{array}}{\begin{array}{c} s^{12} + 47.93s^{11} + 675.7s^{10} + 3374s^9 + 7992s^8 + 9969s^7 + 6769s^6 + 2723s^5 + 820.6s^4 + 175.4s^3 \\ +26.05s^2 + 2.727s + 0.1059 \end{array}}$$

$$W_{22}(s) = \frac{\begin{array}{c} 3497(s^{12} + 48.0412s^{11} + 681.7272s^{10} + 3468.7s^9 + 8553s^8 + 11507s^7 + 8841.9s^6 \\ +4083.5s^5 + 1257.1s^4 + 304.55s^3 + 47.6122s^2 + 5.7707s + 0.3452) \end{array}}{\begin{array}{c} s^{12} + 47.93s^{11} + 675.7s^{10} + 3374s^9 + 7992s^8 + 9969s^7 + 6769s^6 + 2723s^5 + 820.6s^4 + 175.4s^3 \\ +26.05s^2 + 2.727s + 0.1059 \end{array}}$$

From Algorithm 2

$$W_{11}(s) = \frac{2454(s^8+3.2559s^7+4.0212s^6+2.4943s^5+0.9478s^4+0.2756s^3+0.0533s^2+0.0075s+0.00064)}{s^8+3.127s^7+3.405s^6+1.749s^5+0.6497s^4+0.1709s^3+0.03134s^2+0.0042s+0.00029}$$
$$W_{12}(s) = \frac{-2400(s^8+3.2517s^7+3.9996s^6+2.4733s^5+0.9313s^4+0.2699s^3+0.0517s^2+0.0071s+0.00062)}{s^8+3.127s^7+3.405s^6+1.749s^5+0.6497s^4+0.1709s^3+0.03134s^2+0.0042s+0.00029}$$
$$W_{21}(s) = \frac{-2400(s^8+3.2513s^7+4.0192s^6+2.5021s^5+0.9592s^4+0.2806s^3+0.0545s^2+0.0075s+0.00064)}{s^8+3.128s^7+3.421s^6+1.782s^5+0.6706s^4+0.1793s^3+0.0331s^2+0.0044s+0.0003}$$
$$W_{22}(s) = \frac{2448(s^8+3.2578s^7+4.0339s^6+2.5364s^5+0.9759s^4+0.2904s^3+0.0565s^2+0.0081s+0.0007)}{s^8+3.128s^7+3.421s^6+1.782s^5+0.6706s^4+0.1793s^3+0.0331s^2+0.0044s+0.0003}$$

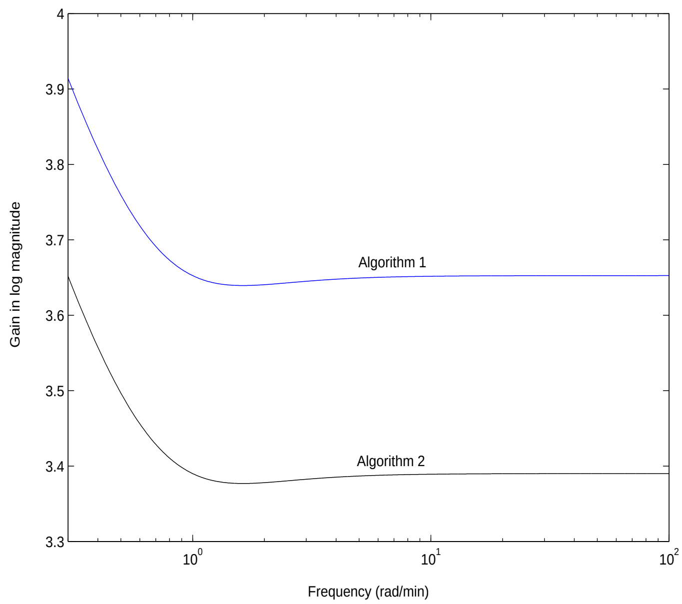

Figure 2.10: Frequency vs. gain plot for W_{11}

In Figures 2.14-2.15, the singular values of the shaped plant have been shown. The dashed lines indicate the boundaries of desired shape, and both the algorithms give satisfactory result. In Figure 2.14, at low frequency region the lower singular value of the shaped plant comes out from the desired boundary, it occurs due to error in data point selection for transfer function fitting.

The condition number of the designed pre-compensator has been shown in Figure 2.16 for both the algorithms. In Algorithm 2, the condition number has been improved significantly. Figures 2.17-2.18 show the closed loop responses for a unit step input (either in input channel-1 or in input channel-2). Due to the condition number minimization in Algorithm 2, the loop deterioration is less compared to Algorithm 1 which

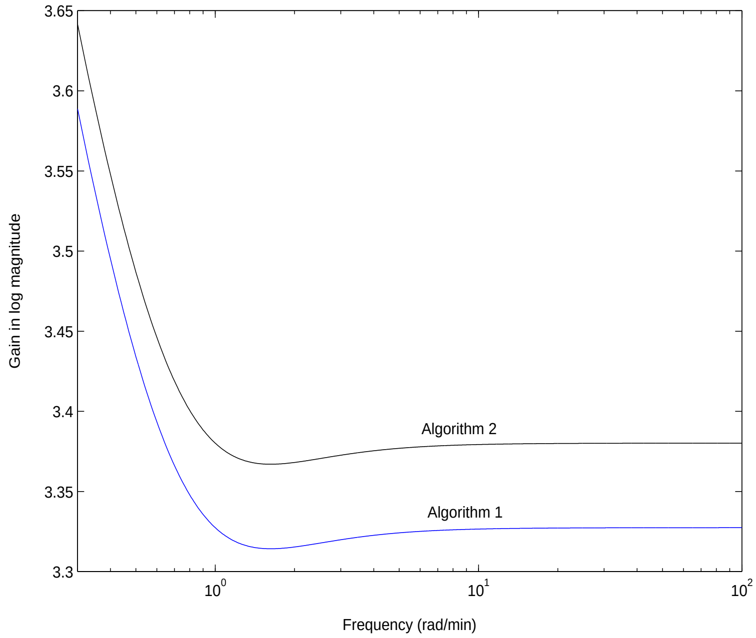

Figure 2.11: Frequency vs. gain plot for W_{12}

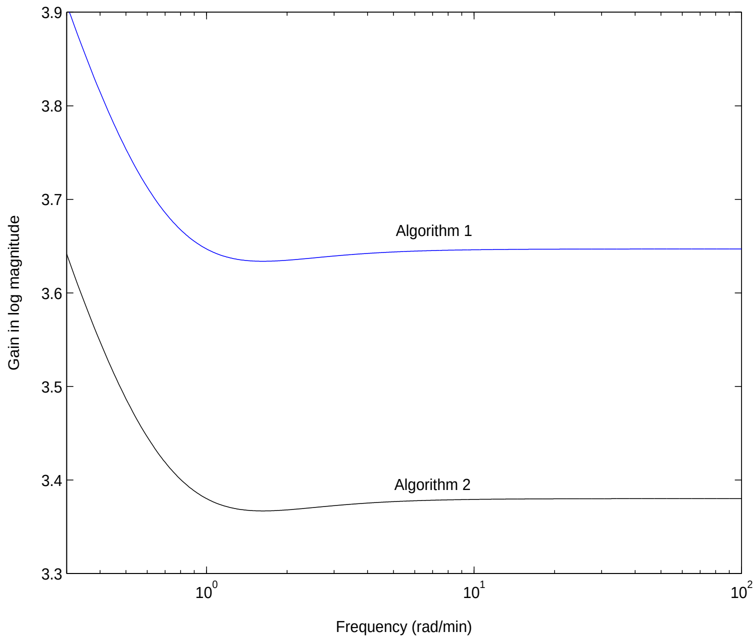

Figure 2.12: Frequency vs. gain plot for W_{21}

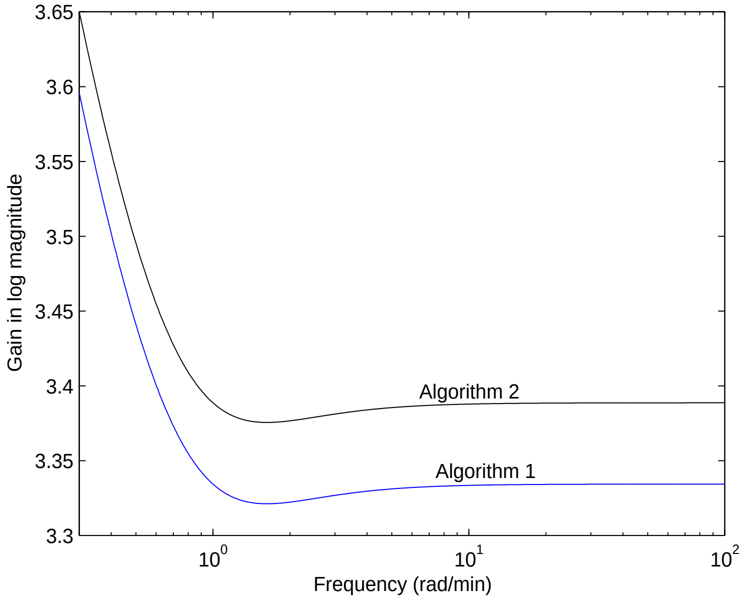

Figure 2.13: Frequency vs. gain plot for W_{22}

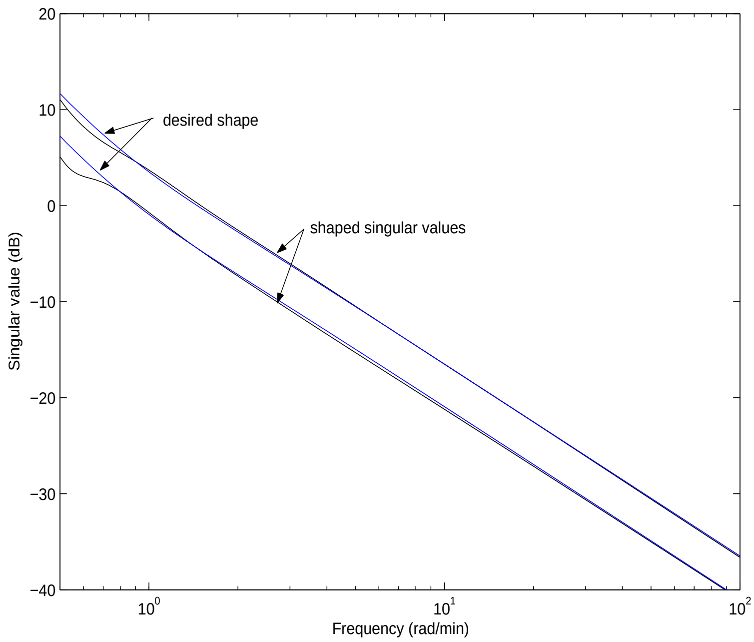

Figure 2.14: Singular values of the shaped plant from Algorithm 1

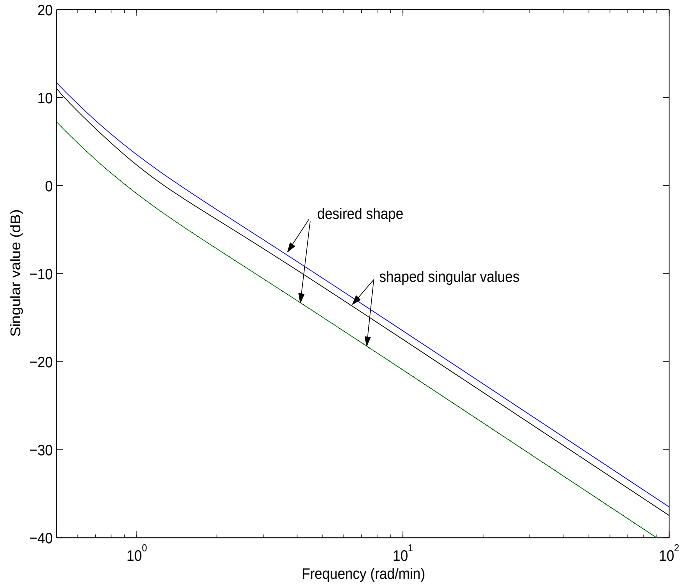

Figure 2.15: Singular values of the shaped plant from Algorithm 2

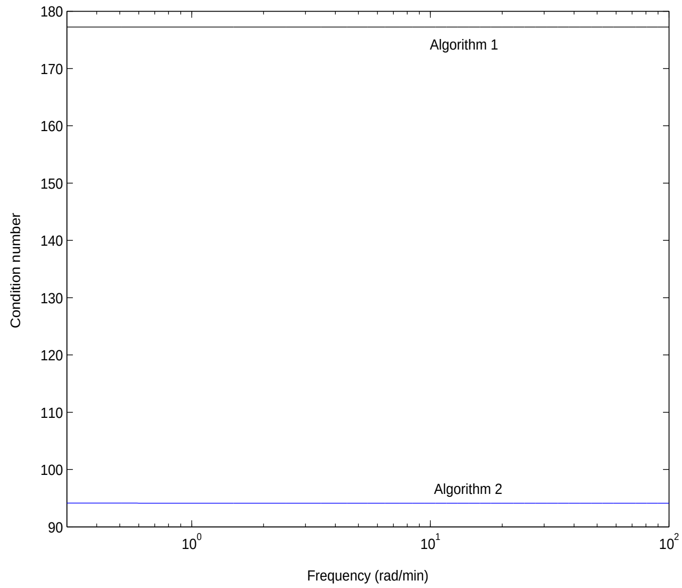

Figure 2.16: Condition number of the pre-compensator

has been shown in Figure 2.19. The calculated γ_{min} values (inverse of robust stability margin) are obtained respectively 3.6377 and 3.1922 from Algorithms 1 and 2. This clearly indicates that the condition number minimization of pre-compensator weighting function in LMI framework results better trade-off between performance and robustness.

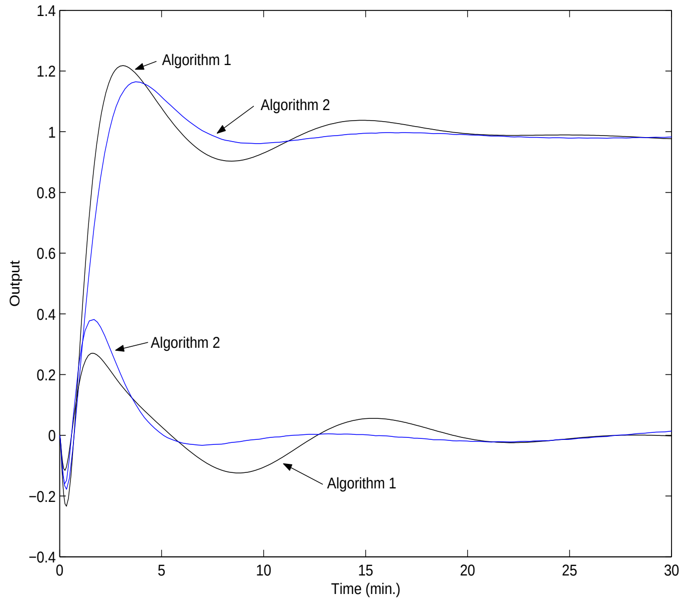

Figure 2.17: Step response due to input in channel-1

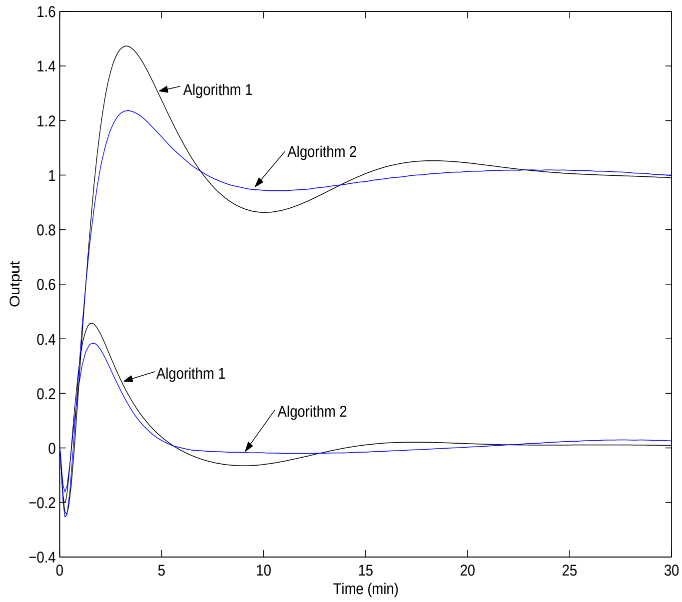

Figure 2.18: Step response due to input in channel-2

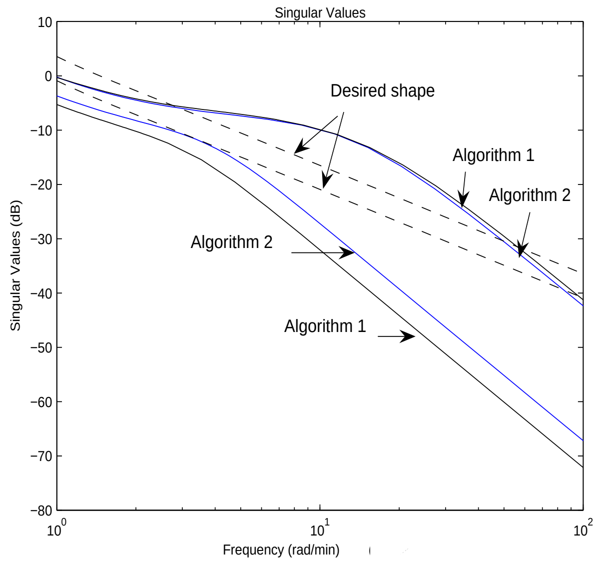

Figure 2.19: Loop deterioration after the inclusion of controller

2.7 Conclusions

In this chapter, a pre-compensator selection procedure has been proposed for H_∞ loop shaping control. The underlying theory of the method is different from the existing results and it gives an alternative and effective procedure. To select pre-compensator, two different algorithms have been introduced where Algorithm 2 leads to minimize the condition number of the pre-compensator in LMI framework. It is necessary to check whether the loop properties are significantly changed in presence of final controller $K = W_1 K_\infty$. If so, a better trade-off between performance and robustness can be achieved by adopting Algorithm 2 which is based on condition number minimization of pre-compensator weighting function. In numerical example, the simulation results obtained from two different algorithms have been presented in a comparative way and both of them give the satisfactory results.

CHAPTER 3

Parametric H_∞ loop shaping control

Compared to McFarlane-Glover method discussed in preceding chapter, the parametric H_∞ loop shaping technique provides more flexible design framework and systemic weight selection procedure for the solution of mixed sensitivity H_∞ control problem [41]. In true sense, both the parametric and McFarlane-Glover H_∞ loop shaping methods ensure robust stability against normalized coprime factor uncertainty description of the shaped plant. The only difference is, parametric structure contains a known scalar parameter in the design framework. Unfortunately, for non-unity parameter the explicit formula proposed in McFarlane-Glover method is no longer applicable and an iterative algorithm is needed to find robust stability margin. In this chapter, a design framework has been proposed for synthesizing the parametric H_∞ loop shaping controller using LMI approach that circumvents the computational difficulty for finding robust stability margin ($\frac{1}{\gamma_{opt}}$). In the sequel, a correspondence has also been drawn with the existing Riccati equation based state-space approach of [41] and finally, the observer based structure of the controller has been realized. The effectiveness of the proposed parametric H_∞ loop shaping control strategy is discussed through simulation studies.

3.1 Introduction

As discussed in Chapter 2, the McFarlane-Glover H_∞ loop shaping method provides some advantageous design steps compared to general H_∞ synthesis problem [26, 65]. In this method, the explicit formula for robust stability margin reduces design efforts and advances the technique one step ahead in robust control theory due to a general unstructured uncertainty description of the system. Later in [41], a more general framework for H_∞ loop shaping control has been proposed. In this structure, a free parameter λ appears in performance index that, in turn, gives a compromise in between the sensitivity and complementary sensitivity transfer functions of the closed-loop system. Unfortunately, this introduced parameter invites some complexities in numerical computations. Most importantly, for non-unit value of this parameter an iterative algorithm is needed to calculate the optimal value of γ and it hampers the main advantage of the loop shaping method. In this chapter, a design platform has been addressed in LMI framework that reduces computation burden for finding the robust stability margin and provides a framework alternative to state-space Riccati equation based approach.

The necessary and sufficient conditions for the existence of parametric H_∞ loop shaping controller have been derived in [41] where the solutions are obtained in state-space framework. The existence of the stabilizing solutions of two AREs indicates the existence of parametric controller. However, interestingly it has been shown that the solution of control ARE is enough to ensure the controller existence whereas the other ARE always gives a stabilizing solution zero and jointly satisfies the γ constraint for H_∞ synthesis. Further in [41], exploiting the disturbance feedforward structure [1] of the generalized plant the observer-based controller has been realized and the problem is posed in state-feedback structure.

On the other hand, the LMI approach leads a remarkably simplified H_∞ controller design [36, 49]. This technique provides a design platform where the number of assumptions is reduced, the robust stability margin is found out by solving a minimization problem and the existing conditions for stabilizing controller are characterized by two symmetric positive-definite matrices. These two matrices are the stabilizing solutions of two ARIs

[1] The generalized plant

$$P = \left[\begin{array}{c|c|c} A & B_1 & B_2 \\ \hline C_1 & 0 & D_{12} \\ \hline C_2 & I & 0 \end{array}\right]$$

is in disturbance feedforward (DF) structure. It has a relationship with the full information (FI) problem. For DF problem, an additional assumption is imposed that is, $A - B_1C_2$ is stable. For detail, see ([114] page-431).

[36, 49]. In [60], a correspondence has been shown between ARIs and AREs, and subsequently for comparison the Doyle-Glover-Khargonekar-Francis (DGKF) method [26], Doyle-Glover method [38] and LMI approach [36, 49] are presented in single platform.

In this chapter, an effort has been made to reformulate the parametric H_∞ loop shaping design problem in LMI framework that in turn, explores a new set of solvability conditions for stabilizing controller and gives an easy way for finding robust stability margin using available LMI solver. The existence conditions for parametric H_∞ loop shaping controller have been characterized by positive definite solutions of two ARIs that correspond to Riccati equation based state-space approach and finally, an observer based structure of the controller has been realized.

The rest of the chapter is organized as follows: The difference between McFarlane-Glover method and parametric H_∞ loop shaping control problem has been discussed in Section 3.2. In Section 3.3, the state-space solutions of the parametric H_∞ loop shaping design problem are presented along with observer-based controller structure and subsequently, the LMI approach is introduced leading to find the solvability conditions of the stabilizing controller. In Section 3.4, a correspondence between ARIs and AREs has been established and in Section 3.5, the observer-based controller structure is realized in LMI approach. A numerical example has been illustrated in Section 3.6 to show the usefulness of the proposed technique and in Section 3.7, the concluding remarks are drawn.

3.2 Parametric H_∞ loop shaping control

Before introducing the parametric H_∞ loop shaping design framework, first in this section, the McFarlane-Glover H_∞ loop shaping method has been described in its state-space form. Referred to Figure 2.2 in Chapter 2, G is the nominal plant, post and pre-compensators are W_2 and W_1, from where the shaped plant $G_S = W_2 G W_1$ is obtained [65]. If the minimal state-space realization of G_S is $\left[\begin{array}{c|c} A & B \\ \hline C & 0 \end{array}\right]$, the state-space realization of the normalized left coprime factors becomes

$$\left[\begin{array}{cc} N & M \end{array}\right] = \left[\begin{array}{c|cc} A + LC & B & L \\ \hline C & 0 & I \end{array}\right], \tag{3.1}$$

where $L = -YC^T$ and $Y = Y^T \geq 0$ is the stabilizing solution of the following Riccati equation

$$AY + YA^T - YC^TCY + BB^T = 0. \tag{3.2}$$

Based on G_S, a controller K_∞ is designed to ensure the internal stability of the closed-loop system for a set of plant $G_p = (M+\Delta_M)^{-1}(N+\Delta_N)$ by minimizing the performance index

$$\|T_{zw}\|_\infty = \left\| \begin{bmatrix} I \\ K_\infty \end{bmatrix} (I - G_S K_\infty)^{-1} M^{-1} \right\|_\infty . \tag{3.3}$$

Here, the performance index is the infinity norm of the transfer function matrix between w (exogenous signal) to z (objective signal[2]) and the design method is known as McFarlane-Glover H_∞ loop shaping method [65]. In parametric H_∞ loop shaping control, the performance index is modified as

$$\|T_{zw}\|_\infty = \left\| \begin{bmatrix} I \\ \lambda K_\infty \end{bmatrix} (I - G_S K_\infty)^{-1} M^{-1} \right\|_\infty \tag{3.4}$$

where, λ is a free scalar parameter [41]. The block-diagram for robust stabilization problem corresponding to (3.4) has been shown in Figure 3.1 with the normalized left coprime factor uncertainty description of the shaped plant.

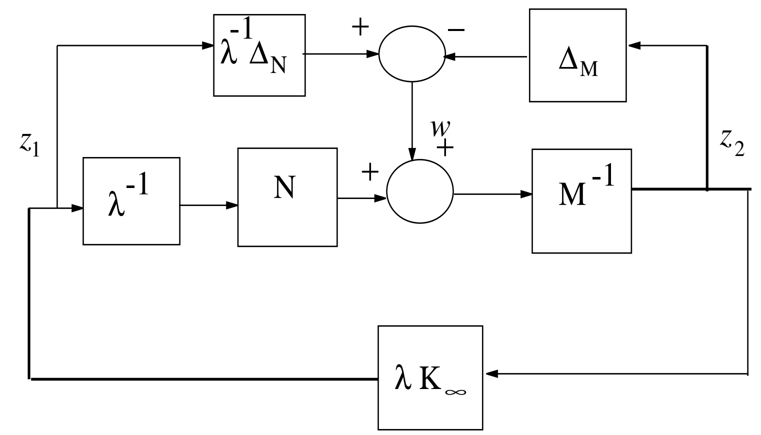

Figure 3.1: Robust stabilization problem in parametric H_∞ loop shaping framework [41]

[2]Here, z is considered as $\begin{bmatrix} z_2^T & z_1^T \end{bmatrix}^T$. Whereas in Section 2.2 of Chapter 2, the objective signal vector was taken as $\begin{bmatrix} z_1^T & z_2^T \end{bmatrix}^T$ and it does not violate any generality of the problem.

Here, λ is a scalar quantity and it does not alter the state-space realization of the normalized coprime factors of the shaped plant as obtained in McFarlane-Glover method. However, it only scales the input matrix of the generalized plant. It means, the parametric H_∞ loop shaping control problem can be posed into two different frameworks. If the parameter enters into the state-space realization of the shaped plant, equation (3.2) becomes parameter dependent and for different values of λ, different normalized coprime factors will be obtained. In other way, if the shaped plant is kept parameter invariant, the normalized left coprime factors can be obtained by using (3.1-3.2). Where λ only scales input of the N block and for a given value of λ, the controller λK_∞ is designed to ensure the stability margin $\left\| \begin{bmatrix} \lambda^{-1}\Delta_N & \Delta_M \end{bmatrix} \right\|_\infty \leq \frac{1}{\gamma}$. When $\lambda = 1$, the parametric loop shaping control problem is similar to McFarlane-Glover method.

From Figure 3.1, the generalized plant is obtained as

$$P_p = \left[\begin{array}{c|c|c} A & -L & \frac{B}{\lambda} \\ \hline C & I & 0 \\ 0 & 0 & I \\ \hline C & I & 0 \end{array} \right] \tag{3.5}$$

Throughout this chapter, it is assumed that $(A, \frac{B}{\lambda}, C)$ is a stabilizable and detectable pair for all $\lambda > 0$. Using the Doyle-Glover method [38], the solvability conditions are derived in [41] and due to disturbance feed-forward structure of the generalized plant, a controller with observer-based structure has been realized. In this chapter, the LMI approach has been applied on generalized plant (3.5) to find the solvability conditions for stabilizing controller and results are compared with the Riccati equation based state-space approach. Moreover, it also has been shown that the LMI technique gives the observer-based controller with similar structure that has been obtained in [41].

3.3 Solvability conditions

For the shaped plant G_S, we assume the number of inputs n_u is more than or equal to the number of outputs n_y and γ_{opt} is the minimum achievable norm of the performance index (3.4) for all stabilizable controllers [41]. We consider the dimension of w is n_w and since M is a square plant, $n_w = n_y$. In the following theorem, the solvability conditions have been stated in state-space form for the existence of a stabilizing controller. For completeness of our discussion, the proof of the theorem has also been discussed briefly.

Theorem 3.1 *[41]: There is a stabilizing controller $\lambda K_\infty(s)$ such that $\gamma_{opt} < \gamma$, if and only if, there exists a stabilizing solution $X_\infty \geq 0$ to the ARE*

$$(A-\phi LC)^T X_\infty + X_\infty(A-\phi LC) - X_\infty(\lambda^{-2}BB^T - \phi LL^T)X_\infty + \phi\gamma^2 C^T C = 0 \quad (3.6)$$

where, $\phi = (\gamma^2-1)^{-1}$. If X_∞ is a stabilizing solution of equation (3.6), the observer-based controller $K_\infty(s)$ becomes

$$K_\infty(s) = \left[\begin{array}{c|c} A+BF_\infty+LC & -L \\ \hline F_\infty & 0 \end{array}\right] \quad (3.7)$$

where, $F_\infty = -\lambda^{-2}B^T X_\infty$.

Proof: The proof of this theorem is straightforward and to find necessary and sufficient conditions for stabilizing controller, Doyle-Glover method has been adopted [38]. Considering the generalized plant P_p as given in (3.5), we have

$$\left.\begin{array}{c} A = A \in \Re^{n\times n},\ B_1 = -L \in \Re^{n\times n_w},\ B_2 = \lambda^{-1}B \in \Re^{n\times n_u}, \\ C_1 = \begin{bmatrix} C \\ 0^{n_u\times n} \end{bmatrix} \in \Re^{(n_w+n_u)\times n}, C_2 = C \in \Re^{n_w\times n}, \\ D_{11} = \begin{bmatrix} I_{n_w} \\ 0_{n_u\times n_w} \end{bmatrix} \in \Re^{(n_w+n_u)\times n_w}, D_{12} = \begin{bmatrix} 0_{n_w\times n_u} \\ I_{n_u} \end{bmatrix} \in \Re^{(n_w+n_u)\times n_u}, \\ D_{21} = I_{n_w} \in \Re^{n_w\times n_w},\ D_{22} = 0 \in \Re^{n_w\times n_u}. \end{array}\right\} \quad (3.8)$$

It satisfies all the required assumptions[3] for applying the Doyle-Glover method. The method states that, there is a stabilizing controller, if and only if, there exists two positive semi-definite solutions X_∞ and Y_∞ satisfying $\rho(X_\infty Y_\infty) \leq \gamma^2$ where, X_∞ and Y_∞ are respectively the two solutions of following algebraic Riccati equations. The AREs

[3]The assumptions are

1. (A, B_2) is stabilizable, (C_2, A) is detectable.
2. $rank(D_{12}) = n_u, rank(D_{21}) = n_w$.
3. $\begin{matrix} A - j\omega I & B_2 \\ C_1 & D_{12} \end{matrix}$ has full column rank for all $\omega \in \Re$.
4. $\begin{matrix} A - j\omega I & B_1 \\ C_2 & D_{21} \end{matrix}$ has full row rank for all $\omega \in \Re$.

are

$$\begin{aligned} X_\infty(A - B_r R^{-1} D_{1\cdot}^T C_1) + (A &- B_r R^{-1} D_{1\cdot}^T C_1)^T X_\infty - X_\infty B_r R^{-1} B_r^T X_\infty \\ &+ C_1^T (I - D_{1\cdot} R^{-1} D_{1\cdot}^T) C_1 = 0 \end{aligned} \tag{3.9}$$

$$\begin{aligned} Y_\infty(A - B_1 D_{\cdot 1}^T \tilde{R}^{-1} C_c)^T &+ (A - B_1 D_{\cdot 1}^T \tilde{R}^{-1} C_c) Y_\infty - Y_\infty C_c^T \tilde{R}^{-1} C_c T_\infty \\ &+ B_1 (I - D_{\cdot 1}^T \tilde{R}^{-1} D_{\cdot 1}) B_1^T = 0 \end{aligned} \tag{3.10}$$

where, $B_r = \begin{bmatrix} B_1 & B_2 \end{bmatrix}$, $C_c = \begin{bmatrix} C_1 \\ C_2 \end{bmatrix}$, $D_{1\cdot} = \begin{bmatrix} D_{11} & D_{12} \end{bmatrix}$, $D_{\cdot 1} = \begin{bmatrix} D_{11} \\ D_{21} \end{bmatrix}$, $D_{11} = \left[\begin{array}{c|c} D_{1111} & D_{1112} \\ \hline D_{1121} & D_{1122} \end{array}\right]$, $R = \left[\begin{array}{c|c} D_{11}^T D_{11} - \gamma^2 I & D_{11}^T D_{12} \\ \hline D_{12}^T D_{11} & D_{12}^T D_{12} \end{array}\right]$ and $\tilde{R} = \left[\begin{array}{c|c} D_{11} D_{11}^T - \gamma^2 I & D_{11} D_{21}^T \\ \hline D_{21} D_{11}^T & D_{21} D_{21}^T \end{array}\right]$.

Now using (3.8), we get

$$R = \begin{bmatrix} (1-\gamma^2)I & 0 \\ 0 & I \end{bmatrix}, \tilde{R} = \begin{bmatrix} (1-\gamma^2)I & 0 & I \\ 0 & -\gamma^2 I & 0 \\ I & 0 & I \end{bmatrix},$$

$$(A - B_r R^{-1} D_{1\cdot}^T C_1) = \left(A - \left(\gamma^2 - 1\right)^{-1} LC\right),$$

$$B_r R^{-1} B_r^T = \lambda^{-2} B B^T - (\gamma^2 - 1)^{-1} L L^T$$

and

$$C_1^T (I - D_{1\cdot} R^{-1} D_{1\cdot}^T) C_1 = \gamma^2 (\gamma^2 - 1)^{-1} C^T C.$$

Replacing these terms in (3.9) and (3.10), and after some algebraic simplification, the AREs become respectively as

$$\begin{aligned} X_\infty(A - (\gamma^2 - 1)^{-1} LC) &+ (A - (\gamma^2 - 1)^{-1} LC)^T X_\infty + \gamma^2 (\gamma^2 - 1)^{-1} C^T C \\ &- X_\infty (\lambda^{-2} B B^T - (\gamma^2 - 1)^{-1} L L^T) X_\infty = 0 \end{aligned} \tag{3.11}$$

and

$$(A + LC) Y_\infty + Y_\infty (A + LC)^T - Y_\infty C^T C Y_\infty = 0. \tag{3.12}$$

Since $(A + LC)$ is stable, $Y_\infty = 0$ is a stabilizing solution of (3.12). Therefore, if there exists a positive semi-definite stabilizing solution X_∞, it always satisfies the requirement

$\rho(X_\infty Y_\infty) \leq \gamma^2$ since $\gamma > 0$, and provides necessary and sufficient conditions for the existence of stabilizing controller.

Now, the controller will be found out when the stabilizing solutions X_∞ and Y_∞ exist. Using Doyle-Glover method [38], a controller K is obtained with the following structure:

$$K = \left[\begin{array}{c|c} A_c & B_c \\ \hline C_c & 0 \end{array}\right]$$

where,

$$A_c = (I - \gamma^{-2} Y_\infty X_\infty)^{-1} \left[(A + (L - Y_\infty C^T)C)(I - \gamma^{-2} Y_\infty X_\infty) - \lambda^{-2} B B^T X_\infty\right],$$

$$B_c = -(I - \gamma^{-2} Y_\infty X_\infty)^{-1}(L - Y_\infty C^T) \text{ and } C_c = -\lambda^{-1} B^T X_\infty.$$

If the controller state is x_c and measured output of the shaped plant is y, the state-space equations of the obtained controller become as follows:

$$\dot{x}_c = (I - \gamma^{-2} Y_\infty X_\infty)^{-1}[A(I - \gamma^{-2} Y_\infty X_\infty)x_c + (L - Y_\infty C^T)C(I - \gamma^{-2} Y_\infty X_\infty)x_c$$
$$-\lambda^{-2} B B^T X_\infty x_c - (L - Y_\infty C^T)y]$$
$$u = -\lambda^{-1} B^T X_\infty x_c.$$

Defining $(I - \gamma^{-2} Y_\infty X_\infty)x_c = x_t$, we have

$$\dot{x}_t = \left[A - \lambda^{-2} B B^T X_\infty (I - \gamma^{-2} Y_\infty X_\infty)^{-1}\right] x_t + (L - Y_\infty C^T)(C x_t - y)$$

and

$$u = -\lambda^{-1} B^T X_\infty (I - \gamma^{-2} Y_\infty X_\infty)^{-1} x_t.$$

This is a realization of the controller with observer-based structure. For $Y_\infty = 0$, it becomes

$$\left.\begin{array}{c} \dot{x}_t = (A + LC)x_t + B\left(-\lambda^{-2} B^T X_\infty\right) x_t - Ly \\ u = \lambda\left(-\lambda^{-2} B^T X_\infty\right) x_t \end{array}\right\}. \tag{3.13}$$

Now defining $F_\infty = -\lambda^{-2} B^T X_\infty$, (3.13) becomes

$$\left.\begin{array}{c} \dot{x}_t = (A + LC + BF_\infty)\, x_t - Ly \\ u = \lambda F_\infty x_t \end{array}\right\} \tag{3.14}$$

which is similar to (3.7) as (3.14) depicts the state-space realization for λK_∞. □

Remark 3.1: *In Theorem 3.1, the stabilizing controller is $\lambda K_\infty(s)$ and its corre-*

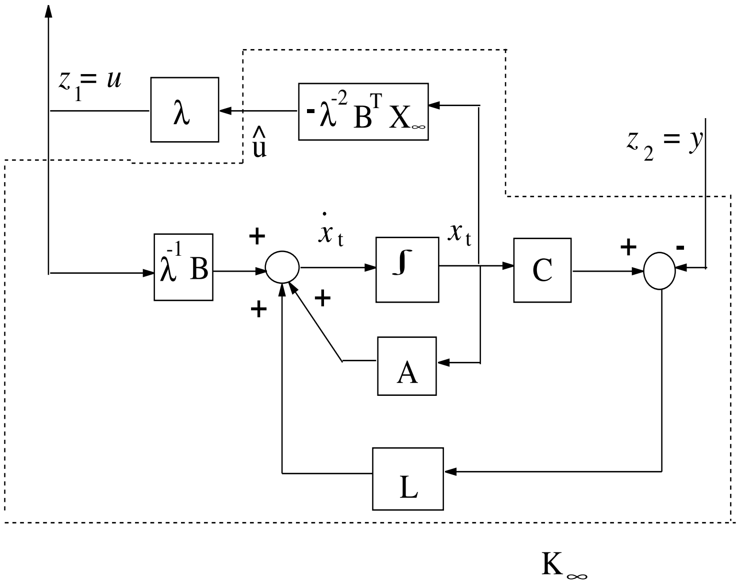

Figure 3.2: Observer-based parametric H_∞ loop shaping controller

sponding block-diagram has been shown in Figure 3.2. Note that, in final step when the parametric H_∞ loop shaping controller is formed by cascading $\lambda^{-1}W_1$ and W_2 with the controller λK_∞, the parameters λ and λ^{-1} are canceled out but K_∞ remains λ dependent.

Now, the parametric H_∞ loop shaping design method has to be reformulated in LMI framework. For the existence of stabilizing controller, a new set of solvability conditions will be derived. Unlike [41], it will be shown that the solvability conditions are involved with the existence of stabilizing solutions of two ARIs. In the sequel, a correspondence also has to be established between ARIs and AREs to compare these results with [41]. Finally in LMI framework, the observer-based structure of the controller will be realized to establish the fact that the proposed method is a parallel approach to [41], however, provides an effective framework for computing optimal value of γ. Assuming the triplet $(A, \frac{B}{\lambda}, C)$ is stabilizable and detectable for a given value $\lambda > 0$, the following theorem can be stated.

Theorem 3.2: *For $\lambda > 0$, there exists a stabilizing controller λK_∞, if and only if*

$R > 0$, $S > 0$, $\gamma > 0$ *and satisfy the following inequalities:*

$$\begin{bmatrix} AR + RA^T - \gamma\lambda^{-2}BB^T & RC^T & -L \\ CR & -\gamma I & I \\ -L^T & I & -\gamma I \end{bmatrix} < 0 \tag{3.15}$$

$$A^TS + SA + C^TL^TS + SLC - \gamma C^TC < 0 \tag{3.16}$$

$$\begin{bmatrix} R & I \\ I & S \end{bmatrix} \geq 0 \tag{3.17}$$

Proof: This theorem will be proved by using the results of [36, 49]. Let, a generalized plant is

$$P = \left[\begin{array}{c|c|c} A & B_1 & B_2 \\ \hline C_1 & D_{11} & D_{12} \\ \hline C_2 & D_{21} & 0 \end{array}\right], \tag{3.18}$$

where (A, B_2, C_2) is stabilizable and detectable. There exists a stabilizing H_∞ controller such that $\|T_{zw}\|_\infty \leq \gamma$, where $\gamma > 0$, if and only if, $R > 0$, $S > 0$ and satisfy the following inequalities:

$$\begin{bmatrix} N_R & 0 \\ 0 & I \end{bmatrix}^T \begin{bmatrix} AR + RA^T & RC_1^T & B_1 \\ C_1R & -\gamma I & D_{11} \\ B_1^T & D_{11}^T & -\gamma I \end{bmatrix} \begin{bmatrix} N_R & 0 \\ 0 & I \end{bmatrix} < 0 \tag{3.19}$$

$$\begin{bmatrix} N_S & 0 \\ 0 & I \end{bmatrix}^T \begin{bmatrix} A^TS + SA & SB_1 & C_1^T \\ B_1^TS & -\gamma I & D_{11}^T \\ C_1 & D_{11} & -\gamma I \end{bmatrix} \begin{bmatrix} N_S & 0 \\ 0 & I \end{bmatrix} < 0 \tag{3.20}$$

$$\begin{bmatrix} R & I \\ I & S \end{bmatrix} \geq 0 \tag{3.21}$$

where, N_R, N_S denote bases of the null spaces of $\begin{bmatrix} B_2^T & D_{12}^T \end{bmatrix}$ and $\begin{bmatrix} C_2 & D_{21} \end{bmatrix}$ respectively. T_{zw} is the transfer function matrix between w to z. Now, comparing the generalized plant (3.5) with (3.18), we have

$$\left.\begin{aligned} A = A, B_1 = -L, B_2 = \lambda^{-1}B, C_1 = \begin{bmatrix} C \\ 0 \end{bmatrix}, C_2 = C \\ D_{11} = \begin{bmatrix} I \\ 0 \end{bmatrix}, D_{12} = \begin{bmatrix} 0 \\ I \end{bmatrix} \text{ and } D_{21} = I. \end{aligned}\right\} \tag{3.22}$$

The bases of the null spaces[4] of $\begin{bmatrix} \lambda^{-1}B^T & 0 & I \end{bmatrix}$ and $\begin{bmatrix} C & I \end{bmatrix}$ can be chosen as $\begin{bmatrix} I & 0 \\ 0 & I \\ -\lambda^{-1}B^T & 0 \end{bmatrix}$ and $\begin{bmatrix} I \\ -C \end{bmatrix}$. Using (3.22) and replacing $N_R = \begin{bmatrix} I & 0 \\ 0 & I \\ -\lambda^{-1}B^T & 0 \end{bmatrix}$ and $N_S = \begin{bmatrix} I \\ -C \end{bmatrix}$ in (3.19) and (3.20), we obtain respectively (3.15) and (3.16). (3.21) is similar to (3.17). □

Remark 3.2: *For a given value of λ, (3.15)-(3.17) can be solved in an LMI framework and an optimal value of γ easily can be found out if it is solved as a minimization problem. Hence, the method proposed in [41] provides conservative results and this can be achieved if one designs the parametric H_∞ loop shaping controller in LMI framework.*

Remark 3.3: *From (3.15), it is obvious that $\begin{bmatrix} -\gamma I & I \\ I & -\gamma I \end{bmatrix} < 0$ is also satisfied. It yields γ is always > 1.*

3.4 Correspondence between LMI and Riccati equation based approach

To draw a correspondence between the Theorems 3.1 and 3.2 the following lemma is presented.

[4] $\lambda^{-1}B^T \quad 0 \quad I \in \Re^{n_u \times (n+n_w+n_u)}$ and $C \quad I \in \Re^{n_w \times (n+n_w)}$. The rank of the null matrices will be $[(n+n_w+n_u)-n_u]$ and $[(n+n_w)-n_w]$ respectively. Hence, these are selected as $\begin{matrix} I_n & 0 & -\lambda^{-1}B \\ 0 & I_{n_w} & 0 \end{matrix}^{T}$ and $\begin{matrix} I_n \\ -C \end{matrix}$.

Lemma 3.1 *[60]: A matrix function is defined as*

$$G(X, A, B, Q) = XA^T + AX + XQX + BB^T$$

and it is assumed that, (A, B) is controllable on the imaginary axis with $Q = Q^T$. Then the following statements are equivalent.
i) There exists a matrix $\hat{X} > 0$ satisfying $G(\hat{X}, A, B, Q) < 0$.
ii) There exists a matrix $X \geq 0$ satisfying $G(X, A, B, Q) = 0$ such that $A+XQ$ is stable.

Further, the relation $\hat{X} > X$ is also satisfied.

Theorem 3.2 states the solvability conditions for the existence of stabilizing controller in LMI framework. Using Schur complement form (see Chapter 1), the following ARI is obtained from (3.15).

$$\left(A + \frac{1}{(1-\gamma^2)}LC\right)R + R\left(A + \frac{1}{(1-\gamma^2)}LC\right)^T - \left(\frac{\gamma}{(1-\gamma^2)}\right)RC^TCR - \left(\frac{\gamma}{(1-\gamma^2)}\right)LL^T - \gamma\lambda^{-2}BB^T < 0. \tag{3.23}$$

Similarly, from (3.16)

$$S(A + LC) + (A + LC)^T S - \gamma C^T C < 0. \tag{3.24}$$

Now, pre and post-multiplying (3.23) and (3.24) by R^{-1} and S^{-1} respectively, we get

$$R^{-1}\left(A + \frac{1}{(1-\gamma^2)}LC\right) + \left(A + \frac{1}{(1-\gamma^2)}LC\right)^T R^{-1} - \left(\frac{\gamma}{(1-\gamma^2)}\right)C^TC - R^{-1}\left(\left(\frac{\gamma}{(1-\gamma^2)}\right)LL^T + \gamma\lambda^{-2}BB^T\right)R^{-1} < 0 \tag{3.25}$$

and

$$(A + LC)S^{-1} + S^{-1}(A + LC)^T - \gamma S^{-1}C^TCS^{-1} < 0. \tag{3.26}$$

Again, multiplying both sides of (3.25) and (3.26) by γ we have

$$(\gamma R^{-1})\left(A + \frac{1}{(1-\gamma^2)}LC\right) + \left(A + \frac{1}{(1-\gamma^2)}LC\right)^T (\gamma R^{-1}) - \left(\frac{\gamma^2}{(1-\gamma^2)}\right)C^TC - (\gamma R^{-1})\left(\left(\frac{1}{(1-\gamma^2)}\right)LL^T + \lambda^{-2}BB^T\right)(\gamma R^{-1}) < 0 \tag{3.27}$$

and

$$(A+LC)(\gamma S^{-1})+(\gamma S^{-1})(A+LC)^T-(\gamma S^{-1})C^TC(\gamma S^{-1})<0. \tag{3.28}$$

Now changing the variables as $\tilde{X}_\infty = \gamma R^{-1}$ and $\tilde{Y}_\infty = \gamma S^{-1}$, we get two ARIs as follows:

$$\begin{aligned}
&\tilde{X}_\infty\left(A-\left(\gamma^2-1\right)^{-1}LC\right)+\left(A-\left(\gamma^2-1\right)^{-1}LC\right)^T\tilde{X}_\infty \\
&\quad -\tilde{X}_\infty\left(\lambda^{-2}BB^T-\left(\gamma^2-1\right)^{-1}LL^T\right)\tilde{X}_\infty+\gamma^2\left(\gamma^2-1\right)^{-1}C^TC<0
\end{aligned} \tag{3.29}$$

$$(A+LC)\tilde{Y}_\infty+\tilde{Y}_\infty(A+LC)^T-\tilde{Y}_\infty C^TC\tilde{Y}_\infty<0. \tag{3.30}$$

These two ARIs are the counterpart of AREs which have been obtained in state-space approach (see (3.11) and (3.12)). Since the pair $\left(\left(A-\left(\gamma^2-1\right)^{-1}LC\right),\left(\gamma\left(1-\gamma^2\right)^{-\frac{1}{2}}C\right)\right)$ is observable on the imaginary axis, using the Lemma 3.1, it can be stated that if (3.29) has stabilizing solution $\tilde{X}_\infty$, then ARE (3.11) also has stabilizing solutions X_∞ and satisfies the following relation $\tilde{X}_\infty > X_\infty \geq 0$. On the other hand, $\tilde{Y}_\infty > Y_\infty = 0$ and it satisfies $\rho(X_\infty Y_\infty) < \rho(\tilde{X}_\infty\tilde{Y}_\infty) \leq \gamma^2$.

3.5 Controller construction

In Theorem 3.2, the solvability conditions for stabilizing controller are characterized by two positive definite matrices R and S. If these solutions exist, a controller

$$K=\left[\begin{array}{c|c} A_c & B_c \\ \hline C_c & D_c \end{array}\right]$$

can be obtained by using the results of [35] and in this regard, the following steps have been adopted. Note that, from parametric H_∞ loop shaping framework the generalized plant (3.5) can be obtained and comparing it with (3.18), we have

$$A=A\in\Re^{n\times n},\ B_1=-L\in\Re^{n\times n_w},\ B_2=\lambda^{-1}B\in\Re^{n\times n_u},$$

$$C_1=\begin{bmatrix} C \\ 0^{n_u\times n}\end{bmatrix}\in\Re^{(n_w+n_u)\times n}, C_2=C\in\Re^{n_w\times n}, D_{11}=\begin{bmatrix} I_{n_w} \\ 0^{n_u\times n_w}\end{bmatrix}\in\Re^{(n_w+n_u)\times n_w},$$

$$D_{12}=\begin{bmatrix} 0^{n_w\times n_u} \\ I_{n_u}\end{bmatrix}\in\Re^{(n_w+n_u)\times n_u},\ D_{21}=I_{n_w}\in\Re^{n_w\times n_w},\ D_{22}=0\in\Re^{n_w\times n_u}$$

First, the matrix D_c has to be found out from the following relation

$$D_c = \left(D_{12}^{\dagger} D_{12}\right) D_0 \left(D_{21} D_{21}^{\dagger}\right) \tag{3.31}$$

where, $\bar{\sigma}\left(D_{11} + D_{12}D_0D_{21}\right) < \gamma$. From (3.15), we get $\gamma > 1$ (see Remark 3.3) and using the definition of pseudo inverse, we have

$$D_{12}^{\dagger} = \left(D_{12}^T D_{12}\right)^{-1} D_{12}^T = \begin{bmatrix} 0_{n_u \times n_w} & I_{n_u} \end{bmatrix}, \; D_{21}^{\dagger} = \left(D_{21}^T D_{21}\right)^{-1} D_{21}^T = I_{n_u}.$$

Now simplifying $D_{11} + D_{12}D_0D_{21}$, we have

$$D_{11} + D_{12}D_0D_{21} = \begin{bmatrix} I_{n_w} \\ 0_{n_u \times n_w} \end{bmatrix} + \begin{bmatrix} 0_{n_w \times n_u} \\ I_{n_u} \end{bmatrix} D_0 = \begin{bmatrix} I_{n_w} \\ D_0 \end{bmatrix}.$$

Hence, $D_0 = 0_{n_u \times n_w}$ is a valid choice that always satisfies $\bar{\sigma}\left(D_{11} + D_{12}D_0D_{21}\right) < \gamma$ and from (3.31), we have $D_c = 0$.

The explicit relations for other controller matrices are as follows [35]:

$$B_c = N_p^{-1}\theta_B^T, \quad C_c = \theta_C \left(M_p^T\right)^{-1}$$

$$A_c = -N_p^{-1}\Big[SB_2\theta_C + \theta_B^T C_2 R + SAR + A^T + \begin{bmatrix} SB_1 + \theta_B^T D_{21} & C_1^T \end{bmatrix} \\ \left(-\nabla^{-1}\right)\begin{bmatrix} B_1^T \\ C_1R + D_{12}\theta_c \end{bmatrix}\Big] (M_p^T)^{-1}$$

where M_p, N_p are two invertible matrices and satisfy the relation $M_pN_p^T = I - RS$, and here, $M_p = R$ and $N_p^T = \left(R^{-1} - S\right)$ have been selected. The ∇ is defined as $\nabla := \begin{bmatrix} -\gamma I_{n_w} & D_{11}^T \\ D_{11} & -\gamma I_{n_w \times n_u} \end{bmatrix} \in \Re^{2n_w + n_u}$ and the unknowns θ_B and θ_C are obtained by solving the following two least-square problems. θ_x and θ_y are two variables and the problems are

$$\left.\begin{array}{l} \left(\begin{array}{c|c} 0 & \begin{bmatrix} D_{21} & 0 \end{bmatrix} \\ \hline \begin{bmatrix} D_{21}^T \\ 0 \end{bmatrix} & \nabla \end{array}\right)\left(\begin{array}{c} \theta_B \\ \hline \theta_x \end{array}\right) = -\left(\begin{array}{c} C_2 \\ \hline B_1^T S \\ C_1 \end{array}\right) \\ \left(\begin{array}{c|c} 0 & \begin{bmatrix} 0 & D_{12}^T \end{bmatrix} \\ \hline \begin{bmatrix} 0 \\ D_{12} \end{bmatrix} & \nabla \end{array}\right)\left(\begin{array}{c} \theta_C \\ \hline \theta_y \end{array}\right) = -\left(\begin{array}{c} B_2^T \\ \hline B_1^T \\ C_1 R \end{array}\right) \end{array}\right\} \tag{3.32}$$

Simplifying the first equation of (3.32), we have

$$\begin{bmatrix} D_{21} & 0 \end{bmatrix} \theta_x = -C_2 \text{ and } \begin{bmatrix} D_{21}^T \\ 0 \end{bmatrix} \theta_B + \nabla \theta_x = -\begin{bmatrix} B_1^T S \\ C_1 \end{bmatrix}. \tag{3.33}$$

From (3.33) we have,

$$\begin{bmatrix} D_{21} & 0 \end{bmatrix} \nabla^{-1} \begin{bmatrix} D_{21}^T \\ 0 \end{bmatrix} \theta_B + \begin{bmatrix} D_{21} & 0 \end{bmatrix} \theta_x = -\begin{bmatrix} D_{21} & 0 \end{bmatrix} \nabla^{-1} \begin{bmatrix} B_1^T S \\ C_1 \end{bmatrix}$$

$$\Rightarrow \begin{bmatrix} D_{21} & 0 \end{bmatrix} \nabla^{-1} \begin{bmatrix} D_{21}^T \\ 0 \end{bmatrix} \theta_B = C_2 - \begin{bmatrix} D_{21} & 0 \end{bmatrix} \nabla^{-1} \begin{bmatrix} B_1^T S \\ C_1 \end{bmatrix}. \tag{3.34}$$

Similarly, simplifying the second equation of (3.32) we get

$$\begin{bmatrix} 0 & D_{12}^T \end{bmatrix} \nabla^{-1} \begin{bmatrix} 0 \\ D_{12} \end{bmatrix} \theta_C = B_2^T - \begin{bmatrix} 0 & D_{12}^T \end{bmatrix} \nabla^{-1} \begin{bmatrix} B_1^T \\ C_1 R \end{bmatrix}. \tag{3.35}$$

Since $\nabla^{-1} = \begin{bmatrix} \gamma^{-1}\left(D_{11}^T \left(D_{11}D_{11}^T - \gamma^2 I\right)^{-1} D_{11} - I_{n_w}\right) & D_{11}^T \left(D_{11}D_{11}^T - \gamma^2 I\right)^{-1} \\ \left(D_{11}D_{11}^T - \gamma^2 I\right)^{-1} D_{11} & \gamma\left(D_{11}D_{11}^T - \gamma^2 I\right)^{-1} \end{bmatrix}$

$$= \begin{bmatrix} \gamma\left(1-\gamma^2\right)^{-1} I_{n_w} & \begin{bmatrix} \left(1-\gamma^2\right)^{-1} & 0_{n_w \times n_u} \end{bmatrix} \\ \begin{bmatrix} \left(1-\gamma^2\right)^{-1} I_{n_w} \\ 0_{n_u \times n_w} \end{bmatrix} & \begin{bmatrix} \gamma\left(1-\gamma^2\right)^{-1} I_{n_w} & 0_{n_w \times n_u} \\ 0_{n_u \times n_w} & -\gamma^{-1} I_{n_u} \end{bmatrix} \end{bmatrix},$$

Now considering the left hand side of (3.34), we have

$$\begin{aligned} \begin{bmatrix} D_{21} & 0 \end{bmatrix} \nabla^{-1} \begin{bmatrix} D_{21}^T \\ 0 \end{bmatrix} &= \begin{bmatrix} I_{n_w} & 0_{n_w \times (n_w+n_u)} \end{bmatrix} \nabla^{-1} \begin{bmatrix} I_{n_w} \\ 0_{(n_w+n_u) \times n_w} \end{bmatrix} \\ &= \gamma\left(1-\gamma^2\right)^{-1} I_{n_w} \end{aligned} \tag{3.36}$$

and right hand side of (3.34)

$$C_2 - \begin{bmatrix} D_{21} & 0 \end{bmatrix} \nabla^{-1} \begin{bmatrix} B_1^T S \\ C_1 \end{bmatrix} = C - \begin{bmatrix} I_{n_w} & 0_{n_w \times (n_w+n_u)} \end{bmatrix} \nabla^{-1} \begin{bmatrix} -L^T S \\ \begin{bmatrix} C \\ 0_{n_u} \end{bmatrix} \end{bmatrix}$$

$$
\begin{aligned}
&= C - \left(-\gamma\left(1-\gamma^2\right)^{-1} L^T S + \left(1-\gamma^2\right)^{-1} C\right) \\
&= \gamma\left(1-\gamma^2\right)^{-1} L^T S + \left(1 - \left(1-\gamma^2\right)^{-1}\right) C \\
&= \gamma\left(1-\gamma^2\right)^{-1} L^T S - \gamma^2\left(1-\gamma^2\right)^{-1} C. \qquad (3.37)
\end{aligned}
$$

Now replacing (3.36) and (3.37) in (3.34), we have

$$
\theta_B = \gamma^{-1}\left(1-\gamma^2\right)\left[\gamma\left(1-\gamma^2\right)^{-1} L^T S - \gamma^2\left(1-\gamma^2\right)^{-1} C\right] = L^T S - \gamma C. \qquad (3.38)
$$

Similarly simplifying (3.35), we have

$$
\begin{bmatrix} 0 & D_{12}^T \end{bmatrix} \nabla^{-1} \begin{bmatrix} 0 \\ D_{12} \end{bmatrix} = \begin{bmatrix} 0_{n_u \times n_u} & \begin{bmatrix} 0_{n_u \times n_w} & I_{n_u} \end{bmatrix} \end{bmatrix} \nabla^{-1} \begin{bmatrix} 0_{n_u \times n_u} \\ 0_{n_w \times n_u} \\ I_{n_u} \end{bmatrix} = -\gamma^{-1} I_{n_u}
$$

and $B_2^T - \begin{bmatrix} 0 & D_{12}^T \end{bmatrix} \nabla^{-1} \begin{bmatrix} B_1^T \\ C_1 R \end{bmatrix}$

$$
= \lambda^{-1} B^T - \begin{bmatrix} 0_{n_u \times n_u} & \begin{bmatrix} 0_{n_u \times n_w} & I_{n_u} \end{bmatrix} \end{bmatrix} \nabla^{-1} \begin{bmatrix} -L^T \\ \begin{bmatrix} CR \\ 0 \end{bmatrix} \end{bmatrix} = \lambda^{-1} B^T.
$$

Simplifying (3.35), we have $\theta_C = -\lambda^{-1}\gamma B^T$. Hence,

$$
\begin{aligned}
B_c = N_p^{-1}\theta_B^T &= \left(R^{-1} - S\right)^{-1}\left(L^T S - \gamma C\right)^T \\
&= \left[S\left(S^{-1}R^{-1} - I\right)\right]^{-1}\left(SL - \gamma C^T\right) \\
&= \left(S^{-1}R^{-1} - I\right)^{-1}\left(L - \gamma S^{-1} C^T\right), \qquad (3.39)
\end{aligned}
$$

$$
C_c = \theta_C \left(M_p^T\right)^{-1} = -\lambda^{-1}\gamma B^T R^{-1} \qquad (3.40)
$$

and $A_c = -N_p^{-1}\Big[SB_2\theta_C + \theta_B^T C_2 R + SAR + A^T + \begin{bmatrix} SB_1 + \theta_B^T D_{21} & C_1^T \end{bmatrix}$

$$
\left(-\nabla^{-1}\right)\begin{bmatrix} B_1^T \\ C_1 R + D_{12}\theta_c \end{bmatrix}\Big] (M_p^T)^{-1}
$$

$$
\begin{aligned}
&= -N_p^{-1}\left[-\lambda^{-2}\gamma SBB^T + \left(L^T S - \gamma C\right)^T CR + SAR + A^T + C^T L^T\right]\left(M_p^T\right)^{-1} \\
&= -\left(R^{-1} - S\right)^{-1} \\
&\quad \left[-\lambda^{-2}\gamma SBB^T R^{-1} + \left(L^T S - \gamma C\right)^T C + SA + A^T R^{-1} + C^T L^T R^{-1}\right] \\
&= -\left(S^{-1}R^{-1} - I\right)^{-1} \\
&\quad \left[-\lambda^{-2}\gamma BB^T R^{-1} + LC - \gamma S^{-1}C^T C + A + S^{-1}A^T R^{-1} + S^{-1}C^T L^T R^{-1}\right]
\end{aligned} \tag{3.41}
$$

Proposition 3.1: *If $R > 0$ and $S > 0$ are the solutions of LMIs obtained from Theorem 3.2, then the controller $K = \left[\begin{array}{c|c} A_c & B_c \\ \hline C_c & 0 \end{array}\right]$ where, A_c, B_c and C_c are respectively given in (3.41), (3.39) and (3.40), can be realized in an observer-based structure.*

Proof: (3.15) and (3.16) of Theorem 3.2 can be simplified respectively to (3.29) and (3.30) by changing the variables $\tilde{X}_\infty = \gamma R^{-1}$ and $\tilde{Y}_\infty = \gamma S^{-1}$ (see Section 3.4). Now, replacing $R^{-1} = \gamma^{-1}\tilde{X}_\infty$ and $S^{-1} = \gamma^{-1}\tilde{Y}_\infty$ in (3.39)-(3.41), we get

$$
\begin{aligned}
A_c = \left(I - \gamma^{-2}\tilde{Y}_\infty\tilde{X}_\infty\right)^{-1}\Big[&\left(A + LC - \lambda^{-2}BB^T\tilde{X}_\infty\right) \\
&+ \left(\gamma^{-2}\tilde{Y}_\infty A^T\tilde{X}_\infty - \tilde{Y}_\infty C^T C + \gamma^{-2}\tilde{Y}_\infty C^T L^T \tilde{X}_\infty\right)\Big]
\end{aligned}
$$

$$
\begin{aligned}
B_c &= -\left(I - \gamma^{-2}\tilde{Y}_\infty\tilde{X}_\infty\right)^{-1}\left(L - \tilde{Y}_\infty C^T\right) \\
C_c &= -\lambda^{-1}B^T\tilde{X}_\infty.
\end{aligned}
$$

Considering respectively the controller state and measured output of the shaped plant as x_c and y, the controller state-space equations become

$$
\begin{aligned}
\dot{x}_c = \left(I - \gamma^{-2}\tilde{Y}_\infty\tilde{X}_\infty\right)^{-1}\Big\{\Big[&(A + LC + \lambda^{-1}BF) + (\gamma^{-2}\tilde{Y}_\infty A^T\tilde{X}_\infty - \tilde{Y}_\infty C^T C \\
&+ \gamma^{-2}\tilde{Y}_\infty C^T L^T\tilde{X}_\infty)\Big] x_c - (L - \tilde{Y}_\infty C^T)y\Big\}
\end{aligned}
$$

and $u = Fx_c$,

where $F = -\lambda^{-1}B^T\tilde{X}_\infty$. Simplifying the state equation, it becomes

$$\begin{aligned}\left(I-\gamma^{-2}\tilde{Y}_\infty\tilde{X}_\infty\right)\dot{x}_c = Ax_c+\lambda^{-1}BFx_c \quad &+ \quad \left(L-\tilde{Y}_\infty C^T\right)(Cx_c-y)\\ &+ \quad \gamma^{-2}\tilde{Y}_\infty(A+LC)^T\tilde{X}_\infty x_c. \end{aligned} \tag{3.42}$$

Since, $\tilde{Y}_\infty$ satisfies the inequality (3.30)

$$\tilde{Y}_\infty(A+LC)^T+(A+LC)\tilde{Y}_\infty-\tilde{Y}_\infty C^TC\tilde{Y}_\infty<0,$$

there must exists η , $\eta>0$ such that

$$\tilde{Y}_\infty(A+LC)^T+(A+LC)\tilde{Y}_\infty-\tilde{Y}_\infty C^TC\tilde{Y}_\infty+\eta I=0. \tag{3.43}$$

From (3.43), $\tilde{Y}_\infty(A+LC)^T = -(A+LC)\tilde{Y}_\infty+\tilde{Y}_\infty C^TC\tilde{Y}_\infty-\eta I$ and replacing it in (3.42),

$$\begin{aligned}\left(I-\gamma^{-2}\tilde{Y}_\infty\tilde{X}_\infty\right)\dot{x}_c &= Ax_c+\lambda^{-1}BFx_c+\left(L-\tilde{Y}_\infty C^T\right)(Cx_c-y)\\ &-\gamma^{-2}A\tilde{Y}_\infty\tilde{X}_\infty x_c-\gamma^{-2}LC\tilde{Y}_\infty\tilde{X}_\infty x_c+\gamma^{-2}\tilde{Y}_\infty C^TC\tilde{Y}_\infty\tilde{X}_\infty x_c-\eta\gamma^{-2}\tilde{X}_\infty x_c\\ &= A\left(I-\gamma^{-2}\tilde{Y}_\infty\tilde{X}_\infty\right)x_c \quad + \quad \left(L-\tilde{Y}_\infty C^T\right)\left(C\left(I-\gamma^{-2}\tilde{Y}_\infty\tilde{X}_\infty\right)x_c-y\right)\\ &\quad + \quad \lambda^{-1}BFx_c-\eta\gamma^{-2}\tilde{X}_\infty x_c. \end{aligned} \tag{3.44}$$

Now defining $\left(I-\gamma^{-2}\tilde{Y}_\infty\tilde{X}_\infty\right)x_c = x_t$, (3.44) becomes

$$\begin{aligned}\dot{x}_t = Ax_t+\left(L-\tilde{Y}_\infty C^T\right)(Cx_t-y) \quad &- \quad \lambda^{-2}BB^T\tilde{X}_\infty\left(I-\gamma^{-2}\tilde{Y}_\infty\tilde{X}_\infty\right)^{-1}x_t\\ &- \quad \eta\gamma^{-2}\tilde{X}_\infty\left(I-\gamma^{-2}\tilde{Y}_\infty\tilde{X}_\infty\right)^{-1}x_t. \end{aligned} \tag{3.45}$$

Again,

$$u = Fx_c = -\lambda^{-1}B^T\tilde{X}_\infty\left(I-\gamma^{-2}\tilde{Y}_\infty\tilde{X}_\infty\right)^{-1}x_t = \lambda\hat{u} \tag{3.46}$$

where, $\hat{u} = -\lambda^{-2}B^T\tilde{X}_\infty\left(I-\gamma^{-2}\tilde{Y}_\infty\tilde{X}_\infty\right)^{-1}x_t$.
Equations (3.45) and (3.46) have been realized in block-diagram form as shown in Figure 3.3 and these are the equations of an observer-based controller. □

In Figure 3.3, the controller block-diagram has been shown. The output of Q block be-

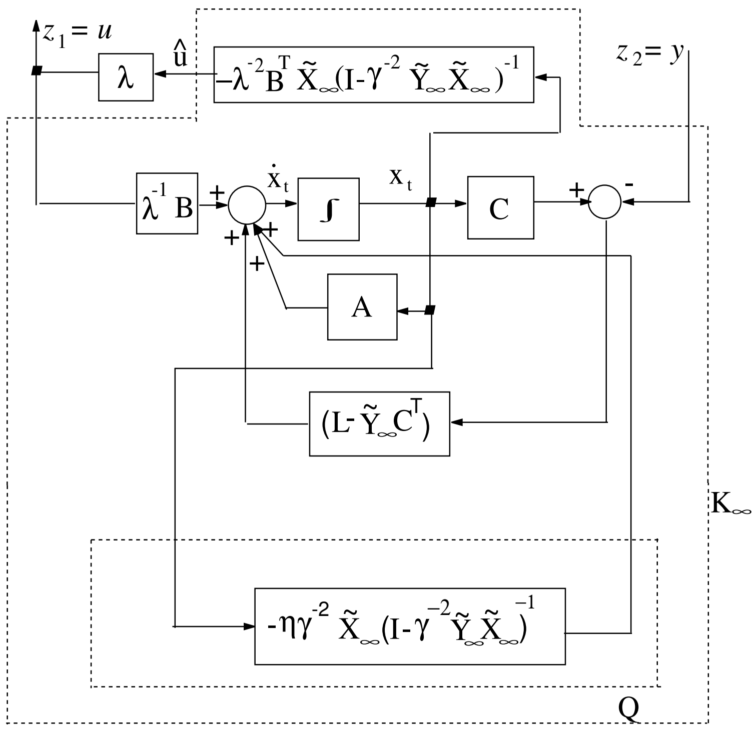

Figure 3.3: Parametric H_∞ loop shaping controller in LMI approach

comes zero when $\eta = 0$, and it explores a controller K_∞ which has the similar structure as obtained from state-space Riccati equation based approach [41].

Remark 3.4: *In (3.43), a parameter η has been introduced to obtain the equality condition that finally gives the controller state-equation (3.45). Even though the value of η is very small, the role of η can not be neglected as this equality condition is necessary to realize the controller in its observer form.*

3.6 Numerical example

In this section, a numerical example has been demonstrated to illustrate the proposed design technique. Here, the linearized mathematical model of longitudinal dynamics of F-8 aircraft has been considered whose state-space model is as follows [52].

$$\dot{x} = \begin{bmatrix} -0.8 & -0.0006 & -12 & 0 \\ 0 & -0.014 & -16.64 & -32.2 \\ 1 & -0.0001 & -1.5 & 0 \\ 1 & 0 & 0 & 0 \end{bmatrix} x + \begin{bmatrix} -19 & -3 \\ -0.66 & -0.5 \\ -0.16 & -0.5 \\ 0 & 0 \end{bmatrix} u$$

$$y = \begin{bmatrix} 0 & 0 & 0 & 1 \\ 0 & 0 & -1 & 1 \end{bmatrix} x,$$

where x is the state vector, u is the input vector and y is the output vector. The detail description of these three vectors can be found in [52] and here, the effect of input saturation is not taken into account. For controller synthesis, the post-compensator is taken as an identity matrix with proper dimension. Since, the plant is open loop stable and minimum phase system, there is no such restriction on closed-loop bandwidth which is a major consideration for pre-compensator selection. In this example, the specified design goals are as follows: the steady state error should not exceed $\pm 2\%$ for step input commands and closed-loop stability should be guaranteed. To satisfy these requirements a pre-compensator

$$W_1 = \begin{bmatrix} \frac{10(s+0.3)}{s(s+8)} & 0 \\ 0 & \frac{20(s+1.5)}{s(s+1)} \end{bmatrix}$$

has been selected and the corresponding robust stability margin for the shaped plant is obtained as 0.398 (i.e.,γ= 2.511) by solving the optimization problem of Theorem 3.2 subject to minimize the γ. This indicates that the closed-loop stability is ensured upto 39.8% perturbation of the normalized coprime factors of the shaped plant.

Iterative algorithm of [41]			Using LMI approach
Initial guess (μ_0)	γ_{opt}	λ	γ_{opt}
10	1.8748	0.3544	1.8758
5	2.003	0.4635	2.004
1	2.2856	0.7435	2.2875
0.5	2.3742	0.8417	2.3763
0	Can not be found	1	2.5111
-0.5	2.7683	1.330	2.7697
-0.9	3.695	2.4550	3.6985

Table 3.1: γ_{opt} for different values of λ

Table 3.1 shows the optimal values of γ for different λs and these results are compa-

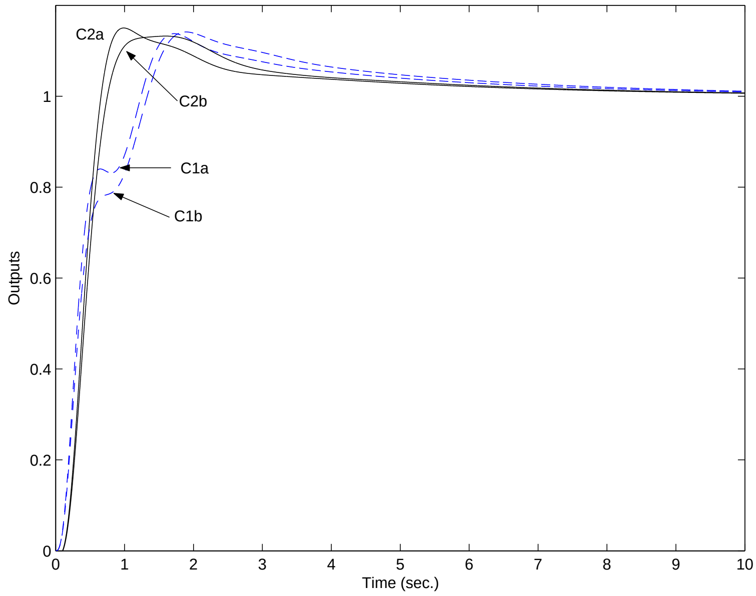

Figure 3.4: a: $\lambda = 1.0$, b: $\lambda = 0.8417$, C1a and C1b for channel-1 output, C2a and C2b for channel-2 output with unit step command inputs in both the channels

rable for both the methods. For the iterative method of [41], an initial guess(μ_0) is set to calculate γ_{opt}. However, it has been observed that this algorithm does not work when $\mu_0 \leq -1$, and a definite guideline is needed which is not addressed in [41]. Moreover from sequential steps of this algorithm one can not obtain γ_{opt} for a fixed value of λ. Here the reverse order is followed; first γ_{opt} is calculated and then, the corresponding λ is found out which is not in general practical. Meanwhile it is important to note that, although the McFarlane-Glover method is a special case of parametric H_∞ loop shaping control, the iterative algorithm of [41] does not work when $\lambda = 1$. However, the proposed LMI technique is applicable for any choice of λ and subsequently computes the corresponding γ_{opt}.

The output responses for unit step command in both the channels have been shown in Figure 3.4. For two different values of λ, the parametric H_∞ loop shaping controllers have been designed and their corresponding performances are demonstrated. When $\lambda = 1$, the controller is similar to McFarlane-Glover H_∞ loop shaping controller, whereas at $\lambda = 0.8417$, larger robust stability margin is obtained. Similarly, the controller can also be designed for other values of λ as mentioned in Table 3.1 for which the larger robust stability margin will be obtained.

3.7 Conclusions

In this chapter, the design of parametric H_∞ loop shaping controller has been reformulated in LMI framework and a new set of solvability conditions is established for the existence of such controller. Further, a correspondence is drawn with [41] and it is shown that, the proposed technique can also impart an observer based structure of the controller. In numerical example, the drawbacks of the method given in [41] have been discussed and subsequently, the advantages of the proposed technique are pointed out. Interestingly, if we change the value of λ, different γ's are obtained which are related to performance and stability of the closed-loop system. More specifically, the parameter λ affects the bases of null-spaces for the generalized plant and subsequently the stabilizing solution of H_∞ controller that in turn affects performance and stability of the closed-loop system. In order to have more degrees of freedom in design, the proposed parametric H_∞ loop shaping control problem can be investigated in matrix variable form instead of a free parameter λ. It may be noted that the design of McFarlane-Glover H_∞ loop shaping controller is the special case of parametric H_∞ loop-shaping control problem when the value of free parameter λ is assigned to 1. It appears that the proposed technique will provide a foundation in understanding the solution of parametric H_∞ loop shaping control problem based on LMI framework.

CHAPTER 4

Static H_∞ loop shaping control

In preceding chapter, the parametric H_∞ loop shaping control problem has been formulated in LMI framework and it depicts the same structure of McFarlane-Glover method when the parameter is set to 1. In this technique, the designed controller is with the same order of the shaped plant. Normally this order is high and the controller is known as full order (FO) H_∞ loop shaping controller. In the present chapter, an attempt has been made to develop an alternate but a simple methodology for designing a static output feedback H_∞ loop shaping controller that effectively yields a lower order controller design method. For the existence of static H_∞ loop shaping controller, a set of sufficient conditions has been derived from four-block H_∞ synthesis framework. These conditions are formulated in LMI form, and are different from those obtained in [74-76] using the normalized coprime factorization approach.

4.1 Introduction

In principle, the requirements for achieving the good robust stability margin, disturbance attenuation, reference command signal tracking and measurement noise rejection can be handled directly by introducing the weighting functions and converting the problem into a H_∞ optimization problem (discussed in Chapter 2). The H_∞ loop shaping method is conceptually a simple yet powerful design technique in frequency domain for robust control of multivariable system against perturbations. In this method, the nominal plant is cascaded with appropriately chosen weights so that the frequency response of the weighted open-loop system is reshaped in order to meet closed-loop performance requirements. Based on this shaped plant, a robust controller is synthesized either in the normalized coprime factor form or in its equivalent four-block H_∞ framework [64, 65] (discussed in Chapter 2). The former approach, though more general for considering unstructured uncertainty, may not be always straightforward for controller design while the presence of input saturation is considered in the plant. Whereas the four-block framework in this case may provide a suitable methodology for robust controller design. Moreover, the later approach provides a sequence of design steps when the pole placement constraint is imposed in the synthesis problem [19]. As a result, there is a need for extending the existing results based on coprime factorization approach to those in general four-block H_∞ framework.

From the implementation point of view, it is quite disadvantageous as the order of the H_∞ controller is generally high and it depends on the order of the compensated plant [65]. Several researchers have shown keen interest to design lower order H_∞ controller without sacrificing the stability margin and performance robustness of the system [16], [65]. In this context, a novel method for designing a static output feedback H_∞ loop shaping controller with high performance has been reported in control system literatures [74-76]. Exploiting the normalized coprime description of the plant, sufficient conditions have been given for the existence of a static controller. These conditions are in LMI form, and easy for implementation to obtain a tractable controller.

The objective of the present chapter is to develop a suitable method for designing a static H_∞ loop shaping output feedback controller in four-block H_∞ framework. In true sense, mere replacement of the generalized plant for four-block H_∞ framework in [76] can not give directly the linear sufficient conditions for the existence of static controller, and some extra effort is needed to reformulate the constraints in LMI form. This has been done by introducing an additional matrix obtained from the stabilizing solution of a Riccati equation. The method proposed in this chapter provides an alternate but a simple approach for designing static H_∞ loop shaping controller utilizing a set of coupled matrix inequality conditions.

The rest of the chapter is organized as follows. In Section 4.2, some preliminary results have been discussed. An alternate design technique for static H_∞ loop shaping controller and solvability conditions are presented in Section 4.3. To show the effectiveness of the proposed method two numerical examples have been illustrated in Section

4.4. In Section 4.5, a case study on load frequency control of interconnected power system has been carried out to illustrate the design procedure of static H_∞ loop shaping controller.

4.2 Preliminary results

We consider the state-space realization of the compensated plant $G_S = \left[\begin{array}{c|c} A & B \\ \hline C & 0 \end{array}\right]$, where (A, B, C) is stabilizable and detectable, and $A \in \Re^{n\times n}$, $B \in \Re^{n\times n_u}$ and $C \in \Re^{n_y\times n}$. For simplicity, G_S is considered as a strictly proper shaped plant and $D \neq 0$ does not give any extra insight to the present work. Based on the compensated or shaped plant G_S, a stabilizing full order (FO) controller is synthesized by following the design procedure given in Section 2.2 of Chapter 2. For completeness of this chapter, we again describe briefly the state-space formulation of H_∞ loop shaping control problem that has already been presented in previous chapter.

Let, the normalized left coprime factorization of G_S is described as $M^{-1}N$, where the state-space realization of M, N is

$$\left[\begin{array}{cc} N & M \end{array}\right] = \left[\begin{array}{c|cc} A+LC & B & L \\ \hline C & 0 & I \end{array}\right] \tag{4.1}$$

where, $L = -YC^T$ is an observer gain matrix and Y is the symmetric positive semi-definite stabilizing solution of the algebraic Riccati equation:

$$AY + YA^T - YC^TCY + BB^T = 0. \tag{4.2}$$

In normalized coprime factor robust stabilization framework, the uncertainties are presented as perturbations of M and N, and the stabilizing static controller[1] K_s is synthesized by satisfying

$$\inf_{K_s \text{ stabilizing}} \left\| \left[\begin{array}{c} K_s \\ I \end{array}\right] (I - G_S K_s)^{-1} M^{-1} \right\|_\infty \leq \frac{1}{\epsilon_{\max}} = \gamma_{opt} \leq \gamma \tag{4.3}$$

where, $\epsilon_{\max}$ is the maximum achievable robust stability margin and the shaped plant G_S is formed combining the nominal system and weighting TFM [65]. The weighting

[1] In order to indicate the static controller, suffix 's' has been used whereas in full order case (dynamic controller), it is denoted as ∞.

matrices are chosen such that G_S contains no hidden unstable modes to ensure the internal stability of the closed-loop system. The sufficient conditions for the existence of static H_∞ loop shaping output feedback controller for the normalized coprime factor robust stabilization problem have been stated in the following theorem [76].

Theorem 4.1 *[76]: There is a static controller K_s such that (4.3) is satisfied, if $\gamma > 1$ and there exists a symmetric positive definite matrix R such that*

$$(A + LC)\,R + R\,(A + LC)^T < 0 \tag{4.4}$$

$$\begin{bmatrix} AR + RA^T - \gamma BB^T & RC^T & -L \\ CR & -\gamma I & I \\ -L^T & I & -\gamma I \end{bmatrix} < 0 \tag{4.5}$$

are satisfied where L is defined as in (4.1) and (4.2).

The proof of this theorem can be found in [76]. These conditions are numerically tractable as these are deduced in LMI form. Now, related to the static controller we also state some important results which are required to establish the main results of this chapter.

Lemma 4.1 *[74]: With the stabilizable and detectable realization of a plant* $G_S = \left[\begin{array}{c|c} A & B \\ \hline C & 0 \end{array}\right]$*, there exists a static output feedback controller, if and only if, the following inequalities are satisfied:*

$$\left.\begin{aligned} AR + RA^T - \sigma BB^T < 0 \\ AR + RA^T - \sigma RC^T CR < 0 \end{aligned}\right\} \tag{4.6}$$

where $R = R^T > 0$ and $\sigma > 0$.

Apart from this, the necessary and sufficient conditions for the existence of static output feedback controller that satisfies the performance bound, will be presented in the following theorem to describe the H_∞ synthesis problem.

Theorem 4.2 *[14]: If the state-space realization of a generalized plant is*

$$P_g = \left[\begin{array}{c|c|c} A & B_1 & B_2 \\ \hline C_1 & D_{11} & D_{12} \\ \hline C_2 & D_{21} & 0 \end{array}\right]$$

where (A, B_2, C_2) is stabilizable and detectable, there exists a static output feedback H_∞ controller such that $\|T_{zw}\|_\infty \leq \gamma$, if and only if, the following inequalities are satisfied for $R = R^T > 0,\ S = S^T > 0$ and $\gamma > 0$:

$$\begin{bmatrix} N_R & 0 \\ 0 & I \end{bmatrix}^T \begin{bmatrix} AR + RA^T & RC_1^T & B_1 \\ C_1 R & -\gamma I & D_{11} \\ B_1^T & D_{11}^T & -\gamma I \end{bmatrix} \begin{bmatrix} N_R & 0 \\ 0 & I \end{bmatrix} < 0 \tag{4.7}$$

$$\begin{bmatrix} N_S & 0 \\ 0 & I \end{bmatrix}^T \begin{bmatrix} A^T S + SA & SB_1 & C_1^T \\ B_1^T S & -\gamma I & D_{11}^T \\ C_1 & D_{11} & -\gamma I \end{bmatrix} \begin{bmatrix} N_S & 0 \\ 0 & I \end{bmatrix} < 0 \tag{4.8}$$

$$R = S^{-1} \tag{4.9}$$

where, N_R, N_S denote the bases of the null spaces of $\begin{bmatrix} B_2^T & D_{12}^T \end{bmatrix}$ and $\begin{bmatrix} C_2 & D_{21} \end{bmatrix}$ respectively. Note that, T_{zw} is the transfer function matrix from w to z where these are respectively the exogenous and objective signal vectors.

4.3 Alternative method for static H_∞ loop shaping controller design

In normalized left coprime factorization framework, as $MM^* + NN^* = I$ and $\left\| \begin{bmatrix} N & M \end{bmatrix} \right\|_\infty = 1$, the following expression can be seen in [65] (also see in Chapter 2) from where the equivalent relationship between the two frameworks of H_∞ loop shaping control is established.

$$\|T_{zw}\|_\infty = \left\| \begin{bmatrix} K_s \\ I \end{bmatrix} (I - G_S K_s)^{-1} M^{-1} \right\|_\infty$$

$$= \left\| \begin{bmatrix} K_s \\ I \end{bmatrix} (I - G_S K_s)^{-1} M^{-1} \begin{bmatrix} N & M \end{bmatrix} \right\|_\infty$$

$$= \left\| \begin{bmatrix} K_s \\ I \end{bmatrix} (I - G_S K_s)^{-1} \begin{bmatrix} G_S & I \end{bmatrix} \right\|_\infty$$

Now (4.3) can be restated as, find a stabilizing controller K_s such that

$$\|T_{zw}\|_\infty = \inf_{K_s \text{ stabilizing}} \left\| \begin{bmatrix} K_s \\ I \end{bmatrix} (I - G_S K_s)^{-1} \begin{bmatrix} G_S & I \end{bmatrix} \right\|_\infty \leq \frac{1}{\epsilon_{\max}} \leq \gamma \quad (4.10)$$

is satisfied. It may be observed in (4.10), the transfer function matrix whose ∞-norm has to be minimized, has four blocks transfer functions from two exogenous signal vectors to two objective signal vectors that explores the four-block synthesis problem related to H_∞ loop shaping control (shown in Figure 4.1).

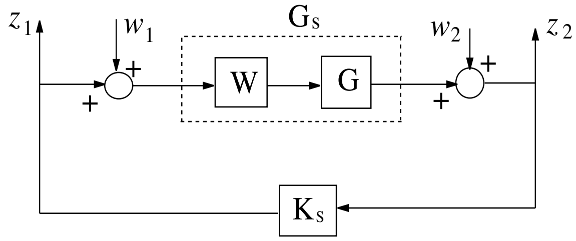

Figure 4.1: Four-block synthesis framework for static H_∞ loop shaping control

In the following subsection, parallel to Theorem 4.1, a new set of sufficient conditions for the existence of static H_∞ loop shaping controller has to be established from four-block H_∞ synthesis framework.

4.3.1 Solvability conditions

Theorem 4.3: *There exists a static H_∞ loop shaping controller K_s for the system G_S such that (4.10) is satisfied, if $\beta > 1$, $P = P^T > 0$ and the following inequalities hold:*

$$\begin{bmatrix} AP + PA^T - \beta BB^T & PC^T \\ CP & -\beta I \end{bmatrix} < 0, \quad (4.11)$$

$$\begin{bmatrix} AP + PA^T + YC^TCY - YC^TCP - PC^TCY & B \\ B^T & -I \end{bmatrix} < 0 \quad (4.12)$$

where, Y is the symmetric positive semi-definite solution of (4.2) and $\beta = \left(\gamma^2 - 1\right)$.

Proof: These sufficient conditions are derived in the four-block H_∞ synthesis framework. Since the coprime factors are normalized, (4.10) is equivalent to (4.3) and we need the generalized plant for the four-block structure $\left(\begin{bmatrix} w_2 \\ w_1 \end{bmatrix} \text{to} \begin{bmatrix} z_2 \\ z_1 \end{bmatrix}\right)$, as shown in Figure 4.1, based on which the robust stabilization problem is solved.

In Figure 4.1, in order to shape the open-loop plant, the pre-compensator is selected as W and the post-compensator is taken as an identity matrix with proper dimension. Considering the state-space minimal realization of G_S as earlier, the generalized plant becomes

$$P_{GS} = \left[\begin{array}{c|cc|c} A & 0 & B & B \\ \hline C & I & 0 & 0 \\ 0 & 0 & 0 & I \\ \hline C & I & 0 & 0 \end{array}\right] \tag{4.13}$$

Comparing (4.13) with Theorem 4.2, we have $A = A$, $B_1 = \begin{bmatrix} 0 & B \end{bmatrix}$, $B_2 = B$, $C_1 = \begin{bmatrix} C \\ 0 \end{bmatrix}$, $D_{11} = \begin{bmatrix} I & 0 \\ 0 & 0 \end{bmatrix}$, $D_{12} = \begin{bmatrix} 0 \\ I \end{bmatrix}$, $C_2 = C$ and $D_{21} = \begin{bmatrix} I & 0 \end{bmatrix}$. If the bases of the null spaces of $\begin{bmatrix} B_2^T & D_{12}^T \end{bmatrix} = \begin{bmatrix} B^T & 0 & I \end{bmatrix}$ and $\begin{bmatrix} C_2 & D_{21} \end{bmatrix} = \begin{bmatrix} C & I & 0 \end{bmatrix}$ are taken as $N_R = \begin{bmatrix} I & 0 \\ 0 & I \\ -B^T & 0 \end{bmatrix}$ and $N_S = \begin{bmatrix} -I & 0 \\ C & 0 \\ 0 & I \end{bmatrix}$ respectively, applying Theorem 4.2, the necessary and sufficient conditions for the existence of static H_∞ loop shaping controller are obtained as follows. The static H_∞ controller K_s exists, if and only if, the following inequalities hold

$$\begin{bmatrix} AR + RA^T - \gamma BB^T & RC^T & 0 & B \\ CR & -\gamma I & I & 0 \\ 0 & I & -\gamma I & 0 \\ B^T & 0 & 0 & -\gamma I \end{bmatrix} < 0 \tag{4.14}$$

$$\begin{bmatrix} A^T S + SA - \gamma C^T C & -SB \\ -B^T S & -\gamma I \end{bmatrix} < 0, \tag{4.15}$$

$$R = S^{-1} \tag{4.16}$$

with $R > 0,\ S > 0$ and $\gamma > 1$.
Here, (4.14) and (4.15) are the two LMI constraints with the variables R and R^{-1}

respectively. To avoid inversion of the variable, the following steps are carried out where the constraints are presented in LMI form with a new variable. Using Schur complement form in (4.14), after some algebraic simplifications, we have

$$\begin{bmatrix} AP + PA^T - \beta BB^T & PC^T \\ CP & -\beta I \end{bmatrix} < 0 \tag{4.17}$$

where $P = \gamma R$ and $\beta = \left(\gamma^2 - 1\right)$. Note that β is a positive number as $\gamma > 1$. Further, using Schur complement form in (4.15), one can rewrite (4.15) as

$$A^T S + SA - \gamma CC^T + \gamma^{-1} SBB^T S < 0. \tag{4.18}$$

Pre and post-multiplying (4.18) by S^{-1} and using (4.16), we have

$$PA^T + AP - PC^T CP + BB^T < 0. \tag{4.19}$$

Since $\beta > 0$, (4.17) fulfills the first constraint of (4.6) but its second can not be always satisfied by (4.19). To establish the second constraint of (4.6), one can rewrite (4.19) as

$$PA^T + AP - \beta PC^T CP + (\beta - 1)PC^T CP + BB^T < 0$$

$$\Rightarrow \; PA^T + AP - \beta PC^T CP < (1 - \beta)PC^T CP - BB^T. \tag{4.20}$$

It may be noted that (4.20) is achieved from (4.19) and they are equivalent to each other. For $\beta > 1$, $PA^T + AP - \beta PC^T CP < 0$ is always satisfied; hence, the second condition of (4.6) holds for the existence of static controller.

Note that the two inequalities (4.17) and (4.19) are involved with a variable P instead of R and R^{-1} but (4.19) is not in LMI form due to the products of same variable. To obtain the linear inequality condition, we introduce a matrix Y that is a stabilizing solution of (4.2) which, in turn, results the matrix $\left(A - YC^T C\right)$ is stable. Now, for all P, $(Y - P)^T C^T C \,(Y - P) \geq 0$ that implies

$$-PC^T CP \leq YC^T CY - YC^T CP - PC^T CY. \tag{4.21}$$

Using (4.19) and (4.21), if

$$PA^T + AP + YC^T CY - YC^T CP - PC^T CY + BB^T < 0 \tag{4.22}$$

is satisfied, (4.19) also will obviously be satisfied. Again from (4.2), $BB^T = -AY - YA^T + YC^TCY$ and replacing it in (4.22), we get

$$(P-Y)\left(A-YC^TC\right)^T + \left(A-YC^TC\right)(P-Y) < 0. \tag{4.23}$$

The solution of the above Lyapunov matrix inequality $(P-Y) = (P-Y)^T > 0$ exists as $\left(A-YC^TC\right)$ is Hurwitz. In (4.22), the unknown matrix is P and it is an LMI constraint. Using the Schur complement form, (4.22) can be rewritten as

$$\begin{pmatrix} AP + PA^T + YC^TCY - YC^TCP - PC^TCY & B \\ B^T & -I \end{pmatrix} < 0$$

hence, (4.12) is established. □

Remark 4.1: *From (4.20) it is clear that, we may have the feasible solution P with $0 < \beta < 1$, i.e., even though there exists the static controller it can not be obtained by using Theorem 4.3.*

Remark 4.2: *For the stable shaped plant, another set of sufficient conditions for the existence of static H_∞ loop shaping controller can also be obtained. If $\beta > 0$ and there exists a feasible solution $P = P^T > 0$ such that (4.11) and $PA^T + AP + BB^T < 0$ are satisfied, then, there exists static H_∞ loop shaping controller that satisfies (4.10).*

4.3.2 Controller reconstruction

In Theorem 4.3, the positive definite matrix P is obtained by solving the following optimization problem.

$$\begin{aligned} \text{Minimize} \quad & \beta \\ \text{Subject to} \quad & (4.11), (4.12) \text{ and } \beta > 1 \end{aligned} \tag{4.24}$$

From $\beta = \gamma^2 - 1$, the maximum robust stability margin $\left(\frac{1}{\gamma}\right)$ is calculated and since $P = \gamma R$, R is easily obtained. Here, P and β are the LMI variables which are involved with $\left(\frac{n(n+1)}{2} + 1\right)$ number of decision variables. Compared to [75]-[76], the numbers of LMI variables as well as decision variables are same with the proposed method. In this framework, the designed control law is $u = K_s y$ and from (4.13), the closed-loop system between w to z becomes

$$T_{zw} = \left[\begin{array}{c|c} A_{cl} & B_{cl} \\ \hline C_{cl} & D_{cl} \end{array}\right]$$

where $A_{cl} = A + BK_sC$, $B_{cl} = \begin{bmatrix} BK_s & B \end{bmatrix}$, $C_{cl} = \begin{bmatrix} C \\ K_sC \end{bmatrix}$ and $D_{cl} = \begin{bmatrix} I & 0 \\ K_s & 0 \end{bmatrix}$. Now using bounded real lemma, the closed-loop system is stable and $\|T_{zw}\|_\infty \leq \gamma$, if and only if, $R = R^T > 0$ such that

$$\begin{bmatrix} A_{cl}R + RA_{cl}^T & RC_{cl}^T & B_{cl} \\ C_{cl}R & -\gamma I & D_{cl} \\ B_{cl}^T & D_{cl}^T & -\gamma I \end{bmatrix} < 0. \tag{4.25}$$

Replacing closed-loop matrices in (4.25), we have

$$\begin{bmatrix} AR + RA^T + BK_sCR + RC^TK_s^TB^T & RC^T & RC^TK_s^T & BK_s & B \\ CR & -\gamma I & 0 & I & 0 \\ K_sCR & 0 & -\gamma I & K_s & 0 \\ K_s^TB^T & I & K_s^T & -\gamma I & 0 \\ B^T & 0 & 0 & 0 & -\gamma I \end{bmatrix} < 0. \tag{4.26}$$

Now, (4.26) can be written in the following form

$$\Psi + \varphi K_s \Phi + \Phi^T K_s^T \varphi^T < 0 \tag{4.27}$$

where,

$$\Psi = \begin{bmatrix} AR + RA^T & RC^T & 0 & 0 & B \\ CR & -\gamma I & 0 & I & 0 \\ 0 & 0 & -\gamma I & 0 & 0 \\ 0 & I & 0 & -\gamma I & 0 \\ B^T & 0 & 0 & 0 & -\gamma I \end{bmatrix}, \ \varphi = \begin{bmatrix} B \\ 0 \\ I \\ 0 \\ 0 \end{bmatrix}, \ \Phi = \begin{bmatrix} RC^T \\ 0 \\ 0 \\ I \\ 0 \end{bmatrix}^T.$$

The LMI (4.27) can be solved by using MATLAB LMI toolbox and subsequently the corresponding controller K_s is then found out. Finally, combining weight with the static controller K_s, as shown in Figure 4.1, the H_∞ loop shaping controller WK_s is obtained whose order is equal to the order of W. The design steps are illustrated below.

4.3.3 Design steps

1. Select pre and/or post-compensator(s) to meet closed-loop design specifications.
2. Realize the shaped plant in state-space form. Solve the optimization problem (4.24) and find P and β.
3. From β, find γ using the relation $\gamma = \sqrt{1+\beta}$. Then $R = \gamma^{-1}P$.
4. Solve controller LMI (4.27) to obtain the static controller K_s.
5. The final H_∞ loop shaping controller is obtained as $W_1K_sW_2$ where W_1 and W_2 are respectively the pre and post-compensator.

4.4 Numerical examples

Example 1[75]: The state-space realization of the shaped plant is

$$A = \begin{bmatrix} -0.0366 & 0.0271 & 0.0188 & -0.4555 \\ 0.0482 & -1.01 & 0.0024 & -4.0208 \\ 0.1002 & 0.3681 & -0.707 & 1.42 \\ 0 & 0 & 1 & 0 \end{bmatrix}, B = \begin{bmatrix} -0.4422 & 0.1676 \\ 3.5446 & -7.5922 \\ -5.52 & 4.49 \\ 0 & 0 \end{bmatrix}, C = \begin{bmatrix} 0 \\ 1 \\ 0 \\ 0 \end{bmatrix}^T$$

Applying Theorems 4.1 and 4.3, we obtain respectively $\gamma = 2.770$ and 2.773. To find these optimal values, the *'mincx'* command of LMI toolbox has been used [37]. In *'mincx'*, the optimal value is found out by an iterative method and the numbers of iterations are respectively 15 and 12, and subsequently the designed static controller gains are $\begin{bmatrix} -1.433 & 2.1477 \end{bmatrix}^T$ and $\begin{bmatrix} -1.4274 & 2.1493 \end{bmatrix}^T$.

Example 2 [112]: A transfer function model of VAR compensator has been taken into account to show the effectiveness of the proposed method. The nominal plant model is

$$G(s) = \frac{1}{(s+0.2124)(s^2+0.2492s+12.55)} \times$$
$$\begin{bmatrix} 0.2307s(s+33.56) & -3.2226(s^2+0.0934s+7.944) \\ -27.556(s+0.2308) & 3.5807(s+1.723)(s-1.261) \end{bmatrix}$$

In [112], a full order (FO) H_∞ loop shaping controller has been designed and we consider the same pre-compensator $W = \text{diag}\left(\frac{a(s+0.2)}{s}, \frac{b(s+0.2)}{s}\right)$ for designing static H_∞ loop shaping controller. For different values of a and b, the following results have been obtained.

In this example, with minimal realization of the shaped plant the order is 7 and the pre-compensator is with order 2. Hence, the designed full order and static controller (WK_s) have respectively the orders 7 and 2. In Theorem 4.1, the number of iterations is more compared to that of Theorem 4.3 and robust stability margins (γ) are almost same in both the methods. In Figures 4.2-4.5, the simulation results have been shown for a=0.1, b=0.2. The full order controller gives better performance, whereas the responses for static controllers which are obtained from Theorems 4.1 and 4.3 are overlapped.

a, b	γ			Iteration		K_s	
	Th4.1	Th4.3	FO	Th4.1	Th4.3	Th4.1	Th4.3
a=0.1, b=0.2	2.3572	2.3569	1.4723	28	23	$\begin{matrix} 0.2491 & 0.713 \\ 1.5807 & -1.2855 \end{matrix}$	$\begin{matrix} 0.2561 & 0.7103 \\ 1.614 & -1.3067 \end{matrix}$
a=0.1, b=0.3	2.2355	2.2347	1.5406	25	22	$\begin{matrix} 0.1252 & 0.8064 \\ 1.5005 & -1.196 \end{matrix}$	$\begin{matrix} 0.1262 & 0.8061 \\ 1.507 & -1.2005 \end{matrix}$
a=0.3, b=0.5	2.3477	2.3476	1.7093	26	22	$\begin{matrix} 0.0687 & 0.8995 \\ 1.0965 & -1.4062 \end{matrix}$	$\begin{matrix} 0.0694 & 0.8998 \\ 1.098 & -1.4084 \end{matrix}$

Table 4.1: Results of example 2

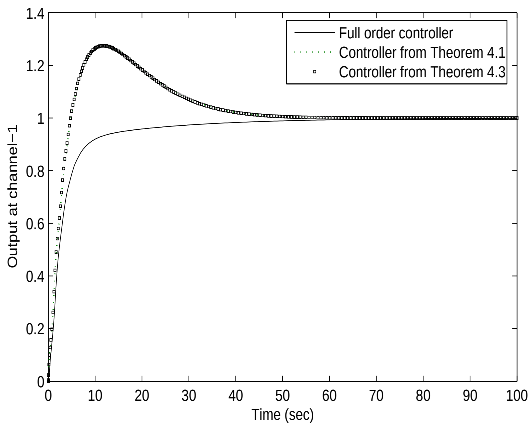

Figure 4.2: Output at channel-1 due to unit step change in channel-1 (for a=0.1, b=0.2)

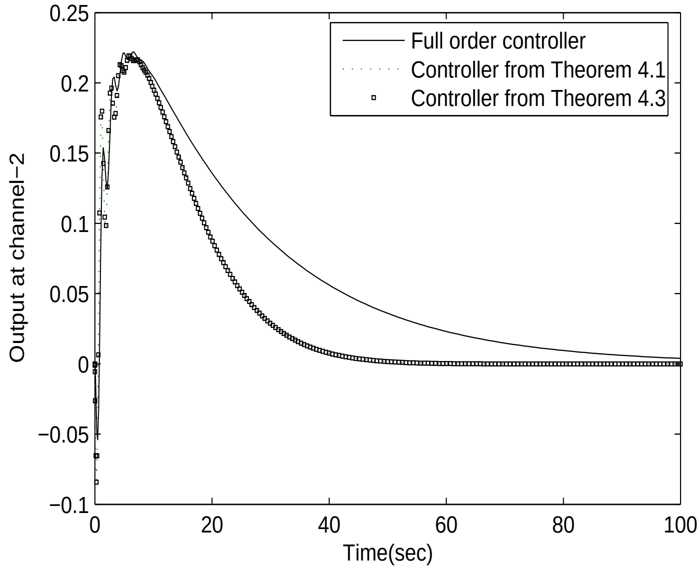

Figure 4.3: Output at channel-2 due to unit step change in channel-1(for a=0.1, b=0.2)

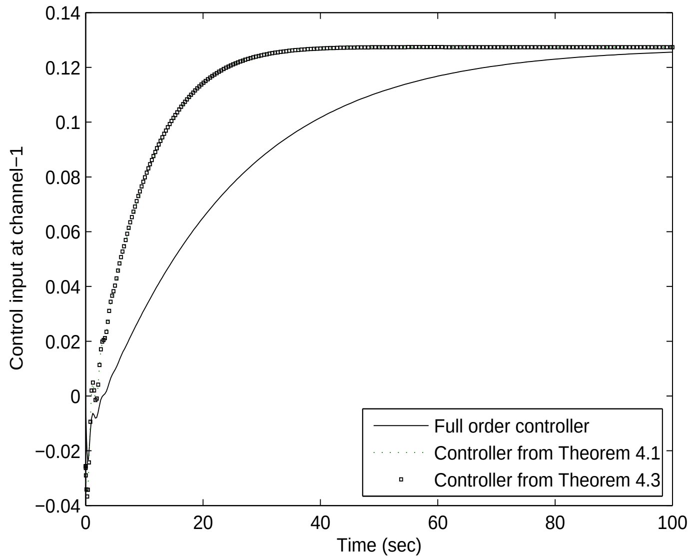

Figure 4.4: Control effort at channel-1(for a=0.1, b=0.2)

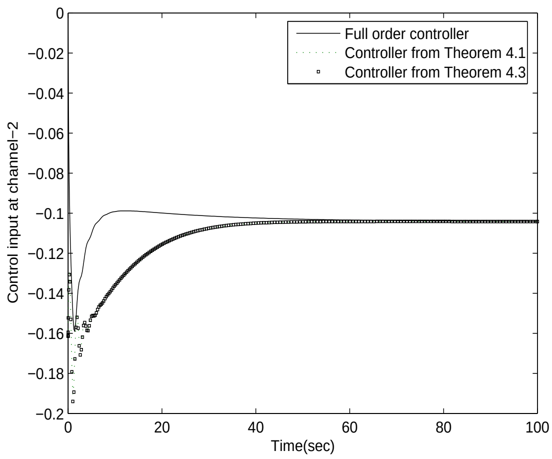

Figure 4.5: Control effort at channel-2 (for a=0.1, b=0.2)

4.5 Case study: Load frequency control of inter-connected power system

In this section, the load frequency control problem of power system has been studied. For this system, a static H_∞ loop controller is designed to ensure robustness of the closed-loop system. The design is challenging as the system has structured uncertainty. In simulation study, a simplified model of two-area interconnected power system has been considered and in the following, a brief overview has been given for load frequency control problem.

In power system, keeping the frequency within acceptable bounds requires to continuously maintain a balance between power generation and demand in presence of some uncertainties and disturbances of the system. This security action is performed by the load frequency control of power system that results output variations to generating units, through operation of speed governor, automatic generation control (AGC) and also through collective decisions of operators. The main objective is to regulate the output power of each generating unit at prescribed levels while keeping the frequency fluctuations within pre-specified limits. In an interconnected power system, due to change in load demand the frequency deviation occurs which has an adverse effect on both the consumer and supply side and it is also cause for the fluctuation of power flow in tie-lines. To suppress these effects, a closed-loop control scheme is required. Towards this objective, in last few decades several methods have been proposed based on some classical and modern techniques [2, 15, 29, 32, 58, 85, 89]. Usually, the load frequency controllers are lower order classical Proportional and Integral (PI) type and, are tuned online by trial-error methods. These techniques usually do not consider the effects of uncertainty and disturbances of the system. Recently, some robust and adaptive control schemes have been developed to deal with parameter variation as well as to improve the performance of interconnected power systems [12, 13, 77]. In this direction, H_∞ control becomes a popular design technique that optimally achieves the robust performance and stability of the inter-connected power system in presence of parametric uncertainty. It gives higher order controller which is a drawback of this method. This order is same with the order of augmented plant and it is usually high due to presence of design weights. The implementation of higher order controllers will lead to high cost, poor reliability and potential problems in realization. In [12], a different technique has been proposed to design a lower order load frequency controller with PI structure using LMI approach. Interestingly, the lower order H_∞ loop shaping controller proposed in this chapter is free from these drawbacks. In power systems, the design techniques described in [64, 65] have already been applied for robust controller synthesis and relevant to this, some research works can also be found in the literatures [31, 62, 115].

In this section, the LFC problem has been studied leading to two major contributions: the application static (lower order) H_∞ loop shaping controller to LFC problem and guaranteeing stability in presence of parametric uncertainty of the system using real structured singular value (μ) analysis. For simulation study, a two-area interconnected power system model has been adopted. The performance of the proposed designed controller has also been compared with the full order H_∞ loop shaping controller. To analyze stability with respect to parametric uncertainty of the system, the mathematical model is simplified to a standard LFT structure. Then, the real μ-analysis has been carried out to ensure the robust stability of the system.

4.5.1 Modeling of two-area interconnected power system

We have considered a two-area interconnected power steam plants [29, 77] whose model in state-space form can be described as

$$\left.\begin{aligned} \dot{x}(t) &= A_m x(t) + B_m u(t) + \Gamma_m p(t) \\ y(t) &= C_m x(t) + d(t) \end{aligned}\right\} \tag{4.28}$$

where, $x(t), u(t), p(t), d(t)$ are respectively the state vector, control vector, the step change in load demand and disturbances at the output with proper dimensions. The state vector is $x = \begin{bmatrix} \Delta f_1 & \Delta P_{g1} & \Delta X_{g1} & \Delta P_{tie} & \Delta f_2 & \Delta P_{g2} & \Delta X_{g2} \end{bmatrix}^T$, where Δf_i is the frequency deviation, the turbine-generator output is ΔP_{gi} and ΔX_{gi} is the governor output for $i = 1, 2$. The tie-line power of the system is ΔP_{tie}. The outputs $y_1 = \Delta ACE_1 = \Delta f_1 + \Delta P_{tie}$ and $y_2 = \Delta ACE_2 = \Delta f_2 - \Delta P_{tie}$ are known as area control errors. The load demand and disturbance vectors have been considered as $p = \begin{bmatrix} \Delta P_{d1} & \Delta P_{d2} \end{bmatrix}^T$ and $d = \begin{bmatrix} d_1 & d_2 \end{bmatrix}^T$ respectively. Now, the system matrices for the two-area interconnected power system are given as below [29].

$$A_m = \begin{bmatrix} -\frac{1}{T_{P1}} & \frac{K_{P1}}{T_{P1}} & 0 & -\frac{K_{P1}}{T_{P1}} & 0 & 0 & 0 \\ 0 & -\frac{1}{T_{T1}} & \frac{1}{T_{T1}} & 0 & 0 & 0 & 0 \\ -\frac{1}{R_1 T_{G1}} & 0 & -\frac{1}{T_{G1}} & 0 & 0 & 0 & 0 \\ T_{12} & 0 & 0 & 0 & -T_{12} & 0 & 0 \\ 0 & 0 & 0 & \frac{K_{P2}}{T_{P2}} & -\frac{1}{T_{P2}} & \frac{K_{P2}}{T_{P2}} & 0 \\ 0 & 0 & 0 & 0 & 0 & -\frac{1}{T_{T2}} & \frac{1}{T_{T2}} \\ 0 & 0 & 0 & 0 & -\frac{1}{R_2 T_{G2}} & 0 & -\frac{1}{T_{G2}} \end{bmatrix}$$

$$B_m = \begin{bmatrix} 0 & 0 & \frac{1}{T_{G1}} & 0 & 0 & 0 & 0 \\ 0 & 0 & 0 & 0 & 0 & 0 & \frac{1}{T_{G2}} \end{bmatrix}^T, \Gamma_m = \begin{bmatrix} -\frac{K_{P1}}{T_{P1}} & 0 & 0 & 0 & 0 & 0 & 0 \\ 0 & 0 & 0 & 0 & -\frac{K_{P2}}{T_{P2}} & 0 & 0 \end{bmatrix}^T.$$

T_G^0 (sec)	T_{12}^0 (p.u.)	T_T^0 (sec)	T_P^0 (sec)	K_P^0 (Hz/p.u. MW)	R^0 (Hz/p.u. MW)	K_E^0 (p.u./Hz MW)
0.080	0.545	0.3	20	120	2.4	0.425

Table 4.2: Nominal values of the parameters of two-area interconnected power system

In Table 4.2 the nominal values of the plant parameters have been given as described in [29]. The nominal values are same for both the areas, as for example, $T_P^0 = T_{P1}^0 = T_{P2}^0 = 20sec$. Assuming the parameter variation around the normalized value of K_E is equal to zero, the ranges of the other system parameters are considered as follows:

$$0.04 \leq \frac{1}{T_P} \leq 0.06,\ 4.8 \leq \frac{K_P}{T_P} \leq 7.2,\ 2.664 \leq \frac{1}{T_T} \leq 3.996,$$

$$4.1666 \leq \frac{1}{RT_G} \leq 6.25,\ 10 \leq \frac{1}{T_G} \leq 15.$$

That is, $\pm 20\%$ perturbation with respect to the nominal values of the parameters has been considered.

4.5.2 State-space parametric uncertainty

In state-space model it has been observed that, there are five ratio variables from where the uncertainty originates in the system. To capture all these distributed uncertain parameters in a single block Δ, the following steps have been carried out.

The nominal state-space matrices of the system are defined as A_0, B_0, Γ_0 and C_0. Now, corresponding to varying ratios $\frac{1}{T_P}, \frac{K_P}{T_P}, \frac{1}{T_T}, \frac{1}{RT_G}$ and $\frac{1}{T_G}$, the following five real parameters $\delta_1, \delta_2, \delta_3, \delta_4$ and δ_5 have been considered and the state-space model (4.28) can be represented as

$$\left.\begin{aligned} \dot{x}(t) &= \left(A_0 + \textstyle\sum_{i=1}^{5} \delta_i A_i\right) x(t) + (B_0 + \delta_3 B_3)u(t) + (\Gamma_0 + \delta_2 \Gamma_2)p(t) \\ y(t) &= C_0 x(t) + d(t) \end{aligned}\right\} \tag{4.29}$$

where, $\delta_i \in \begin{bmatrix} -1 & 1 \end{bmatrix}, i = 1, \ldots, 5$. Here, $\pm 20\%$ perturbation is considered and it yields, the nominal values of varying ratios in $A_i, i = 1, \ldots, 5, B_3$ and Γ_2 should be multiplied with 0.2 to keep all the five real parameters in the range -1 to +1. Now, from the state-space matrices A_m, B_m and Γ_m, we have

$$A_1 = \begin{bmatrix} -\frac{1}{5T_{P1}^0} & 0 & 0 & 0 & 0 & 0 & 0 \\ 0 & 0 & 0 & 0 & 0 & 0 & 0 \\ 0 & 0 & 0 & 0 & 0 & 0 & 0 \\ 0 & 0 & 0 & 0 & 0 & 0 & 0 \\ 0 & 0 & 0 & 0 & -\frac{1}{5T_{P2}^0} & 0 & 0 \\ 0 & 0 & 0 & 0 & 0 & 0 & 0 \\ 0 & 0 & 0 & 0 & 0 & 0 & 0 \end{bmatrix},$$

$$B_3 = \begin{bmatrix} 0 & 0 & \frac{1}{5T_{G1}^0} & 0 & 0 & 0 & 0 \\ 0 & 0 & 0 & 0 & 0 & 0 & \frac{1}{5T_{G2}^0} \end{bmatrix}^T, \Gamma_2 = \begin{bmatrix} -\frac{K_{P1}^0}{5T_{P1}^0} & 0 & 0 & 0 & 0 & 0 & 0 \\ 0 & 0 & 0 & 0 & -\frac{K_{P2}^0}{5T_{P2}^0} & 0 & 0 \end{bmatrix}^T,$$

and A_2, A_3, A_4, A_5 easily can be found as we obtain A_1. Now, the state equation of

(4.29) can be written as follows:

$$\dot{x}(t) = (A_0 x(t) + B_0 u(t) + \Gamma_0 p(t)) + U\Delta(\bar{A}x(t) + \bar{B}u(t) + \bar{\Gamma}p(t))$$

where, $U = \begin{bmatrix} I_7 & I_7 & I_7 & I_7 & I_7 & I_7 & I_7 \end{bmatrix}$, $\bar{A} = \begin{bmatrix} A_1^T & A_2^T & 0 & A_3^T & 0 & A_4^T & A_5^T \end{bmatrix}^T$, $\bar{B} = \begin{bmatrix} 0 & 0 & 0 & 0 & B_3^T & 0 & 0 \end{bmatrix}^T$, $\bar{\Gamma} = \begin{bmatrix} 0 & 0 & \Gamma_2^T & 0 & 0 & 0 & 0 \end{bmatrix}^T$ and the uncertainty block $\Delta = diag(\ \delta_1 I_7,\ \ \delta_2 I_{14},\ \ \delta_3 I_{14},\ \ \delta_4 I_7,\ \ \delta_5 I_7\ )$. With this uncertainty description, the two-area interconnected power system can be represented by a block-diagram as shown in Figure 4.6. Here, $K_L = W K_s = \left[\begin{array}{c|c} A_{kL} & B_{kL} \\ \hline C_{kL} & 0 \end{array}\right]$ is the H_∞ loop shaping

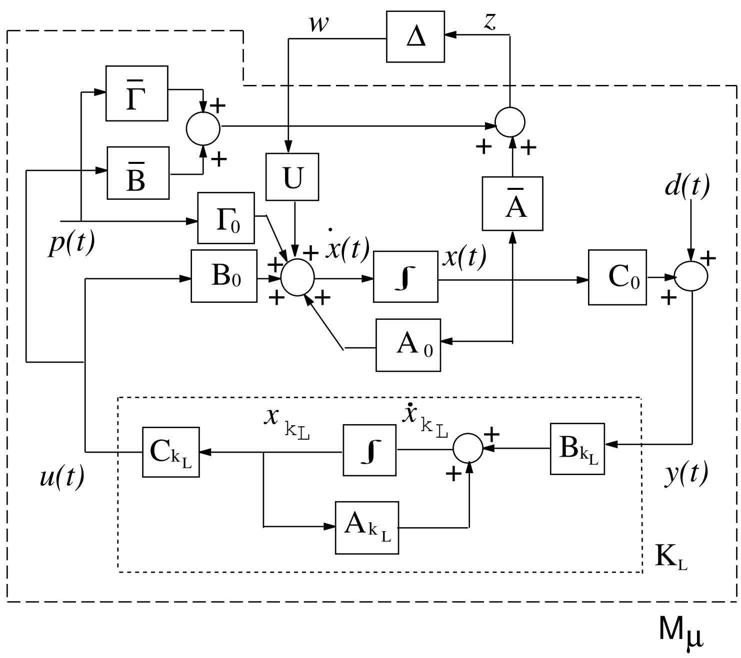

Figure 4.6: Block-diagram for two-area interconnected power system

controller that has to be designed using the method described in preceding section. To ensure robust stability against structured uncertainty of the two-area interconnected power system, the state-space model is represented as shown in Figure 4.6. Here, the parameters of the system that structurally vary within a given range, have been taken out and accumulated in a single block. This block, Δ is structured and essentially indicates the uncertainty of the system and simplifies the framework for robust stability analysis of the closed-loop system. Towards this notion, for the designed controller K_L

the real μ-analysis has been carried out and the block-diagram is simplified as shown in Figure 4.7. There an interconnected transfer function matrix M_μ is formed with

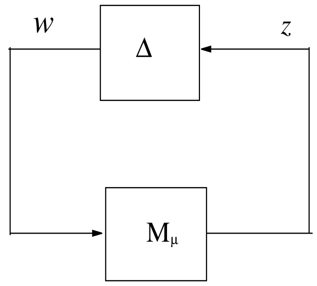

Figure 4.7: μ analysis for robust stabilization

respect to the uncertainty set Δ and for this framework, the structured singular value μ is defined as

$$\mu(M_\mu) = \frac{1}{\min_{\Delta \in S}\{\bar{\sigma}(\Delta) : \det(I - M_\mu \Delta) = 0\}}$$

where, S is the set of allowable perturbations. Now, as $\delta_i \in \begin{bmatrix} -1 & 1 \end{bmatrix}$, the $sup_{\omega \in R}$ $\mu(M_\mu(j\omega)) < 1$ ensures the robust stability of the closed-loop two-area interconnected power system for $\pm 20\%$ perturbations of the nominal values.

4.5.3 Controller design and simulation results

From Table 4.2, we have the nominal system matrices for the two-area interconnected power system as follows.

$$A_0 = \begin{bmatrix} -0.05 & 6.0 & 0 & -6.0 & 0 & 0 & 0 \\ 0 & -3.33 & 3.33 & 0 & 0 & 0 & 0 \\ -5.2083 & 0 & -12.5 & 0 & 0 & 0 & 0 \\ 0.545 & 0 & 0 & 0 & -0.545 & 0 & 0 \\ 0 & 0 & 0 & 6.0 & -0.05 & 6.0 & 0 \\ 0 & 0 & 0 & 0 & 0 & -3.33 & 3.33 \\ 0 & 0 & 0 & 0 & -5.2083 & 0 & -12.5 \end{bmatrix}$$

$$B_0 = \begin{bmatrix} 0 & 0 & 12.5 & 0 & 0 & 0 & 0 \\ 0 & 0 & 0 & 0 & 0 & 0 & 12.5 \end{bmatrix}^T, \Gamma_0 = \begin{bmatrix} -6.0 & 0 & 0 & 0 & 0 & 0 & 0 \\ 0 & 0 & 0 & 0 & -6.0 & 0 & 0 \end{bmatrix}^T$$

$$C_0 = \begin{bmatrix} 1 & 0 & 0 & 1 & 0 & 0 & 0 \\ 0 & 0 & 0 & -1 & 1 & 0 & 0 \end{bmatrix}$$

To suppress the effects of change in load demand on frequency deviation and area control error, a pre-compensator is selected to shape the singular values of the open-loop plant. Post-compensator is taken as an identity matrix with proper dimension. The pre-compensator contains a pole at origin to make the steady state error zero as well as to attenuate the effect of disturbances at the output of the system. In the design procedure the pre-compensator is selected as

$$\frac{1.4(s+0.5)}{s(s+1)} I_2.$$

The singular values of the shaped and nominal plant have been shown in Figure 4.8.

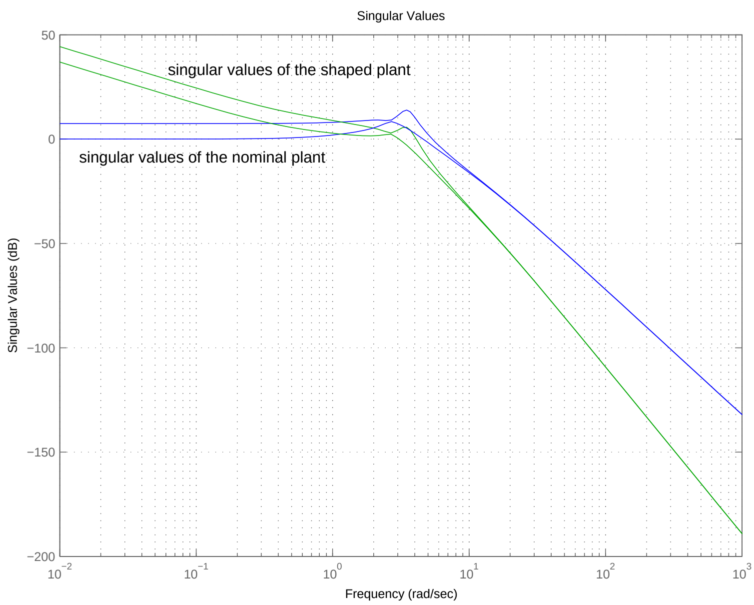

Figure 4.8: Singular values of the shaped and nominal plant

From this shaped plant, the robust stability margin has been calculated. For full order controller $\gamma = 2.1466$ and in lower order case (static controller case), it is obtained 4.7226. Hence, the lower order controller ensures less robust stability margin compared to full order controller.

In Figures 4.9-4.12, the performance of the controllers has been studied. With 10% change in load demand, the frequency deviation and area control error in both the

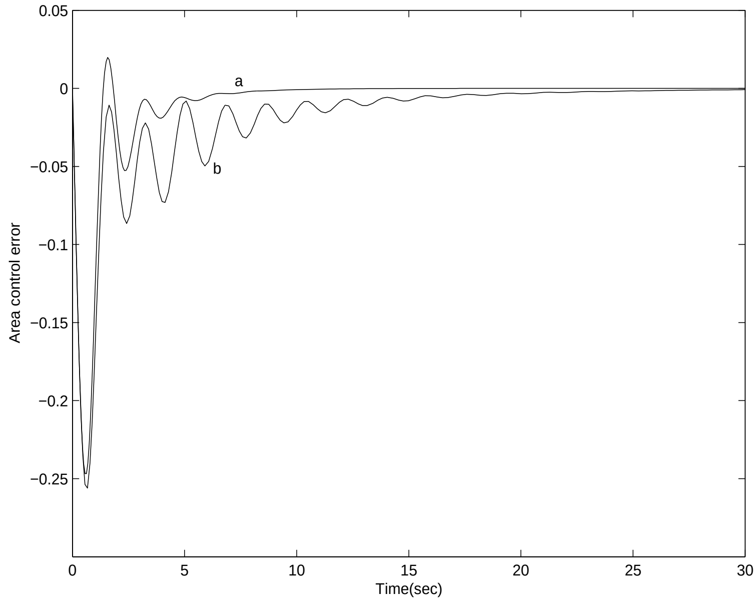

Figure 4.9: Area control error in area-1 due to 10% change in load demand in area-1, a: full order controller b: lower order controller

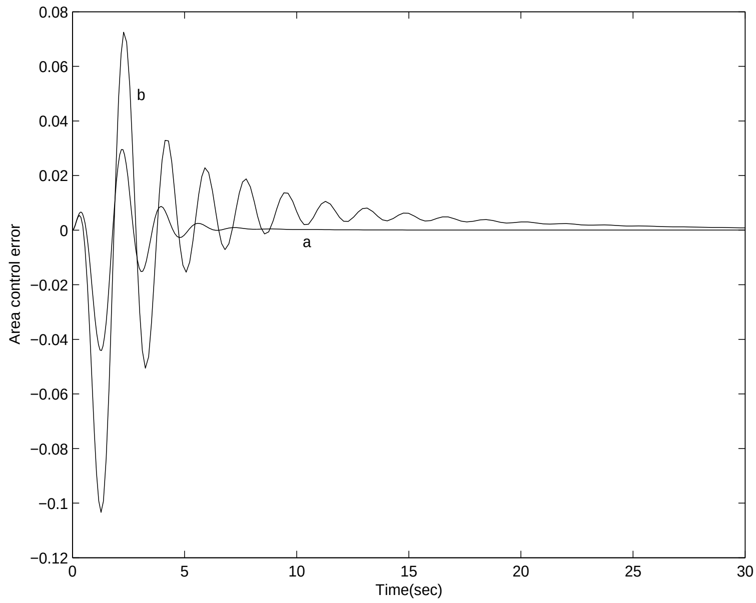

Figure 4.10: Area control error in area-2 due to 10% change in load demand in area-1, a: full order controller b: lower order controller

areas have been shown. The full order controller gives better performance compared to lower order controller. In case of lower order controller, there is more oscillation in the transient part leading to more peak overshoot and settling time of the system. The designed static controller is

$$K_s = \begin{bmatrix} -0.2394 & -0.0235 \\ -0.0222 & -0.2396 \end{bmatrix}.$$

Finally, the static H_∞ loop shaping controller is obtained by combining the pre-compensator with K_s. Due to slowly varying load demand in area 1, the area control error in the same area has been shown in Figure 4.13 and both the controllers give satisfactory performance.

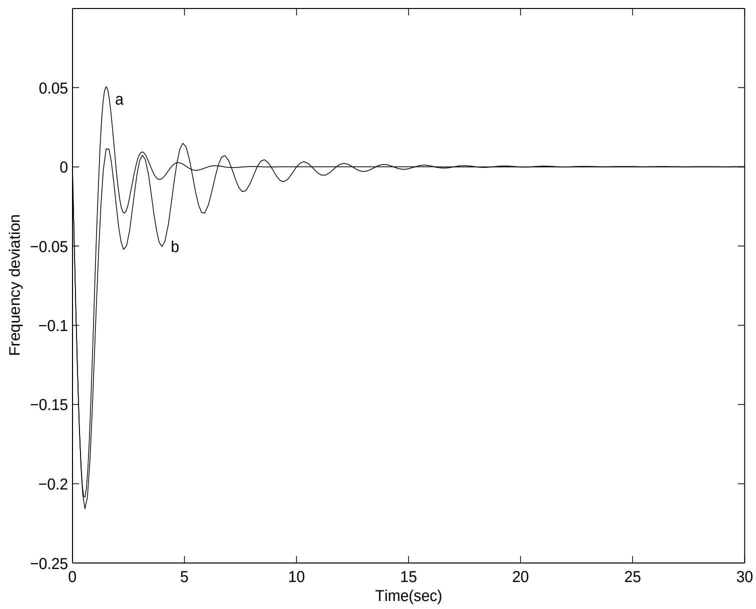

Figure 4.11: Frequency deviation in area-1 due to 10% change in load demand in area-1, a: full order controller, b: lower order controller

Now, we analyze the robust stability of the system in face of ±20% perturbation of the parameters. As the H_∞ loop shaping controller is designed based on unstructured normalized coprime factor uncertainty description, the controller can not ensure the closed-loop stability in presence of parametric uncertainty of the system. Here, the real μ-analysis has been performed to show stability of the system. In all frequencies, if the structured singular value (μ) of M_μ (see Figure 4.7) becomes less than one, it ensures robust stability of the system within specified (±20%) parameter variation. In Figure 4.14, the μ plot for both the controllers has been shown that indicates, the full order controller can take more perturbation than the lower order controller.

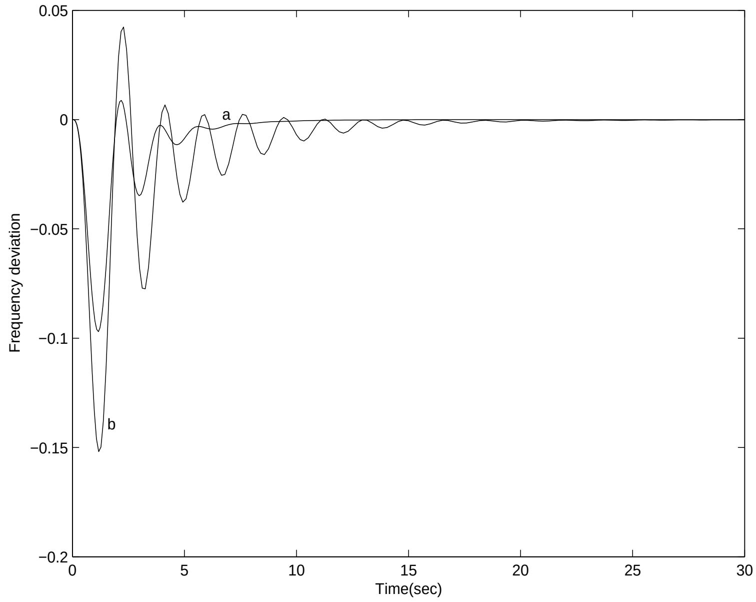

Figure 4.12: Frequency deviation in area-2 due to 10% change in load demand in area-1, a: full order controller, b: lower order controller

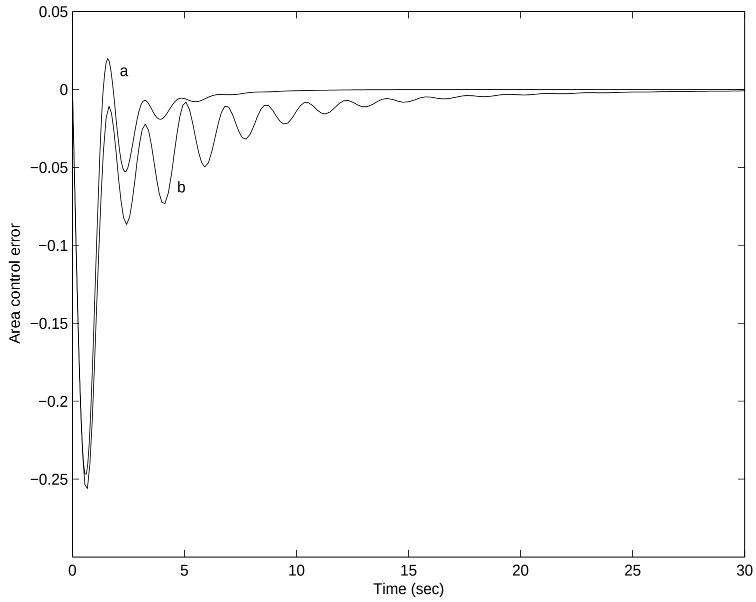

Figure 4.13: Area control error in area-1 due to 0.1(1+sin0.001t)% change in load demand in area-1, a: full order controller, b: lower order controller

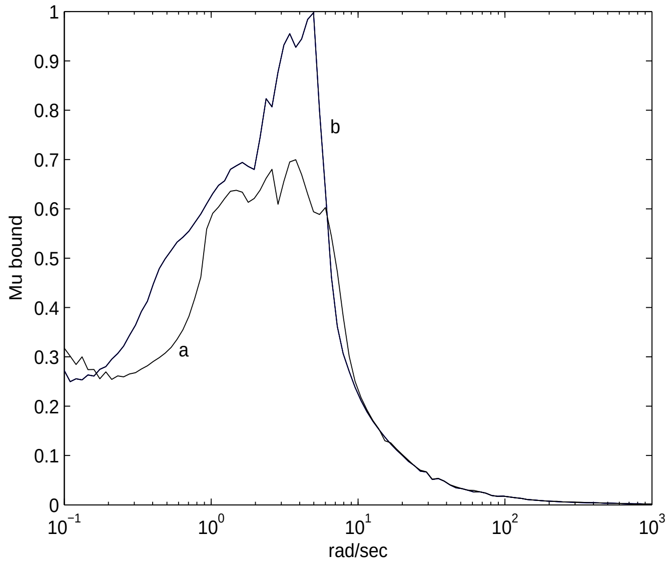

Figure 4.14: μ plot for robust stability, a: full order controller, b: lower order controller

4.6 Conclusions

In this chapter, a new set of sufficient conditions for the existence of static H_∞ loop shaping controller has been proposed. The results are obtained in four-block H_∞ synthesis framework which is equivalent to the normalized coprime factor robust stabilization problem. This result has been compared with [76] and from the present work, it is obvious that the minimum achievable γ can not be less than equal to 1.414 (since, $\beta > 1, \gamma = \sqrt{1+\beta}$). The work is numerically attractive as the constraints are posed in LMI form that can be solved efficiently with standard MATLAB LMI solvers [37]. In Remark 4.2, a different set of sufficient conditions for the existence of static H_∞ loop shaping controller has also been derived for the stable shaped plant. The effectiveness of the proposed method has been elucidated through two numerical examples. Also note that, the proposed method may provide an alternative but a simple platform for designing the static output feedback H_∞ loop shaping controller for the LTI plant which is subject to input saturation as well as for the problem with pole placement constraint.

In Section 4.5, the proposed method has been applied to load frequency control problem of inter-connected power system to verify the efficacy of the proposed control algorithm. The robustness of the system is ensured against the load disturbances and parametric uncertainty of the system. To this objective, the real μ-analysis has been performed to study the stability of the plant with structured model uncertainty. The performance of static H_∞ loop shaping controller has been compared with the full-order H_∞ loop shaping controller. It has been observed that the system with full order H_∞ controller can withstand more structured perturbation than the static (lower order) H_∞ loop shaping controller.

CHAPTER 5

Local stabilization with bounded control inputs via H_∞ loop shaping approach

So far, the constraint on control input is not yet considered in the design problems. In practical situations, the control input constraints to the plant can not be avoided and needs extra care for controller synthesis. Ignoring control input constraints, if a controller is designed and is placed in closed-loop structure, the system's performance will be deteriorated when large control input signal appears to the plant that exceeds the specified bound, and even, it may cause for instability too. In this chapter, control input bounds have been taken into account while parametric H_∞ loop shaping output feedback controller is designed to achieve local stability of the closed-loop system. The problem addressed in this chapter is basically a special case of actuator saturation control problem where control inputs to the plant are never allowed to reach into saturation region. In the proposed method, the uncertainty of the plant is presented as perturbations to normalized left coprime factors of the shaped plant. Finally, two numerical examples have been elucidated to show the effectiveness of the proposed method.

5.1 Introduction

In recent years, a class of research workers has shown keen interest on the stabilization problem of LTI plant with bounded control inputs ([44, 47, 52, 110] and references therein). Specifically, the LTI plant with actuator saturation is a practical situation where, the design of controller to stabilize such system is a challenging task and it is mainly directed into two approaches. In first approach, quite often the controller synthesis is carried out ignoring the effects of saturation, where some retro fitted schemes (anti-windup) and analytical methods are adopted for improving performance and stability of the closed-loop system. However, in analytical framework it is trivial fact that, an internally stable system always explore a local stability region in state-space while it is subjected to bounded control inputs or actuator saturation, but only challenge is to design feedback control law that can achieve a domain of attraction large enough.

On the other hand, the second approach is involved with more complex design framework where the control input constraints are taken into synthesis phase. In literatures, several state and output feedback controller design methods have been addressed for the stabilization of LTI plant in local or global sense [44, 47, 84]. For open-loop stable plant, the global or semi-global stability can be achieved with bounded control inputs, whereas in absence of open-loop stability assumption, a linear feedback controller can only reveal the local stability of the closed-loop system [44]. In local stabilization problem, the involved interest is mainly to synthesize a stabilizing controller that maximizes region of attraction and subsequently, gives an estimation of it. Meanwhile in global stability, the region of attraction becomes the whole state-space. On the other hand, the construction of stabilizing feedback law with constraint inputs or with actuator saturation addressed as semi-global stabilization problem while the estimated stability region encloses a priori given bounded set (arbitrarily large) in the state-space. Interestingly it has to be noted that, the bounded control input problem is the linear case of actuator saturation control problem, that is, the control inputs never go into saturation. However, if the input to saturation element is bounded, the actuator can be modeled locally and it falls into sector bounded stabilizing solution of control problem. In that case, all state vectors belong to the region of attraction also satisfy the sector-bound condition which has been addressed in this next chapter.

Here, an output feedback controller has been designed to achieve the local stability of uncertain LTI plant with bounded control inputs. By introducing a free scalar parameter, the design has been performed in parametric H_∞ loop shaping framework where the unstructured uncertainty of the plant is presented as perturbations to normalized coprime factors of the shaped plant [41, 65]. In the proposed technique, no open-loop stability assumption is made that leads the design approach to local stabilization problem. To show the stability of closed-loop system, a quadratic type Lyapunov function is considered and subsequently, an estimation is also provided for the region or domain of attraction. For the existence of stabilizing controller, a set of sufficient conditions is established in LMI form.

The chapter is organized as follows:

In Section 5.2, the local stabilization problem of LTI plant with bounded control inputs has been described. Then in Section 5.3, the problem statements are given and in Section 5.4, using H_∞ loop shaping approach the local stabilization problem has been solved for LTI plant with bounded control inputs. It consists of two parts; in first part, the uncertainty of the plant is not considered and in second part, a stability bound is found out leading to establish the local stability of an uncertain LTI plant. Subsequently, the region of attraction has also been maximized. In Section 5.5, two numerical examples have been considered to show the effectiveness of the proposed method. Finally, the concluding remarks are drawn in Section 5.6.

5.2 Local stability of LTI plant with bounded control inputs

Let us consider an LTI plant G whose state-space model is

$$\left.\begin{aligned} \dot{x_n} &= A_n x_n + B_n u_n \\ y_n &= C_n x_n + D_n u_n \end{aligned}\right\} \tag{5.1}$$

where $x_n \in \Re^n$, $u_n \in \Re^m$ and $y_n \in \Re^p$. We assume (A_n, B_n, C_n) is stabilizable and detectable, and no assumption is made for open-loop stability of the system (5.1). The control input $u_n = [u_{n1}, \ldots, u_{nm}]^T$ is bounded where at i^{th} channel, $u_{ni} \in \begin{bmatrix} -u_{0i} & u_{0i} \end{bmatrix}$, $u_{0i} > 0,\ i = 1, \ldots, m$. Without loss of generality, it can be rewritten as $u_{ni} \in \begin{bmatrix} -1 & 1 \end{bmatrix}$, $i = 1, \ldots, m$ by appropriately scaling the matrices B_n and D_n. Now, considering an output feedback controller

$$\left.\begin{aligned} \dot{x_c} &= A_c x_c + B_c y_n \\ u_n &= C_c x_c \end{aligned}\right\} \tag{5.2}$$

where $x_c \in \Re^{n_c}$, the closed-loop system becomes

$$\dot{x_{cl}} = A_{cl} x_{cl} \tag{5.3}$$

where, $x_{cl} = \begin{bmatrix} x_n^T & x_c^T \end{bmatrix}^T \in \Re^{n+n_c}$ and $A_{cl} = \begin{bmatrix} A_n & B_n C_c \\ B_c C_n & A_c + B_c D_n C_c \end{bmatrix}$.

Definition 5.1 [47]: *With bounded control inputs as mentioned above, a dynamic controller (5.2) has to be designed such that the closed-loop system (5.3) is quadratically stable and subsequently, a set D_0 of initial state vectors has to be estimated such that $\forall\ x_{cl}^0 \in D_0$, the trajectories of (5.3) converge to origin as time tends to infinity. This problem is known as the local stabilization problem of LTI plant with bounded control inputs.*

Definition 5.2 [47]: *The set D_0 is the region of attraction for the closed-loop system (5.3) with respect to the equilibrium point origin, namely*

$$D_0 = \left\{ x_{cl}^0 \in \Re^{n+n_c} : \lim_{t\to\infty} x_{cl}(t) = 0\ \forall x_{cl}(0) = x_{cl}^0 \right\}.$$

5.3 Problem statements

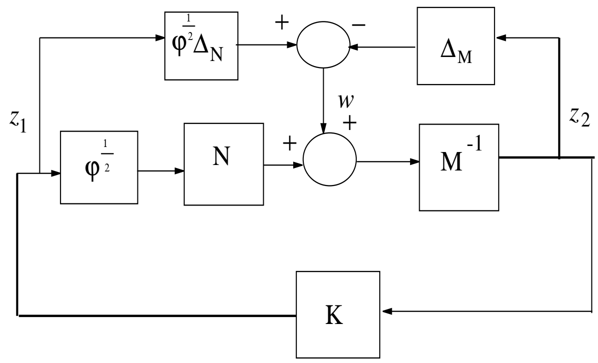

Figure 5.1: Block-diagram for parametric H_∞ loop shaping control

The nominal plant (5.1) is given whose control inputs are bounded, $u_{ni} \in \begin{bmatrix} -1 & 1 \end{bmatrix}$, $i = 1, \ldots, m$. An output feedback controller (5.2) has to be designed to achieve local stability of the closed-loop system. To fulfill this objective, a design framework based on parametric H_∞ loop shaping control has been adopted which is shown in Figure 5.1.

In this figure, the blocks M and N are the normalized left coprime factors of the shaped plant $G_S = W_2GW_1$ where, W_2 and W_1 are respectively the post and pre-compensator selected in order to meet design specifications[1].

Remark 5.1: *In H_∞ loop shaping control (discussed in preceding chapters), the compensators are selected to satisfy closed-loop design specifications like, disturbance attenuation, tracking performance, robust stability margin etc. However, for local stabilization problem as mentioned in Definition 5.1, these specifications are not the primary concern. In case of uncertain LTI plant, the compensators have to be selected such that the shaped plant depicts a good robust stability margin.*

Remark 5.2: *The loop shaping controller is $\varphi^{\frac{1}{2}}W_1KW_2$ whereas the controller K is designed based on the shaped plant $\varphi^{\frac{1}{2}}W_2GW_1$. Since there is constraint on control input, the singular values of the shaped plant do not remain in desired values when input exceeds the limit, that in turn affects on controller synthesis and explores a complicated design task. In the proposed framework, φ can be viewed as a tuning parameter of controller gain which is selected from a given range by solving an optimization problem. The range is selected by the designer and by changing this range, the controller performance can be improved.*

Remark 5.3: *φ is an unknown scalar design parameter. The design framework shown in Chapter 3 can be obtained by replacing $\varphi = \lambda^{-2}$, however it is different as λ was considered in Chapter 3 as a known given parameter.*

Let the selected post and pre-compensators be respectively

$$W_2 = \left[\begin{array}{c|c} A_{w2} & B_{w2} \\ \hline C_{w2} & 0 \end{array}\right] \text{ and } W_1 = \left[\begin{array}{c|c} A_{w1} & B_{w1} \\ \hline C_{w1} & 0 \end{array}\right],$$

where, $A_{w2} \in \Re^{n_{w2} \times n_{w2}}$ and $A_{w1} \in \Re^{n_{w1} \times n_{w1}}$. Defining the state vectors of post and pre-compensator respectively as x_{w2} and x_{w1}; output of W_2 as y_{w2} and input to W_1 as

[1]To generalize the design framework, the post and pre-compensators have been considered.

u_{w1}, the shaped plant $G_S = W_2 G W_1$ becomes

$$\left[\begin{array}{c} \dot{x_n} \\ \dot{x_{w2}} \\ \dot{x_{w1}} \\ \hline y_{w2} \end{array}\right] = \left[\begin{array}{ccc|c} A_n & 0 & B_n C_{w1} & 0 \\ B_{w2} C_n & A_{w2} & B_{w2} D_n C_{w1} & 0 \\ 0 & 0 & A_{w1} & B_{w1} \\ \hline 0 & C_{w2} & 0 & 0 \end{array}\right] \left[\begin{array}{c} x_n \\ x_{w2} \\ x_{w1} \\ \hline u_{w1} \end{array}\right]$$

$$\Rightarrow \left[\begin{array}{c} \dot{x_s} \\ \hline y_{w2} \end{array}\right] = \left[\begin{array}{c|c} A & B \\ \hline C & 0 \end{array}\right] \left[\begin{array}{c} x_s \\ \hline u_{w1} \end{array}\right], \tag{5.4}$$

where $x_s = \left[\begin{array}{ccc} x_n^T & x_{w2}^T & x_{w1}^T \end{array}\right]^T$. Let we assume, (A, B, C) is stabilizable and detectable. Then, the normalized left coprime factorization of $G_S = M^{-1}N$ whose state-space realization becomes as follows [65].

$$\left[\begin{array}{c|c} N & M \end{array}\right] = \left[\begin{array}{c|cc} A + LC & B & L \\ \hline C & 0 & I \end{array}\right], \tag{5.5}$$

where $L = -ZC^T$ is a stabilizing observer gain and Z is the symmetric positive semi-definite solution of the algebraic Riccati equation

$$AZ + ZA^T - ZC^T CZ + BB^T = 0. \tag{5.6}$$

In parametric H_∞ loop shaping framework shown in Figure 5.1, the parameter φ scales each channel of the input matrix, however, does not alter the state-space realization of the normalized coprime factors of the shaped plant. In this figure, considering the objective signal vector as $\left[\begin{array}{cc} z_2^T & z_1^T \end{array}\right]^T$ and exogenous signal as w, the generalized plant in linear fractional transformation (LFT) structure becomes

$$P_p = \left[\begin{array}{c|c|c} A & -L & \varphi^{\frac{1}{2}} B \\ \hline C & I & 0 \\ 0 & 0 & I \\ \hline C & I & 0 \end{array}\right]. \tag{5.7}$$

Now, we assume $(A, \varphi^{\frac{1}{2}} B, C)$ is stabilizable and detectable for all $\varphi > 0$. Then, there exists a stabilizing controller $\varphi^{\frac{1}{2}} K$, if and only if, the control ARE has a positive semi-definite solution X_∞ (see Theorem 3.1 in Chapter 3). Since P_p is with disturbance feedforward structure, the controller K can be realized in an observer form and it becomes

$$K(s) = \left[\begin{array}{c|c} A - \varphi BB^T X_\infty + LC & -L \\ \hline -(\varphi)^{\frac{1}{2}} B^T X_\infty & 0 \end{array}\right]. \tag{5.8}$$

In Chapter 3, the LMI formulation of parametric H_∞ loop shaping control has already been discussed. Here for the parameter φ, the solvability conditions are again presented for completeness of this chapter.

Lemma 5.1: *For a given positive value of φ, there exists a stabilizing controller $\varphi^{\frac{1}{2}}K$, if and only if the following inequalities*

$$\begin{bmatrix} AR + RA^T - \gamma\varphi BB^T & RC^T & -L \\ CR & -\gamma I & I \\ -L^T & I & -\gamma I \end{bmatrix} < 0 \tag{5.9}$$

$$A^T S + SA + C^T L^T S + SLC - \gamma C^T C < 0 \tag{5.10}$$

$$\begin{bmatrix} R & I \\ I & S \end{bmatrix} \geq 0 \tag{5.11}$$

are satisfied with $R = R^T > 0$, $S = S^T > 0$, $\gamma > 0$.

The proof of this lemma is discussed in Chapter 3 (See Theorem 3.3). Interestingly from Lemma 5.1, one can derive two ARIs if there exists the stabilizing solutions $R > 0$ and $S > 0$. Now using the Schur complement form, the following ARIs are obtained. Here, (5.9) is simplified as

$$\left(A + \frac{1}{(1-\gamma^2)}LC\right)R + R\left(A + \frac{1}{(1-\gamma^2)}LC\right)^T - \left(\frac{\gamma}{(1-\gamma^2)}\right)RC^TCR - \left(\frac{\gamma}{(1-\gamma^2)}\right)LL^T$$
$$-\gamma\varphi BB^T < 0 \tag{5.12}$$

and from (5.10), we have

$$S(A + LC) + (A + LC)^T S - \gamma C^T C < 0. \tag{5.13}$$

Now, after some simplifications and changing the variables $\tilde{X}_\infty = \gamma R^{-1}$ and $\tilde{Y}_\infty = \gamma S^{-1}$, (5.12) and (5.13) are respectively simplified as follows (see Section 3.4).

$$\tilde{X}_\infty \left(A - \left(\gamma^2 - 1\right)^{-1} LC\right) + \left(A - \left(\gamma^2 - 1\right)^{-1} LC\right)^T \tilde{X}_\infty$$

$$-\tilde{X}_\infty\left(\varphi BB^T-\left(\gamma^2-1\right)^{-1}LL^T\right)\tilde{X}_\infty+\gamma^2\left(\gamma^2-1\right)^{-1}C^TC<0 \tag{5.14}$$

$$(A+LC)\tilde{Y}_\infty+\tilde{Y}_\infty(A+LC)^T-\tilde{Y}_\infty C^TC\tilde{Y}_\infty<0. \tag{5.15}$$

It may be noted that, for an unknown value of φ, the inequality constraints posed in Lemma 5.1 do not remain in LMI form and subsequently, the computational complexity will arise. In the proposed method, we keep this parameter free and considering the controller structure as same as (5.8), an output feedback controller will be designed to achieve local stability of the closed-loop system with bounded control inputs.

Problem 5.1: *The nominal plant (5.1) is subject to bounded control inputs,* $u_{ni}\in\begin{bmatrix}-1 & 1\end{bmatrix}$, $i=1,\dots,m$. *In absence of control input constraint, the compensators* W_2 *and* W_1 *are selected to form the shaped plant (5.4). By satisfying the control input constraints, find a symmetric positive definite solution* X_∞ *and* φ *such that the controller (5.8) will quadratically stabilize the closed-loop system, where the loop shaping controller becomes* $\varphi^{\frac{1}{2}}W_1KW_2$. *Subsequently, the designed controller also will maximize the region of attraction and provide an estimate of it with the least conservatism*

Note that when there is no uncertainty, Δ_M and Δ_N shown in Figure 5.1 are zero, that implies $w=0$. For this case, by solving the Problem 5.1 we can achieve the local stability of the nominal plant (5.1). However in presence of unstructured uncertainty, the controller K can ensure internal stability of the closed-loop system for the uncertainty bound $\|\begin{bmatrix}\Delta_M & \varphi^{\frac{1}{2}}\Delta_N\end{bmatrix}\|_\infty<\epsilon_{max}$. Without any constraint on control inputs, for a given value of φ this bound can easily be found out from Lemma 5.1 and it becomes $\epsilon_{max}=\frac{1}{\gamma_{opt}}$. But this bound is no longer applicable when constraints are imposed on control inputs. In that case, the stability conditions established in Problem 5.1 need to be modified that, in turn, satisfy the constraints of Lemma 5.1 as well as ensure quadratic stability of the closed-loop system without exceeding the control input bounds. From the modified conditions, the obtained γ will provide the uncertainty level for which the local stability of the system is ensured.

Problem 5.2: *A nominal plant (5.1) is given which has unstructured uncertainty and it is represented as perturbations to normalized coprime factors of the shaped plant as shown in Figure 5.1. The control input of the plant* u_{ni} *is bounded as given in Problem 5.1. By satisfying the control input bounds, find a symmetric positive definite solution* X_∞ *and* φ *such that the controller (5.8) will quadratically stabilize the shaped plant (5.4)* *and subsequently, it maximizes the uncertainty limit ϵ_{max} and region of attraction of the closed-loop system.*

5.4 Controller synthesis

The controller structure shown in preceding section is involved with two unknown variables φ and X_∞. The scalar variable φ is introduced to increase design flexibility and it effectively scales the gain of pre-compensator in H_∞ loop shaping framework. In this section, a controller with similar structure as in (5.8) has to be designed that simultaneously solves the Problems 5.1 and 5.2. In order to achieve this goal, first, a set of sufficient conditions has been derived for existence of solvability conditions of the controller that quadratically stabilizes the closed-loop system with bounded control inputs and subsequently gives an estimation of region of attraction. Then these conditions have been modified to maximize the region of attraction. Finally, another set of sufficient conditions are derived for local stabilization of an uncertain LTI plant leading to have solution of Problem 5.2.

5.4.1 Local stabilization of LTI plant

Theorem 5.1: *A nominal plant G is given with bounded control inputs $|u_{ni}| \leq 1, i = 1, \ldots, m$. By selecting proper compensators W_2 and W_1, the shaped plant is obtained as $W_2 G W_1$ whose minimal state-space realization and normalized left coprime factors are respectively given in (5.4) and (5.5). For a given r, there exists a controller $(\varphi)^{\frac{1}{2}} K$ where,*

$$K = \left[\begin{array}{c|c} A - \varphi B B^T Q^{-1} + LC & -L \\ \hline -(\varphi)^{\frac{1}{2}} B^T Q^{-1} & 0 \end{array}\right] \tag{5.16}$$

that quadratically stabilizes the closed-loop system, if

$$\begin{bmatrix} U\left(A + LC\right)^T + \left(A + LC\right)U & UC^T L^T \\ LCU & QA^T + AQ - 2\varphi BB^T \end{bmatrix} < 0 \tag{5.17}$$

$$C_{Roi}\left(Q + U\right)C_{Roi}^T \leq 1 \; for \; i = 1, \cdots, m \tag{5.18}$$

$$0 < \varphi < r, \quad Q > 0, \quad U > 0 \tag{5.19}$$

are satisfied where $C_{Roi} = \left[\begin{array}{cc} 0_{1\times(n_n+n_{w2})} & C_{w1i} \end{array}\right]$, C_{w1i} *is the* i^{th} *row of* C_{w1} *matrix. The above controller can be designed by solving the following optimization problem:*

$$\begin{aligned} &\textit{Maximize} && \varphi \\ &\textit{subject to} && (5.17)-(5.19). \end{aligned} \tag{5.20}$$

The ellipsoid $\varepsilon_1(P)$ *defined as* $\{x_{cl}^T P x_{cl} \leq 1 : \forall x_{cl} \neq 0, P = P^T > 0\}$ *describes a region of attraction where,*

$$P = \left[\begin{array}{c|c} U^{-1} & -U^{-1} \\ \hline -U^{-1} & U^{-1}+Q^{-1} \end{array}\right].$$

Proof: Let $x_c \in \Re^{n_c}$ and $x_s \in \Re^{n_s}$ are respectively the state vectors of controller and the shaped plant where $n_c = n_s$, then the closed-loop system becomes

$$\left[\begin{array}{c} \dot{x}_s \\ \hline \dot{x}_c \end{array}\right] = \left[\begin{array}{c|c} A & -\varphi BB^TQ^{-1} \\ \hline -LC & A-\varphi BB^TQ^{-1}+LC \end{array}\right] \left[\begin{array}{c} x_s \\ \hline x_c \end{array}\right]. \tag{5.21}$$

$$\Rightarrow \dot{x}_{cl} = A_{cl}x_{cl}$$

To prove quadratic stability of the closed-loop system, a quadratic type Lyapunov function $V(x_{cl}) = x_{cl}^T P x_{cl}$ is considered where, $x_{cl} = \left[\begin{array}{cc} x_s^T & x_c^T \end{array}\right]^T$ and the unknown matrix $P = P^T > 0$. In stable region of state-space, the derivative of $V(x_{cl})$ with respect to time becomes negative definite. Since, $\dot{V}(x_{cl}) = x_{cl}^T(A_{cl}^TP+PA_{cl})x_{cl}$, it becomes negative definite if $(A_{cl}^TP+PA_{cl}) < 0$. Now partitioning P with compatible dimension as

$$P = \left[\begin{array}{c|c} P_{11} & P_{12} \\ \hline P_{12}^T & P_{22} \end{array}\right], \tag{5.22}$$

we have, $A_{cl}^TP + PA_{cl}$

$$= \left[\begin{array}{cc} A & -\varphi BB^TQ^{-1} \\ -LC & A-\varphi BB^TQ^{-1}+LC \end{array}\right]^T \left[\begin{array}{cc} P_{11} & P_{12} \\ P_{12}^T & P_{22} \end{array}\right] + \left[\begin{array}{cc} P_{11} & P_{12} \\ P_{12}^T & P_{22} \end{array}\right] \left[\begin{array}{cc} A & -\varphi BB^TQ^{-1} \\ -LC & A-\varphi BB^TQ^{-1}+LC \end{array}\right]. \tag{5.23}$$

Simplifying (5.23), we have $A_{cl}^T P + PA_{cl} = \left[\begin{array}{c|c} S_{11} & S_{12} \\ \hline S_{21} & S_{22} \end{array}\right]$ where,

$$\begin{aligned} S_{11} &= A^T P_{11} - C^T L^T P_{12}^T + P_{11}A - P_{12}LC && (5.24) \\ S_{12} &= A^T P_{12} - C^T L^T P_{22} + P_{12}A - \varphi P_{12}BB^T Q^{-1} \\ &+ P_{12}LC - \varphi P_{11}BB^T Q^{-1} && (5.25) \\ S_{21} &= S_{12}^T && (5.26) \\ S_{22} &= A^T P_{22} - \varphi Q^{-1}BB^T P_{22} + C^T L^T P_{22} - \varphi Q^{-1}BB^T P_{12} + P_{22}A \\ &- \varphi P_{22}BB^T Q^{-1} + P_{22}LC - \varphi P_{12}^T BB^T Q^{-1}. && (5.27) \end{aligned}$$

Now $(A_{cl}^T P + PA_{cl}) < 0$, if $S_{11} < 0$ and $S_{22} - S_{21}S_{11}^{-1}S_{12} < 0$ are satisfied. In this context to obtain $S_{11} < 0$, we choose $-P_{12}^T = -P_{12} = P_{11}$ and (5.24) becomes

$$S_{11} = (A + LC)^T P_{11} + P_{11}(A + LC). \qquad (5.28)$$

Since, $(A + LC)$ is stable, there always exists $P_{11} > 0$ such that $S_{11} < 0$. Now, replacing $-P_{12}^T = -P_{12} = P_{11}$ in (5.22), we have

$$P = \left[\begin{array}{c|c} P_{11} & -P_{11} \\ \hline -P_{11} & P_{22} \end{array}\right]. \qquad (5.29)$$

P will be a positive definite matrix if $P_{11} > 0$ and $P_{22} - P_{11}P_{11}^{-1}P_{11} = P_{22} - P_{11} > 0$ hold. Hence to satisfy $P_{22} > P_{11}$, we choose $P_{22} = P_{11} + V$ where V is an unknown symmetric positive define matrix. Now, replacing $-P_{12}^T = -P_{12} = P_{11}$ and $P_{22} = P_{11} + V$ in (5.25) and (5.27), we respectively have

$$\begin{aligned} S_{12} &= -A^T P_{11} - C^T L^T P_{11} - C^T L^T V - P_{11}A + \varphi P_{11}BB^T Q^{-1} - P_{11}LC - \varphi P_{11}BB^T Q^{-1} \\ &= -\left[(A + LC)^T P_{11} + P_{11}(A + LC) + C^T L^T V\right] && (5.30) \end{aligned}$$

$$\begin{aligned} S_{22} &= A^T P_{11} + A^T V - \varphi Q^{-1}BB^T P_{11} - \varphi Q^{-1}BB^T V + C^T L^T P_{11} + C^T L^T V \\ &+ \varphi Q^{-1}BB^T P_{11} + P_{11}A + VA - \varphi P_{11}BB^T Q^{-1} - \varphi VBB^T Q^{-1} \\ &+ P_{11}LC + VLC + \varphi P_{11}BB^T Q^{-1} && (5.31) \end{aligned}$$

For simplification, we choose $V = Q^{-1}$ and (5.31) becomes

$$S_{22} = (A+LC)^T P_{11} + P_{11}(A+LC) + (A-\varphi BB^T V + LC)^T V + V(A-\varphi BB^T V + LC) \tag{5.32}$$

Now,

$$\begin{aligned} S_{22} - S_{21}S_{11}^{-1}S_{12} &= (A-\varphi BB^T V)^T V + V(A-\varphi BB^T V) \\ &\quad -VLC\left[(A+LC)^T P_{11} + P_{11}(A+LC)\right]^{-1} C^T L^T V \end{aligned}$$

Hence, $S_{22} - S_{21}S_{11}^{-1}S_{12} < 0$ implies

$$\begin{aligned} &A^T V - \varphi VBB^T V + VA - \varphi VBB^T V \\ &\quad -VLC\left[(A+LC)^T P_{11} + P_{11}(A+LC)\right]^{-1} C^T L^T V < 0. \end{aligned}$$

Pre and post-multiplying by V^{-1} and since $Q = V^{-1}$, we have

$$QA^T - \varphi BB^T + AQ - \varphi BB^T - LC\left[(A+LC)^T P_{11} + P_{11}(A+LC)\right]^{-1} C^T L^T < 0. \tag{5.33}$$

Using Schur form, (5.33) can be written as

$$\begin{bmatrix} QA^T + AQ - 2\varphi BB^T & LC \\ C^T L^T & (A+LC)^T P_{11} + P_{11}(A+LC) \end{bmatrix} < 0. \tag{5.34}$$

Inequality (5.34) can also be written as

$$\begin{bmatrix} P_{11}^{-1}(A+LC)^T + (A+LC)P_{11}^{-1} & P_{11}^{-1}C^T L^T \\ LCP_{11}^{-1} & QA^T + AQ - 2\varphi BB^T \end{bmatrix} < 0. \tag{5.35}$$

Defining $U = P_{11}^{-1}$ in (5.35), we have the inequality similar to (5.17). Hence, if (5.35) holds, $(A_{cl}^T P + PA_{cl}) < 0$.

Since the output of W_1 is the input of G, without loss of generality it can be shown that if $|y_{w1i}| \leq 1$, where y_{w1i} is the output of W_1 at i^{th} channel, $i = 1, \ldots, m$, control inputs never exceed the specified bounds. As $y_{w1} = C_{w1}x_{w1}$, y_{w1i} can be written as follows:

$$\begin{aligned} y_{w1i} &= \begin{bmatrix} 0 & 0 & C_{w1i} & 0 \end{bmatrix} \begin{bmatrix} x_n^T & x_{w2}^T & x_{w1}^T & x_c^T \end{bmatrix}^T \\ &= C_{Ri}x_{cl}, \end{aligned}$$

where $C_{Ri} = \begin{bmatrix} 0 & 0 & C_{w1i} & 0 \end{bmatrix}$, $x_{cl} = \begin{bmatrix} x_n^T & x_{w2}^T & x_{w1}^T & x_c^T \end{bmatrix}^T$ and C_{w1i} is the i^{th} row of C_{w1}. Now, defining an ellipsoid $\varepsilon_1(P) = \{x_{cl} : x_{cl}^T P x_{cl} \leq 1 \; \forall \; x_{cl} \neq 0, P = P^T > 0\}$, we have,

$$1 - x_{cl}^T P x_{cl} \geq 0.$$

Using Schur complement, it can be written as

$$\begin{aligned} \begin{bmatrix} 1 & x_{cl}^T \\ x_{cl} & P^{-1} \end{bmatrix} &\geq 0 \\ \Rightarrow P^{-1} - x_{cl} x_{cl}^T &\geq 0 \end{aligned} \tag{5.36}$$

Pre and post-multiplying (5.36) by respectively C_{Ri} and C_{Ri}^T, we have

$$C_{Ri} x_{cl} x_{cl}^T C_{Ri}^T \leq C_{Ri} P^{-1} C_{Ri}^T. \tag{5.37}$$

Again, at i^{th} channel the control inputs never exceed the bounds if

$$C_{Ri} x_{cl} x_{cl}^T C_{Ri}^T \leq 1. \tag{5.38}$$

From (5.37) and (5.38), it is obvious that x_{cl} belongs to the ellipsoid $\varepsilon_1(P)$ as well satisfies (5.38), if

$$C_{Ri} P^{-1} C_{Ri}^T \leq 1. \tag{5.39}$$

Using Schur complement form, (5.39) can be written as

$$\begin{bmatrix} 1 & C_{Ri} \\ C_{Ri}^T & P \end{bmatrix} \geq 0. \tag{5.40}$$

Now, replacing (5.29) in (5.40) and since, $P_{11} = U^{-1}$ and $P_{22} = U^{-1} + Q^{-1}$, we have

$$\begin{bmatrix} 1 & C_{Roi} & 0_{1\times n_c} \\ C_{Roi}^T & U^{-1} & -U^{-1} \\ 0_{n_c\times 1} & -U^{-1} & U^{-1} + Q^{-1} \end{bmatrix} \geq 0, \tag{5.41}$$

where $C_{Ri} = \begin{bmatrix} C_{Roi} & 0_{1\times n_c} \end{bmatrix} = \begin{bmatrix} \begin{bmatrix} 0_{1\times n_n} & 0_{1\times n_{w2}} & C_{w1i} \end{bmatrix} & 0_{1\times n_c} \end{bmatrix}$. Using Schur complement form, (5.41) is simplified as

$$\begin{bmatrix} 1 & C_{Roi} \\ C_{Roi}^T & (Q+U)^{-1} \end{bmatrix} \geq 0. \tag{5.42}$$

(5.42) is equivalent to

$$C_{Roi}\,(Q+U)\,C_{Roi}^T \leq 1. \tag{5.43}$$

In each channel the control input does not exceed the bound, if (5.43) is satisfied for $i = 1, \ldots, m$. □

Remark 5.4: *By solving the optimization problem of Theorem 5.1, we get a controller that quadratically stabilizes the closed-loop system and simultaneously estimates a region of attraction. However, it does not maximize the region. To obtain it, one can minimize the trace of* U^{-1} *and* Q^{-1} *which in turn minimizes the determinant of* P*, that is, the volume of ellipsoid is maximized [14]. Also note that, the range in which* φ *is varied, can be changed according to design requirements.*

5.4.2 Maximizing the region of attraction

Defining the ellipsoid $\epsilon_\varrho(P) = \{x_{cl} : x_{cl}^T P x_{cl} \leq \varrho \;\forall\; x_{cl} \neq 0, P = P^T > 0\}$, (5.39) can be written as

$$C_{Ri} P^{-1} C_{Ri}^T \leq \varrho^{-1}. \tag{5.44}$$

To maximize the region of attraction, (5.43) has to be modified by changing the variable $\nu = \varrho^{-1}$ as follows:

$$C_{Roi}\,(Q+U)\,C_{Roi}^T \leq \nu \text{ for } i = 1, \cdots, m. \tag{5.45}$$

Corollary 5.1: *The controller* $(\varphi)^{\frac{1}{2}}K$*, where* K *is as given in(5.16), quadratically stabilizes the closed-loop system and subsequently maximizes the region of attraction, if the optimization problem is solved as follows:*

Minimize $(\nu - \varphi)$

Subject to

$$\begin{bmatrix} U\,(A+LC)^T + (A+LC)\,U & UC^T L^T \\ LCU & QA^T + AQ - 2\varphi BB^T \end{bmatrix} < 0 \tag{5.46}$$

$$C_{Roi}\left(Q+U\right)C_{Roi}^{T}\leq\nu \text{ for } i=1,\cdots,m \tag{5.47}$$

$$0<\varphi<r,\quad Q>0,\quad U>0. \tag{5.48}$$

The ellipsoid $\varepsilon_{\varrho}(P)$ *defined as* $\{x_{cl}^{T}Px_{cl}\leq\ \nu^{-1}:\forall x_{cl}\neq 0, P=P^{T}>0\}$ *describes a region of attraction where*

$$P=\left[\begin{array}{c|c} U^{-1} & -U^{-1} \\ \hline -U^{-1} & U^{-1}+Q^{-1}\end{array}\right].$$

Corollary 5.1 solves the Problem 5.1. Now we consider the unstructured uncertainty of the LTI plant G which is presented as perturbations to normalized coprime factors of the shaped plant as shown in Figure 5.1. In presence of control input constraint, an output feedback controller has to be designed that quadratically stabilizes the closed-loop system for a certain level of uncertainty bound. In preceding theorem, already a set of sufficient conditions has been derived for local stabilization of LTI plant with bounded control inputs, however, the uncertainty of the plant is not yet addressed. Now, a new set of sufficient conditions will be derived that satisfies the constraints of Theorem 5.1 as well as Lemma 5.1 from where a stability bound can be obtained for uncertain LTI plant.

5.4.3 Local stabilization of uncertain LTI plant

Corollary 5.2: *A nominal plant (5.1) is given which has unstructured uncertainty represented as perturbations to normalized coprime factors of the shaped plant as shown in Figure 5.1. The control input of the plant* u_n *is bounded where* $|u_{ni}|\leq 1, i=1,\ldots,m$*. For a given* r*, there exists a controller* $(\varphi)^{\frac{1}{2}}K$ *where,*

$$K=\left[\begin{array}{c|c} A-\varphi BB^{T}Q^{-1}+LC & -L \\ \hline -(\varphi)^{\frac{1}{2}}B^{T}Q^{-1} & 0\end{array}\right] \tag{5.49}$$

that quadratically stabilizes the closed-loop system with an uncertainty bound $\left(\sqrt{(1+\eta)}\right)^{-1}$, *if*

$$\left[\begin{array}{cc} U\left(A+LC\right)^{T}+\left(A+LC\right)U & UC^{T}L^{T} \\ LCU & QA^{T}+AQ-2\varphi BB^{T}\end{array}\right]<0 \tag{5.50}$$

$$\begin{bmatrix} AQ+QA^T-\varphi BB^T & QC^T & L-QC^T \\ CQ & -I & 0 \\ L^T-CQ & 0 & -\eta I \end{bmatrix} < 0 \tag{5.51}$$

$$C_{Roi}\,(Q+U)\,C_{Roi}^T \leq \nu \text{ for } i=1,\cdots,m \tag{5.52}$$

$$0<\varphi<r, \quad Q>0, \quad U>0, \quad \eta>0 \tag{5.53}$$

are satisfied. The controller can be obtained by solving the following optimization problem.

$$\begin{aligned} &\textit{Minimize } (\eta+\nu-\varphi) \\ &\textit{Subject to } \ (5.50)-(5.53). \end{aligned}$$

The ellipsoid $\varepsilon_\varrho(P)$ defined as $\{x_{cl}^T P x_{cl} \leq \nu^{-1} : \forall x_{cl} \neq 0, P=P^T>0\}$ describes a region of attraction where

$$P = \left[\begin{array}{c|c} U^{-1} & -U^{-1} \\ \hline -U^{-1} & U^{-1}+Q^{-1} \end{array}\right].$$

Proof: In absence of uncertainty it has already been proved that, if (5.50), (5.52) and (5.53) are satisfied, the controller (5.49) quadratically stabilizes the closed-loop system with bounded control inputs and also estimates a region of attraction as mentioned above. For uncertain plant, the constraints of Lemma 5.1 also have to be satisfied to ensure robustness along with local stability of the LTI plant with bounded control inputs. Meanwhile it is important to note that, if (5.50) holds, this implies that U satisfies (5.15) which is the second inequality derived from Lemma 5.1. Now using Schur complement form, (5.51) can be written as

$$(AQ+QA^T-\varphi BB^T)+\begin{bmatrix} QC^T & (L-QC^T) \end{bmatrix}\begin{bmatrix} I & 0 \\ 0 & \eta^{-1}I \end{bmatrix}\begin{bmatrix} CQ \\ (L^T-CQ) \end{bmatrix} < 0 \tag{5.54}$$

Defining $\alpha=\eta^{-1}$, (5.54) is simplified as

$$AQ-\alpha LCQ+QA^T-\alpha QC^TL^T-\varphi BB^T+\alpha LL^T+(1+\alpha)QC^TCQ<0 \tag{5.55}$$

$$\Rightarrow (A-\alpha LC)Q+Q(A-\alpha LC)^T-(\varphi BB^T-\alpha LL^T)+(1+\alpha)QC^TCQ<0 \tag{5.56}$$

Hence if (5.56) holds, Q also satisfies (5.14) which is the first inequality derived from Lemma 5.1. Now comparing with (5.14), we have $\tilde{X}_\infty = Q^{-1}$ and $\gamma = \sqrt{1+\eta}$, that provides the robust stability margin as $\left(\sqrt{1+\eta}\right)^{-1}$. □

The Corollary 5.2 solves the Problem 5.2. Interestingly, all problems in this section are formulated in LMI form that can easily be solved by using LMI toolbox [37]. In the following section, two numerical examples are illustrated to show the effectiveness of the proposed method.

5.5 Numerical examples

Example 1:

The linearized longitudinal dynamics of F-8 aircraft model has been considered whose state-space matrices are given as follows [52]:

$$A_n = \begin{bmatrix} -0.8 & -0.006 & -12 & 0 \\ 0 & -0.014 & -16.64 & -32.2 \\ 1 & -0.0001 & -1.5 & 0 \\ 1 & 0 & 0 & 0 \end{bmatrix}, \; B_n = \begin{bmatrix} -19 & -3 \\ -0.66 & -0.5 \\ -0.16 & -0.5 \\ 0 & 0 \end{bmatrix},$$

$$C_n = \begin{bmatrix} 0 & 0 & 0 & 1 \\ 0 & 0 & -1 & 1 \end{bmatrix}$$

The states of the system are pitch rate (rad/sec), forward velocity (ft/sec), angle of attack (rad) and pitch angle(rad); whereas the measured outputs are pitch angle and flight path angle (rad). Two control inputs, elevator angle (degree) and flaperon angle (degree) are subject to actuator saturation with the limits $\pm 15^0$. Here the design objectives are specified as follows: the steady state error does not exceed $\pm 2\%$ and in presence of nominal plant uncertainty, the system stability should be guaranteed. In order to achieve these objectives, using loop shaping concept (discussed in Chapter 2) a pre-compensator is selected to shape singular values of the open-loop plant. The selected pre-compensator is

$$W_1 = \begin{bmatrix} \frac{10(s+0.3)}{s(s+8)} & 0 \\ 0 & \frac{20(s+1.5)}{s(s+1)} \end{bmatrix}$$

and the post-compensator is considered as an identity matrix with proper dimension. With these selected compensators, the local stabilization problem has been solved.

	φ		ϱ		$(\sqrt{1+\eta})^{-1}$
	Cor 5.1	Cor 5.2	Cor 5.1	Cor 5.2	from Cor 5.2
$\pm 10^0$	0.9996	0.9997	128.27	3.39	0.3919
$\pm 15^0$	0.9998	0.9996	291.44	4.84	0.3948
$\pm 100^0$	0.9998	0.9997	397.26	39.78	0.3979

Table 5.1: Results of example-1

In Table 5.1, the results have been shown for different control input bounds. When the bounding limits are increased, the estimated region of attraction is also increased. Here the range of φ is chosen from 0 to 1. The local stabilization problem has been solved using both the Corollaries 5.1 and 5.2 where Corollary 5.2 can take care of the uncertainty of the LTI plant. The controller given below is designed for the bound $\pm 15^0$ which is obtained by solving the optimization problem of Corollary 5.2. Finally, the H_∞ loop shaping controller is formed by cascading the pre-compensator W_1 with $(\varphi)^{\frac{1}{2}}K = \left[\begin{array}{c|c} A_c & B_c \\ \hline C_c & 0 \end{array}\right]$ where

$$A_c = 10^4 * \begin{bmatrix} -0.0001 & -0.0000 & -0.0016 & -0.0010 & -0.0047 & -0.0029 & -0.0008 & -0.0011 \\ 0 & -0.0000 & -0.0005 & 0.0003 & -0.0002 & -0.0001 & -0.0001 & -0.0002 \\ 0.0001 & -0.0000 & -0.0005 & -0.0002 & -0.0000 & -0.0000 & -0.0001 & -0.0002 \\ 0.0001 & 0 & -0.0000 & -0.0005 & 0 & 0 & 0 & 0 \\ 0.6097 & -0.0006 & -1.3557 & 3.6329 & -2.4362 & -2.6753 & -0.4996 & -0.7266 \\ 0 & 0 & -0.0000 & 0.0000 & 0.0001 & 0 & 0 & 0 \\ 0.5101 & -0.0004 & -0.9552 & 2.8422 & -1.9985 & -2.0920 & -0.5411 & -0.7924 \\ 0 & 0 & 0.0003 & -0.0002 & 0 & 0 & 0.0001 & 0 \end{bmatrix},$$

$$B_c = \begin{bmatrix} 14.0531 & -4.3022 \\ -47.0678 & 11.9008 \\ 5.4834 & -3.4309 \\ 5.2983 & -0.1851 \\ -0.3355 & -0.0274 \\ -0.2001 & -0.1151 \\ -2.7071 & 4.4689 \\ -1.0314 & 2.6038 \end{bmatrix},$$

$$C_c = 10^4 * \begin{bmatrix} 1.5243 & -0.0014 & -3.3893 & 9.0822 & -6.0885 & -6.6883 & -1.2491 & -1.8166 \\ 0.6377 & -0.0005 & -1.1945 & 3.5530 & -2.4981 & -2.6151 & -0.6763 & -0.9905 \end{bmatrix}.$$

Let, we consider an initial state vector

$$x_{cl}^{0} = \left[\begin{array}{cccccccccccccccc} 7 & 6 & 1 & 1 & 0 & 0 & 0 & 0 & 0 & 0 & 0 & 0 & 0 & 0 & 0 & 0 \end{array} \right]^{T}.$$

For this initial condition, ${x_{cl}^{0}}^{T} P x_{cl}^{0} = 3.2526$ that indicates, the initial state vector is inside the estimated region (since $\varrho = 4.84$). For this initial condition, the state responses are shown in Figures 5.2 and 5.3, whereas the control inputs are depicted in Figure 5.4. In this case, the robust stability margin 0.3948 is ensured for normalized coprime factor uncertainty description of the shaped plant. Note that, since the Corollary 5.2 is involved with uncertainty of the plant, it estimates smaller region of attraction compared to Corollary 5.1. On the other hand, if uncertainty of the plant is not considered, the local stabilization problem can be solved via Corollary 5.1 that gives comparably larger region of attraction. We consider

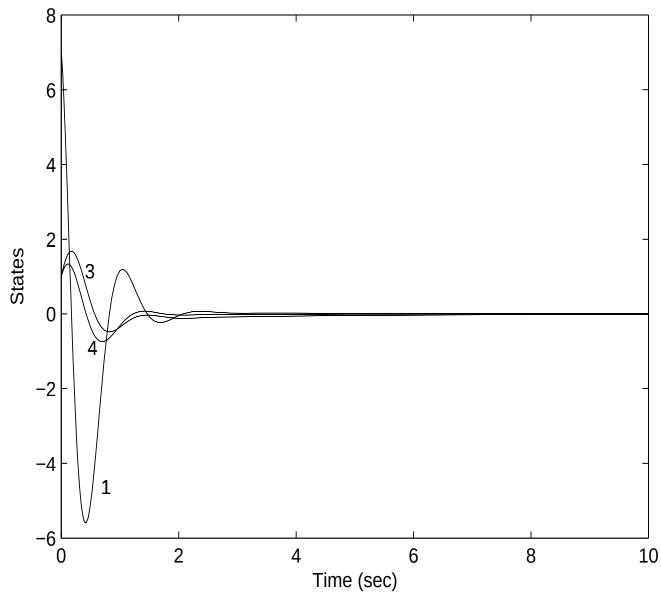

Figure 5.2: State-1 (curve 1 in rad/sec), state-3 (curve 3 in rad) and state-4 (curve 4 in rad) of the nominal plant

$$x_{cl}^{0} = \left[\begin{array}{cccccccccccccccc} 25 & 20 & 7 & 7 & 0 & 0 & 0 & 0 & 0 & 0 & 0 & 0 & 0 & 0 & 0 & 0 \end{array} \right]^{T},$$

for which ${x_{cl}^{0}}^{T} P x_{cl}^{0} = 286.59$ is obtained that indicates, the state vector inside the estimated region (since $\varrho = 291.44$). For this initial condition, the state responses have

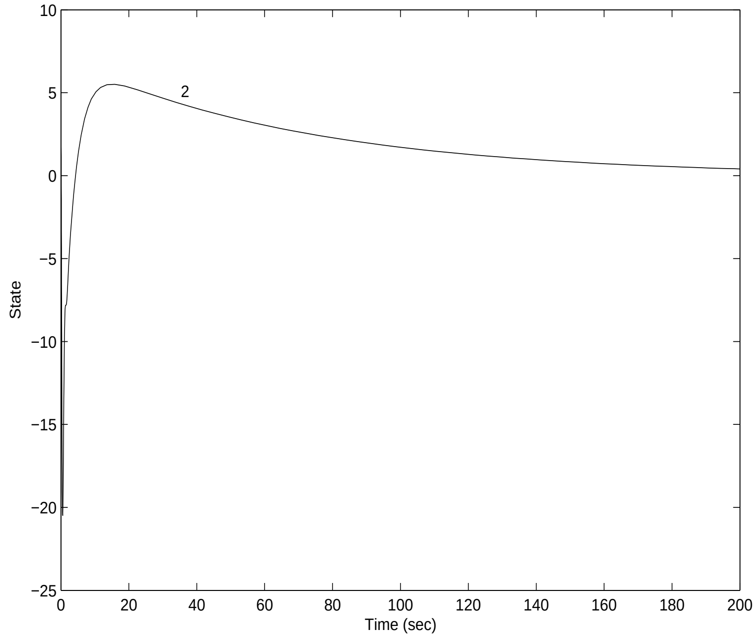

Figure 5.3: State-2 (curve 2 in ft/sec) of the nominal plant

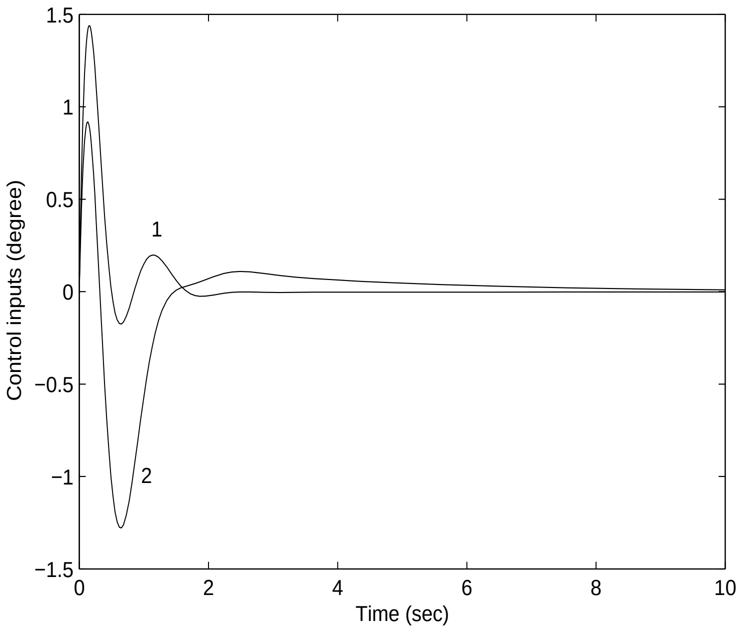

Figure 5.4: Curve 1: control input at channel-1; Curve 2: control input at channel-2

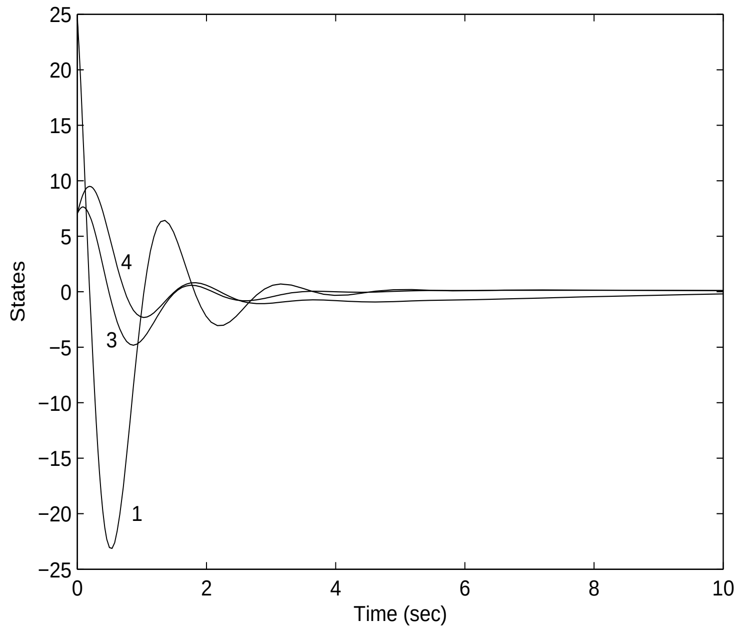

Figure 5.5: State-1 (curve 1 in rad/sec), state-3 (curve 3 in rad) and state-4 (curve 4 in rad) of the nominal plant

been shown in Figures 5.5 and 5.6 and the control inputs are depicted in Figure 5.7. It may be noted that the response of control signals are all well inside the specified bounds and never enters into saturation region.

In the following, another numerical example has been considered where, the control input bounds are not same for each channel.

Example 2:

We consider another example where the vertical plane dynamics of aircraft model has been considered. The state-space matrices of the nominal plant are given as follows:

$$A_n = \begin{bmatrix} 0 & 0 & 1.132 & 0 & -1 \\ 0 & -0.0538 & -0.1712 & 0 & 0.0705 \\ 0 & 0 & 0 & 1 & 0 \\ 0 & 0.0485 & 0 & -0.8556 & -1.013 \\ 0 & -0.2909 & 0 & 1.0532 & -0.6859 \end{bmatrix}, \; B_n = \begin{bmatrix} 0 & 0 & 0 \\ -.12 & 1 & 0 \\ 0 & 0 & 0 \\ 4.419 & 0 & -1.665 \\ 1.575 & 0 & -0.0732 \end{bmatrix},$$

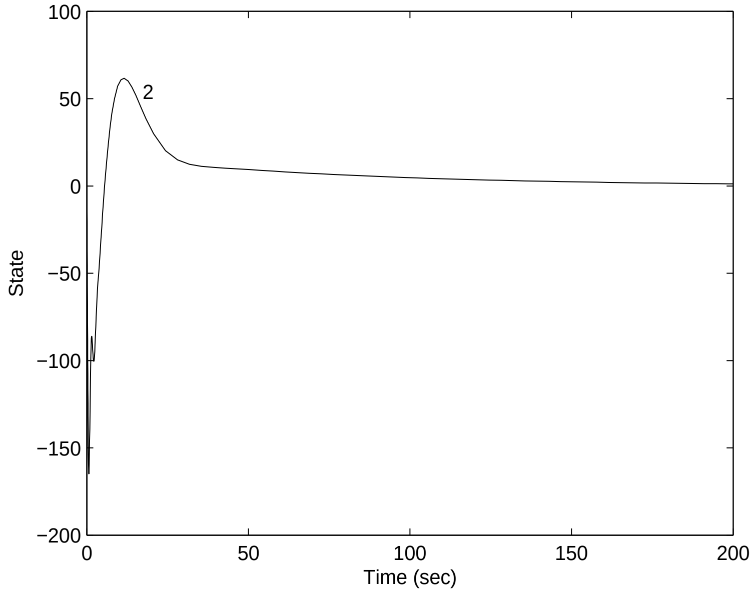

Figure 5.6: State-2 (curve 2 in ft/sec) of the nominal plant

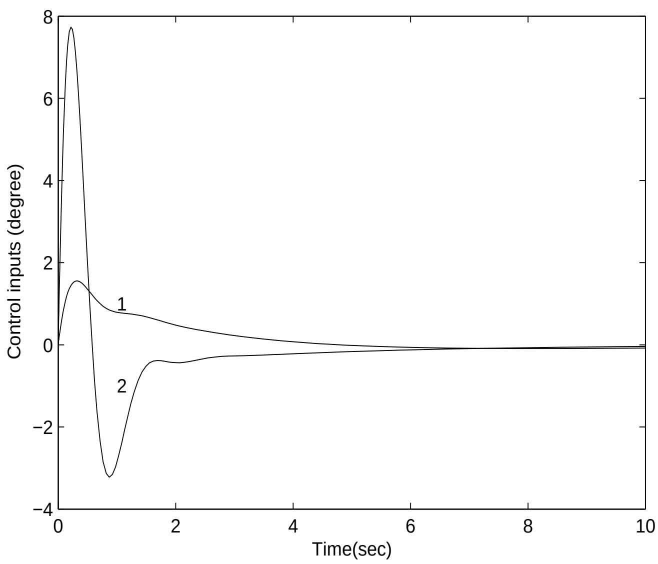

Figure 5.7: Curve 1: control input at channel-1; Curve 2: control input at channel-2

$$C_n = \begin{bmatrix} 1 & 0 & 0 & 0 & 0 \\ 0 & 1 & 0 & 0 & 0 \\ 0 & 0 & 1 & 0 & 0 \end{bmatrix}.$$

The detail description of the plant model as well as closed-loop specifications are given in [65]. For solving the local stabilization problem, here we consider the same type pre-compensator used in [65] and it is

$$W_1 = \begin{bmatrix} 24\frac{s+0.4}{s(s+1)} & 0 & 0 \\ 0 & 12\frac{s+0.4}{s(s+1)} & 0 \\ 0 & 0 & 24\frac{s+0.4}{s(s+1)} \end{bmatrix}.$$

In first and third channel, the control input bounds are $\pm 40^0$ whereas in second channel, it is $\pm 10\ m/sec^2$.

	φ		ϱ		$(\sqrt{1+\eta})^{-1}$
	Cor 5.1	Cor 5.2	Cor 5.1	Cor 5.2	from Cor 5.2
$\pm 20^0$ and $\pm 5m/sec^2$	0.9994	0.9997	66.20	1.2691	0.2118
$\pm 40^0$ and $\pm 10m/sec^2$	0.9998	0.9997	172.77	3.6733	0.2124
$\pm 100^0$ and $\pm 20m/sec^2$	0.9997	0.9997	88.33	11.313	0.2126

Table 5.2: Results of example-2

In Table 5.2, the results have been shown for different input bounds. The range of φ is taken from 0 to 1. In the following, the state-space matrices of the designed controller has been shown which is obtained by solving the optimization problem of Corollary 5.2 with the bounds $\pm 40^0$ and $\pm 10m/sec^2$. In H_∞ loop shaping framework, the designed controller is $(\varphi)^{\frac{1}{2}} W_1 K$ where,

$$(\varphi)^{\frac{1}{2}} K = \left[\begin{array}{c|c} A_c & B_c \\ \hline C_c & 0 \end{array}\right].$$

$A_c = 10^5 *$

$$\begin{bmatrix} -0.00004 & 0 & 0.00002 & 0 & 0 & 0 & 0 \\ 0 & -0.00004 & 0 & 0 & 0 & 0 & 0 \\ 0.00001 & 0 & -0.0007 & 0.00001 & 0 & 0 & 0 \\ 0.00007 & 0.00002 & -0.00029 & -0.00001 & -0.00001 & 0.00013 & 0.0001 \\ 0.0001 & 0.00001 & -0.00016 & 0.00001 & 0 & 0.00005 & 0.00003 \\ -0.22846 & -0.01304 & -0.38113 & -0.07754 & 0.14548 & -0.03863 & -0.03088 \\ 0.00001 & 0 & 0 & 0 & 0 & 0 & 0 \\ -0.00244 & -0.00073 & -0.00492 & -0.00105 & 0.00168 & -0.00074 & -0.0006 \\ 0.0000007 & -0.000006 & -0.0000006 & 0 & 0 & 0 & 0 \\ 0.66179 & 0.03142 & 1.0449 & 0.20957 & -0.41373 & 0.08746 & 0.06941 \\ 0.00001 & 0 & 0.00001 & 0 & 0 & 0 & 0 \end{bmatrix}$$

$$
\left.\begin{matrix}
0 & 0 & 0 & 0 \\
0.00003 & 0.00002 & 0 & 0 \\
0 & 0 & 0 & 0 \\
0 & 0 & -0.00005 & -0.00004 \\
0 & 0 & 0 & 0 \\
-0.00298 & -0.00215 & 0.08746 & 0.07452 \\
0 & 0 & 0 & 0 \\
-0.00074 & -0.0006 & 0.00111 & 0.00964 \\
0.000005 & 0 & 0 & 0 \\
0.00444 & 0.00271 & -0.24128 & -0.20519 \\
0 & 0 & 0 & 0
\end{matrix}\right] ,
$$

$$
B_c = \begin{bmatrix}
4.06560 & 0.10908 & -1.26337 \\
0.10908 & 4.35854 & -0.26391 \\
-1.26337 & -0.26391 & 7.62643 \\
-7.40136 & -2.04402 & 29.91413 \\
-10.49870 & -1.34436 & 16.03193 \\
-2.67532 & -0.68614 & 4.35446 \\
-1.16960 & -0.08637 & 0.90970 \\
-0.12415 & 2.65510 & 0.19239 \\
-0.07959 & 0.66087 & 0.06535 \\
-2.33792 & -0.03988 & -2.74258 \\
-1.93480 & 0.00380 & -1.15188
\end{bmatrix} ,
$$

$$
C_c = 10^4 *
$$

$$
\begin{bmatrix}
-0.2856 & -0.0163 & -0.4763 & -0.0969 & 0.1818 & -0.04828 & -0.0386 & -0.0037 & -0.0026 & 0.1093 & 0.0931 \\
-0.0061 & -0.0017 & -0.01231 & -0.0026 & 0.0042 & -0.0018 & -0.0015 & -0.0018 & -0.0015 & 0.0027 & 0.0024 \\
0.8272 & 0.03928 & 1.3060 & 0.2619 & -0.5171 & 0.1093 & 0.0867 & 0.0055 & 0.0033 & -0.3015 & -0.2564
\end{bmatrix}
$$

Now considering an initial state vector as

$$
x_{cl}^0 = \begin{bmatrix} 0.7 & 0.6 & 0.6 & 0.7 & 0.6 & 0_{1\times 17} \end{bmatrix}^T ,
$$

we have ${x_{cl}^0}^T P x_{cl}^0 = 3.5646$ (it is inside the estimated region, since $\varrho = 3.6733$) and in Figure 5.8, the state responses have been shown. Figures 5.9 and 5.10 show the control inputs that never exceed the bounds. In this case, the obtained robust stability margin is 0.2124.

Without considering uncertainty, a larger estimated region can be obtained by solving the optimization problem of Corollary 5.1 as shown in Table 5.2. We consider an initial state vector

$$
x_{cl}^0 = \begin{bmatrix} 5 & 2.6 & 2.6 & 2.7 & 2.6 & 0_{1\times 17} \end{bmatrix}^T ,
$$

that yields ${x_{cl}^0}^T P x_{cl}^0 = 147.8386$. In Figures 5.11, 5.12 and 5.13, the states and control inputs are respectively shown.

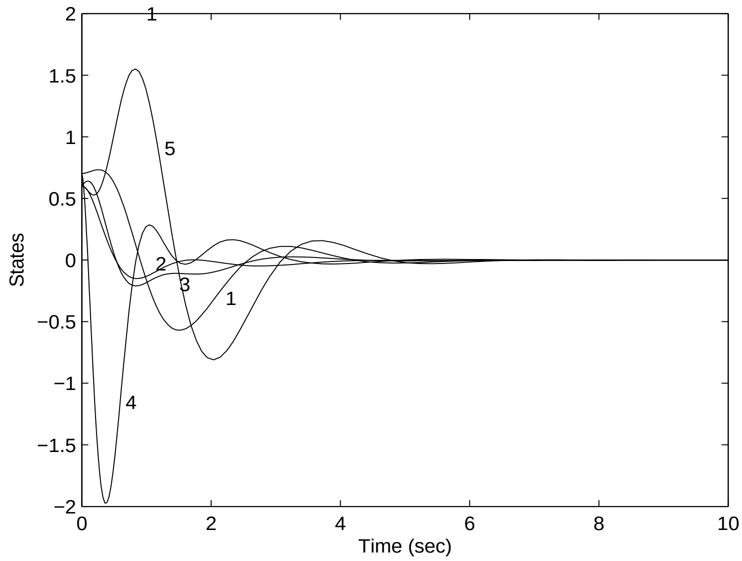

Figure 5.8: State-1 (curve 1 in m), state-2 (curve 2 in m/sec), state-3 (curve 3 in degree), state-4 (curve 4 in degree/sec) and state-5 (curve 5 in m/sec) of the nominal plant

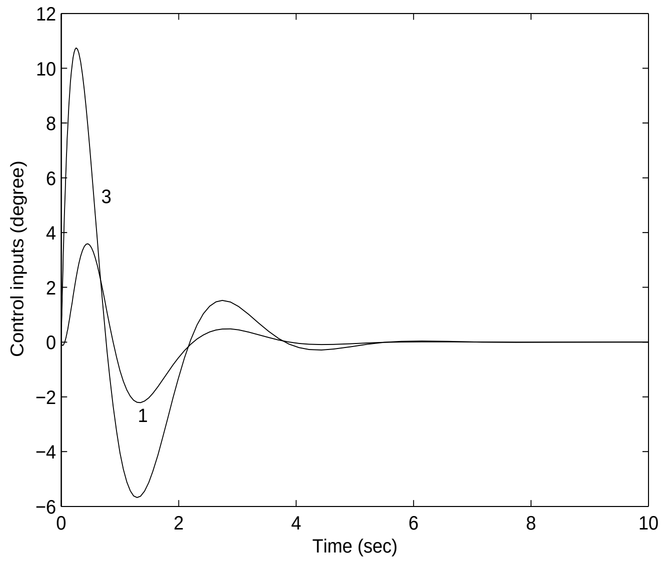

Figure 5.9: Curve 1: control input at channel-1; Curve 3: control input at channel-3

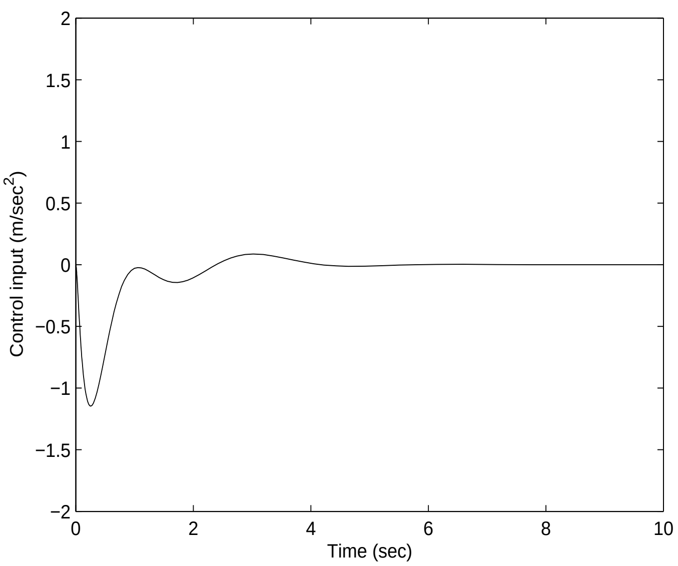

Figure 5.10: Control input at channel-2

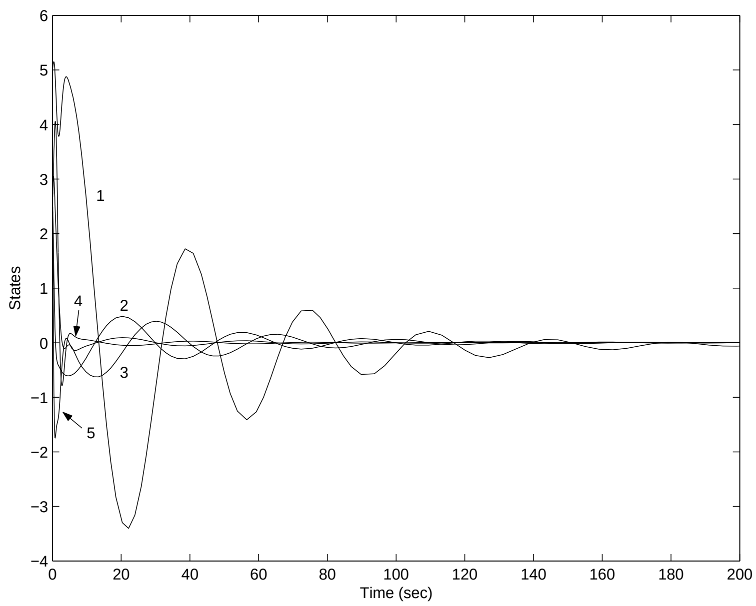

Figure 5.11: State-1 (curve 1 in m), state-2 (curve 2 in m/sec), state-3 (curve 3 in degree), state-4 (curve 4 in degree/sec) and state-5 (curve 5 in m/sec) of the nominal plant

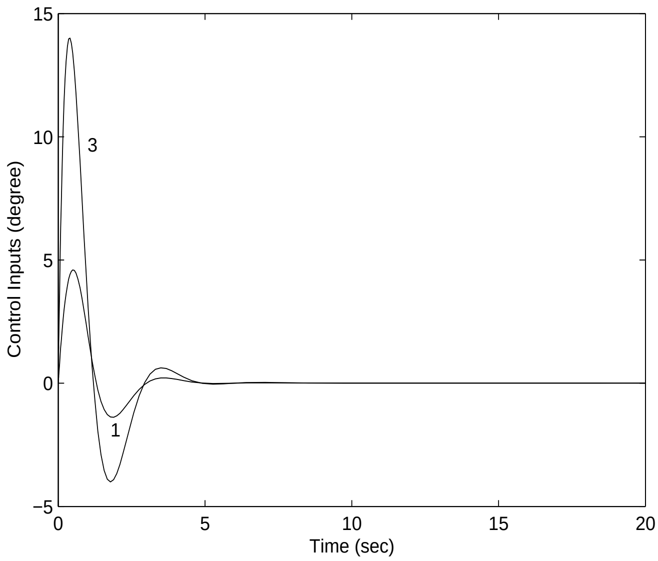

Figure 5.12: Curve 1: control input at channel-1; Curve 3: control input at channel-3

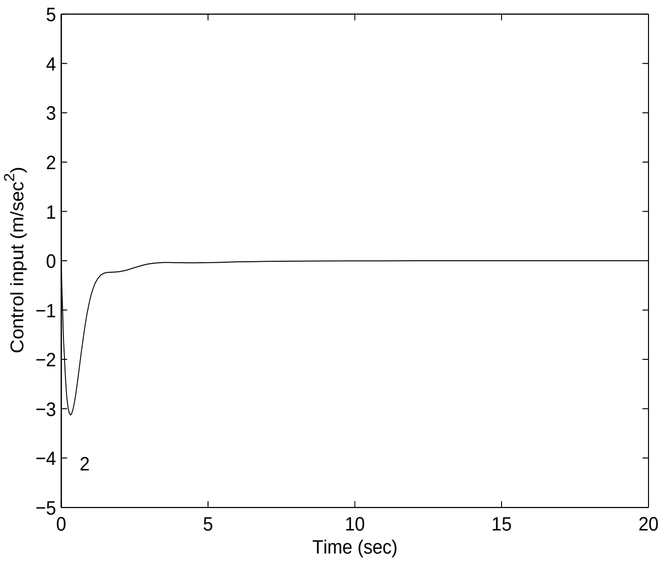

Figure 5.13: Control input at channel-2

5.6 Conclusions

In this chapter, an output feedback controller has been designed for local stabilization of an uncertain LTI plant with bounded control inputs. The unstructured uncertainty of the system is described as perturbations to normalized coprime factors of the shaped plant. The proposed technique is posed in parametric H_∞ loop shaping framework where a scalar parameter φ is introduced to increase flexibility of the design method. This parameter effectively scales the gain of pre-compensator. In this method, open-loop stability assumption has not been considered that leads it to local stabilization problem. To prove quadratic stability of the closed-loop system, a quadratic Lyapunov function has been considered and the derived sufficient conditions are posed in LMI form. To show the effectiveness of the proposed method, two numerical examples have been elucidated.

CHAPTER 6

Robust control with input saturation: H_∞ loop shaping approach

In preceding chapter, the local stabilization problem of LTI plant has been discussed with bounded control input constraint. Specifically, it is a part of actuator saturation problem using H_∞ loop shaping approach where control inputs never enter into saturation zone. On the other hand, if maximum limit of the control input to actuator is specified and it enters into saturation region, this situation equivalently can be treated as a nonlinear static function that satisfies a local sector bound. Considering this fact, a design framework has been proposed in the present chapter to achieve robust performance and stability of the LTI plant with input saturation constraint. Two different techniques based on polytopic linear parameter varying (LPV) approach and Popov stability criteria have been adopted to design robust controller in H_∞ loop shaping framework. The effectiveness of the proposed design techniques is illustrated through simulation results.

6.1 Introduction

Quite often, the robustness of an LTI plant is seriously affected by actuator saturation and even, it may cause for instability too. To this end, a large volume of works can be found in control system literatures where the design problem has been addressed to achieve robust performance and stability of the system with a priori given level of actuator saturation in presence of bounded exogenous inputs ([45, 47, 52, 72, 83, 90] and references therein). The given saturation level indicates, the maximum control input to actuator is specified that in turn, satisfies a local sector-bound. In some synthesis problems, this level of saturation has also been maximized subject to stability of the closed-loop system [44, 45]. Meanwhile, with actuator saturation constraint the robustness issue against uncertainty of the plant has also become an active area of research in last few years [43, 44].

In the present chapter, using H_∞ loop shaping approach two design frameworks have been addressed to achieve robust performance and stability of the LTI plant when control inputs are subject to actuator saturation. Adopting the H_∞ loop shaping method, the main objective is to achieve an acceptable trade-off between the robust performance and stability against the general unstructured uncertainty of the plant. Although, the H_∞ loop shaping technique provides a good design platform for linear robust control theory, however, it is not so straightforward to apply for actuator saturation control problem. When control inputs are saturated, singular values of the shaped plant alter from desired location that deteriorates the performance and stability of the closed-loop system. Moreover, in H_∞ loop shaping framework the stability margin obtained from linear region of saturation element is no longer applicable when control input enters into saturation region. In this context, modification of compensators in an adaptive way may be a remedial step to tackle the effects of saturation in H_∞ loop shaping control, however, it imparts a difficult task to designer. Related to this problem, some 'retro-fitted' schemes and ad-hoc methods can be found in the literatures. In [48], several anti-windup schemes have been reported and their performances are compared to provide an insight related to stability of the closed-loop system. Although, the reported techniques have been successfully applied to some practical examples but still, these existing methods are unable to provide a generic solution for designing a robust controller. In [78], the loop shaping weight has been modified for constrained control inputs but it is an ad-hoc method and no such definite robust stability margin can be specified in the design cycle. In [20], the describing function method has been adopted to tackle the effects of saturation in H_∞ loop shaping framework.

In this chapter, two different design techniques have been proposed to design robust controller for an LTI plant with input saturation constraint. The design of H_∞ loop shaping controller is carried out in its equivalent four-block framework that leads an easier synthesis structure for saturation control problem. In the first method, the shaped plant with input saturation has been represented as an equivalent polytopic LPV system. Then, using vertex property of the polytopic LPV plant, H_∞ loop shaping controllers have been designed at each vertex of the polytope, and subsequently these controllers are scheduled by adopting certain interpolation technique. The scheduled controller locally ensures robust stability and L_2-performance of the closed-loop system due to vertex property of the polytopic LPV shaped plant. Whereas in second method, the H_∞ loop shaping framework with input saturation nonlinearity has been transformed into an equivalent Lur'e type system and subsequently, Popov stability criteria is used to design a robust controller that ensures certain level of stability margin against the unstructured uncertainty of the plant. A numerical example has been considered to show the effectiveness of the proposed methods.

This chapter is organized as follows:

In Section 6.2, some definitions and preliminary works related to the main results of this chapter have been presented. Section 6.3 describes the design of robust controller in H_∞ loop shaping framework using LPV approach. In Section 6.4, a different design approach is considered that transforms an actuator saturation H_∞ loop shaping control problem to an equivalent Lur'e type control problem and subsequently, stability analysis is studied through Popov absolute stability criteria. In Section 6.5, a numerical example has been considered to demonstrate the effectiveness of the proposed methods. Finally, the concluding remarks are drawn in Section 6.6.

6.2 Preliminaries

Some preliminary results relevant to the design techniques proposed in this chapter are presented. These will be required to develop main results of this chapter. In first part, the preliminary results on LPV system have been demonstrated, whereas the later part briefly provides a description on Lur'e type system.

An LPV system can be represented in its state-space form where the system matrices are the function of some varying vector of real parameters. We consider an LPV system

$$\left.\begin{aligned} \dot{x} &= A(\theta)x + B(\theta)u \\ y &= C(\theta)x + D(\theta)u \end{aligned}\right\} \tag{6.1}$$

where x, u and y are respectively the state, input and output vectors and θ is the time varying vector of real parameters.

Definition 6.1 [6]: *The time-varying parameter θ is said to vary in a polytope Ω of vertices $\omega_1, \ldots, \omega_r$ if $\theta \in \Omega := Co\{\omega_1, \ldots, \omega_r\}$ where, r is the number of vertices of the polytope.*

Definition 6.2 [6]: *An LPV system is polytopic when the state-space matrices are dependent on θ through an affine relation and the parameter vector θ varies in a fixed polytope.*

We now consider the state equation of an unforced LPV system

$$\dot{x} = A(\theta)x \tag{6.2}$$

where θ lies in a compact set and $A(\theta) \in \Re^{n\times n}$. The quadratic stability of the system (6.2) can be stated as follows:

Lemma 6.1 [10]: *The system is quadratically stable over the compact set Ω in which θ varies, if there exist $P \in \Re^{n\times n},\ P = P^T > 0$, such that for all θ the inequality*

$$A^T(\theta)P + PA(\theta) < 0 \tag{6.3}$$

holds.

Definition 6.3 [10]: *The L_2-norm of a quadratically stable LPV system (6.1) can be defined as*

$$\|G\| = \sup_{\theta\in\Omega} \sup_{\|u\|_2\neq 0,\ u\in L_2} \frac{\|y\|_2}{\|u\|_2} \tag{6.4}$$

where S is the compact set. y and u are respectively the output and input vectors.

Now, a generalized LPV system for the quadratic H_∞-performance problem has been considered as follows:

$$\left.\begin{aligned} \dot{x} &= A(\theta)x + B_1(\theta)w + B_2(\theta)u \\ z &= C_1(\theta)x + D_{11}(\theta)w + D_{12}(\theta)u \\ y &= C_2(\theta)x + D_{21}(\theta)w + D_{22}(\theta)u \end{aligned}\right\} \tag{6.5}$$

where x, z, y, w and u are the state, objective signal, measured output, exogenous signal and control input vectors respectively. The state-space matrices are parameter dependent with compatible dimensions and θ belongs to a compact set. In other words, the system matrices depend on the time varying vector $\theta(t)$ that is assumed to be measured or estimated in real time. The designer will seek a feedback controller $\begin{bmatrix} A_c(\theta) & B_c(\theta) \\ C_c(\theta) & D_c(\theta) \end{bmatrix}$ in independence on θ to the actual plant such that the closed-loop system becomes quadratically stable and the L_2-induced norm of the system between w to z is bounded by γ. If $D_{22} = 0$, combining the state vectors x and x_c as $x_{cl} \begin{bmatrix} x^T & x_c^T \end{bmatrix}^T$, where x_c is state vector of the controller, we have the closed-loop system $\begin{bmatrix} A_{cl}(\theta) & B_{cl}(\theta) \\ C_{cl}(\theta) & D_{cl}(\theta) \end{bmatrix}$ where,

$$A_{cl} = \begin{bmatrix} A + B_2C_cC_2 & B_2C_c \\ B_cC_2 & A_c \end{bmatrix}, \quad B_{cl} = \begin{bmatrix} B_1 + B_2D_cD_{21} \\ B_cD_{21} \end{bmatrix},$$

$$C_{cl} = \begin{bmatrix} C_1 + D_{12}D_cC_2 & D_{12}C_c \end{bmatrix} \text{and } D_{cl} = D_{11} + D_{12}D_cD_{21}.$$

The dependence on θ is omitted for brevity. Now, the quadratic H_∞ performance problem for the above mentioned closed-loop LPV system can be stated as follows.

Lemma 6.2 [6]: *The closed-loop system* $\begin{bmatrix} A_{cl}(\theta) & B_{cl}(\theta) \\ C_{cl}(\theta) & D_{cl}(\theta) \end{bmatrix}$ *has the quadratic* H_∞ *performance* γ, *if and only if, there exist a matrix* $P = P^T > 0$ *such that it satisfies*

$$\begin{pmatrix} A_{cl}^T(\theta)P + PA_{cl}(\theta) & PB_{cl}(\theta) & C_{cl}^T(\theta) \\ B_{cl}^T(\theta)P & -\gamma I & D_{cl}^T(\theta) \\ C_{cl}(\theta) & D_{cl}(\theta) & -\gamma I \end{pmatrix} < 0 \tag{6.6}$$

for all $\theta \in \Omega$.

Remark 6.1: *Applying the bounded real lemma, the quadratic H_∞ performance problem has been posed in an inequality constraint as shown in (6.6), where the parameter independent single Lyapunov solution P has been considered for the LPV system. The equivalent condition for parameter dependent Lyapunov solution $P(\theta)$ can be found in [5, 10] that yields infinite number of LMI constraints for ensuring the quadratic H_∞ performance γ. Interestingly for polytopic LPV plant, (6.6) is reduced to a set of finite number of LMI constraints. Using the vertex property of the polytopic LPV plant it can be said that, for a single Lyapunov function if (6.6) is satisfied at each vertex of the polytope, all plants that lie in that polytope also will satisfy (6.6) for the same Lyapunov function [6].*

Theorem 6.1 [6]: *For the polytopic LPV plant described as*

$$\begin{pmatrix} A(\theta) & B(\theta) \\ C(\theta) & D(\theta) \end{pmatrix} \in Co\left\{ \begin{pmatrix} A_i & B_i \\ C_i & D_i \end{pmatrix} := \begin{pmatrix} A(\omega_i) & B(\omega_i) \\ C(\omega_i) & D(\omega_i) \end{pmatrix}, i = 1, \ldots, r \right\}, \tag{6.7}$$

the following statements are equivalent:

1. *The LPV system is stable with H_∞ quadratic performance γ ;*

2. *There exists a single Lyapunov solution (parameter independent) $P = P^T > 0$ such that*
$$\begin{pmatrix} A^T(\theta)P + PA(\theta) & PB(\theta) & C^T(\theta) \\ B^T(\theta)P & -\gamma I & D^T(\theta) \\ C(\theta) & D(\theta) & -\gamma I \end{pmatrix} < 0 \tag{6.8}$$
for all trajectories of θ in the polytope;

3. *Lyapunov solution P satisfies the system of LMIs*
$$\begin{pmatrix} A_i^T P + PA_i & PB_i & C_i^T \\ B_i^T P & -\gamma I & D_i^T \\ C_i & D_i & -\gamma I \end{pmatrix} < 0, i = 1, \ldots, r; \tag{6.9}$$

Finally, we present the solvability conditions for the existence of an LPV controller in convex optimization framework [6]. Considering the generalized plant (6.5), we assume i) $D_{22} = 0$, ii) $B_2(\theta), C_2(\theta), D_{12}(\theta), D_{21}(\theta)$ are parameter independent and iii) $(A(\theta), B_2(\theta), C_2(\theta))$ is stabilizable and detectable for all the trajectories of θ. Now, if the parameter trajectories are in the polytope $\Theta = \{\sum_{i=1}^{r} \alpha_i \omega_i : \alpha_i \geq 0, \sum_{i=1}^{r} \alpha_i = 1\}$, the following theorem can be stated as follows.

Theorem 6.2 [6]: *Let the above assumptions be fulfilled. Then, there exists an LPV controller with the quadratic H_∞ performance bound γ for all the parameter trajectories in Θ, if and only if, there exists two symmetric matrices R and S such that the following LMIs are satisfied for every $i = 1, \ldots, r$.*

$$\left.\begin{array}{r} \begin{pmatrix} N_R & 0 \\ 0 & I \end{pmatrix}^T \begin{pmatrix} A_i R + R A_i^T & R C_{1i}^T & B_{1i} \\ C_{1i} R & -\gamma I & D_{11i} \\ B_{1i}^T & D_{11i}^T & -\gamma I \end{pmatrix} \begin{pmatrix} N_R & 0 \\ 0 & I \end{pmatrix} < 0 \\ \begin{pmatrix} N_S & 0 \\ 0 & I \end{pmatrix}^T \begin{pmatrix} A_i^T S + S A_i & S B_{1i} & C_{1i}^T \\ B_{1i}^T S & -\gamma I & D_{11i}^T \\ C_{1i} & D_{11i} & -\gamma I \end{pmatrix} \begin{pmatrix} N_S & 0 \\ 0 & I \end{pmatrix} < 0 \\ \begin{pmatrix} R & I \\ I & S \end{pmatrix} \geq 0 \end{array}\right\} \tag{6.10}$$

where N_R and N_S are the bases of the null spaces of $\begin{bmatrix} B_2^T & D_{12}^T \end{bmatrix}$ and $\begin{bmatrix} C_2 & D_{21} \end{bmatrix}$ respectively.

We now describe the structure of a Lur'e type system which will be required to establish the second design technique of this chapter.

Lur'e system [53]

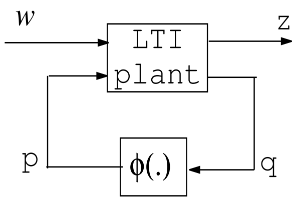

Figure 6.1: Block diagram for Lur'e system

A Lur'e system is a feedback system whose forward path consists of an LTI plant, and an uncertain nonlinear element that satisfies a sector-bound constraint is connected in a feedback path. In state-space form, a Lur'e system can be described as follows.

$$\begin{aligned}\dot{x} &= Ax + B_p p + B_w w \\ q &= C_q x \\ z &= C_z x\end{aligned}$$

where, $p_i(t) = \phi_i(q_i(t)),\ i = 1\ldots, n_p, p(t) \in \Re^{n_p}$ and, ϕ_i satisfies the sector condition $0 \leq q_i\phi_i(q_i) \leq q_i^2\ \forall q_i \in \Re$.

6.3 Robust H_∞ loop shaping controller design with input saturation constraint: polytopic LPV approach

In Figure 6.2, the H_∞ loop shaping design framework with input saturation has been depicted where W is the pre-compensator selected in order to satisfy the closed-loop design specifications. The effect of saturation is not considered in pre-compensator selection and without loss of generality, the post-compensator is taken as an identity matrix with proper dimension. The block-diagram shown in Figure 6.2 is the equivalent four-block synthesis framework for H_∞ loop shaping control (see Chapter 2) where $w = \begin{bmatrix} w_1^T & w_2^T \end{bmatrix}^T$ and $z = \begin{bmatrix} z_1^T & z_2^T \end{bmatrix}^T$ are respectively considered as the exogenous and objective signal vectors. In absence of saturation nonlinearity, the robust controller K_∞ is designed to ensure the internal stability of the perturbed normalized coprime factor shaped plant $G_p = (M + \Delta_M)^{-1}(N + \Delta_N)$ (see Figure 2.3) where the nominal shaped plant is $G_S = GW = M^{-1}N$. The controller is designed by satisfying the following constraint [65]:

$$\inf_{K_\infty \text{ stabilizing}} \left\| \begin{bmatrix} K_\infty \\ I \end{bmatrix} (I - G_S K_\infty)^{-1} M^{-1} \right\|_\infty \leq \frac{1}{\epsilon} = \gamma \tag{6.11}$$

where γ is the performance bound. Unfortunately, this bound is no longer applicable when the system operates in saturation mode. The objective of this section is to provide a systematic design procedure for H_∞ loop shaping control that depicts certain level of robustness in presence of input saturation constraint.

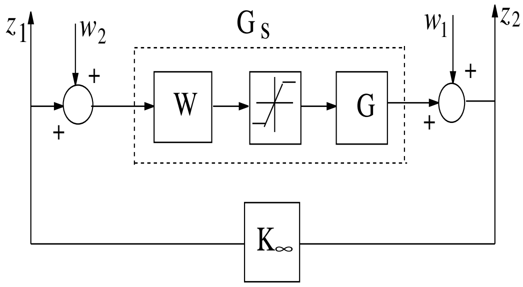

Figure 6.2: Four-block synthesis framework for H_∞ loop shaping control with input saturation

Let us consider the state space models of the nominal plant, $G(s)$ as

$$\left.\begin{aligned} \dot{x}_n &= A_n x_n + B_n u_n \\ y_n &= C_n x_n + D_n u_n \end{aligned}\right\} \tag{6.12}$$

and the pre-compensator, W as

$$\left.\begin{aligned} \dot{x}_w &= A_w x_w + B_w u_w \\ y_w &= C_w x_w + D_w u_w \end{aligned}\right\} \tag{6.13}$$

where, x_n, u_n and y_n are respectively state, control input and output vectors of the nominal plant and x_w, u_w and y_w are the state, input and output vectors for pre-compensator W. Here, we also consider the decoupled, sector-bounded, static saturation nonlinearity with an assumption, at j^{th} channel the maximum input to actuator is $y_{wmax,j}$. The maximum limit yields, the control input does not exceed the bound and it is assumed to be known to the designer. $sat(y_w)$ is the saturation function and for m number of channels, it becomes $SAT(y_w) = \begin{bmatrix} sat_1(y_{w1}), & \dots & , sat_m(y_{wm}) \end{bmatrix}^T$ where the input vector is $y_w = \begin{bmatrix} y_{w1}, & \dots & , y_{wm} \end{bmatrix}^T$. The saturation nonlinearity in normalized form can be defined as follows:

$$sat_j(y_{wj}) = \begin{cases} -1 & y_{wj} < -1, \\ y_{wj} & |y_{wj}| \leq 1, \\ +1 & y_{wj} > 1. \end{cases} \tag{6.14}$$

Graphically the nonlinearity has been shown in Figure 6.3 and as the maximum control input in each channel is specified, the corresponding slope β_j at j^{th} channel is also a known quantity to the designer.

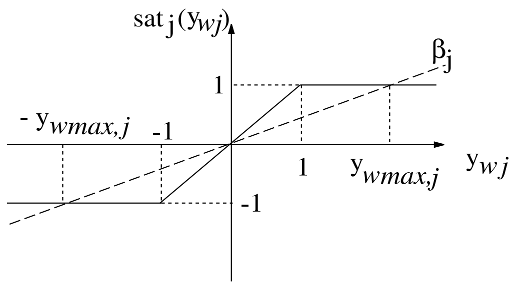

Figure 6.3: Saturation nonlinearity: y_{wj} is the j^{th} output of the pre-compensator (input to the j^{th} actuator)

Let us define, $sat_j(y_{wj}) = \theta_j y_{wj}$ where, $j = 1, \ldots, m$ and θ_j is defined as

$$\theta_j = \begin{cases} \frac{1}{y_{wj}} & y_{wj} > 1, \\ 1 & |y_{wj}| \leq 1, \\ -\frac{1}{y_{wj}} & y_{wj} < -1. \end{cases} \tag{6.15}$$

Here, θ_j is a function of y_{wj}. In the sequel, as $-y_{wmax,j} \leq y_{wj} \leq y_{wmax,j}$, it implies $\frac{1}{y_{wmax,j}} \leq \theta_j \leq 1$. In other way, $\beta_j \leq \theta_j \leq 1$ and for the multivariable system with m number of input channels, it can be written as $SAT(y_w) = \Theta y_w$ where, $\Theta = diag(\theta_1, \ldots, \theta_m)$ and $y_w = \begin{bmatrix} y_{w1}, & \ldots & , y_{wm} \end{bmatrix}^T$.

Proposition 6.1: *In H_∞ loop shaping framework, the shaped plant is obtained by cascading the nominal plant G with the pre-compensator W and they are described in (6.12) and (6.13) respectively. The shaped plant can be expressed as an equivalent polytopic LPV system when saturation nonlinearity appears in between the pre-compensator and nominal plant.*

Proof: As shown in Figure 6.2, in H_∞ loop shaping framework without considering the saturation constraint the shaped plant is GW but in presence of saturation nonlinearity, using (6.12), (6.13) and $SAT(y_w) = \Theta y_w$, the state-space model of the shaped plant can be derived as follows.

$$\left.\begin{aligned}\dot{x}_n &= A_n x_n + B_n \Theta C_w x_w + B_n \Theta D_w u_w\\ \dot{x}_w &= A_w x_w + B_w u_w\\ y_n &= C_n x_n + D_n \Theta C_w x_w + D_n \Theta D_w u_w\end{aligned}\right\} \tag{6.16}$$

Now, if the shaped plant is defined as $\begin{bmatrix} A_s & B_s \\ C_s & D_s \end{bmatrix}$, from (6.16) the state-space matrices are as follows:

$$\left.\begin{aligned}A_s &= \begin{bmatrix} A_n & B_n\Theta C_w \\ 0 & A_w \end{bmatrix} = \begin{bmatrix} A_n & B_n C_w \\ 0 & A_w \end{bmatrix} + \begin{bmatrix} B_n \\ 0 \end{bmatrix}(I-\Theta)\begin{bmatrix} 0 & -C_w \end{bmatrix}\\ B_s &= \begin{bmatrix} B_n\Theta D_w \\ B_w \end{bmatrix} = \begin{bmatrix} B_n D_w \\ B_w \end{bmatrix} + \begin{bmatrix} B_n \\ 0 \end{bmatrix}(I-\Theta)(-D_w)\\ C_s &= \begin{bmatrix} C_n & D_n\Theta C_w \end{bmatrix} = \begin{bmatrix} C_n & D_n C_w \end{bmatrix} + D_n (I-\Theta)\begin{bmatrix} 0 & -C_w \end{bmatrix}\\ D_s &= D_n\Theta D_w = D_n D_w + D_n (I-\Theta)(-D_w)\end{aligned}\right\} \tag{6.17}$$

where, $(I-\Theta) \in \Re^{m\times m}$. Further, we define $\Phi = (I-\Theta)$. Since $\beta_j \le \theta_j \le 1$, $0 \le \phi_j \le (1-\beta_j)$, where

$$\Phi = \mathrm{diag}(\phi_1, \ldots, \phi_m). \tag{6.18}$$

Replacing $(I-\Theta)$ with Φ in (6.17), we have

$$\left.\begin{aligned}A_s = \bar{A} + B_0\Phi C_0,\ B_s = \bar{B} + B_0\Phi D_0,\\ C_s = \bar{C} + D\Phi C_0 \text{ and } D_s = \bar{D} + D\Phi D_0,\end{aligned}\right\} \tag{6.19}$$

where $\bar{A}, \bar{B}, \bar{C}, \bar{D}, B_0, C_0$ and D_0 can be easily obtained by comparing (6.19) with (6.17). In (6.19), the state-space matrices are dependent on Φ through an affine relation where, Φ belongs to a given polytope as β_j is known in each channel, and hence using the Definition 6.2, the shaped plant along with the nonlinearity can be considered as a polytopic LPV system. □

Remark 6.2: *The shaped plant with saturation nonlinearity has been represented as a polytopic LPV system in (6.19). From linear differential inclusion (LDI) result [14], it is true that all trajectories of the nonlinear shaped plant can be represented by trajectories of the polytopic LVP system. However, the converse is not true. Some trajectories of (6.19) are not the trajectories of the nonlinear shaped plant and hence, some con-*

servatism is imposed in the design when the nonlinear plant is described as a polytopic LPV system.

Theorem 6.3: *Let the nominal plant and pre-compensator are strictly proper and $-y_{wmax,j} \leq y_{wj} \leq y_{wmax,j}$ is the known bound for j^{th} channel where $j = 1, \ldots, m$, then the shaped plant with input saturation can be represented as a Polytopic LPV system $\begin{bmatrix} A_s & B_s \\ C_s & 0 \end{bmatrix}$ as defined in (6.19). If the triplet (A_s, B_s, C_s) is stabilizable and detectable for all Φ in the polytope $\Omega = \left\{\sum_{i=1}^{2^m} \alpha_i \omega_i : \alpha_i \geq 0, \sum_{i=1}^{2^m} \alpha_i = 1\right\}$, where $B_s = \tilde{B} = \begin{bmatrix} 0 \\ B_w \end{bmatrix}$ and $C_s = \tilde{C} = \begin{bmatrix} C_n & 0 \end{bmatrix}$, there exists an LPV controller for $\gamma \geq 1$ with $\sup_{\Phi \in \Omega} \sup_{\|w\|_2 \neq 0,\ w \in L_2} \frac{\|z\|_2}{\|w\|_2} \leq \gamma$ where $z = \begin{bmatrix} z_1^T & z_2^T \end{bmatrix}^T$ and $w = \begin{bmatrix} w_1^T & w_2^T \end{bmatrix}^T$ (shown in Figure 6.2), if and only if, the following matrix inequalities hold for every $i = 1, \ldots, 2^m$*

$$\begin{pmatrix} N_R & 0 \\ 0 & I \end{pmatrix}^T \begin{pmatrix} A_{si}R + R{A_{si}}^T & R\begin{bmatrix} 0 & \tilde{C}^T \end{bmatrix} & \begin{bmatrix} 0 & \tilde{B} \end{bmatrix} \\ \begin{bmatrix} 0 \\ \tilde{C} \end{bmatrix} R & -\gamma I & \begin{bmatrix} 0 & 0 \\ I & 0 \end{bmatrix} \\ \begin{bmatrix} 0 \\ \tilde{B}^T \end{bmatrix} & \begin{bmatrix} 0 & I \\ 0 & 0 \end{bmatrix} & -\gamma I \end{pmatrix} \begin{pmatrix} N_R & 0 \\ 0 & I \end{pmatrix} < 0 \quad (6.20)$$

$$\begin{pmatrix} N_S & 0 \\ 0 & I \end{pmatrix}^T \begin{pmatrix} {A_{si}}^T S + S A_{si} & S\begin{bmatrix} 0 & \tilde{B} \end{bmatrix} & \begin{bmatrix} 0 & \tilde{C}^T \end{bmatrix} \\ \begin{bmatrix} 0 \\ \tilde{B}^T \end{bmatrix} S & -\gamma I & \begin{bmatrix} 0 & I \\ 0 & 0 \end{bmatrix} \\ \begin{bmatrix} 0 \\ \tilde{C} \end{bmatrix} & \begin{bmatrix} 0 & 0 \\ I & 0 \end{bmatrix} & -\gamma I \end{pmatrix} \begin{pmatrix} N_S & 0 \\ 0 & I \end{pmatrix} < 0 \quad (6.21)$$

and

$$\begin{pmatrix} R & I \\ I & S \end{pmatrix} \geq 0 \quad (6.22)$$

where, $R > 0$, $S > 0$, N_R and N_S are the bases of the null spaces of $\begin{bmatrix} \tilde{B}^T & I & 0 \end{bmatrix}$ and $\begin{bmatrix} \tilde{C} & I & 0 \end{bmatrix}$ respectively.

Proof: It is assumed that the nominal plant and pre-compensator are strictly proper. Hence, referring to the state-space models defined in (6.12) and (6.13), we have $D_n = 0$

and $D_w = 0$ and from (6.17), $B_s = \tilde{B} = \begin{bmatrix} 0 \\ B_w \end{bmatrix}, C_s = \tilde{C} = \begin{bmatrix} C_n & 0 \end{bmatrix}$ and $D_s = 0$ are obtained. From Figure 6.2, the generalized plant for H_∞ loop shaping control in four-block synthesis framework can be obtained as

$$\left.\begin{aligned} \dot{\bar{x}} &= A_s\bar{x} + \tilde{B}w_2 + \tilde{B}u \\ z_1 &= u \\ z_2 &= \tilde{C}\bar{x} + w_1 \\ y &= \tilde{C}\bar{x} + w_1 \end{aligned}\right\} \tag{6.23}$$

where, $\bar{x} = \begin{bmatrix} x_n^T & x_w^T \end{bmatrix}^T$ and $y = z_2$. Comparing (6.23) with (6.5), we have $A = A_s, B_1 = \begin{bmatrix} 0 & \tilde{B} \end{bmatrix}, B_2 = \tilde{B}, C_1 = \begin{bmatrix} 0 \\ \tilde{C} \end{bmatrix}, C_2 = \tilde{C}, D_{11} = \begin{bmatrix} 0 & 0 \\ I & 0 \end{bmatrix}, D_{12} = \begin{bmatrix} I \\ 0 \end{bmatrix}, D_{21} = \begin{bmatrix} I & 0 \end{bmatrix}$ and $D_{22} = 0$. Since the control input is bounded in each channel, from Proposition 6.1, it is obvious that Φ will be in a given polytope Ω where $\omega_i = 1, \ldots, 2^m$ are the vertices of the polytope and it depicts (6.23) as a generalized polytopic LPV system. As it satisfies all the assumptions for Theorem 6.2, the theorem can be applied directly for the generalized plant (6.23) in order to obtain the conditions (6.20)-(6.22) and this in turn, ensures the existence of a stabilizing controller with a performance bound γ. □

Remark 6.3: *The pre-compensator and nominal plant are assumed to be strictly proper in order to satisfy the assumption (ii) of Theorem 6.2. In [6], a technique has been discussed where the assumption (ii) is enforced by pre and/or post-filtering the control input and/or measure output of the generalized plant.*

Controller construction

For m number of input channels, the polytope has 2^m number of vertices and in Theorem 6.3, the numbers of LMI constraints are $(2^{m+1}+1)$. If the solvability conditions are satisfied, we have R, S and γ and this, in turn, indicates there exists an LPV controller. The idea is now to construct controllers for the vertices of the polytope and to use a convex combination of these controllers for an arbitrary point of the convex polytope.

Let the LPV controller $\Lambda(\Phi)$ be

$$\begin{bmatrix} A_c(\Phi) & B_c(\Phi) \\ C_c(\Phi) & D_c(\Phi) \end{bmatrix} \tag{6.24}$$

and it will be obtained by following the procedure given in [6]. From (6.23) and (6.24), the closed-loop system becomes

$$\left[\begin{array}{c} \dot{\bar{x}} \\ \dot{x}_c \\ \hline z_1 \\ z_2 \end{array}\right] = \left[\begin{array}{cc|cc} A_s + \tilde{B}D_c\tilde{C} & \tilde{B}C_c & \tilde{B}D_c & \tilde{B} \\ B_c\tilde{C} & A_c & B_c & 0 \\ \hline D_c\tilde{C} & C_c & D_c & 0 \\ \tilde{C} & 0 & I & 0 \end{array}\right] \left[\begin{array}{c} \bar{x} \\ x_c \\ \hline w_1 \\ w_2 \end{array}\right] \tag{6.25}$$

$$\Rightarrow \left.\begin{array}{r} \dot{x}_{cl} = A_{cl}x_{cl} + B_{cl}w \\ z = C_{cl}x_{cl} + D_{cl}w \end{array}\right\} \tag{6.26}$$

where x_c is the controller state, $x_{cl} = \begin{bmatrix} \bar{x}^T & x_c^T \end{bmatrix}^T$, $w = \begin{bmatrix} w_1^T & w_2^T \end{bmatrix}^T$ and $z = \begin{bmatrix} z_1^T & z_2^T \end{bmatrix}^T$. Here, the dependence on Φ is not shown for simplicity and A_{cl}, B_{cl}, C_{cl} and D_{cl} are the closed-loop state-space matrices with proper dimensions. Now, these matrices can be written as follows:

$$\left.\begin{array}{r} A_{cl} = A_0^c + B^c\Lambda\Pi, B_{cl} = B_0^c + B^c\Lambda E_{21}, \\ C_{cl} = C_0^c + E_{12}\Lambda\Pi, D_{cl} = D_0^c + E_{12}\Lambda E_{21} \end{array}\right\} \tag{6.27}$$

where,

$$\left.\begin{array}{l} A_0^c = \begin{bmatrix} A_s & 0 \\ 0 & 0 \end{bmatrix}, B_0^c = \begin{bmatrix} 0 & \tilde{B} \\ 0 & 0 \end{bmatrix}, C_0^c = \begin{bmatrix} 0 & 0 \\ \tilde{C} & 0 \end{bmatrix}, D_0^c = \begin{bmatrix} 0 & 0 \\ I & 0 \end{bmatrix} \\ B^c = \begin{bmatrix} 0 & \tilde{B} \\ I & 0 \end{bmatrix}, \Pi = \begin{bmatrix} 0 & I \\ \tilde{C} & 0 \end{bmatrix}, E_{21} = \begin{bmatrix} 0 & 0 \\ I & 0 \end{bmatrix}, E_{12} = \begin{bmatrix} 0 & I \\ 0 & 0 \end{bmatrix} \end{array}\right\} \tag{6.28}$$

B^c, Π, E_{21}, E_{12} are parameter independent and the state-space matrices A_{cl}, B_{cl}, C_{cl} and D_{cl} are the affine functions of Λ. Now, after having the two stabilizing solutions R and S from Theorem 6.3, the closed-loop Lyapunov matrix P correspond to (6.26) is obtained as the unique solution of the following linear equation (see Appendix-B)

$$\begin{bmatrix} S & I \\ \tilde{N}^T & 0 \end{bmatrix} = P \begin{bmatrix} I & R \\ 0 & \tilde{M}^T \end{bmatrix} \tag{6.29}$$

where $\tilde{M}$ and $\tilde{N}$ are full rank matrices with $\tilde{M}\tilde{N}^T = I - RS$. When P is known, at i^{th} vertex the controller Λ_i is calculated by solving the following matrix inequality which is obtained from Lemma 6.2.

$$\begin{pmatrix} A_{cl}^T(\omega_i)P + PA_{cl}(\omega_i) & PB_{cl}(\omega_i) & C_{cl}^T(\omega_i) \\ B_{cl}^T(\omega_i)P & -\gamma I & D_{cl}^T(\omega_i) \\ C_{cl}(\omega_i) & D_{cl}(\omega_i) & -\gamma I \end{pmatrix} < 0 \tag{6.30}$$

where, $A_{cl}, B_{cl}, C_{cl}, D_{cl}$ are the closed-loop state-space matrices as defined in (6.27)-(6.28) and $\omega_i, i = 1, \ldots, 2^m$ are the vertices of the polytope. The controller LMI can easily be formed from (6.30) (see Section A.1 in Appendix-A) and 2^m number of controllers are designed at vertices of the polytope. These controllers are scheduled based on a strategy when Φ varies in the given polytope [6] (see Section A.2 in Appendix A). Finally, combining pre-compensator with $\Lambda(\Phi)$ the LPV H_∞ loop shaping controller is obtained.

Remark 6.4: *Since (6.23) is a generalized polytopic LPV system, using vertex property presented in Theorem 6.1, the performance bound γ is ensured in the given polytope Ω. The controllers at each vertices are designed off-line and based on the varying parameter in the polytope, the controllers are interpolated. The designed controller is also a polytopic LPV controller.*

Remark 6.5: *The γ is obtained for all the shaped plants that lie in a given polytope. Hence, γ^{-1} accounts robust stability margin for the normalized coprime factor uncertainty of the shaped plant when input saturation remains in a pre-specified limit.*

6.4 Robust controller design with input saturation using Popov stability criteria

In this section, using H_∞ loop shaping approach a different design technique has been proposed to achieve robustness of an LTI plant with input saturation constraint. Like in preceding section, here it is also assumed that in each channel, the maximum input to actuator is limited that indicates, the saturation nonlinearity satisfies a local sector-bound. With this sector-bound condition, the H_∞ loop shaping synthesis framework has been transformed into an equivalent Lur'e type system and then, adopting the Popov absolute stability criteria a robust controller has been designed to ensure certain robustness. Here, the upper bound of L_2-gain between the exogenous and objective signal is minimized to improve the performance and stability of the closed-loop system. This effectively yields the robust stability margin for normalized coprime factor uncertainty description of the shaped plant. The design constraints are formulated in BMI framework [9].

Note that, the BMI design constraint is well-known in robust control theory. However, the complexity due to its non-convex characteristics makes it hard to apply BMIs to control synthesis problems. Even though several algorithms have been proposed, their performances depend on how to relax given BMI problems. Iterative method is one of the simplest technique that can be adopted for solving BMI problem but no convergence algorithm is yet addressed that can reduce the computational burden [105]. The existing algorithms all are iterative in nature, and the basic idea lies in the technique to convert the BMI constraint into LMI form by fixing some variables. One such popular algorithm is the V-K iteration [8, 9]. In this algorithm, the first step employs a convex optimization problem to find out the Popov parameters by fixing the controller matrices. On the other hand, K-iteration is the synthesis step, where the controller matrices with optimal performance bound are found out by fixing the Popov parameters. However, in the present work we have used the LMI based iterative method tom solve synthesis problem with BMI constraints. This LMI based iterative method helps to analyze the convergency of V-K algorithm.

6.4.1 H_∞ loop shaping control with input saturation: Lur'e type system representation

Figure 6.4 depicts the equivalent four-block synthesis structure for H_∞ loop shaping control which is already shown in Figure 6.2[1]. Here, we consider the state-space models of nominal plant G and pre-compensator W as given in (6.12) and (6.13) respectively. The dimensions of state-space matrices are given as follows: $A_n \in \Re^{n_n \times n_n}$, $B_n \in \Re^{n_n \times m}$, $C_n \in \Re^{n_y \times n_n}$, $D_n \in \Re^{n_y \times m}$, $A_w \in \Re^{n_w \times n_w}$, $B_w \in \Re^{n_w \times m}$, $C_w \in \Re^{m \times n_w}$, $D_w \in$

[1]Here, the position of exogenous input vectors w_1 and w_2 has been interchanged, however, it does not lose any generality (see Section 2.4 in Chapter 2).

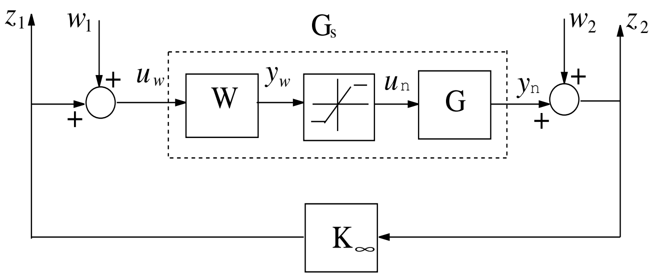

Figure 6.4: Four-block synthesis framework for H_∞ loop shaping control with input saturation constraint

$\Re^{m\times m}$. In normalized form, the saturation nonlinearity has been defined in (6.14).

Now, the block-diagram shown in Figure 6.4 has to be transformed into a Lur'e type system by replacing the saturation block with dead-zone nonlinearity in combination with a linear part that has been shown in Figure 6.5 [45].

Defining the dead-zone nonlinearity as $dzn(y_w)$, we have $u_n = sat(y_w) = y_w - dzn(y_w)$ and at j^{th} channel, if the saturation nonlinearity satisfies the sector condition

$$\beta_j y_{wj}^2 \leq sat_j(y_{wj})y_{wj} \leq y_{wj}^2$$

where $\beta_j = \frac{1}{y_{wmax,j}}$ for $j = 1, \ldots, m$, we have

$$-y_{wj}^2 \leq -sat_j(y_{wj})y_{wj} \leq -\beta_j y_{wj}^2$$

$$\Rightarrow\ 0 \leq y_{wj}(y_{wj} - sat_j(y_{wj})) \leq y_{wj}^2(1-\beta_j)$$

$$\Rightarrow\ 0 \leq y_{wj}\ dzn(y_{wj}) \leq y_{wj}^2(1-\beta_j).$$

For simplicity, we assume that the maximum bounds of input signals at each channel are same and it is $y_{wmax,j} = \nu$ for $j = 1, \ldots, m$ and $\beta = \frac{1}{\nu}$. In Figure 6.5, we have defined $z_s = y_w$ and output of the dead-zone nonlinear element is w_s. Then, considering the objective and exogenous signal vectors respectively as $[z_s^T\ z_2^T\ z_1^T]^T$ and $[w_s^T\ w_2^T\ w_1^T]^T$, and assuming $D_w = 0$, we have a generalized plant

$$\left.\begin{aligned} \dot{x}_s &= A_a x_s + B_{w_s}^{\beta} w_s + B_w^e w + B_u u \\ z_s &= C_{z_s} x_s \\ z &= C_z x_s + D_{w_s z}^{\beta} w_s + D_{wz} w + D_{uz} u \\ y &= C_y x_s + D_{w_s y}^{\beta} w_s + D_{wy} w \end{aligned}\right\} \tag{6.31}$$

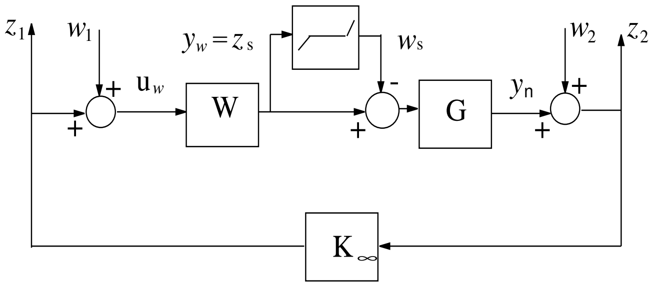

Figure 6.5: Four-block synthesis framework for H_∞ loop shaping control with dead-zone nonlinearity

where, $x_s = [x_n^T\ x_w^T]^T,\ y = z_2,\ u = z_1,\ z = [z_2^T\ z_1^T]^T$ and $w = [w_2^T\ w_1^T]^T$. The matrices $B_{w_s}^\beta,\ D_{w_s z}^\beta$ and $D_{w_s y}^\beta$ are obtained respectively by multiplying $B_{w_s} = \begin{bmatrix} -B_n \\ 0 \end{bmatrix}$, $D_{w_s z} = \begin{bmatrix} -D_n \\ 0 \end{bmatrix}$ and $D_{w_s y} = -D_n$ with $(1-\beta)$ and the structure of the matrices are shown below:

$$A_a = \begin{bmatrix} A_n & B_n C_w \\ 0_{n_w \times n_n} & A_w \end{bmatrix},\ B_{w_s}^\beta = \begin{bmatrix} -(1-\beta)B_n \\ 0_{n_w \times m} \end{bmatrix},\ B_w^e = \begin{bmatrix} 0_{n_n \times n_y} & 0_{n_n \times m} \\ 0_{n_w \times n_y} & B_w \end{bmatrix},$$

$$B_u = \begin{bmatrix} 0_{n_n \times m} \\ B_w \end{bmatrix}, C_{z_s} = \begin{bmatrix} 0_{m \times n_n} & C_w \end{bmatrix},\ C_z = \begin{bmatrix} C_n & D_n C_w \\ 0_{m \times n_n} & 0_{m \times n_w} \end{bmatrix},$$

$$C_y = \begin{bmatrix} C_n & D_n C_w \end{bmatrix}, D_{w_s z}^\beta = \begin{bmatrix} -(1-\beta)D_n \\ 0_{m \times m} \end{bmatrix}, D_{wz} = \begin{bmatrix} I_{n_y} & 0_{n_y \times m} \\ 0_{m \times n_y} & 0_{m \times m} \end{bmatrix},$$

$$D_{uz} = \begin{bmatrix} 0_{n_y \times m} \\ I_m \end{bmatrix}, D_{w_s y}^\beta = -(1-\beta)D_n,\ D_{wy} = \begin{bmatrix} I_{n_y} & 0_{n_y \times m} \end{bmatrix}.$$

Note that after scaling, the nonlinearity $\frac{dzn_j(z_{sj})}{(1-\beta)}$ remains in the sector bound [0 1].

Let us consider the state-space model of the controller as

$$\left.\begin{aligned} \dot{x}_c &= A_c x_c + B_c y \\ u &= C_c x_c + D_c y \end{aligned}\right\} \tag{6.32}$$

where, $x_c \in \Re^{(n_n + n_w = n_c)}$ is the controller state vector and $A_c,\ B_c,\ C_c,\ D_c$ are with proper dimensions. Combining (6.31) and (6.32), the closed-loop system becomes

$$\left[\begin{array}{c} \dot{x}_s \\ \dot{x}_c \\ \hline z_s \\ \hline z \end{array}\right] = \left[\begin{array}{cc|c|c} A_a + B_u D_c C_y & B_u C_c & B^{\beta}_{w_s} + B_u D_c D^{\beta}_{w_s y} & B^{e}_{w} + B_u D_c D_{wy} \\ B_c C_y & A_c & B_c D^{\beta}_{w_s y} & B_c D_{wy} \\ \hline C_{z_s} & 0 & 0 & 0 \\ \hline C_z + D_{uz} D_c C_y & D_{uz} C_c & D^{\beta}_{w_s z} + D_{uz} D_c D^{\beta}_{w_s y} & D_{wz} + D_{uz} D_c D_{wy} \end{array}\right] \left[\begin{array}{c} x_s \\ x_c \\ \hline w_s \\ \hline w \end{array}\right].$$

Now, considering the closed-loop state vector as $x_{cl} = [x_s^T \ x_c^T]^T$, in state-space model it can be written as

$$\left.\begin{array}{l} \dot{x}_{cl} = A^{cl} x_{cl} + B^{cl}_{w_s} w_s + B^{cl}_{w} w \\ z_s = C^{cl}_{z_s} x_{cl} \\ z = C^{cl}_{z} x_{cl} + D^{cl}_{w_s z} w_s + D^{cl}_{wz} w \end{array}\right\} \tag{6.33}$$

where,

$$A^{cl} = \begin{bmatrix} A_a + B_u D_c C_y & B_u C_c \\ B_c C_y & A_c \end{bmatrix}, \ B^{cl}_{w_s} = \begin{bmatrix} B^{\beta}_{w_s} + B_u D_c D^{\beta}_{w_s y} \\ B_c D^{\beta}_{w_s y} \end{bmatrix},$$

$$B^{cl}_{w} = \begin{bmatrix} B^{e}_{w} + B_u D_c D_{wy} \\ B_c D_{wy} \end{bmatrix}, C^{cl}_{z_s} = \begin{bmatrix} C_{z_s} & 0_{m \times n_c} \end{bmatrix}, C^{cl}_{z} = \begin{bmatrix} C_z + D_{uz} D_c C_y & D_{uz} C_c \end{bmatrix},$$

$$D^{cl}_{w_s z} = D^{\beta}_{w_s z} + D_{uz} D_c D^{\beta}_{w_s y}, \ D^{cl}_{wz} = D_{wz} + D_{uz} D_c D_{wy}.$$

In block-diagram form, (6.33) can be represented as follows:

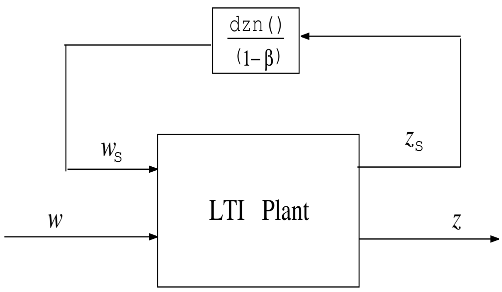

Figure 6.6: Lur'e type system

Note that, the system shown in Figure 6.6 is in the form of a Lur'e system (see Figure 6.1). Now in synthesis framework, a controller (6.32) has to be designed such that the robust stability will be ensured leading to minimize the L_2-gain between w and z. In order to achieve this objective, the Popov absolute stability criteria has been adopted with a Lyapunov function of the following form [14]

$$V(x_{cl}) = x_{cl}^T P x_{cl} + 2\sum_{j=1}^{m} \xi_j \int_0^{C_{z_s,j}^{cl} x_{cl}} \phi_j(\zeta) d\zeta \tag{6.34}$$

where, $C_{z_s,j}^{cl}$ is the j^{th} row of the matrix $C_{z_s}^{cl}$, $j = 1, \ldots, m$ and $\phi_j(.) = \frac{dzn_j(.)}{(1-\beta)}$.

6.4.2 Controller synthesis

The system described in (6.33) is the equivalent Lur'e type system representation of the H_∞ loop shaping control framework when input saturation is taken into account. Note that, the minimized upper bound of L_2-gain between w and z will account (inverse of this gain) the robust stability margin for the normalized coprime factor uncertainty description of the shaped plant when control input does not exceed the pre-specified saturation level. To minimize L_2 gain between w and z, the following theorem is presented.

Theorem 6.4 [14]: *The upper bound on the L_2-gain between w and z is finite if there exists a Lyapunov function in the form (6.34) and satisfies*

$$\begin{bmatrix} PA^{cl} + A^{cl^T}P + C_z^{cl^T}C_z^{cl} & A^{cl^T}C_{z_s}^{cl^T}\Upsilon + PB_{w_s}^{cl} + C_z^{cl^T}D_{w_sz}^{cl} + C_{z_s}^{cl^T}T & PB_w^{cl} + C_z^{cl^T}D_{wz}^{cl} \\ \Upsilon C_{z_s}^{cl}A^{cl} + B_{w_s}^{cl^T}P + D_{w_sz}^{cl^T}C_z^{cl} + TC_{z_s}^{cl} & \Upsilon C_{z_s}^{cl}B_{w_s}^{cl} + B_{w_s}^{cl^T}C_{z_s}^{cl^T}\Upsilon + D_{w_sz}^{cl^T}D_{w_sz}^{cl} - 2T & \Upsilon C_{z_s}^{cl}B_w^{cl} + D_{w_sz}^{cl^T}D_{wz}^{cl} \\ B_w^{cl^T}P + D_{wz}^{cl^T}C_z^{cl} & B_w^{cl^T}C_{z_s}^{cl^T}\Upsilon + D_{wz}^{cl^T}D_{w_sz}^{cl} & D_{wz}^{cl^T}D_{wz}^{cl} - \gamma^2 I \end{bmatrix} \leq 0 \tag{6.35}$$

where $\gamma^2 > 0$, $\Upsilon = diag(\xi_1, \ldots, \xi_m) \geq 0$ and $T = diag(\tau_1, \ldots, \tau_m)$, and the bound can be obtained by solving the following optimization problem:

$$\left.\begin{array}{r} \textit{Minimize} \ \ \gamma^2 \\ \textit{Subject to} \ \ (6.35), P > 0, \Upsilon \geq 0, T \geq 0 \end{array}\right\} \tag{6.36}$$

Proof: See Section A.3 in Appendix A. □

In Theorem 6.4, a sufficient condition has been presented for the existence of the Lyapunov function of Lur'e type leading to ensure absolute stability of the system (6.33) by minimizing the upper bound of L_2-gain between w and z. The unknown variables are symmetric positive definite matrix P, T and the scalar terms $\xi_j,\ j = 1, \dots, m$ which are placed with the integration term as shown in (6.34). The existence of feasible solutions yield the existence of (6.34) that in turn, establishes a sufficient condition for absolute stability of the Lur'e system (6.33). Furthermore, by solving the problem (6.36) in LMI framework one can easily find the L_2-gain γ.

Remark 6.6: *Note that, when the controller matrices (A_c, B_c, C_c and D_c) are known, (6.36) is an LMI problem that provides an analytical framework for LTI plant with input saturation constraint. However, applying this theorem the controller (6.32) can not be synthesized straightforwardly as (6.36) consists of some product terms involving with unknown matrices A_c, B_c, C_c and D_c.*

In the following, a procedure has been given for designing a strictly proper controller ($D_c = 0$)[9]. Note that, with unknown $A_c, B_c, C_c, \Upsilon, P$ and γ, (6.35) is a nonlinear matrix inequality constraint. After some simplifications and changing the variables, this problem can be formulated into the BMI framework. To obtain it, first, the nonlinear constraint (6.35) has to be rewritten in such a way that the variable matrix A_c will be eliminated. In the following steps, this procedure has been illustrated in detail. From (6.33) (with $D_c = 0$), we have

$$A^{cl} = \begin{bmatrix} A_a & B_u C_c \\ B_c C_y & 0_{n_c \times n_c} \end{bmatrix} + \begin{bmatrix} 0_{n_c \times n_c} \\ I_{n_c} \end{bmatrix} A_c \begin{bmatrix} 0_{n_c \times n_c} & I_{n_c} \end{bmatrix} = \bar{A}_0 + J A_c J^T \tag{6.37}$$

where $\bar{A}_0 = \begin{bmatrix} A_a & B_u C_c \\ B_c C_y & 0_{n_c \times n_c} \end{bmatrix}$ and $J = \begin{bmatrix} 0_{n_c \times n_c} \\ I_{n_c} \end{bmatrix}$. Replacing $A^{cl} = \bar{A}_0 + J A_c J^T$ in (6.35), we have

$$\left[\begin{array}{ccc} P\bar{A}_0 + \bar{A}_0^T P + {C_z^{cl}}^T C_z^{cl} & \bar{A}_0^T {C_{z_s}^{cl}}^T \Upsilon + P B_{w_s}^{cl} + {C_z^{cl}}^T D_{w_s z}^{cl} + {C_{z_s}^{cl}}^T T & P B_w^{cl} + {C_z^{cl}}^T D_{wz}^{cl} \\ \Upsilon C_{z_s}^{cl} \bar{A}_0 + {B_{w_s}^{cl}}^T P + {D_{w_s z}^{cl}}^T C_z^{cl} + T C_{z_s}^{cl} & \Upsilon C_{z_s}^{cl} B_{w_s}^{cl} + {B_{w_s}^{cl}}^T {C_{z_s}^{cl}}^T \Upsilon + {D_{w_s z}^{cl}}^T D_{w_s z}^{cl} - 2T & \Upsilon C_{z_s}^{cl} B_w^{cl} + {D_{w_s z}^{cl}}^T D_{wz}^{cl} \\ {B_w^{cl}}^T P + {D_{wz}^{cl}}^T C_z^{cl} & {B_w^{cl}}^T {C_{z_s}^{cl}}^T \Upsilon + {D_{wz}^{cl}}^T D_{w_s z}^{cl} & {D_{wz}^{cl}}^T D_{wz}^{cl} - \gamma^2 I \end{array} \right]$$

$$
+\begin{bmatrix} PJ \\ \Upsilon C_{z_s}^{cl} J \\ 0_{(n_y+m)\times n_c} \end{bmatrix} A_c \begin{bmatrix} J^T & 0_{n_c\times m} & 0_{n_c\times(n_y+m)} \end{bmatrix}
$$

$$
+\begin{bmatrix} J \\ 0_{m\times n_c} \\ 0_{(n_y+m)\times n_c} \end{bmatrix} A_c^T \begin{bmatrix} J^T P & J^T {C_{z_s}^{cl}}^T \Upsilon & 0_{n_c\times(n_y+m)} \end{bmatrix} < 0. \tag{6.38}
$$

Note that, $C_{z_s}^{cl} J = 0_{m\times n_c}$ and defining $\Pi^T = \begin{bmatrix} J^T P & 0_{n_c\times m} & 0_{n_c\times(n_y+m)} \end{bmatrix}$ and $\Xi^T = \begin{bmatrix} J^T & 0_{n_c\times m} & 0_{n_c\times(n_y+m)} \end{bmatrix}$, (6.38) can be written in the following form

$$
\Psi + \Pi A_c \Xi^T + \Xi A_c^T \Pi^T < 0, \tag{6.39}
$$

where Ψ is the first term of the inequality (6.38). Now, taking the orthogonal complements of Π^T and Ξ^T respectively as

$$
\Pi_\perp = \begin{bmatrix} P^{-1} J_\perp & 0 & 0 \\ 0 & I_m & 0 \\ 0 & 0 & I_{(n_y+m)} \end{bmatrix} \text{ and } \Xi_\perp = \begin{bmatrix} J_\perp & 0 & 0 \\ 0 & I_m & 0 \\ 0 & 0 & I_{(n_y+m)} \end{bmatrix},
$$

and applying the elimination lemma (see Chapter 1), we have a solution A_c from (6.39), if and only if,

$$
\Xi_\perp^T \Psi \Xi_\perp < 0 \text{ and } \Pi_\perp^T \Psi \Pi_\perp < 0 \tag{6.40}
$$

hold, where $J_\perp = \begin{bmatrix} I_{n_c} \\ 0_{n_c\times n_c} \end{bmatrix}$ is the orthogonal complement of J^T. To find the solution, P and P^{-1} are partitioned as

$$
P = \begin{bmatrix} \tilde{P} & \tilde{M} \\ \tilde{M}^T & \tilde{R} \end{bmatrix},\ P^{-1} = \begin{bmatrix} \tilde{Q} & \tilde{N} \\ \tilde{N}^T & \tilde{S} \end{bmatrix} \tag{6.41}
$$

where $\tilde{N}\tilde{M}^T = I - \tilde{Q}\tilde{P}$. Then replacing P and P^{-1} in (6.40) and defining $Y = C_c \tilde{N}^T$ and $Z = \tilde{M} B_c$, (6.40) is simplified as follows (see A.4 in Appendix-A):

$$
\left[\begin{matrix} \tilde{P} A_a + Z C_y + A_a^T \tilde{P} + C_y^T Z^T + {C_z^{cl}}^T C_z^{cl} \\ \Upsilon C_{z_s}^{cl} A_a + {D_{w_s y}^{\beta}}^T Z^T + {B_{w_s}^{\beta}}^T \tilde{P} + {D_{w_s z}^{\beta}}^T C_z + T C_{z_s} \\ B_w^T \tilde{P} + D_{wy}^T Z^T + D_{wz}^T C_z \end{matrix} \right.
$$

$$\left.\begin{matrix} (.)^T & (.)^T \\ \Upsilon C_{z_s} B^{\beta}_{w_s} + {B^{\beta}_{w_s}}^T C^T_{z_s}\Upsilon + {D^{\beta}_{w_s z}}^T D^{\beta}_{w_s z} - 2T & (.)^T \\ B^T_w C^T_{z_s}\Upsilon + D^T_{wz} D^{\beta}_{w_s z} & D^T_{wz} {D^{\beta}_{w_s z}}^T - \gamma^2 I \end{matrix}\right] < 0 \tag{6.42}$$

$$\left[\begin{matrix} A_a\tilde{Q} + B_u Y + \tilde{Q}A^T_a + Y^T B^T_u \\ \Upsilon C_{z_s} A_a \tilde{Q} + \Upsilon C_{z_s} B_u Y + {D^{\beta}_{w_s z}}^T C_z \tilde{Q} + {D^{\beta}_{w_s z}}^T D_{uz} Y + T C_{z_s}\tilde{Q} + {B^{\beta}_{w_s}}^T \\ B^T_w + C_z\tilde{Q} + D_{uz} Y \\ C_z\tilde{Q} + D_{uz} Y \end{matrix}\right.$$

$$\left.\begin{matrix} (.)^T & (.)^T & (.)^T \\ \Upsilon C_{z_s} B^{\beta}_{w_s} + {B^{\beta}_{w_s}}^T C^T_{z_s}\Upsilon + {D^{\beta}_{w_s z}}^T D^{\beta}_{w_s z} - 2T & (.)^T & (.)^T \\ B^T_w C^T_{z_s}\Upsilon + D^T_{wz} D^{\beta}_{w_s z} & D^T_{wz} D_{wz} - \gamma^2 I & (.)^T \\ 0 & 0 & -I \end{matrix}\right] < 0. \tag{6.43}$$

The inequality (6.43) is not linear as there are some product terms comprising $\Upsilon, T, \tilde{Q}$ and Y. When T and Υ are fixed, (6.43) is an LMI in $\tilde{Q}, Y$ and for fixed $\tilde{Q}, Y$, (6.43) is an LMI in Υ, T. The positive definite constraint on $\tilde{P}, \tilde{Q}$ is imposed from the existence of symmetric matrices U_1 and U_2 such that [9]

$$\begin{bmatrix} U_1 & Z^T & 0 & 0 \\ Z & \tilde{P} & I & 0 \\ 0 & I & \tilde{Q} & Y^T \\ 0 & 0 & Y & U_2 \end{bmatrix} > 0. \tag{6.44}$$

Hence, finally the optimization problem becomes

$$\left.\begin{matrix} \text{Minimize} \;\; \gamma^2 \\ \text{Subject to} \;\; (6.42), (6.43), (6.44), \Upsilon \geq 0, T \geq 0 \end{matrix}\right\}. \tag{6.45}$$

Design steps

1. Without considering the effect of saturation, for a given nominal plant G, a H_∞ loop shaping controller is designed. The selected pre-compensator is W.

2. With known controller matrices which are obtained from step 1, (6.36) is solved to find the optimal Υ and T.

3. For each diagonal element of Υ and T, grid the range from 0 to its optimal value.

Finer grid depicts better result.

4. At each node, fix Υ and T in (6.45). Then, LMI (6.45) is solved to find $\gamma, \tilde{P}$, $\tilde{Q}$, Y, Z, U_1 and U_2. This step is carried out for each node and find the minimum γ.

5. Corresponding to the node where minimum γ is obtained, $\tilde{P}, \tilde{Q}, Y, Z, U_1$ and U_2 are calculated.

6. Then, $\tilde{M}$ and $\tilde{N}$ are selected such that $\tilde{N}\tilde{M}^T = I - \tilde{Q}\tilde{P}$ and using the relations $Y = C_c\tilde{N}^T$ and $Z = \tilde{M}B_c$, the controller matrices C_c and B_c are found out.

7. The closed-loop Lyapunov matrix P is found out and then, A_c is calculated by solving the LMI constraint (6.39).

8. Combining weight with the controller, the H_∞ loop shaping controller is obtained.

6.5 Numerical example

In control system literatures, many researchers have studied the linearized longitudinal dynamics of F-8 Aircraft model as an example of saturation control to show the effectiveness of their proposed methods [28, 51, 52] (already discussed in Chapters 3 and 5). The same example has been considered here.

The linearized state space model of the longitudinal dynamics of F-8 aircraft is shown below [52]:

$$\dot{x_n} = \begin{bmatrix} -0.8 & -0.0006 & -12 & 0 \\ 0 & -0.014 & -16.64 & -32.2 \\ 1 & -0.0001 & -1.5 & 0 \\ 1 & 0 & 0 & 0 \end{bmatrix} x_n + \begin{bmatrix} -19 & -3 \\ -0.66 & -0.5 \\ -0.16 & -0.5 \\ 0 & 0 \end{bmatrix} u_s$$

$$y_n = \begin{bmatrix} 0 & 0 & 0 & 1 \\ 0 & 0 & -1 & 1 \end{bmatrix},$$

where x_n is the state vector, u_s is the saturated input vector and y_n is the output vector. When there is no saturation, $u_s = u$. The physical interpretation of these three vectors is described in Chapter 5. The post-compensator is taken as an identity matrix and, since the plant is open loop stable and minimum phase system, there is no such restriction on closed-loop band width which is a major consideration for pre-compensator selection.

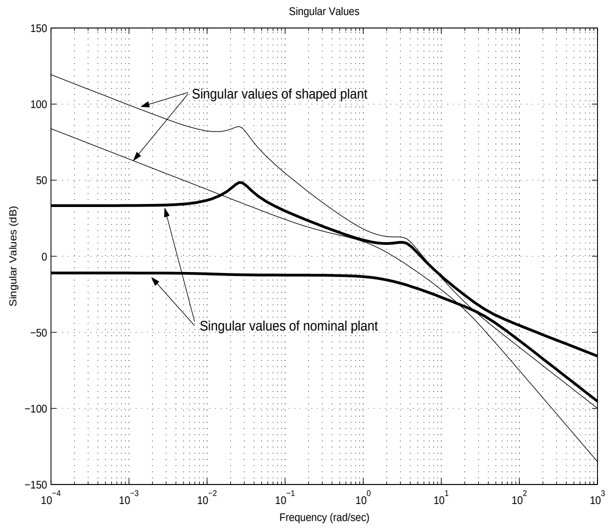

Figure 6.7: Singular values of the nominal and shaped plant

The saturation limits are considered as $\pm 8^\circ$ in both the input channels. The closed-loop specifications are as follows: the steady state error does not exceed $\pm 2\%$ for the step commands and in presence of actuator saturation, the stability of the closed-loop system should be ensured leading to graceful performance degradation. To satisfy these closed-loop requirements, a pre-compensator W is selected and in absence of saturation, it is enough to meet the design objectives (γ= 2.517). The selected pre-compensator is

$$W = \begin{bmatrix} \frac{10(s+0.3)}{s(s+8)} & 0 \\ 0 & \frac{20(s+1.5)}{s(s+1)} \end{bmatrix}$$

and in Figure 6.7, the singular values of the shaped and nominal plant have been shown. Without considering the saturation constraint, an LTI H_∞ loop shaping controller has been designed (controller state-space matrices are given in Section A.5 in Appendix A). In Figures 6.8-6.11, the output responses and control inputs at both the channels have been demonstrated for this controller with and without considering the saturation. However, in presence of input saturation nothing can be said about the performance bound of the closed-loop system while the LTI controller is used.

6.5.1 Controller synthesis using LPV approach

In the proposed LPV approach, the same pre-compensator has been considered and, ϕ_1 and ϕ_2 are defined as two varying parameters to indicate the level of saturation of the

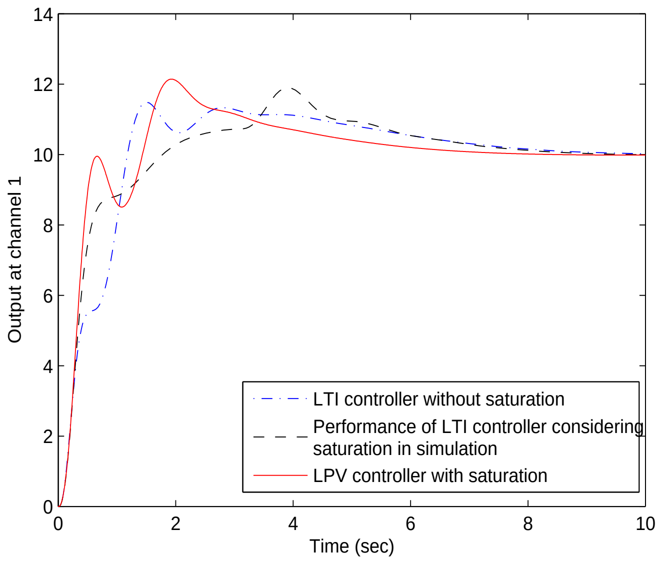

Figure 6.8: Output response of the plant at channel-1 when reference input is 10

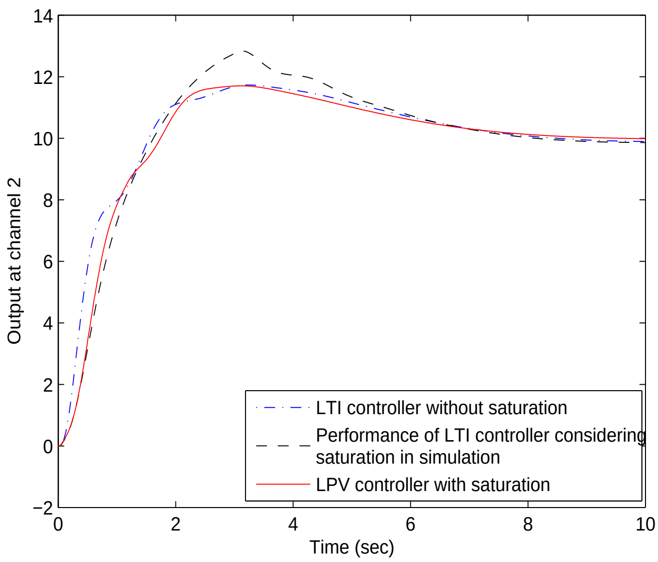

Figure 6.9: Output response of the plant at channel-2 when reference input is 10

system in both the channels. It is also assumed that the parameters lie in between 0 to 0.7 (i.e., slope β_j, j =1, 2 in Figure 6.3 vary in between 1 to 0.3) that corresponds to

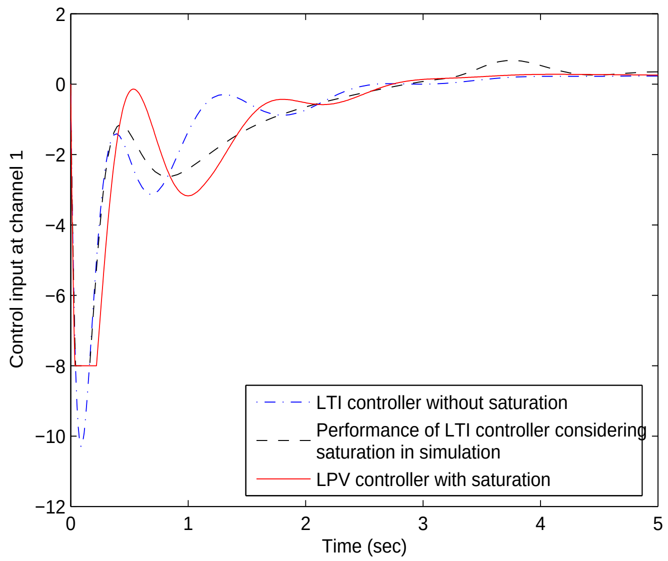

Figure 6.10: Control input at channel-1

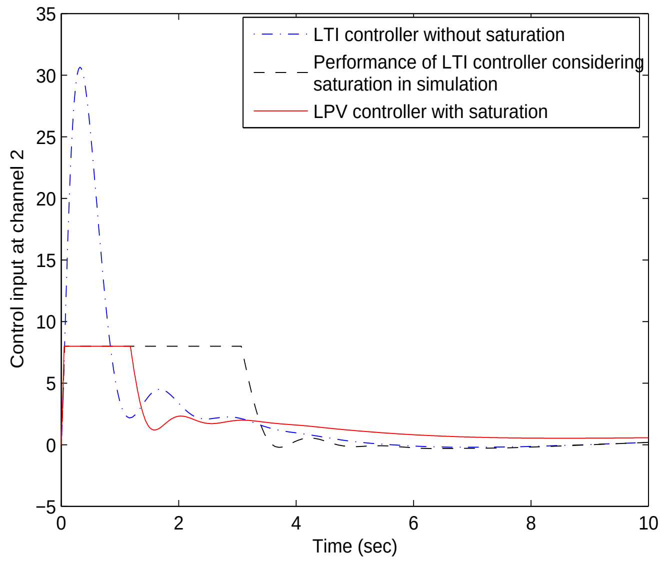

Figure 6.11: Control input at channel-2

a polytope with vertices at $(0, 0)$, $(0, 0.7)$, $(0.7, 0)$ and $(0.7, 0.7)$. Following the design method given in Section 6.3, four different controllers have been designed corresponding to four vertices of the polytope and the optimal value of γ is achieved as 3.522 by solving the optimization problem posed in Theorem 6.3. The LPV gain scheduled controller following the procedure given in A.2 (Appendix-A) has been simulated in MATLAB environment and the output responses as well as the control inputs of the system have been illustrated in Figures 6.8-6.11. The scheduling variables ϕ_1 and ϕ_2 are shown in Figure 6.12 which do not exceed the limit 0.7 (i.e., the slope remains in the pre-specified range (1 to 0.3) that in turn indicates, the maximum control input to saturation element does not exceed the limit $y_{wmax,j}, \jmath = 1, 2$ as shown in Figure 6.3). It appears that the LPV controller gives better result than the LTI controller due to gain scheduling synthesis when control inputs reach to saturation. Moreover with input saturation, the LPV approach gives a robust stability margin ($\epsilon = \frac{1}{\gamma} = 0.284$) for the normalized coprime factor uncertainty of the shaped plant.

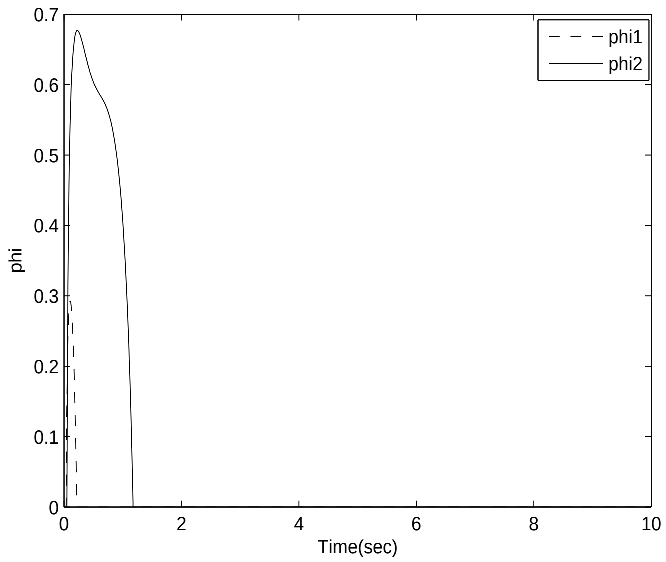

Figure 6.12: Time-varying scheduling parameters

6.5.2 Controller design using Popov stability criteria

Now, another H_∞ loop shaping controller will be designed using the second approach discussed in Section 6.4. In normalized scale, for both the channels $y_{wmax,j}, j = 1, 2$ are pre-specified. Using the design procedure given in Section 6.4, the following results are obtained. First, without considering saturation, an LTI H_∞ loop shaping controller is designed for the same shaped plant which is formed in the first approach. Now, fixing the controller matrices in (6.36), the optimal $\Upsilon = diag(\xi_1,\ \xi_2)$ and $T = diag(\tau_1,\ \tau_2)$ are obtained. For different values of $y_{wmax,j}, j = 1, 2$, the optimal solutions are given in Table 6.1. Note that, the specified $y_{wmax,j}$ is same for both the channels.

$y_{wmax,j}, j = 1, 2$	ξ_1	ξ_2	τ_1	τ_2
1.5	0.0443387	0.0012097	96.6599049	1.5751209
2.0	0.1373460	0.0025723	182.9571205	2.6613832
2.5	0.1438812	0.0021810	276.0224989	3.5904587
3.0	0.1509746	0.0019397	372.8507782	4.4125657
3.5	0.1753650	0.0019012	483.2929637	5.2045033

Table 6.1: Optimal multiplier parameters for different choice of y_{wmax}

Here, the four ranges from 0 to their optimal values for ξ_1, ξ_2, τ_1 and τ_2 are grided. Then for a given $y_{wmax,j}, j = 1, 2$, the LMI (6.45) is solved at each node by fixing the values of Υ and T. The values of multipliers are given in Table 6.2 corresponding to that node where minimum γ is obtained. After finding this node, the controller is designed using the design steps mentioned in Section 6.4. In Table 6.2, it is shown that, when the level of saturation is increased (i.e., $y_{wmax,j}$ is increased) γ is also increased. That is, the robust stability margin is decreased.

$y_{wmax,j}, j = 1, 2$	γ	ξ_1	ξ_2	τ_1	τ_2
1.5	2.7118	0.0147795	0.0004032	96.6599049	1.5751209
2.0	2.9488	0.0457820	0.0008574	182.9271205	2.6613832
2.5	3.1387	0.0479604	0.0007270	184.0149993	3.5904987
3.0	3.4267	0.05032486	0.0006465	186.4253891	4.4125657
3.5	3.6122	0.0584550	0.0006337	241.6464818	2.6022516

Table 6.2: Optimal γ for different y_{wmax}

6.6 Conclusions

In this chapter, using H_∞ loop shaping approach two different design techniques have been proposed in order to achieve robustness of an LTI plant with input saturation constraint. In first approach, the shaped plant has been presented as a polytopic LPV system considering input saturation. Then in LMI framework, an LPV H_∞ loop shaping controller has been designed by adopting the vertex property of the polytopic LPV plant.

Note that, the assumption on nominal plant and pre-compensator, i.e., strictly properness leads to a conservative design procedure. For controller synthesis, the parameter independent Lyapunov function approach has been adopted due to vertex property of the polytopic LPV plant. The designed controllers are scheduled on basis of the time-varying parameters which are defined to capture the information of saturation level of the closed-loop system. In the second approach, the H_∞ loop shaping design framework with input saturation constraint has been transformed into Lur'e type system. Then, Popov absolute stability criteria has been applied to ensure closed-loop stability of the system and subsequently, its L_2-performance bound is minimized. The design constraints are posed in BMI framework. Fixing the multiplier parameters, the problem has been converted into LMI form. Then solving the LMI constraints, controller has been designed. Also note that, using this method only a full order strictly proper controller can be designed which is a drawback of this approach. To illustrate both the techniques, a numerical example has been elucidated.

In comparison, the LPV approach is superior than the Lur'e type system representation approach to design a H_∞ loop shaping controller considering input saturation constraint. In the second approach, the design constraints are formulated in BMI form that imparts more computational burden to the designer. Further, using this approach one can only design a strictly proper controller which is a drawback of this method.

CHAPTER 7

Conclusions

This work presents the robust controller design technique for LTI plant using H_∞ loop shaping approach. The synthesis problems have been formulated in LMI framework that leads some computational advantages for controller design. In the following section, the main contributions of this thesis are summarized and subsequently, related to this work some future research directions have also been discussed.

7.1 Thesis Summary

The main contributions of this thesis are given as follows:

- In Chapter 2, some important design aspects of H_∞ loop shaping method have been discussed in detail along with some useful remarks and derivations. For shaping open-loop singular values, a new method for pre-compensator selection has been proposed that comprises two different algorithms. The first algorithm is simple, however, does not include condition number minimization of the pre-compensator in weight selection procedure. Whereas in second algorithm, pre-compensator is selected by minimizing its condition number in LMI framework that in turn, reduces loop deterioration. The second algorithm is posed in LMI framework which is numerically attractive.

- In Chapter 3, the parametric H_∞ loop shaping control problem has been formulated in LMI framework. In parallel with Riccati equation based state-space approach, a new set of solvability conditions has been derived for the existence of stabilizing controller. With non-unity parameter, the proposed method circumvents the computational burden for calculating the optimal performance bound. In addition, a complete correspondence between Riccati equation based state-space method and LMI approach has been established. In the proposed technique, the observer-based structure of the controller has also been realized. The effectiveness of the proposed technique has been demonstrated through a numerical example.

- In Chapter 4, a new set of sufficient conditions for the existence of static H_∞ loop shaping controller has been proposed. The results are obtained in four-block H_∞ synthesis framework which is equivalent to normalized coprime factor robust stabilization problem. The work is numerically attractive as the design constraints are formulated in LMI form. Two numerical examples are illustrated to show the effectiveness of the proposed method. Further, this method has been applied to load frequency control problem of inter-connected power system. The performance robustness of the system against the load disturbances and parametric uncertainty has been carried out by adopting the real μ-analysis technique. The performance of static controller has been compared with full-order H_∞ loop shaping controller through simulation studies.

- With bounded control inputs, the local stabilization problem of LTI plant has been addressed in Chapter 5. For stabilization, a parametric H_∞ loop shaping controller has been designed leading to maximize the region of attraction of the closed-loop system when control inputs are bounded by pre-specified limits. The introduced parameter is selected from design constraints to achieve a better trade-off among design objectives. Further, this design problem has also been extended for uncertain LTI plant whose uncertainty is described as perturbations to normalized coprime factors of the shaped plant. By this approach, an output feedback H_∞ loop shaping controller has been designed such that, with bounded control inputs the local stabilization is accomplished for certain level of uncertainty of the LTI plant and subsequently, the region of attraction is also maximized. The synthesis problems are formulated in LMI framework and two numerical examples are provided to illustrate the effectiveness of the proposed method.

- In Chapter 6, adopting the H_∞ loop shaping method, robust controller has been designed for LTI plant with input saturation constraint. The design is performed in four-block synthesis framework which is equivalent to the normalized coprime factor robust stabilization problem. In this chapter, two different design approaches have been proposed. In first approach, the controller has been designed by representing the shaped plant as polytopic LPV system when input saturation is taken into account. Exploiting the vertex property of the polytopic LPV plant, in LMI framework different controllers have been designed at vertices of the polytope. These controllers are scheduled on basis of the time-varying parameters that are employed to capture the information of saturation level of the closed-loop system. In this approach, a specified performance bound is guaranteed as the shaped plant is assumed to be lying in a given polytope. In second approach, the design framework for H_∞ loop shaping control with input saturation has been transformed into Lur'e type system. For controller synthesis, the Popov absolute stability has been adopted that ensures a robust performance bound for certain level of actuator saturation limit. The design constraints are posed in BMI framework and an iterative algorithm is used to find the robust controller.

7.2 Scopes for future Work

Related to this work, some future scopes are outlined here in which directions the research work can be carried out.

- It is possible to extend the method of Chapter 2 by introducing an optimization problem that simultaneously minimizes the performance bound γ and condition number of the compensator to achieve less loop deterioration.

- For parameter varying system or the LTI plant with input saturation, a systematic weight (compensator) selection procedure can be developed that will maintain the open-loop gain in spite of parameter variation or input saturation constraint.

- Instead of a scalar parameter, a gain matrix can be introduced in parametric H_∞ loop shaping control to increase design flexibility.

- For stable open loop plant, it is worthwhile to study the semi-global and global stability with bounded control inputs using H_∞ loop shaping approach.

- With input saturation, a robust anti-windup scheme for H_∞ loop shaping control can be proposed. Subsequently, an investigation can also be made for anti-windup compensation design for polytopic systems by adopting parameter dependent Lyapunov function approach and H_∞ loop shaping design technique.

- To investigate the improvement of results, the parameter dependent Lyapunov function approach can be applied to first method of Chapter 6 where polytopic LPV approach has been used to design robust controller.

- Development of decentralized H_∞ loop shaping control scheme for a system subject to input saturation can be investigated.

Appendix **A**

Appendix-A

A.1 Controller LMI

We rewrite (6.30).

$$\begin{pmatrix} A_{cl}^T(\omega_i)P + PA_{cl}(\omega_i) & PB_{cl}(\omega_i) & C_{cl}^T(\omega_i) \\ B_{cl}^T(\omega_i)P & -\gamma I & D_{cl}^T(\omega_i) \\ C_{cl}(\omega_i) & D_{cl}(\omega_i) & -\gamma I \end{pmatrix} < 0 \tag{A.1}$$

where $A_{cl}, B_{cl}, C_{cl}, D_{cl}$ are the closed-loop state-space matrices defined in (6.27)-(6.28) and $\omega_i, i = 1, \ldots, 2^m$ are the vertices of the polytope. For simplicity of notation, dependence on ω_i is omitted and using (6.27)-(6.28) in (A.1), we have

$$\begin{pmatrix} (A_0^{cT} + \Pi^T\Lambda^T B^{cT})P + P(A_0^c + B^c\Lambda\Pi) & P(B_0^c + B^c\Lambda E_{21}) & C_0^{cT} + \Pi^T\Lambda^T E_{12}^T \\ (B_0^{cT} + E_{21}^T\Lambda^T B^{cT})P & -\gamma I & D_0^{cT} + E_{21}^T\Lambda^T E_{12}^T \\ C_0^c + E_{12}\Lambda\Pi & D_0^c + E_{12}\Lambda E_{21} & -\gamma I \end{pmatrix} < 0$$

$$\Rightarrow \Psi + U^T\Lambda^T V + V^T\Lambda U < 0 \tag{A.2}$$

where,

$$\Psi = \begin{pmatrix} A_0^{cT}P + PA_0^c & PB_0^c & C_0^{cT} \\ B_0^{cT}P & -\gamma I & D_0^{cT} \\ C_0^c & D_0^c & -\gamma I \end{pmatrix}, U^T = \begin{pmatrix} \Pi^T \\ E_{21}^T \\ 0 \end{pmatrix} \text{ and } V^T = \begin{pmatrix} PB^c \\ 0 \\ E_{12} \end{pmatrix}.$$

Since P is known, Ψ, U, V are also known matrices. Using MATLAB LMI toolbox, (A.2) is solved at each vertex of the polytope. The obtained solution is Λ that comprises the state-space matrices of the controller.

A.2 Gain scheduling

Let we consider, $\begin{bmatrix} A_{ci} & B_{ci} \\ C_{ci} & D_{ci} \end{bmatrix}, i = 1, \ldots, 2^m$ are the designed controller at different vertices of the polytope. Then the LPV controller will be scheduled in the following way [6].

$$\begin{pmatrix} A_c(\Phi) & B_c(\Phi) \\ C_c(\Phi) & D_c(\Phi) \end{pmatrix} = \sum_{i=1}^{2^m} \alpha_i \begin{pmatrix} A_{ci} & B_{ci} \\ C_{ci} & D_{ci} \end{pmatrix}$$

where, $0 \leq \alpha_i \leq 1$ and $\sum_{i=1}^{2^m} \alpha_i = 1$.

for $m = 1$:

The variable is ϕ_1 and $\phi_{1,min} \leq \phi_1 \leq \phi_{1,max}$. Then $\alpha_1 = v1$ and $\alpha_2 = (1 - v1)$ where $v1 = \frac{\phi_{1,max} - \phi_1}{\phi_{1,max} - \phi_{1,min}}$.

for $m = 2$:

The variables are ϕ_1 and ϕ_2 where $\phi_{1,min} \leq \phi_1 \leq \phi_{1,max}$, $\phi_{2,min} \leq \phi_2 \leq \phi_{2,max}$. Then, $\alpha_1 = v1v2$, $\alpha_2 = (1 - v1)v2$, $\alpha_3 = v1(1 - v2)$, $\alpha_4 = (1 - v1)(1 - v2)$ where $v1 = \frac{\phi_{1,max} - \phi_1}{\phi_{1,max} - \phi_{1,min}}$ and $v2 = \frac{\phi_2 - \phi_{2,min}}{\phi_{2,max} - \phi_{2,min}}$.

Similarly for $m = 3, 4, \ldots,$ the scheduling can be done.

A.3 Proof of Theorem 6.4[14]

For all x_{cl} and w that satisfy (6.33), the L_2-gain of the system (6.33) does not exceed γ if there exists a Lyapunov function (6.34) and $\gamma \geq 0$ such that

$$\frac{d}{dt} V(x_{cl}) \leq \gamma^2 w^T w - z^T z \tag{A.3}$$

is satisfied. Simplifying (A.3), we have

$$2(x_{cl}^T P + w_s^T \Upsilon C_{z_s}^{cl})(A^{cl} x_{cl} + B_{w_s}^{cl} w_s + B_w^{cl} w) \leq \gamma^2 w^T w - z^T z.$$

Now, replacing $z = C_z^{cl} x^{cl} + D_{w_s z}^{cl} w_s + D_{wz}^{cl} w$, it is simplified as

$$\begin{aligned} &2(x_{cl}^T P + w_s^T \Upsilon C_{z_s}^{cl})(A^{cl} x_{cl} + B_{w_s}^{cl} w_s + B_w^{cl} w) - \gamma^2 w^T w \\ &\qquad + (C_z^{cl} x^{cl} + D_{w_s z}^{cl} w_s + D_{wz}^{cl} w)^T (C_z^{cl} x^{cl} + D_{w_s z}^{cl} w_s + D_{wz}^{cl} w) \leq 0 \end{aligned} \tag{A.4}$$

where x_{cl} satisfies the sector condition

$$w_{sj}(w_{sj} - C_{z_s j}^{cl} x_{cl}) \leq 0, \quad j = 1, \ldots, m. \tag{A.5}$$

Using S-procedure (see Chapter 1), if there exists $T = diag(\tau_1, \ldots, \tau_m) \geq 0$ such that

$$\begin{aligned} &2(x_{cl}^T P + w_s^T \Upsilon C_{z_s}^{cl})(A^{cl} x_{cl} + B_{w_s}^{cl} w_s + B_w^{cl} w) - \gamma^2 w^T w \\ &+ (C_z^{cl} x^{cl} + D_{w_s z}^{cl} w_s + D_{wz}^{cl} w)^T (C_z^{cl} x^{cl} + D_{w_s z}^{cl} w_s + D_{wz}^{cl} w) - 2 \sum_{j=1}^{m} \tau_j w_{sj}(w_{sj} - C_{z_s j}^{cl} x_{cl}) \leq 0 \end{aligned} \tag{A.6}$$

is satisfied, then (A.3) holds. Simplifying (A.6), we have

$$\begin{gathered} x_{cl}^T P A^{cl} x_{cl} + x_{cl}^T P B_{w_s}^{cl} w_s + w_s^T \Upsilon C_{z_s}^{cl} A^{cl} x_{cl} + w_s^T \Upsilon C_{z_s}^{cl} B_{w_s}^{cl} w_s + x_{cl}^T {A^{cl}}^T P x_{cl} + \\ x_{cl}^T {A^{cl}}^T {C_{z_s}^{cl}}^T \Upsilon w_s + x_{cl}^T P B_w^{cl} w + w_s^T \Upsilon C_{z_s}^{cl} B_w^{cl} w + w^T {B_w^{cl}}^T P x_{cl} + w^T {B_w^{cl}}^T {C_{z_s}^{cl}}^T \Upsilon w_s \\ + w_s^T {B_{w_s}^{cl}}^T P x_{cl} + w_s^T {B_{w_s}^{cl}}^T {C_{z_s}^{cl}}^T \Upsilon w_s - \gamma^2 w^T w + x_{cl}^T {C_z^{cl}}^T C_z^{cl} x_{cl} + x_{cl}^T {C_z^{cl}}^T D_{w_s z}^{cl} w_s + \\ x_{cl}^T {C_z^{cl}}^T D_{wz}^{cl} w + w_s^T {D_{w_s z}^{cl}}^T C_z^{cl} x_{cl} + w_s^T {D_{w_s z}^{cl}}^T D_{w_s z}^{cl} w_s + w_s^T {D_{w_s z}^{cl}}^T D_{wz}^{cl} w + w^T {D_{wz}^{cl}}^T C_z^{cl} x_{cl} + \\ w^T {D_{wz}^{cl}}^T D_{w_s z}^{cl} w_s + w^T {D_{wz}^{cl}}^T D_{wz}^{cl} w - 2 w_s^T T w_s + w_s^T T C_{z_s}^{cl} x_{cl} + x_{cl}^T {C_{z_s}^{cl}}^T T w_s \leq 0. \end{gathered}$$

Now, this inequality can be written in the following form

$$\begin{bmatrix} x_{cl}^T & w_s^T & w^T \end{bmatrix} W \begin{bmatrix} x_{cl} \\ w_s \\ w \end{bmatrix} \leq 0$$

where,

$$W = \begin{bmatrix} PA^{cl} + {A^{cl}}^T P + {C_z^{cl}}^T C_z^{cl} & {A^{cl}}^T {C_{z_s}^{cl}}^T \Upsilon + PB_{w_s}^{cl} + {C_z^{cl}}^T D_{w_s z}^{cl} + {C_{z_s}^{cl}}^T T \\ \Upsilon C_{z_s}^{cl} A^{cl} + {B_{w_s}^{cl}}^T P + {D_{w_s z}^{cl}}^T C_z^{cl} + T C_{z_s}^{cl} & \Upsilon C_{z_s}^{cl} B_{w_s}^{cl} + {B_{w_s}^{cl}}^T {C_{z_s}^{cl}}^T \Upsilon + {D_{w_s z}^{cl}}^T D_{w_s z}^{cl} - 2T \\ {B_w^{cl}}^T P + {D_{wz}^{cl}}^T C_z^{cl} & {B_w^{cl}}^T {C_{z_s}^{cl}}^T \Upsilon + {D_{wz}^{cl}}^T D_{w_s z}^{cl} \end{bmatrix}$$

$$\begin{bmatrix} PB_w^{cl} + {C_z^{cl}}^T D_{wz}^{cl} \\ \Upsilon C_{z_s}^{cl} B_w^{cl} + {D_{w_s z}^{cl}}^T D_{wz}^{cl} \\ {D_{wz}^{cl}}^T D_{wz}^{cl} - \gamma^2 I \end{bmatrix}.$$

It is similar to (6.35) and γ can be calculated by solving the optimization problem (6.36).

A.4 BMI constraints

$$\Xi_\perp^T \Psi \Xi_\perp = \begin{bmatrix} J_\perp^T & 0 & 0 \\ 0 & I & 0 \\ 0 & 0 & I \end{bmatrix} \times$$

$$\begin{bmatrix} P\bar{A}_0 + \bar{A}_0^T P + {C_z^{cl}}^T C_z^{cl} & \bar{A}_0^T {C_{z_s}^{cl}}^T \Upsilon + PB_{w_s}^{cl} + {C_z^{cl}}^T D_{w_s z}^{cl} + {C_{z_s}^{cl}}^T T \\ \Upsilon C_{z_s}^{cl} \bar{A}_0 + {B_{w_s}^{cl}}^T P + {D_{w_s z}^{cl}}^T C_z^{cl} + T C_{z_s}^{cl} & \Upsilon C_{z_s}^{cl} B_{w_s}^{cl} + {B_{w_s}^{cl}}^T {C_{z_s}^{cl}}^T \Upsilon + {D_{w_s z}^{cl}}^T D_{w_s z}^{cl} - 2T \\ {B_w^{cl}}^T P + {D_{wz}^{cl}}^T C_z^{cl} & {B_w^{cl}}^T {C_{z_s}^{cl}}^T \Upsilon + {D_{wz}^{cl}}^T D_{w_s z}^{cl} \end{bmatrix}$$

$$\begin{bmatrix} PB_w^{cl} + {C_z^{cl}}^T D_{wz}^{cl} \\ \Upsilon C_{z_s}^{cl} B_w^{cl} + {D_{w_s z}^{cl}}^T D_{wz}^{cl} \\ {D_{wz}^{cl}}^T D_{wz}^{cl} - \gamma^2 I \end{bmatrix} \times \begin{bmatrix} J_\perp & 0 & 0 \\ 0 & I & 0 \\ 0 & 0 & I \end{bmatrix}$$

$$= \begin{bmatrix} J_\perp^T \quad P\bar{A}_0 + \bar{A}_0^T P + {C_z^{cl}}^T C_z^{cl} \quad J_\perp & J_\perp^T \quad \bar{A}_0^T {C_{z_s}^{cl}}^T \Upsilon + PB_{w_s}^{cl} + {C_z^{cl}}^T D_{w_s z}^{cl} + {C_{z_s}^{cl}}^T T \\ \Upsilon C_{z_s}^{cl} \bar{A}_0 + {B_{w_s}^{cl}}^T P + {D_{w_s z}^{cl}}^T C_z^{cl} + T C_{z_s}^{cl} \quad J_\perp & \Upsilon C_{z_s}^{cl} B_{w_s}^{cl} + {B_{w_s}^{cl}}^T {C_{z_s}^{cl}}^T \Upsilon + {D_{w_s z}^{cl}}^T D_{w_s z}^{cl} - 2T \\ {B_w^{cl}}^T P + {D_{wz}^{cl}}^T C_z^{cl} \quad J_\perp & {B_w^{cl}}^T {C_{z_s}^{cl}}^T \Upsilon + {D_{wz}^{cl}}^T D_{w_s z}^{cl} \end{bmatrix}$$

$$\begin{bmatrix} J_\perp^T \left(PB_w^{cl} + {C_z^{cl}}^T D_{wz}^{cl} \right) \\ \Upsilon C_{z_s}^{cl} B_w^{cl} + {D_{w_s z}^{cl}}^T D_{wz}^{cl} \\ {D_{wz}^{cl}}^T D_{wz}^{cl} - \gamma^2 I \end{bmatrix}$$

Now, simplifying the block matrices and substituting the expressions for $\bar{A}_0, C_z^{cl}, B_w^{cl}$ etc., we have

$$\text{(1,1) block:} J_\perp^T \left(P\bar{A}_0 + \bar{A}_0^T P + {C_z^{cl}}^T C_z^{cl}\right) J_\perp = J_\perp^T P \bar{A}_0 J_\perp + J_\perp^T \bar{A}_0^T P J_\perp + J_\perp^T {C_z^{cl}}^T C_z^{cl} J_\perp$$

$$= \begin{bmatrix} I & 0 \end{bmatrix} \begin{bmatrix} \tilde{P} & \tilde{M} \\ \tilde{M}^T & \tilde{R} \end{bmatrix} \begin{bmatrix} A_a & B_u C_c \\ B_c C_y & 0 \end{bmatrix} \begin{bmatrix} I \\ 0 \end{bmatrix} + (.)^T +$$

$$\begin{bmatrix} I & 0 \end{bmatrix} \begin{bmatrix} C_z^T \\ C_c^T D_{uz}^T \end{bmatrix} \begin{bmatrix} C_z & D_{uz} C_c \end{bmatrix} \begin{bmatrix} I \\ 0 \end{bmatrix}$$

$$= \tilde{P} A_a + \tilde{M} B_c C_y + A_a^T \tilde{P} + C_y^T B_c^T \tilde{M}^T + C_z^T C_z = \tilde{P} A_a + Z C_y + A_a^T \tilde{P} + C_y^T Z^T + C_z^T C_z$$

$$\text{(2, 1) block:} \Upsilon C_{z_s}^{cl} \bar{A}_0 J_\perp + {B_{w_s}^{cl}}^T P J_\perp + {D_{w_s z}^{cl}}^T C_z^{cl} J_\perp + T C_{z_s}^{cl} J_\perp$$

$$= \begin{bmatrix} \Upsilon C_{z_s} & 0 \end{bmatrix} \begin{bmatrix} A_a & B_u C_c \\ B_c C_y & 0 \end{bmatrix} \begin{bmatrix} I \\ 0 \end{bmatrix} + \begin{bmatrix} {B_{w_s}^{\beta}}^T & {D_{w_s y}^{\beta}}^T B_c^T \end{bmatrix} \begin{bmatrix} \tilde{P} & \tilde{M} \\ \tilde{M}^T & \tilde{R} \end{bmatrix} \begin{bmatrix} I \\ 0 \end{bmatrix}$$

$$+ {D_{w_s z}^{\beta}}^T \begin{bmatrix} C_z & D_{uz} C_c \end{bmatrix} \begin{bmatrix} I \\ 0 \end{bmatrix} + \begin{bmatrix} T C_{z_s} & 0 \end{bmatrix} \begin{bmatrix} I \\ 0 \end{bmatrix}$$

$$= \Upsilon C_{z_s} A_a + {B_{w_s}^{\beta}}^T \tilde{P} + {D_{w_s y}^{\beta}}^T B_c^T \tilde{M}^T + {D_{w_s z}^{\beta}}^T C_z + T C_{z_s}$$

$$= \Upsilon C_{z_s} A_a + {B_{w_s}^{\beta}}^T \tilde{P} + {D_{w_s y}^{\beta}}^T Z^T + {D_{w_s z}^{\beta}}^T C_z + T C_{z_s}$$

$$\text{(3, 1) block:} {B_w^{cl}}^T P J_\perp + {D_{wz}^{cl}}^T C_z^{cl} J_\perp$$

$$= \begin{bmatrix} {B_w^e}^T & D_{wy}^T B_c^T \end{bmatrix} \begin{bmatrix} \tilde{P} & \tilde{M} \\ \tilde{M}^T & \tilde{R} \end{bmatrix} \begin{bmatrix} I \\ 0 \end{bmatrix} + D_{wz}^T \begin{bmatrix} C_z & D_{uz} C_c \end{bmatrix} \begin{bmatrix} I \\ 0 \end{bmatrix}$$

$$= {B_w^e}^T \tilde{P} + D_{wy}^T B_c^T \tilde{M}^T + B_{wz}^T C_z = {B_w^e}^T \tilde{P} + D_{wy}^T Z^T + B_{wz}^T C_z$$

$$\text{(2, 2) block:} \Upsilon C_{z_s}^{cl} B_{w_s}^{cl} + {B_{w_s}^{cl}}^T {C_{z_s}^{cl}}^T \Upsilon + {D_{w_s z}^{cl}}^T D_{w_s z}^{cl} - 2T$$

$$= \begin{bmatrix} \Upsilon C_{z_s} & 0 \end{bmatrix} \begin{bmatrix} B_{w_s}^{\beta} \\ B_c D_{w_s y}^{\beta} \end{bmatrix} + \begin{bmatrix} {B_{w_s}^{\beta}}^T & {D_{w_s y}^{\beta}}^T B_c^T \end{bmatrix} \begin{bmatrix} C_{z_s}^T \Upsilon \\ 0 \end{bmatrix} + D_{w_s z}^{\beta} D_{w_s z}^{\beta} - 2T$$

$$= \Upsilon C_{z_s} B_{w_s}^{\beta} + {B_{w_s}^{\beta}}^T C_{z_s}^T \Upsilon + D_{w_s z}^{\beta} D_{w_s z}^{\beta} - 2T$$

(3, 2) block: ${B_w^{cl}}^T {C_{z_s}^{cl}}^T \Upsilon + {D_{wz}^{cl}}^T D_{w_s z}^{cl}$

$$= \begin{bmatrix} {B_w^e}^T & D_{wy}^T B_c^T \end{bmatrix} \begin{bmatrix} C_{z_s}^T \Upsilon \\ 0 \end{bmatrix} + D_{wz}^T D_{w_s z}^{\beta} = {B_w^e}^T C_{z_s}^T \Upsilon + D_{wz}^T D_{w_s z}^{\beta}$$

(3, 3) block: ${D_{wz}^{cl}}^T D_{wz}^{cl} - \gamma^2 I = D_{wz}^T D_{wz} - \gamma^2 I$

Hence, $\Xi_\perp^T \Psi \Xi_\perp < 0$ implies

$$\begin{bmatrix} \tilde{P} A_a + Z C_y + A_a^T \tilde{P} + C_y^T Z^T + C_z^T C_z & (.)^T & (.)^T \\ \Upsilon C_{z_s} A_a + {B_{w_s}^{\beta}}^T \tilde{P} + {D_{w_s y}^{\beta}}^T Z^T + {D_{w_s z}^{\beta}}^T C_z + T C_{z_s} & \Upsilon C_{z_s} B_{w_s}^{\beta} + {B_{w_s}^{\beta}}^T C_{z_s}^T \Upsilon + D_{w_s z}^{\beta} D_{w_s z}^{\beta} - 2T & (.)^T \\ {B_w^e}^T \tilde{P} + D_{wy}^T Z^T + B_{wz}^T C_z & {B_w^e}^T C_{z_s}^T \Upsilon + D_{wz}^T D_{w_s z}^{\beta} & D_{wz}^T D_{wz} - \gamma^2 I \end{bmatrix} < 0$$

Similarly, $\Pi_\perp^T \Psi \Pi_\perp$

$$= \begin{bmatrix} J_\perp^T P^{-1} & 0 & 0 \\ 0 & I & 0 \\ 0 & 0 & I \end{bmatrix} \times$$

$$\begin{bmatrix} P \bar{A}_0 + \bar{A}_0^T P + {C_z^{cl}}^T C_z^{cl} & \bar{A}_0^T {C_{z_s}^{cl}}^T \Upsilon + P B_{w_s}^{cl} + {C_z^{cl}}^T D_{w_s z}^{cl} + {C_{z_s}^{cl}}^T T & P B_w^{cl} + {C_z^{cl}}^T D_{wz}^{cl} \\ \Upsilon C_{z_s}^{cl} \bar{A}_0 + {B_{w_s}^{cl}}^T P + {D_{w_s z}^{cl}}^T C_z^{cl} + T C_{z_s}^{cl} & \Upsilon C_{z_s}^{cl} B_{w_s}^{cl} + {B_{w_s}^{cl}}^T {C_{z_s}^{cl}}^T \Upsilon + {D_{w_s z}^{cl}}^T D_{w_s z}^{cl} - 2T & \Upsilon C_{z_s}^{cl} B_w^{cl} + {D_{w_s z}^{cl}}^T D_{wz}^{cl} \\ {B_w^{cl}}^T P + {D_{wz}^{cl}}^T C_z^{cl} & {B_w^{cl}}^T {C_{z_s}^{cl}}^T \Upsilon + {D_{wz}^{cl}}^T D_{w_s z}^{cl} & {D_{wz}^{cl}}^T D_{wz}^{cl} - \gamma^2 I \end{bmatrix} \times \begin{bmatrix} P^{-1} J_\perp & 0 & 0 \\ 0 & I & 0 \\ 0 & 0 & I \end{bmatrix}$$

$$= \begin{bmatrix} J_\perp^T P^{-1} \; P \bar{A}_0 + \bar{A}_0^T P + {C_z^{cl}}^T C_z^{cl} \; P^{-1} J_\perp & J_\perp^T P^{-1} \; \bar{A}_0^T {C_{z_s}^{cl}}^T \Upsilon + P B_{w_s}^{cl} + {C_z^{cl}}^T D_{w_s z}^{cl} + {C_{z_s}^{cl}}^T T & J_\perp^T P^{-1} \left(P B_w^{cl} + {C_z^{cl}}^T D_{wz}^{cl} \right) \\ \Upsilon C_{z_s}^{cl} \bar{A}_0 + {B_{w_s}^{cl}}^T P + {D_{w_s z}^{cl}}^T C_z^{cl} + T C_{z_s}^{cl} \; P^{-1} J_\perp & \Upsilon C_{z_s}^{cl} B_{w_s}^{cl} + {B_{w_s}^{cl}}^T {C_{z_s}^{cl}}^T \Upsilon + {D_{w_s z}^{cl}}^T D_{w_s z}^{cl} - 2T & \Upsilon C_{z_s}^{cl} B_w^{cl} + {D_{w_s z}^{cl}}^T D_{wz}^{cl} \\ {B_w^{cl}}^T P + {D_{wz}^{cl}}^T C_z^{cl} \; P^{-1} J_\perp & {B_w^{cl}}^T {C_{z_s}^{cl}}^T \Upsilon + {D_{wz}^{cl}}^T D_{w_s z}^{cl} & {D_{wz}^{cl}}^T D_{wz}^{cl} - \gamma^2 I \end{bmatrix}$$

Now, simplifying the following block matrices, we have
(1, 1) block:

$$J_\perp^T P^{-1}\left(P\bar{A}_0 + \bar{A}_0^T P + {C_z^{cl}}^T C_z^{cl}\right)P^{-1}J_\perp = J_\perp^T \bar{A}_0 P^{-1}J_\perp + (.)^T + J_\perp^T P^{-1}{C_z^{cl}}^T C_z^{cl} P^{-1}J_\perp$$

$$= \begin{bmatrix} I & 0 \end{bmatrix}\begin{bmatrix} A_a & B_uC_c \\ B_cC_y & 0 \end{bmatrix}\begin{bmatrix} \tilde{Q} & \tilde{N} \\ \tilde{N}^T & \tilde{S} \end{bmatrix}\begin{bmatrix} I \\ 0 \end{bmatrix} + (.)^T +$$

$$\begin{bmatrix} I & 0 \end{bmatrix}\begin{bmatrix} \tilde{Q} & \tilde{N} \\ \tilde{N}^T & \tilde{S} \end{bmatrix}\begin{bmatrix} C_z^T \\ C_c^T D_{uz}^T \end{bmatrix}\begin{bmatrix} C_z & D_{uz}C_c \end{bmatrix}\begin{bmatrix} \tilde{Q} & \tilde{N} \\ \tilde{N}^T & \tilde{S} \end{bmatrix}\begin{bmatrix} I \\ 0 \end{bmatrix}$$

$$= A_a\tilde{Q} + B_uC_c\tilde{N}^T + \tilde{Q}A_a^T + \tilde{N}C_c^T B_u^T + \left(\tilde{Q}C_z^T + \tilde{N}C_c^T D_{uz}^T\right)\left(C_z\tilde{Q} + D_{uz}C_c\tilde{N}^T\right)$$

$$= A_a\tilde{Q} + B_uY + \tilde{Q}A_a^T + Y^T B_u^T + \left(\tilde{Q}C_z^T + Y^T D_{uz}^T\right)\left(C_z\tilde{Q} + D_{uz}Y\right)$$

(2, 1) block: $\left(\Upsilon C_{z_s}^{cl}\bar{A}_0 + {B_{w_s}^{cl}}^T P + {D_{w_sz}^{cl}}^T C_z^{cl} + TC_{z_s}^{cl}\right)P^{-1}J_\perp$

$$= \begin{bmatrix} \Upsilon C_{z_s} & 0 \end{bmatrix}\begin{bmatrix} A_a & B_uC_c \\ B_cC_y & A_c \end{bmatrix}\begin{bmatrix} \tilde{Q} & \tilde{N} \\ \tilde{N}^T & \tilde{S} \end{bmatrix}\begin{bmatrix} I \\ 0 \end{bmatrix} + \begin{bmatrix} {B_{w_s}^\beta}^T & {B_{w_sy}^\beta}^T B_c^T \end{bmatrix}\begin{bmatrix} I \\ 0 \end{bmatrix} +$$

$${D_{w_sz}^\beta}^T\begin{bmatrix} C_z & D_{uz}C_c \end{bmatrix}\begin{bmatrix} \tilde{Q} & \tilde{N} \\ \tilde{N}^T & \tilde{S} \end{bmatrix}\begin{bmatrix} I \\ 0 \end{bmatrix} + \begin{bmatrix} Tc_{z_s} & 0 \end{bmatrix}\begin{bmatrix} \tilde{Q} & \tilde{N} \\ \tilde{N}^T & \tilde{S} \end{bmatrix}\begin{bmatrix} I \\ 0 \end{bmatrix}$$

$$= \Upsilon C_{z_s}A_a\tilde{Q} + \Upsilon C_{z_s}B_uC_c\tilde{N}^T + {B_{w_s}^\beta}^T + {D_{w_sz}^\beta}^T C_z\tilde{Q} + {D_{w_sz}^\beta}^T D_{uz}C_c\tilde{N}^T + TC_{z_s}\tilde{Q}$$

$$= \Upsilon C_{z_s}A_a\tilde{Q} + \Upsilon C_{z_s}B_uY + {B_{w_s}^\beta}^T + {D_{w_sz}^\beta}^T C_z\tilde{Q} + {D_{w_sz}^\beta}^T D_{uz}Y + TC_{z_s}\tilde{Q}$$

(3, 1) block: $\left({B_w^{cl}}^T P + {D_{wz}^{cl}}^T C_z^{cl}\right)P^{-1}J_\perp$

$$= \begin{bmatrix} {B_w^e}^T & D_{wy}^T B_c^T \end{bmatrix}\begin{bmatrix} I \\ 0 \end{bmatrix} + D_{wz}^T\begin{bmatrix} C_z & D_{uz}C_c \end{bmatrix}\begin{bmatrix} \tilde{Q} & \tilde{N} \\ \tilde{N}^T & \tilde{S} \end{bmatrix}\begin{bmatrix} I \\ 0 \end{bmatrix}$$

$$= {B_w^e}^T + D_{wz}^T C_z\tilde{Q} + D_{wz}^T D_{uz}C_c\tilde{N}^T = {B_w^e}^T + D_{wz}^T C_z\tilde{Q} + D_{wz}^T D_{uz}Y$$

(2,2), (3, 2) and (3, 3) blocks are already simplified in earlier stage and hence, $\Pi_\perp^T\Psi\Pi_\perp < 0$ implies

$$\left[\begin{array}{c} A_a\tilde{Q} + B_uY + \tilde{Q}A_a^T + Y^T B_u^T + \left(\tilde{Q}C_z^T + Y^T D_{uz}^T\right)\left(C_z\tilde{Q} + D_{uz}Y\right) \\ \Upsilon C_{z_s}A_a\tilde{Q} + \Upsilon C_{z_s}B_uY + {B_{w_s}^\beta}^T + {D_{w_sz}^\beta}^T C_z\tilde{Q} + {D_{w_sz}^\beta}^T D_{uz}Y + TC_{z_s}\tilde{Q} \\ {B_w^e}^T + D_{wz}^T C_z\tilde{Q} + D_{wz}^T D_{uz}Y \end{array}\right.$$

$$
\left.\begin{array}{cc}
(.)^T & (.)^T \\
\Upsilon C_{z_s} B^{\beta}_{w_s} + {B^{\beta}_{w_s}}^T C^T_{z_s} \Upsilon + D^{\beta}_{w_s z} D^{\beta}_{w_s z} - 2T & (.)^T \\
{B^e_w}^T C^T_{z_s} \Upsilon + D^T_{wz} D^{\beta}_{w_s z} & D^T_{wz} D_{wz} - \gamma^2 I
\end{array}\right] < 0
$$

It can be written as

$$
\left[\begin{array}{c}
A_a \tilde{Q} + B_u Y + \tilde{Q} A_a^T + Y^T B_u^T \\
\Upsilon C_{z_s} A_a \tilde{Q} + \Upsilon C_{z_s} B_u Y + {B^{\beta}_{w_s}}^T + {D^{\beta}_{w_s z}}^T C_z \tilde{Q} + {D^{\beta}_{w_s z}}^T D_{uz} Y + T C_{z_s} \tilde{Q} \\
{B^e_w}^T + D^T_{wz} C_z \tilde{Q} + D^T_{wz} D_{uz} Y \\
\left(C_z \tilde{Q} + D_{uz} Y\right)
\end{array}\right.
$$

$$
\left.\begin{array}{ccc}
(.)^T & (.)^T & (.)^T \\
\Upsilon C_{z_s} B^{\beta}_{w_s} + {B^{\beta}_{w_s}}^T C^T_{z_s} \Upsilon + D^{\beta}_{w_s z} D^{\beta}_{w_s z} - 2T & (.)^T & (.)^T \\
{B^e_w}^T C^T_{z_s} \Upsilon + D^T_{wz} D^{\beta}_{w_s z} & D^T_{wz} D_{wz} - \gamma^2 I & (.)^T \\
0 & 0 & -I
\end{array}\right] < 0
$$

A.5 State-space matrices of the controller

LTI H_∞ loop shaping controller without considering saturation

$$
A_c = \begin{bmatrix}
-0.8000 & -0.0006 & -37.1543 & -203.0608 & -47.5000 & -14.2500 & -15.0000 & -11.2500 \\
0 & -0.0140 & 36.8513 & 220.5883 & -1.6500 & -0.4950 & -2.5000 & -1.8750 \\
1.0000 & -0.0001 & -14.6442 & -42.6412 & -0.4000 & -0.1200 & -2.5000 & -1.8750 \\
1.0000 & 0 & -3.6957 & -48.3940 & 0 & 0 & 0 & 0 \\
1.0032 & -0.0000 & -2.9730 & 17.0400 & -12.7631 & -3.6273 & -0.9954 & -0.7498 \\
0 & 0 & -0.3814 & 5.7235 & 1.0000 & 0 & 0 & 0 \\
0.1787 & -0.0001 & 11.0377 & 10.9257 & -0.9954 & -0.1745 & -4.7802 & -2.5410 \\
0 & 0 & 8.1032 & 0.3751 & 0 & 02.0000 & 0 &
\end{bmatrix},
$$

$$
B_c = \begin{bmatrix}
-228.2151 & 25.1543 \\
306.2797 & -53.4913 \\
-55.7854 & 13.1442 \\
-52.0897 & 3.6957 \\
11.9623 & -0.3602 \\
5.3421 & 0.3814 \\
22.0573 & -9.5744 \\
8.4783 & -8.1032
\end{bmatrix},
$$

$$
C_c = \begin{bmatrix}
-0.2508 & 0.0000 & 0.8333 & -1.3595 & 1.1908 & 0.9068 & 0.2488 & 0.1874 \\
-0.0447 & 0.0000 & -0.3658 & 0.3893 & 0.2488 & 0.0436 & 0.9451 & 0.6352
\end{bmatrix}, \quad D_c = \begin{bmatrix} 0 & 0 \\ 0 & 0 \end{bmatrix}.
$$

Appendix-B

Using completion lemma, a matrix $\tilde{P}$ with the dimension $(2n \times 2n)$ can be constructed when there exists two symmetric positive definite matrices P and Q that satisfy

$$\begin{bmatrix} P & I \\ I & Q \end{bmatrix} \geq 0. \tag{B.1}$$

P and Q are respectively the left upper block of $\tilde{P}$ and $\tilde{P}^{-1}$. The following steps are shown in detail to construct $\tilde{P}$.

Let, $\tilde{P} = \begin{bmatrix} P & M \\ M^T & R \end{bmatrix}$ and $\tilde{Q} = \tilde{P}^{-1} = \begin{bmatrix} Q & N \\ N^T & S \end{bmatrix}$. We have $P > 0,\ Q > 0$ and since (B.1) holds, $P - Q^{-1} \geq 0$. Then using the inversion lemma of a matrix in block form [114], we have

$$\tilde{Q} = \tilde{P}^{-1} = \begin{bmatrix} P^{-1} + P^{-1}M\Delta^{-1}M^T P^{-1} & -P^{-1}M\Delta^{-1} \\ -\Delta^{-1}M^T P^{-1} & \Delta^{-1} \end{bmatrix} = \begin{bmatrix} Q & N \\ N^T & S \end{bmatrix} \tag{B.2}$$

where $\Delta = R - M^T P^{-1} M$. From (B.2), we have

$$\text{(2, 2) block:} \quad \Delta^{-1} = \left(R - M^T P^{-1} M\right)^{-1} = S \tag{B.3}$$

$$\text{(1, 2) block:} \quad -P^{-1}M\Delta^{-1} = -P^{-1}MS = N \tag{B.4}$$

$$\text{(1, 1) block:} \quad P^{-1} + P^{-1}MSM^T P^{-1} = Q \tag{B.5}$$

From (B.4) and (B.5), we have

$$P^{-1} + P^{-1}MSM^TP^{-1} = P^{-1} - NM^TP^{-1} = Q.$$

Simplifying it, we get the relation

$$NM^T = I - QP \tag{B.6}$$

Hence, M and N are dependent on P and Q. When P and Q are known, then an invertible matrix M has to be chosen to find the other matrix N by satisfying the relation (B.6). Now, we shall find the matrices R and S.

From (B.5), we have

$$\begin{aligned}
P^{-1} + P^{-1}MSM^TP^{-1} &= Q \\
\Rightarrow I + MSM^TP^{-1} &= PQ \\
\Rightarrow MSM^TP^{-1} &= (PQ - I) \\
\Rightarrow MSM^T &= (PQ - I)P \\
\Rightarrow S = M^{-1}[(PQ - I)P]M^{T^{-1}} &= M^{-1}[P(QP - I)]M^{T^{-1}} \qquad \text{(B.7)}
\end{aligned}$$

Now from (B.6), we have

$$\begin{aligned}
N &= (I - QP)M^{T^{-1}} \\
&= (P^{-1} - Q)PM^{T^{-1}} \\
&= -(Q - P^{-1})PM^{T^{-1}} \qquad \text{(B.8)}
\end{aligned}$$

Using (B.6), (B.7) and (B.8), we have

$$S = M^{-1}P(Q - P^{-1})PM^{T^{-1}} = N^T(Q - P^{-1})^{-1}N \tag{B.9}$$

Now, from (B.3)

$$R = M^TP^{-1}M + S^{-1}.$$

Then, replacing S from (B.7), we have

$$R = M^TP^{-1}M + M^TP^{-1}(PQ - I)^{-1}M = M^T(P - Q^{-1})^{-1}M \tag{B.10}$$

Hence, when we have P, Q, M and N, we can easily find out S and R from (B.9) and (B.10).

In other way, $\tilde{P}$ is the unique solution of

$$\begin{bmatrix} P & I \\ M^T & 0 \end{bmatrix} = \tilde{P} \begin{bmatrix} I & Q \\ 0 & N^T \end{bmatrix} \tag{B.11}$$

(B.11) can be easily verified since, $PQ + MN^T = I$ and $M^TQ + RN^T = 0$. Interestingly note that, $\tilde{P}$ can be written in the following form by which the completion lemma can also be proved.

$$\tilde{P} = \begin{bmatrix} P & M \\ M^T & R \end{bmatrix} = \begin{bmatrix} I & 0 \\ 0 & M^T \end{bmatrix} \begin{bmatrix} P & I \\ I & (P - Q^{-1})^{-1} \end{bmatrix} \begin{bmatrix} I & 0 \\ 0 & M \end{bmatrix}.$$

Bibliography

[1] Agamennoni, O., Figueroa, J. L., Desages, A. C., Palazoglu, A., and Ramagnoli, J. A. A loop shaping technique for feedback control design. *Computers and Chemical Engineering 20*, 1 (1996), 27–37.

[2] Al-Flamouz, Z., and Abdel-Magid, Y. Variable structure load frequency controllers for multiarea power systems. *International Journal of Electric Power and Energy Systems 15*, 5 (1993), 293–300.

[3] Anaparthi, K. K., Pal, B. C., and El-Zobaidi, H. Coprime factorization approach in designing multi-input stabilizer for damping electromechanical oscillations in power systems. *IEE Proceedings- Generation, Transmission and Distribution 152*, 3 (2005), 301–308.

[4] Apkarian, P., and Adams, R. J. Advanced gain-scheduling techniques for uncertain systems. *IEEE Trans. on Control System Technology 6*, 1 (1998), 21–32.

[5] Apkarian, P., and Gahinet, P. A convex characterization of gain-scheduled H_∞ controllers. *IEEE Trans. on Automatic Control 40*, 5 (1995), 853–864.

[6] Apkarian, P., Gahinet, P., and Becker, G. Self-scheduled H_∞ ccontrol of linear parameter varying systems: A design example. *Automatica 31*, 9 (1995), 1251–1261.

[7] Bang, K. H., and Park, H. B. Analysis of robust performance improvement using loop shaping and structured singular value. In *SICE, Tottori* (July, 1996), pp. 1269–1274.

[8] Banjerdpongchai, D. *Parametric Robust Controller Synthesis Using Linear Matrix Inequalities*. Stanford University, Ph.D. Thesis, 1997.

[9] Banjerdpongchi, D., and How, J. P. LMI synthesis of parametric robust H_∞ controllers. In *Proceedings of the American Control Conference, Albuquerque, NM,* (June, 1997), pp. 493–498.

[10] Becker, G., and Packard, A. Robust performance of linear parametrically varying systems using parametrically-dependent linear feedback. *Systems and Control Letters 23*, 3 (1994), 205–215.

[11] Bernstein, D. S., and Michel, A. N. A chronological bibliography on saturating actuators. *International Journal of Robust and Nonlinear Control 5*, 5 (1995), 375–380.

[12] Bevrani, Y., Mitani, Y., and Tsuji, K. Robust decentralized load-frequency control using an iterative linear matrix inequalities algorithm. *IEE Proceedings-Generation, Transmission and Distribution 151*, 3 (2004), 347–354.

[13] Bevrani, Y., Mitani, Y., and Tsuji, K. Sequential design of decentralized load frequency controller using μ synthesis and analysis. *Energy conversion and management 45* (2004), 865–881.

[14] Boyd, S., Feron, E., Ghaoui, E. L., and Balakrishnan, V. *Linear Matrix Inequalities in System and Control Theory.* SIAM, Philadelphia, 1994.

[15] Calovic, M. S. Linear regulator design for a load and frequency control. *IEEE Trans. on Power Apparatus and Systems PAS-91*, 6 (1972), 2271–2285.

[16] Cao, Y., Lam, J., and Sun, Y. Static output feedback stabilization: An LMI approach. *Automatica 34* (1998), 1641–1645.

[17] Cao, Y., Lin, Z., and Shamash, Y. Set invariance analysis and gain-scheduling control for lpv systems subject to actuator saturation. *Systems and Control Letters 46*, 2 (2002), 137–151.

[18] Chen, B. M., Lee, T. H., Peng, K., and Venkataramanan, V. Composite nonlinear feedback control for linear systems with input saturation: Theory and an application. *IEEE Trans. on Automatic Control 48*, 3 (2003), 427–439.

[19] Chilali, M., and Gahinet, P. H_∞ design with pole placement constraints: An LMI approach. *IEEE Trans. on Automatic Control 41*, 3 (1996), 358–367.

[20] Choi, C. T., and Kim, J. S. H_∞ position control of hard nonlinear systems. In *Proceedings of Conference on Control Applications, Dearborn* (1996), pp. 4518–4523.

[21] Citiva, M. L., Papegeorgiou, G., Messner, W. C., and Kanade, T. Design and flight testing of a gain-schduled H_∞ loop shaping controller for wide-envelope flight of a robotic helicopter. In *Proceedings of the American Control Conference, Denver, Colorado* (June, 2003), pp. 4195–4200.

[22] Dehghani, A., Lanzon, A., and Anderson, B. D. O. An H_∞ model referencing design utilizing a two degree of freedom controller scheme. In *Proceedings of 44th IEEE Conference on Decision and Control, and the European Control Conference, Seville, Spain* (December, 2005), pp. 2302–2307.

[23] Ding, Z. Global stabilization of input-saturated systems subject to l_2 disturbances. *IEE Proceedings on Control Theory Applications 147*, 1 (2000), 53–58.

[24] Doreto, P. A historical review of robust control. *IEEE Control System Magazine, April, 1987, 44-47.*

[25] Doyle, J. C., Francis, B., and Tennenbaum, A. *Feedback Control Theory.* Mcmillan Publishing Co., 1990.

[26] Doyle, J. C., Glover, K., Khargonekar, P. P., and Francis, B. A. State-space solutions to standard H_2 and H_∞ control problems. *IEEE Trans. on Automatic Control 34*, 8 (1989), 831–847.

[27] Doyle, J. C., and Stein, G. Multivariable feedback design: Concepts for a classical/modern synthesis. *IEEE Trans. on Automatic Control 26*, 1 (1981), 4–16.

[28] Edwards, C., and Postlethwaite, I. Anti-windup and bumpless transfer schemes. In *UKACC International Conference on Control* (1996), pp. 394–399.

[29] Elgerd, O. I. *Electric energy system theory-an introduction.* McGraw-Hill, New York, 1970.

[30] Farret, D., Duc, G., and Harcaut, J. P. Multirate LPV synthesis: A loop shaping approach for missile control. In *Proceedings of the American Control Conference, Anchorage* (May 2002), pp. 4092–4097.

[31] Farsangi, M. M., Song, Y. H., Fang, W. L., and Wang, X. F. Robust FACTs control design using the H_∞ loop-shaping method. *IEE Proceedings on Generation, Transmission and Distribution 149*, 3 (2002), 352–358.

[32] Fosha, C. E., and Elgered, O. I. The megawatt frequency control problem: A new approach via optimal control theory. *IEEE Trans. on Power Apparatus and Systems PAS-89*, 4 (1970), 563–577.

[33] Francis, B. A. *A Course in H_∞ Control Theory.* Springer Verlag, Lecture notes in Control and Information Sciences, 1987.

[34] Fuller, A. T. In the large stability of relay and saturated control systems with linear controllers. *International Journal of Control 10* (1969), 457–480.

[35] Gahinet, P. Explicit controller formulas for LMI-based H_∞ synthesis. *Automatica 32*, 7 (1996), 1007–1014.

[36] Gahinet, P., and Apkarian, P. A linear matrix inequality approach to H_∞ control. *International Journal of Robust and Nonlinear Control 4* (1994), 421–448.

[37] Gahinet, P., Nemirovski, A., Laub, A. J., and Chilali, M. *LMI Control Toolbox.* The Math Works Inc., 1995.

[38] Glover, K., and Doyle, J. State-space formulae for all stabilizing controllers that satisfy an H_∞ norm bound and relations to risk sensitivity. *System and Control Letters 11* (1988), 167–172.

[39] Glover, K., and McFarlane, D. Robust stabilization of normalized coprime factor plant description with H_∞-bounded uncertainty. *IEEE Trans. on Automatic Control 34*, 8 (1989), 821–830.

[40] Green, M., and Limebeer, D. J. N. *Linear Robust Control.* Prentice Hall, 1995.

[41] Gu, G., Chen, J., and Lee, E. B. Parametric H_∞ loopshaping and weighted mixed sensitivity minimization. *IEEE Trans. on Automatic Control 44*, 4 (1999), 846–852.

[42] Halsey, K. M., and Glover, K. Analysis and synthesis of nested feedback systems. *IEEE Trans. on Automatic Control 50*, 7 (2005), 984–996.

[43] Henrion, D., and Tarbouriech, S. LMI relaxations for robust stability of linear systems with saturating controls. *Automatica 35*, 9 (1999), 1599–1604.

[44] Henrion, D., Tarbouriech, S., and Garcia, G. Output feedback robust stabilization of uncertain linear systems with saturating controls: An LMI approach. *IEEE Trans. on Automatic Control 44*, 11 (1999), 2230–2237.

[45] Hindi, H., and Boyd, S. Analysis of linear systems with saturation using convex optimization. In *Proceedings of the 40th Conference on Decision & Control* (1998), pp. 903–908.

[46] Horn, R. A., and Johnson, C. R. *Matrix Analysis.* Cambridge University Press, 1985.

[47] Hu, T., and Lin, Z. *Control Systems With Actuator Saturation: Analysis and Design.* Barkhauser, 2001.

[48] Hyde, R. A. *The Application of Robust Control to VSTOL Aircraft.* Girton College, Cambridge, Ph.D. Thesis, August, 1991.

[49] Iwasaki, T., and Skelton, R. All solutions for the general H_∞ control pproblem: LMI existence conditions and state-space formulas. *Automatica 30*, 8 (1994), 1307–1317.

[50] Kaithwanidvilai, S., and Parnichkun, M. Position control of a pneumatic servo system by genetic algorithm based fixed-structure robust H_∞ loop shaping control. In *Proceedings of 30th Annual Conference of the IEEE Industrial Electronics Society, and the European Control Conference* (2004), pp. 2246–2251.

[51] Kapasouris, P., Athans, M., and Stein, G. Design of feedback control systems for stable plants with saturating actuators. In *Proceedings of Conference on Decision and Control* (1988), pp. 469–479.

[52] Kapila, V., and Grigoriadis, K. M. *Actuator Saturation Control.* Marcel Decker Inc., 2002.

[53] Khalil, H. K. *Nonlinear System.* Macmillan Edition, 1992.

[54] Kucera, V., and DeSouza, C. E. A necessary and sufficient conditions for output feedback stabilizability. *Automatica 31*, 9 (1995), 1357–1359.

[55] Lanzon, A. Simultaneous synthesis of weights and controller in H_∞ loop shaping. In *Proceedings of the 40th Conference on Decision and Control, Orlando, Florida, USA* (December, 2001).

[56] Lanzon, A. *Weight Selection in Robust Control: An Optimization Approach.* Wolfson College, Cambridge, Ph.D. Thesis, October, 2000.

[57] Lanzon, A., and Tsiotras, P. A combined application of H_∞ loop shaping and μ-synthesis to control high-speed flywheel. *IEEE Trans. on Control System Technology 13*, 5 (2005), 766–777.

[58] Lim, K. Y., Wang, Y., and Zhou, R. Robust decentralized load frequency controllers for multi-area power systems. *IEE Proceedings-Generation, Transmission and Distribution 143*, 5 (1996), 377–386.

[59] Lin, Z. Semi-global stabilization of linear systems with position and rate-limited actuator. *Systems and Control Letters 30*, 1 (1997), 1–11.

[60] Liu, K., and He, R. A simple derivation of ARE solutions to the standard H_∞ control problem based on LMI solution. *Systems and Control Letters 55*, 6 (2006), 487–493.

[61] Lo, K. L., and Khan, L. Hierarchical micro-genetic algorithm paradigm for automatic weight selection in H_∞ loop shaping robust flexible ac transmission system damping control design. *IEE Proceedings-Generation, Transmission and Distribution 151*, 1 (2004), 109–118.

[62] Majumder, R., Chaudhuri, B., El-Zobaidi, H., Pal, B. C., and Jaimoukha, I. M. LMI approach to normalized H_∞ loop shaping design of power system damping controllers. *IEE Proceedings-Generation, Transmission and Distribution 152*, 6 (2005), 952–960.

[63] Matsumura, F., Namerikawa, T., Hagiwara, K., and Fujita, M. Application of gain scheduled H_∞ robust controllers to a magnetic bearing. *IEEE Trans. on Control Systems Technology 4*, 5 (1996), 484–493.

[64] McFarlane, D., and Glover, K. *Robust Control Design Using Normalized Coprime Factor Plant Descriptions.* Springer Verlag, Lecture Notes in Control and Information Sciences, 1990.

[65] McFarlane, D., and Glover, K. A loop shaping design procedure using H_∞ synthesis. *IEEE Trans. on Automatic Control 37*, 6 (1992), 759–769.

[66] Moorari, M., and Zafiriou, E. *Robust Process Control.* Prentice Hall, 1989.

[67] Nguyen, T., and Jabbari, F. Output feedback controllers for disturbance attenuation with actuator amplitude and rate saturation. *Automatica 36*, 9 (2000), 1339–1346.

[68] Nobakhti, A., and Munro, N. A new method for singular value loop shaping in design of multiple-channel controllers. *IEEE Trans. on Automatic Control 49*, 2 (2004), 249–253.

[69] Panagopoulos, H., and Astrom, K. J. PID control design and H_∞ loop shaping. In *Proceedings of the 1999 IEEE International Conference on Control Applications, Kohala Coast-Island of Howai* (Auguest, 1999), pp. 103–108.

[70] Papegeorgiou, G. *Robust Control System Design: H_∞ Loop Shaping and Aerospace Applications.* Darwin College, Cambridge, July, Ph.D. Thesis, 1998.

[71] Papegeorgiou, G., and Glover, K. A systematic procedure for desiging non-diagonal weights to facilitate H_∞ loop shaping. In *Proceedings of the 36th Conference on Decision & Control, San Diego, California, USA* (December, 1997), pp. 2127–2123.

[72] Pittet, C., Tarbouriech, S., and Burgat, C. Stability regions for linear systems with saturating controls via circle and popov criteria. In *Proceedings of the 36th Conference on Decision and Control* (1997), pp. 4518–4523.

[73] Postlethwaite, I., Edmunds, J. M., and McFarlane, A. G. L. Principle gains and principle phases in the analysis of linear multivariable feedback systems. *IEEE Trans. on Automatic Control 26*, 1 (1981), 32–46.

[74] Prempain, E. Static H_∞ loop shaping control. In *Control-2004, University of Bath, UK* (September, 2004).

[75] Prempain, E., and Postlethwaite, I. Static H_∞ loop shaping control of fly-by-wire helicopter. In *Proceedings of the Conference on Decision & Control* (2004), pp. 1188–1195.

[76] Prempain, E., and Postlethwaite, I. Static H_∞ loop shaping control of fly-by-wire helicopter. *Automatica 41* (2005), 1517–1528.

[77] Ray, G., Prasad, A. N., and Prasad, G. D. A new approach to the design of robust load-frequency controller for large scale power systems. *Electric power systems research 51*, 1 (1999), 13–22.

[78] Reinelt, W. Robust control of a two-mass-spring system subject to its input constraints. In *Proceedings of the American Control Conference* (June, 2000), pp. 1817–1821.

[79] Rocha, R., Resende, P., Silvino, S. L., and Bortolus, M. V. Control of stall regulated wind turbine through H_∞ loop shaping method. In *Proceedings of the 2001 IEEE International Conference on Control Applications* (2001), pp. 925–929.

[80] Romanchuk, B. G. Some comments on anti-windup synthesis using LMIs. *International Journal of Robust and Nonlinear Control 9*, 10 (1999), 717–734.

[81] Rosenbrock, H. H. The stability of multivariable systems. *IEEE Trans. on Automatic Control 17*, 1 (1972), 105–107.

[82] Rowe, C., and Maciejowski, J. Tuning MPC using H_∞ loop shaping. In *Proceedings of the American Control Conference, Chicago, Illinois* (June, 2000), pp. 1332–1336.

[83] Saberi, A., Lin, Z., and Teel, A. R. Control of linear systems with saturating actuators. *IEEE Trans. on Automatic Control 41*, 3 (1996), 368–378.

[84] Saurez, R., Ramirez, J. A., and Daun, J. S. Linear systems with bounded inputs: Global stabilization with eigenvalue placement. *International Journal of Robust and Nonlinear Control 7*, 9 (1997), 835–845.

[85] Schulte, R. P. An automatic generation control modification for present demands on interconnected power systems. *IEEE Trans. on Power Systems 11*, 3 (1996), 1286–1294.

[86] Sebastian, A., and Salapaka, S. H_∞ loop shaping design for nano-positioning. In *Proceedings of the American Control Conference, Denver, Colorado, USA* (June, 2003), pp. 3708–3713.

[87] Sefton, J., and Glover, K. Pole/zero cancellations in the general H_∞ problem with reference to a two block design. *Systems and Control Letters 14*, 4 (1990), 295–306.

[88] Shamma, J. S., and Athans, M. Guaranteed properties of gain scheduled control for linear parameter varying plant. *Automatica 27*, 3 (1991), 559–564.

[89] Sheirah, M. A., and Abdel-Fattah, M. M. Improved load frequency self-tuning regulator. *International Journal of Control 39*, 1 (1984), 143–158.

[90] Shewchun, J. M., and Feron, E. High performance control with position and rate limited actuators. *International Journal of Robust and Nonlinear Control 9*, 10 (1999), 617–630.

[91] Skogestad, S., and Postlethwaith, I. *Multivariable Feedback Control: Analysis and Design.* John Wiley and Sons, Ltd, Second edition, 2005.

[92] Stilwell, D. J., and Rugh, W. J. Interpolation of observer state feedback controllers for gain scheduling. In *Proceedings of the American Control Conference, Philadelphia, Pennsylvania* (June, 1998), pp. 1215–1219.

[93] Sznaier, M., Suarez, R., Miani, S., and Ramirez, J. A. Optimal l_2 disturbance attenuation and global stabilization of linear systems with bounded control. *International Journal of Robust and Nonlinear Control 9*, 10 (1999), 659–675.

[94] Takaba, K. Local stability analysis of a saturating feedback system based on LPV descriptor representation. *International Journal of Control 76*, 5 (2003), 478–487.

[95] Tan, W., Liu, J., and Tam, P. K. S. PID tuning based on loop-shaping H_∞ control. *IEE Proceedings on Control Theory Applications 145*, 6 (1998), 485–490.

[96] Tan, W., Marquez, H. J., and Chen, T. Multivariable robust controller design for a boiler system. *IEEE Trans. on Control Systems Technology 10*, 5 (2002), 735–742.

[97] Tan, W., Marquez, H. J., Chen, T., and Liu, J. Multimodel analysis and controller design for nonlinear processes. *Computers and Chemical Engineering 28* (2004), 2667–2675.

[98] Teel, A. R. Linear systems with input nonlinearities: Global stabilization by scheduling a family of H_∞-type controllers. *International Journal of Robust and Nonlinear Control 5*, 5 (1995), 399–411.

[99] Teel, A. R. A nonlinear small gain theorem for the analysis of control systems with saturation. *IEEE Trans. on Automatic Control 41*, 9 (1996), 1256–1270.

[100] Tierno, J., and Glavaski, S. Phase-lead compensation of pitch axis control laws via $McFarlane - Glover\ H_\infty$ loop shaping. In *Proceedings of the 38th Conference on Decision and Control, Pheonix, Arizona, USA* (December, 1999), pp. 1538–1543.

[101] Trofino, N. A., and Kucera, V. Stabilization via static output feedback. *IEEE Trans. on Automatic Control 38*, 9 (1993), 764–765.

[102] Turner, M. C., Hermann, G., and Postlethwaite, I. Discrete time anti-windup part i: Stability and performance. In *Proceedings of European Control Conference* (2003).

[103] Turner, M. C., Hermann, G., and Postlethwaite, I. *An Introduction to LMIs in Control.* Department of Engineering, University of Leicester, Technical Report: 02-04, 2004.

[104] Turner, M. C., and Postlethwaite, I. A new perspective on state and low-order anti-windup compensator synthesis. *International Journal of Control 77* (2004), 27–44.

[105] VanAntwerp, J. G., and Braatz, R. D. A tutorial on linear and bilinear matrix inequalities. *Journal of Process Control 10*, 4 (2000), 363–385.

[106] Vidyasagar, M. *Control System Synthesis: A Factorization Approach.* MIT Press, Chicago, Illinois, United States of America, 1985.

[107] Wang, J. Y., and Tomizuka, M. Gain-scheduled H_∞ loop shaping controller for automated guidance of tractor-semitrailer combination vehicles. In *Proceedings of the American Control Conference* (2000), pp. 2033–2037.

[108] Weston, P. F., and Postlethwaite, I. Linear conditioning for systems containing saturating actuators. *Automatica 36* (2000), 1347–1354.

[109] Whidbrone, J. F., Postlethwaith, I., and Gu, D. W. Robust controller design using H_∞ loop shaping and method of inequalities. *IEEE Trans. on Control System Technology 2*, 4 (1994), 455–461.

[110] Wu, F., Lin, Z., and Zheng, Q. Output fedback stabilization of linear systems with actuator saturation. *IEEE Trans. on Automatic Control 52*, 1 (2007), 122–128.

[111] Wu, F., Yang, X. H., Packard, A., and Becker, G. Induced l_2-norm control for LPV systems with bounded parameter variation rates. *International Journal of Robust and Nonlinear Control 6* (1996), 983–998.

[112] Yano, M., and Ikeda, H. H_∞ loop shaping controller for the static VAR compensator. In *IEEE power electronics specialists conference, PESC* (1994), pp. 1088–1094.

[113] Zames, G. Feedback and optimal sensitivity: Model reference transformations, multiplicative seminorms and approximate inverses. *IEEE Trans. on Automatic Control 26*, 2 (1981), 301–320.

[114] Zhou, K., Doyle, J. C., and Glover, K. *Robust and Optimal Control.* Prentice Hall, 1995.

[115] Zhu, C., Khammash, M., Vittal, V., and Qiu, W. Robust power system stabilizer design using H_∞ loop shaping approach. *IEEE Trans. on Power Systems 18*, 2 (2003), 810–818.

Publications from this Thesis

Published

- S. Patra, S. Sen and G. Ray, 'Design of robust load frequency controller: H_∞ loop shaping approach', *Electric Power Components and Systems, Vol. 35, No. 7, pp. 769-783, July, 2007.*

Provisionally accepted

- S. Patra, S. Sen and G. Ray, 'Alternative method for designing the static H_∞ loop shaping controller using LMI approach'. *Automatica.*

Under revision

- S. Patra, S. Sen and G. Ray, 'Linear matrix inequality approach to parametric H_∞ loop shaping control', *Kybernetika.*

Communicated

- S. Patra, S. Sen and G. Ray, 'A low Order H_∞ loop shaping controller for power system load frequency control: normalized coprime factorization approach', *International Journal of Electrical Power and Energy Systems, Elsevier Publication.*
- S. Patra, S. Sen and G. Ray, 'Weight selection for H_∞ loop shaping control', *Kybernetika.*

Author's Biography

Sourav Patra was born on 12^{th} August 1977 at Contai, Midnapur. He obtained his Bachelor's degree in Electrical Engineering from Jadavpur University, Kolkata in the year 2000. Then he did Master of Engineering specialization in Control Systems from Bengal Engineering and Science University, Shibpur, Howrah in the year 2003. He has a short industrial experience from August, 2000 to February' 2001. After Master of Engineering, he joined in PhD program at the Department of Electrical Engineering, Indian Institute of Technology, Kharagur in the year 2003. His research interest includes robust control, linear matrix inequality and actuator saturation control for multivariable systems.